The Dissertation Committee for Abdoljalil Varavei certifies that this is the approved version of the following dissertation:

Development of an Equation-of-State Thermal Flooding Simulator

Committee:

Kamy Sepehrnoori, Supervisor

Gary A. Pope

Mojdeh Delshad

Chun Huh

Mark Miller

Development of an Equation-of-State Thermal Flooding Simulator

by

Abdoljalil Varavei, B.S; MS.

Dissertation

Presented to the Faculty of the Graduate School of

The University of Texas at Austin

in Partial Fulfillment

of the Requirements

for the Degree of

Doctor of Philosophy

The University of Texas at Austin

May 2009

Dedication

To the memory of my father; Gholamhassan Varavei

and my sisters; Batoul and Fatemeh Varavei

To my mother; Setareh Taimouri

My family

My wife; Mandana

My son; Mohammad Hesam.

Acknowledgments

I am extremely grateful to my supervising professor, Dr. Kamy Sepehrnoori for his support, guidance, encouragement, and providing me the opportunity to learn from him on the subject of this study.

I would like to thank Dr. Pope for his guidance and encouragements, and also I would like to extend my thanks to the other members of my supervising committee, Dr. Mojdeh Delshad, Dr. Chun Huh, and Dr. Mark Miller for their time and efforts.

I wish to express my sincere gratitude to the faculty and the staff of the Petroleum and Geosystem Engineering Department for their help and continuous support. Special thanks to Cheryl Kruzie, Esther Barrientes, Roger Terzian, Tim Guinn and Joanna Castillo for their constant support and willingness help.

I would like to extend my appreciation to Dr. Chowdhury Mamun, Dr. Lee Chin and Jana Cox for taking the time to review my dissertation.

I greatly acknowledge financial support from National Iranian Oil Company and from my supervisor Dr. Sepehrnoori.

Finally, I appreciate my family's love and patience both here and in my home country. My mother, Setareh Taimouri, my wife, and my lovely son Mohammad Hesam for their love, patience, understanding, and encouragement towards my achievements.

Development of an Equation-of-State Thermal Flooding Simulator

Publication No._____

Abdoljalil Varavei, Ph.D.

The University of Texas at Austin, 2009

Supervisor: Kamy Sepehrnoori

In the past thirty years, the development of compositional reservoir simulators using various equations of state (EOS) has been addressed in the literature. However, the development of compositional thermal simulators in conjunction with EOS formulation has been ignored, in particular. Therefore in this work, a fully implicit, parallel, compositional EOS-based simulator has been developed. In this model, an equation of state is used for equilibrium calculations among all phases (oil, gas, and aqueous). Also, the physical properties are calculated based on an equation of state, hence obviating the need for using steam tables for calculation of water/steam properties. The governing equations for the model comprise fugacity equations between the three phases, material balance, pore volume constraint and energy equations. The governing partial differential equations are solved using finite difference approximations. In the steam injection process, the solubility of oil in water-rich phase and the solubility of water in oil phase can be high. This model takes into account the solubility of water in oil phase and the solubility of hydrocarbon components in water-rich phase, using three-phase flash calculations.

This simulator can be used in various thermal flooding processes (i.e. hot water or steam injections). Since the simulator was implemented for parallel computers, it is capable of solving large-scale thermal flooding problems. The simulator is successfully validated using analytical solutions. Also, simulations are carried out to compare this model with commercial simulators.

The use of an EOS for calculation of various properties for each phase automatically satisfies the thermodynamic consistency requirements. On the other hand, using the K-value approach, which is not thermodynamically robust, may lead to results that are thermodynamically inconsistent. This simulator accurately tracks all components and mass transfer between phases using an EOS; hence, it will produce thermodynamically consistent results and project accurate prediction of thermal recovery processes.

Electrical heating model, Joule heating and in-situ thermal desorption methods, and hot-chemical flooding model have also been implemented in the simulator. In the electrical heating model, electrical current equation is solved along with other governing equations by considering electrical heat generation. For implementation of the hot-chemical heating model, first the effect of temperature on the phase behavior model and other properties of the chemical flooding model is considered. Next, the material and energy balance and volume constraints equations are solved with a fully implicit method. The models are validated with other solutions and different cases are tested with the implemented models.

Table of contents

List of Tables

List of Figures

Chapter 1: Introduction

1.1 DESCRIPTION OF THE PROBLEM

Black oil models and more general reservoir behavior were originally developed during 1950s by introducing of electronic computers and the restoration of interest in the mathematics of numerical methods. West *et al.* (1954) presented a digital method of solving the equations of unsteady state two-phase flow in oil reservoirs. Douglas *et al.* (1958) developed a numerical method to determine the behavior of a linear water flood with capillary pressure effect. A numerical method to simulate oil displacement by water for multi-dimensional reservoirs was performed by Douglas *et al.* (1959). Sheldon *et al.* (1960) presented a computer method for two-dimensional reservoir simulation on digital computers. Fagin and Stewart (1965) presented an approach for two-dimensional multiphase reservoir simulator.

The models were simple in terms of computer programming and were based on the assumption that oil is nonvolatile and that the vapor phase contains inert gas. With the advancement of computer sciences, new and sophisticated numerical models were developed. Compositional simulators fall into these categories. The compositional simulators address the complexity of fluid and the phase behavior in the thermal recovery process.

The recovery of hydrocarbon using thermal processes has long been a viable option for increasing the production and the ultimate recovery of intermediate to heavy oil from

petroleum reservoirs. Numerical modeling and simulation of recovery processes are required for development and decision-making for increasing oil production using enhanced oil recovery methods. Reservoir simulators are important tools for analysis and optimization of the recovery processes. Thermal recovery methods include processes such as hot water injection, steam injection, in-situ combustion and more exotic processes like coal gasification, electric heating, and even the use of nuclear energy. Originally, the steam injection was aimed at recovery of very viscous oils and tars. The steam increases the temperature of the reservoir and decreases the viscosity of hydrocarbon phases. The consequence of less viscous oil is the enhanced mobility of heavy oil, whereupon oil will flow more freely in the reservoir.

During the past four decades, there have been significant developments in the simulation of heavy oil recovery using thermal methods. Numerical methods were developed ranging from the dead oil model using the implicit pressure-explicit saturation (IMPES) or the sequential solution algorithm to the compositional models that apply the fully implicit solution methods. In addition to viscosity reduction, other methods such as steam distillation, solvent extraction, and thermal expansion also contribute to the general success of thermal recovery process. In the other words, steam injection is used for the recovery of intermediate and lighter oils as well as heavy oil and tar sands.

Another possible benefit of thermal processes is the wettability alteration. The temperature is increased in the reservoir by the injection of either steam or hot water. As a result of the higher reservoir temperature, the wettability can change by desorption of the asphaltenes from the rock surface. Wettability can change from oil-wet to water-wet in naturally fractured carbonate reservoirs and liquid-wet to intermediate gas-wetting in gas condensate reservoirs. These wettability alterations can increase the water flooding efficiency and also increase the liquid mobility in gas condensate reservoirs. The wettability

alteration can also affect surface tension, rock-fluid interaction, relative permeability, and capillary pressure. In other words, in solution gas drive heavy oil reservoirs, with increasing temperature, and consequently with increasing gas relative permeability and mobility, the recovery efficiency is decreased. Therefore, these changes should be modeled accurately. The efficiency of steam-flooding (SF) will be increased if low concentration of alkaline or surfactant is added to the steam. Such methods are referred to as surfactant steam flood (SSF), alkaline steam flood (ASF), and surfactant alkaline steam flood (SASF).

Another application of the thermal model is including the effect of temperature on geo-mechanical properties in the simulations. The steam injection affects the reservoir properties, especially in faulted and fractured reservoirs due to stress changes. The change in stress causes an increase or decrease in facture conductivity; thus, it can affect the direction of flow. Hence, this property should also be modified during thermal recovery.

Electrical heating is another thermal oil recovery method. This recovery method can be used for heavy oil reservoirs, especially with thin pay zone. Due to heat loss from the reservoir, especially due to overburden, steam injection and other thermal recovery methods for this kind of reservoir may not be economical and electromagnetic heating can provide heat to the reservoir more efficient. Modeling of the heating process can be carried out by the current continuity equation, the petrochemical properties, and the heat-generation equation which addresses electrical conduction.

Reservoir simulators are based on the numerical solution of the partial differential equations and the related physical property that describe the fluid flow in the subsurface. Due to intense computational requirements, simulators used in thermal oil recovery processes need to be used in conjunction with high-performance computers to overcome the CPU and the memory requirements so that the simulators can be used on a routine basis in reservoir simulation studies. Parallel processing for reservoir simulation with high-

performance computing clusters can meet the computational requirements for the reservoir simulators. Wang *et al*. (1997) and DeBaun *et al*. (2005) have published articles on parallel processing reservoir simulation development and application. They described the development and advantages of such approaches for performing reservoir simulation studies on parallel and distributed processing modes.

1.2 RESEARCH OBJECTIVES

The main objective of this work is the implementation of a thermal oil recovery module into a general purpose adaptive oil reservoir simulator called GPAS, which was developed at the Center for Petroleum and Geosystems Engineering at The University of Texas at Austin. GPAS encompasses several different modules for simulating various oil recovery processes in conventional and naturally fractured reservoirs. GPAS has the capability of performing compositional gas flooding as well as surfactant/polymer flooding and asphaltene precipitation models. Presently, work is underway to develop and implement a geo-mechanical model into GPAS. Later, a detailed description of GPAS will be given. After the completion of the thermal recovery module, the other modules in GPAS will be modified to include the effect of temperature on recovery processes. The following were the objectives of this research:

1. Development of a four-phase model for GPAS with three-phase flash calculation.
2. Development of the species mass conservation equations and energy balance equation for thermal recovery processes.
3. Discretization of governing partial differential equations using finite difference method.
4. Implementation of the thermal model in GPAS.

5. Implementation of electrical heating processes (in-situ thermal desorption (ISTD) and Joule heating methods) in GPAS.
6. Implementation of hot surfactant model into GPAS.
7. Implementation of the multiphase reaction model for GPAS.
8. Testing and verification of the thermal model.
9. Application of the thermal oil recovery module to realistic problems and comparison with commercial reservoir simulators.

1.3 BRIEF DESCRIPTION OF CHAPTERS

In Chapter 2, a review of the previous work related to compositional simulators and thermal simulators is presented. Chapter 3 presents a new phase behavior module for GPAS. The detailed new phase behavior calculations and case examples are presented in Chapter 3. The new model can handle three hydrocarbon phases in equilibrium, in addition to a separate water phase. The mathematical models, the governing equations, the auxiliary equations, solution technique for GPAS thermal module, and case studies are described in Chapter 4. Chapter 5 describes another thermal process called electrical heating. In this chapter, detailed implemented models including governing equations, method of solving the model equations and case examples are presented. In Chapter 6, another feature of chemical flooding model of GPAS, the hot chemical flooding (including model description), its new equations, and case examples are given. The last chapter presents the summary, conclusions and recommendations for future work.

Chapter 2: Literature Review

2.1 INTRODUCTION

In this chapter, the literature review for the research is presented. First, literatures related to compositional simulators and how the simulators were developed are given. Next, a survey of thermal simulators is presented. Finally, the development of electrical heating model, the hot surfactant, and the multiphase reaction are described.

2.2 LITERATURE REVIEW

The review of previous research is presented in the following sections.

2.2.1 Compositional Simulator

In compositional simulators, mass conservation, and phase equilibrium equations are used to calculate pressure, saturations, phase ratios, and phase compositions of each phase. Kazemi *et al.* (1977) developed a three-dimensional, three-phase, multicomponent numerical reservoir simulator. They used an implicit method to solve the oil phase pressure equation and used explicit equations to calculate overall compositions, water saturation, and oil-gas saturations. Fussell and Fussell (1979) developed the first compositional simulator using an equation-of-state for phase equilibrium and density calculation for gas flooding. Their approach overcomes the non-convergence problem of previous models which did not use equation of state. Inconsistency in fluid properties had led to the non-convergence

problem in previous studies. Coats (1980) developed a fully implicit, three-dimensional and three-phase simulator. Nghiem *et al*. (1981) developed an IMPES compositional, three-phase and three-dimensional simulator. They solved pressure and phase compositions separately. Young and Stephenson (1983) developed a simulator that was more efficient than the Fussell and Fussell's (1979) simulator. The difference between them was the selection of the primary variables and ordering of the equations. Different sets of primary variables depending on fluid conditions were selected in Fussell and Fussell's method. Young and Stephenson's model used one set of primary variables for all conditions. In the Young and Stephenson model, the Jacobian was sparse and close to upper triangular and could be solved more efficiently. Thele *et al*. (1983) compared the models of Nghiem *et al*. (1981), Coats and Young and Stephenson for accuracy, iteration number, and computer time. Acs *et al*. (1985) developed an IMPES simulator by using both Nghiem *et al*. and Young and Stephenson models. Watts (1986) developed a simulator by extending and combining those of Acs *et al*. (1985) and Spillette *et al*. (1973) for sequential implicit compositional simulation. Chien *et al*. (1985) presented another fully implicit formulation with different primary variables than those of Coats (1980). They solved for pressure, overall composition, and equilibrium K-values, but in Coats' formulation the primary variables were pressure, saturation, and phase composition. Collins *et al*. (1986) developed an adaptive implicit simulator. Wong *et al*. (1987) presented the comparison between the Watts and the Young and Stephenson simulators for accuracy and computational efficiency. Chang *et al*. (1990) developed an IMPES compositional simulator (UTCOMP) with a three-phase flash model. Briens *et al*. (1991) developed a fully parallel vectorized compositional reservoir simulator and introduced an algorithm, Sequential Staging of Tasks (SST), which can be used for parallel/ vector processing to speed up the solution of large linear systems equations. Buchwalter and Miller (1993) developed a fully implicit compositional simulator

which combined the conventional black oil equations and a compositional injection component equation. Branco and Rodrigues (1995) described a semi-implicit formulation for compositional reservoir simulation. Wang *et al.* (1997) presented the formulation for a fully implicit parallel EOS compositional simulator. *Wang et al*. (1999) developed the framework approach for EOS compositional simulator and applied for gas injection. Young (2001) described the continuous analog of the volume-balance method for compositional reservoir simulation. Cao and Aziz (2002) developed the IMPSAT (implicit pressure and saturations and explicit component mole fractions) method for reservoir simulation. They described that the method is more stable than the IMPES model and in many cases is less expensive than the fully implicit model. Bowen and Crumpton (2003) presented a formulation for implicit compositional simulator to have more efficient implicit method and CPU advantage. Yan *et al*. (2004) developed a three-dimensional, three-phase compositional simulator using streamline method and applied that to the water-alternating-gas (WAG) process. Li (2004) developed a four-phase streamline simulator and described the model is faster than the finite difference simulators. Voskov and Tchelepi (2008) described a reservoir simulation approach based on adaptive parameterization of the compositional space using the tie-line which obtained from MOC (Method of Characteristics) theory. Rastegar and Jessen (2009) presented an automatic lumping method to reduce number of pseudocomponents for improving the accuracy and CPU time for compositional reservoir simulations.

2.2.2 Thermal Simulator

Hot fluid injection and electrical heating models are described in the following sections.

2.2.2.1 Hot Fluid Injection

Shulter (1969) presented the first steam flooding simulator. He originally developed a three-phase linear model and extended the model to two dimensions in the 1970s. Abdalla and Coats (1971) developed a two-dimensional three-phase flow steam drive simulator. They formulated the equations based on an implicit pressure and explicit saturation model. They neglected the hydrocarbon gas phase; temperature was calculated from saturated steam pressure. This model was extended to three dimensions by Coats *et al*. (1974). Vinsome (1974) introduced an IMPES method to simulate steam-drive and steam-soak processes. Nilsson *et al*. (2005) developed an adaptive simulation model for black-oil steam injection. Coats (1976) introduced the first algorithm to account for distillation and compositional modeling, which was an extension of Coats *et al*. (1974). Ferrer and Farouq Ali (1977) presented a two-dimensional compositional model to simulate steam injection. Their model was similar to Coats' (1976) model, but different in the computation of the heat of vaporization. Coats (1978) developed a three-dimensional, highly implicit formulation for the steam flooding process. Crookston *et al*. (1979) introduced a linearized implicit combustion model. Both of these models were multi-dimensional and could not fully handle the well-bore reservoir coupling implicitly.

Abou-Kassem (1981) presented a two-dimensional, fully-implicit compositional model for steam flooding. He used the sequential implicit method to solve the governing system of equations. The first application of equation of state to calculate the phase properties was developed by Ishimoto in 1985. Ishimoto *et al*. (1987) employed a one-dimensional fully implicit compositional steam flood model. Rubin and Buchanan (1985)

described a general, fully implicit, four-phase, multi-component, multidimensional steam and combustion simulator. This model included a fully implicit well model and had appropriate and powerful iterative techniques for solving large thermal problems. Chein *et al*. (1989) presented a general purpose compositional simulator that contained a thermal option. In this model, the user can select K-values or the equation of state to calculate the fluid properties. Trangenstein (1989) gave an analysis of a two-component, three-phase flow thermal model. The analysis was done to study the effect of thermodynamic principles on flow equations. Brantferger (1991) developed a simulator which had major differences compared to previous formulations. They used an equation of state to calculate thermodynamic properties of each phase. In this model, they considered water as a non-ideal component and used enthalpy as a primary variable. Mifflin *et al*. (1991) introduced a fully coupled, fully implicit oil reservoir simulator. This formulation was implemented in a framework that supports an IMPES and a sequential semi-implicit formulation. Chan and Sarioglu (1992) presented a procedure for incorporating fracture characteristics in a thermal reservoir simulator. Cicek and Eretkin (1996) developed a simulator for steam injection. The simulator was based on a compositional, fully implicit 3D multiphase component mass and energy balance. Godderij *et al*. (1999) introduced a 3D steam drive simulator. They used an interface model, where the single phase steam zone was separated from the two-phase liquid region by a steam condensation front. Cicek (2005) developed and tested the numerical simulation of steam displacement of oil in naturally fractured reservoirs using fully implicit compositional formulation. He investigated the effects of capillary and gravitational forces in the matrix/fracture exchange term. Luo and Barrufet (2005) studied the effect of water-in-oil solubility on oil recovery by using their thermal simulator. They considered water as a pure phase, but mass transfer of water into oil and gas phases was allowed. For a three-phase equilibrium system, each component must have the same

chemical potential in all phases. They performed oil/gas flash calculation in the three-phase system separately. They also had another objective function requiring water chemical potential to be same in oil/gas flash calculation and equal to water chemical potential in water phase.

In thermal processes, the temperature is high. Consequently, the solubility of the water in oil and the solubility of oil in water-rich phase can be increased. These solubilities can affect the crude oil phase behavior and change the density, viscosity, and other properties. Ignoring these solubilities can have a profound effect on the production results. Wang and Chao (1990) showed that water solubility in oil phase can be as high as about 50 percent. Grisworld and Kasch (1942) presented oil/water solubilities at high temperature. They showed that the solubility of water in oil, 54.3°API naphtaha, is 16.18 mole percent at 431.6°F, the solubility of water in oil, 42°API kerosene, is 34.97 mole percent at 507.2°F, and the solubility of the water in oil with 29.3°API at 537.8°F is 43.44 mole percent. Nelson (1956) showed that the solubility of water in oil can be about 42 mole percent at 540°F. Heidman (1985) showed that the solubility of water in liquid C_8 at 500.0°F is 38.7 mole percent. Glandt and Chapman (1995) also showed 33.3 weight percent solubility of water in oil mixture, and they described the effect of this solubility on viscosity.

Before applying the equation of state (EOS) to thermal processes, in other words to handle the phase behavior calculations of water/hydrocarbon and non-hydrocarbon systems, it is necessary to improve and tune the equation. Binary interaction coefficients and volume shift parameters are modified for the EOS for this kind of calculation. Bang (2005) showed good agreement between experimental data for the hydrocarbon/water and hydrocarbon/water/methanol system at different temperatures. They modified the binary interaction coefficient and the volume shift parameter for EOS to match experimental data.

Shinta and Firoozabadi (1997) presented the binary interaction coefficients between water and hydrocarbon for EOS to handle water/hydrocarbon phase behavior calculation.

Al-Hadhrani and Blunt (2000) investigated thermally-induced wettability alteration in fractured reservoirs by core analysis. They also introduced a one-dimensional analytical model for simulating naturally fractured reservoir by steam and hot water injection. They showed that 30% oil recovery could be achieved in a single matrix after 700 days. Tang and Kovscek (2002) experimentally showed that increasing the temperature in the reservoir by hot water injection can change wettability, surface tension, and viscosity ratio and affect the oil recovery. For example, changing the wettability from oil to water-wet can increase the oil recovery. Fahes and Firoozabadi (2005) examined the wettability alteration to intermediate gas-wetting in gas condensate reservoirs at high temperatures. They showed that wettability could change from liquid-wetting to intermediate gas-wetting at high reservoir temperatures and this alteration can increase the liquid mobility at reservoir conditions. Relative permeability is another parameter that can be changed with temperature. Schembre *et al.* (2005) investigated the effect of temperature on relative permeability for heavy-oil diatomite reservoirs and showed water-wettability increasing on account of increasing temperature. They showed the relation of relative permeability to the effect of temperature on surface forces and to rock-fluid interactions.

Shedid and Abbas (2000) conducted an experimental study of alkaline/surfactant/ steam flood in vertical wells. They demonstrated this by using low concentrations of alkaline or surfactant as an additive to steam in water flooded reservoirs. Oil recovery was increased, especially when alkaline and surfactants were added to steam. Abbas *et al*. (2001) investigated the feasibility of steam/chemical flooding through horizontal wells. Their experimental study showed a tertiary oil recovery of heavy oil by using steam, caustic steam, surfactant steam, and caustic-surfactant steam flooding.

Tang and Firoozabadi (2001) carried out a set of experiments to show the effect of gas-oil ratio (GOR), temperature, and initial water saturation on solution-gas-drive heavy-oil reservoirs. They showed that increasing the temperature will decrease the sweep efficiency on account of increasing the mobility of the gas phase.

This thermal model is based on EOS. The phase properties are calculated using EOS. All of the components including water can exist in all of the phases. Water phase is not considered a separate phase; hence flash calculation is used to calculate the phase saturations and the compositions of the phases.

Effect of temperature on relative permeability. One of the most important data for numerical reservoir simulators is relative permeability. Relative permeability usually is described as a function of saturation. The effect of temperature on relative permeability has been presented in literature.

Edmondson (1965) reported that residual oil saturations were decreased with increasing the temperature and relative permeability ratios were decreased with temperature at high water saturations but increased with temperature at low water saturations. Poston *et al*. (1970) reported that with increasing temperature the residual oil saturation decreased and irreducible water saturation increased. They also concluded that the relative permeability of oil and water were increased by increasing of the temperature. Sufi *et al*. (1982) studied the effect of temperature on relative permeability and presented the temperature has no effect on relative permeability data. Their data were obtained from unsteady-state experiment in unconsolidated and Berea sandstone. Torabzadey (1984) presented the relative permeability data in a range of 22ºC to 175ºC. They described that the relative permeability curves were affected by temperature at low interfacial tension and the relative permeability ratio of water to oil was decreased with temperature. They reported that the relative permeability to oil increased and relative permeability to water decreased at a given saturation while residual

oil saturation decreased and irreducible water saturation increased with increasing temperature. Miller and Ramey (1985) studied the laboratory dynamic-displacement relative permeability measurements which were made on unconsolidated and consolidated sand cores with water and a refined white mineral oil. They reported the temperature did not effect on relative permeability. Closmann *et al*. (1985) studied the effect of temperature on tar and brine. They found that the relative permeability curves were shifted to the lower water saturations. Maini and Batycky (1985) studied the temperature effect (in the range of room temperature to 522 ºF) on heavy oil reservoir and stock tank oil and reported that oil relative permeability decreased with increasing the temperature. Polikar *et al*. (1990) studied the effect of temperature on Athabasca bitumen/water relative permeabilities and reported little or no temperature effect on the relative permeabilities to water and bitumen over a range of 100 to 250°C. Akin *et al*. (1999) presented experimental data for the effect of temperature on relative permeability indicating that the relative permeability was not a function of temperature. Ayatollahi *et al*. (2005) presented that the oil relative permeability in gas oil gravity drainage increased by increasing the temperature. They also reported that the aging process has more effect than temperature in thermal oil recovery on oil relative permeability. They described in the case of changing of the wettability of the media, the temperature did not effect on relative permeability unless the effect of temperature was dominant. Schembre *et al*. (2005) presented that by increasing temperature the water relative permeability and residual oil saturation were increased in diatomite rock. They showed that the temperature increased the water wettability too. They explained that the surface properties of the diatomite rock had effect on relative permeability and capillary pressure besides temperature. Hamouda *et al*. (2008) addressed the effect of temperature on relative permeability in a range of 23ºC to 130ºC. They described that relative permeability

curve was shifted toward more water-wet up to the temperature less than 80° C. But for higher temperature, 130°C, the relative permeability curves showed more oil-wet.

2.2.2.2 Electrical Heating Model

The electrical heating enhanced oil recovery model is based on passing electrical current through the conductive formation and resistive heating of the reservoir. As a result, the oil viscosity is reduced. There are many researchers working on electrical enhanced oil recovery. One of the earliest electrical EOR methods was presented by Workman (1930). His method hinged on conducting electricity in the water legs of the reservoir for releasing gases (such as oxygen and hydrogen). The released gases are absorbed by oil; oil becomes lighter and more mobile; oil then releases from the sand and moves to top of the water in the well. The method of using high density electrical currents to carbonize hydrocarbons in order to increase the recovery was proposed by Sarapuu (1957). Bell (1957) proposed the driving of oil from reservoir to production wells via high-density direct electrical current. Using the alternating current to heat up the reservoir and decreasing the viscosity to increase oil recover was presented by Gill (1970, 1972) and Crowson and Gill (1971). Hilbert (1986) developed a numerical simulator of the electrical pre-heat and steam-drive bitumen recovery process for oil sands. Killough and Kossack (1987) developed a fully implicit electrical heating simulator for enhanced oil recovery.

Chilingar *et al.* (1968, 1970, and 1997) at The University of Southern California carried out laboratory experiments, which suggested that this low power drain mechanism can be used for enhanced oil recovery. Tikhomolova (1993) presented electro-osmosis as a method for enhanced oil recovery. McGee *et al*. (1999) presented a field-study of electrical heating with horizontal and vertical wells in Canadian heavy oil fields. The case study evaluated the efficiency of low-frequency alternating current (AC). Chute and Vermeulen

(1988) showed the application of electro-magnetic (EM) heating and radio-frequency (RF) induction to oil recovery via reduction of oil viscosity near well-bore by using the down-hole resistive heaters for heating near the well-bore.

Research and development of different companies have analyzed different electrical heating methods such as DC, AC, RF, EM and down-hole heater for enhanced oil recovery. Electro-Petroleum, Inc. (EPI) has presented the direct electrical simulation in its electro-enhanced oil recovery laboratory and field data. It also presented the Joule-heating electro-enhanced oil recovery. Bell and Titus (1973, 1974, and 1985), Titus *et al*. (1985), and Wittle and Bell (2005) from the research and development group of electro-enhanced oil recovery (EEOR) presented different patterns in electrical enhanced oil recovery.

Wittle *et al*. (2008) presented EEOR and compared it with other technologies. They showed that it can have beneficial chemical changes in production fluids. They also showed that EEOR had competitive cost with the steam-flooding method in shallow reservoir and in deeper fields. In this process, there is no thief zone and no depth limit. Water is not necessary in this process other than the working fluid, and it reduces the water cut.

In-Situ Thermal Desorption (ISTD) is a soil heating remediation technology that uses conductive heating process to remove, vaporize, and destroy contaminants in-situ and transport them to surface. Stegemeier and Vinegar (1995 and 2001), Baker and Bierschenk (2001), Vinegar *et al*. (1997 and 1999), Hansen *et al*. (1998) and Iben *et al*. (1966) presented different applications of ISTD for remediation organic components. Elliot *et al*. (2003) showed the application of this method to the remediation of contaminants below the water table.

2.2.2.3 Hot Chemical Flooding

Tertiary oil recovery processes such as chemical flooding and hot chemical flooding to increase oil recovery are very effective. There are many oil reserves which are oil-wet

carbonate. Therefore, injection of hot chemical flood (hot surfactant flooding, steam surfactant flooding) is effective in achieving higher oil recovery. Novosad (1982) showed that increasing temperature can change the middle phase microemulsion of the anionic surfactant to lower phase microemulsion.

Healy and Reed (1976) showed that increasing the temperature can decrease the solubilization of oil in the microemulsion phase and increase solubilization of water in the microemulsion phase at constant salinity. Novosad (1982) showed that phase changes from Type III to Type II (-) occur when temperature is increased. Healy and Reed (1976) also showed the effect of temperature on solubility ratios at two different temperatures. Puerto and Reed (1983) displayed that the optimum solubilization decreases with increasing temperature. Aoudia and Wade (1995) showed a reduction of optimum solubilization with increasing temperature. Austad and Skule (1996) corroborated the same trend. Dwarakanath and Pope (2000) showed that the optimum salinity increases with temperature and the solubilization ratios in different temperature range versus normalized salinity (salinity divided by optimum salinity) are constant. Healy and Reed (1976) and Ziegler (1988) showed the effect of temperature on interfacial tensions at constant salinity. Novosad (1982), studying the effect of temperature on optimum salinity for two anionic surfactants in Berea cores, showed that temperature can decrease the surfactant concentration in trapped oil phase, whereupon surfactant retention is decreased.

Noll (1991) demonstrated critical micelle concentration CMC measurement for three commercial sulfonate surfactants that are used to produce foam. He showed that CMC increases with temperature. Bourrel and Schechter (1988) presented some of the Flokhart data regarding the temperature dependence of CMC of dodecyl sulfate. They showed that CMC is a linear function of temperature.

2.2.3 Multi-Phase Reaction for Thermal Model

In-situ combustion is a thermal recovery process that can be used as an alternative to steam injection. In this process, the air is injected into a reservoir to oxidize a portion of the hydrocarbons to produce heat and pressure. Ali (1977), Crookston *et al*. (1979), and Youngern (1980) provided a comprehensive review of a few in-situ combustion processes. Coast (1980) presented a more general numerical model of in-situ combustion. Fassihi *et al*. (1983) showed that the combustion of crude oil follows several conservative reactions. They also presented the modeling of their observations. Abu-Khamsin *et al*. (1988) presented reaction kinetics of fuel formation during in-situ combustion. Kristensen *et al*. (2007) presented coupling kinetics and flashes in reactive, thermal, and compositional reservoir simulators. They used a kinetic cell model to develop their algorithm. The kinetic cell model was also used for modeling interaction between chemical kinetics and phase behavior. They compared a K-value-correlation-based approach with an equation of state-based approach for phase equilibrium. They showed that phase behavior may significantly affect reaction paths. Cinar *et al*. (2008) presented a technique to improve the analysis of the kinetics of crude-oil in-situ combustion. They provided a free model technique to evaluate the activation energy and the multi-step reactions. For a given sample, reaction kinetics can be calculated by using different heating rates and multiple experiments.

Chapter 3: General Purpose Adaptive Compositional Reservoir Simulator (GPAS), Four-Phase Model

3.1 INTRODUCTION

The oil industry currently requires much more detailed analyses with a greater demand for reservoir simulation with geological, physical, and chemical models in much greater detail than in the past. Reservoir simulation has become an increasingly widespread and important tool for analyzing and optimizing oil recovery projects and reducing risk in development decisions.

Numerical simulation of large petroleum reservoirs with complex recovery processes is computationally challenging because of the problem size and the detailed property calculations involved. This problem is compounded by the finer resolution needed to model such processes accurately. Traditionally, such simulations have been performed on workstations or high-end desktop computers. These computers restrict the problem size because of their addressable memory limit; moreover, simulation studies of the entire project life become time-consuming. Parallel reservoir simulation, especially on low cost, high-performance computing clusters has alleviated these issues to a certain extent. Recent publications describe the development of such approaches and emphasize the necessity and advantages of using parallel processing (Wang *et al*., 1997; Zhang *et al*., 2001; Dogru *et al*., 2002; Habiballah *et al*., 2003; Gai *et al*., 2003).

Compositional reservoir simulators that are based on EOS formulations do not handle the modeling of aqueous phase behavior and those that are designed for chemical flood modeling typically assume simplified hydrocarbon phase behavior. There are needs

for a single reservoir simulator capable of combining both approaches to benefit from the advantages of both models. The overall objective of GPAS is to develop such technology using a computational framework that also allows parallel processing. The initial stage of development involved the formulation of a fully implicit, parallel, EOS compositional simulator (Wang *et al*., 1997). The description of the framework approach used for modular code development and the application to gas injection are given in Wang *et al*. (1999).

3.2 GENERAL PURPOSE ADAPTIVE SIMULATOR (GPAS)

A fully implicit, parallel, compositional, equation-of-state simulator for large-scale reservoir simulation has been developed at the Center of Petroleum and Geosystems Engineering (CPGE). The simulator called GPAS, is developed under a framework called Integrated Parallel Accurate Reservoir Simulator (IPARS) and is constructed using a Newton-type formulation. The Peng-Robinson EOS has been used for this simulator. For solving the linear system of equations, the linear solver from Portable Extension Toolkit for Scientific Computation (PETSc) package developed in Argonne National Laboratory (ANL) is used (Balay *et al*., 1998). The output/input, table lookup, memory allocation for FORTRAN arrays, decomposition of domain, and the message passing interface between the processors in overlapping regions for updating the parameters are provided by the framework. The communication between processors for linear solver is maintained by PETSc.

3.2.1 The Description of Governing Equation

The flow in porous media for multiphase and multi-component fluids is demonstrated by the following equations:

- Partial differential equation of component-mass balance is used for component flow, employing Darcy's law for computing phase rates.
- Equilibrium equation(s) between the phases to describe component mass transfer between the phases. If two phases are in equilibrium, there is one equation; for the case of three phases in equilibrium, there are two sets of this type of equation.
- Phase saturation or pore volume constraint equation.
- Energy equation which describes the heat flow in the reservoir. This equation is ignored when the code is working with the isothermal option.

GPAS can handle both EOS-compositional and chemical flooding models, which are described later.

3.2.2 Solution Procedure

The component mass-balance equations and the energy-balance equation for the transmissibility term were discretized by using one-point upstream weighting. These equations are non-linear and are solved by Newton's method. These equations and other governing equations, equilibrium fugacity equations and pore volume equations, are linearized in terms of the independent variables. Therefore, there are different numbers of linear system of equations to solve for different options.

- There are $2n_c + 2$ equations (n_c equilibrium fugacity equations, n_c component mass balance equations, one pore volume equation and one water mass balance equation) for each gridblock or $(2n_c + 2)n_b$ equations for the reservoir in the case of isothermal, three-phase model (oil, gas phases in equilibrium) where the solubility between water and hydrocarbon is negligible.

- There are $3n_c + 2$ equations for each gridblock or $(3n_c + 2)n_b$ for reservoir in the case of isothermal four-phase model (oil, gas, second hydrocarbon liquid phases in equilibrium) where again the solubility between water and hydrocarbon is negligible. Four-phase physics can be relevant during CO_2 injection at low temperatures. The second liquid phase compositions are close to that of the gas phase but of higher density.
- There are $3n_c + 1$ equations ($2n_c$ equilibrium fugacity equations, n_c component mass-balance equations and one pore volume equation) for each gridblock or $(3n_c + 1)n_b$ equations for the reservoir in the case of isothermal; three-phase model (oil, gas, and aqueous phases in equilibrium). When water is considered a component, n_c includes water.
- There are $3n_c + 2$ equations ($2n_c$ equilibrium fugacity equations, n_c component mass-balance equations, one pore volume equation, and one energy-balance equation) for each gridblock or $(3n_c + 2)n_b$ equations for the reservoir in the case of non-isothermal three-phase model (oil, gas, and aqueous phases in equilibrium). When water is considered a component, n_c includes water.
- There are $3n_c + 3$ equations ($2n_c$ equilibrium fugacity equations, n_c component mass-balance equations, one pore volume equation, energy-balance equation and one electrical current equation) for each gridblock or $(3n_c + 3)n_b$ equations for the reservoir in the case of electrical heating model which is also a non-isothermal three-phase model (oil, gas, and aqueous phases in equilibrium). When water is considered a component, n_c includes water.

- There are $(n_c + n_A + 2)$ equations ($(n_c + n_A)$ component mass-balance equations, one pore volume equation, and one water mass-balance equation) for each gridblock or $(n_c + n_A + 2)n_b$ equations for the reservoir in case of isothermal chemical flooding. n_A is the number of aqueous components.
- There are $(n_c + n_A + 3)$ equations ($(n_c + n_A)$ component mass-balance equations, one pore volume equation, one water mass balance equation, and one energy balance equation) for each gridblock or $(n_c + n_A + 3)n_b$ equations for the reservoir in case of non-isothermal chemical flooding.
- There are $(n_c + n_A + 4)$ equations ($(n_c + n_A)$ component mass-balance equations, one pore volume equation, one water mass-balance equation, one energy-balance equation, and one electrical current equation) for each gridblock or $(n_c + n_A + 4)n_b$ equations for the reservoir in case of electrical heating model in conjunction with non-isothermal chemical flooding.

The solution procedure involves computing the values of several independent variable sets. There are several choices for independent or primary variables. In GPAS, the primary variables P, N_1, N_2, ...,N_w, LnK_1, LnK_2,..., LnK_{nc} are selected as the best choice, since they make fugacity equations more linear. The system of equations is solved, after linearization using Newton's method, by PETSc solver. After solving the system of equations for the entire reservoir, a phase stability test is used to determine the number of phases should the new condition change the number of phases at each gridblock. The flash calculation is performed to determine composition, amount, and properties of the phases when the number of phases is two or three. The phase stability and phase splitting calculations are done for the initialization as well.

3.2.3 Framework

IPARS was developed as a framework for parallel reservoir simulation research (Gropp *et al*., 1996; Parashar *et al*., 1997; Wheeler *et al*., 1999). One of several reservoir simulation models that have been developed and tested using this framework is the compositional model EOSCOMP (Wang *et al*., 1997, 1999). Extensive testing of this and other models, in IPARS, has been performed on both parallel supercomputers and clusters of PCs with excellent scaling on large numbers of processors running in parallel (Wang *et al*., 1999).

Several physical models have been developed under this framework, such as two-phase water-oil and black oil model in IMPES method and fully implicit formulations. GPAS is one of the simulators that contain different physics, which will be explained in the following sections.

Input/Output. IPARS allows each processor to read the whole input but processes only the portion that the processor is responsible for. The output is collected by the master processor (processor 0) and then sent to the output files.

Domain splitting. The reservoir domain is divided into sub-domains equal to the selected number of processors. The computation for each division or sub-domain is assigned to each processor.

Memory allocation. Memory for grid-element arrays is allocated by the framework. The format of each variable is *I, J, and K* (first three indices) which indicate the coordinate direction. For the corner-point option, there is one index instead of three indices for the node location. The fourth and fifth indices are component and phase number, if the gridblock variables contain component and phase indices. For each physical model, we can make as many grid-element arrays as necessary. Each new variable should have a name, ID

in memory and the size of dimension. The variable ID is assigned by the framework using C language when it is made and stored in a common block to be used in different subroutines.

Message passing between processors. The necessary message sending and receiving between the processors is done by message passing interface (MPI) in the framework. In each physical model, this task is done by calling the function UPDATE. It is performed when evaluating the residual of the component mass-balances and the energy-balance equations, the averaging of physical properties (i.e., saturation and pressure), and also when generating well data. It is necessary in the update call to provide the property name and ID in the memory for the properties which need to be updated for all processors in the overlapping region.

The framework handles some common calculations which are necessary by almost all physical models. These calculations include:

- The identification of the overlapping region of all processors.
- Calculation of the constant part of the transmissibility between two adjacent gridblocks.
- Using the data from table look-up of the relative permeability and the capillary pressure to take the values and their derivatives with respect to phase saturations.
- Calculation of well location and productivity indices.
- Performing simulation run tasks and computer platform which include dimensioning of the non-grid-element variables for FORTRAN arrays, dimensions of the well specification, and estimating the message size in bytes for passing between the processors.

3.3 FOUR PHASE MODEL, MATHEMATICAL MODEL

The main objective here is to present the development a four-phase three-dimensional fully implicit compositional simulator. In this model, three hydrocarbon phases are in equilibrium and water is a separate phase. The model can be used for the system in which water is considered a component; hence, in that system there are three phases (two hydrocarbon phases and an aqueous phase) in equilibrium.

GPAS can handle two phases in equilibrium with a separate aqueous phase. In the water phase, there are not any hydrocarbon components and in the oil and gas phases there is no water component. When three phases are in equilibrium, it is necessary to use the three-phase model. The following processes need to have three phases in equilibrium:

1. Miscible flooding when solvents such as CO_2 are used at low temperature.
2. Recovery of very heavy oil with steam and solvents (i.e. VAPEX).
3. Solvent stimulation of gas condensate reservoirs.
4. Asphaltene precipitation.
5. Hydrate formation.

In other words, in the GPAS thermal model, water is considered a component with three phases in equilibrium (oil, gas, and aqueous phases). Before the implementation of the thermal model, we need to implement the three-phase model for GPAS.

3.3.1 Assumptions, Features and Model Specification

Assumptions used to develop the mathematical model of the three-phase equilibrium model of GPAS are as follows:

1. Isothermal condition
2. No flow boundary conditions
3. Local equilibriums

4. Phase equilibria
5. No dispersion

Featured used for this model are as follows:

1. Full permeability tensor
2. Non-orthogonal grid option
3. Unstructured grid option

The model can handle four phases, with three hydrocarbon phases in equilibrium with the water phase, as in CO_2 injection at low temperature (Orr *et al*. 1981; Turek *et al*. 1988). If H_2O is not a component, then the aqueous phase is modeled and there are up to four phases. But, if water is a component, then the aqueous phase is not modeled and there are up to three phases.

3.3.2 Mass Component Conservation Equations

The mass component conservation equation states that the net rate of accumulation of each component in the volume V_b is equal to the component's net rate across the volume plus any source term.

$$V_b \frac{\partial(\phi N_i)}{\partial t} + V_b \nabla \cdot \sum_{j=1}^{n_p} (x_{ij}.\xi_j.\vec{v}_j) = \dot{q}_i + R_i \qquad i = 1 \ldots n_c + 1 \tag{3.3.1}$$

The term $\dot{q}_i$ represents molar rate of the point source or sink of component *i*. The subscripts of *a, v, o* represent aqueous, vapor and oleic, respectively, N_i is the number of moles of *i* component per pore volume, x_{ij} is the mole fraction of component *i* in phase *j*, ξ_j is the molar density of phase *j* and $\vec{v}_j$ is the volumetric flux of phase *j*.

Darcy's law is used to compute the flux for each phase. The generalized Darcy's law is

$$\vec{v}_j = -\vec{\vec{K}} \cdot \lambda_{rj} (\nabla P_j - \gamma_j \nabla D) \tag{3.3.2}$$

where $\vec{\vec{K}}$ is the permeability tensor defined as

$$\vec{\vec{K}} = \begin{bmatrix} k_{xx} & k_{xy} & k_{xz} \\ k_{yx} & k_{yy} & k_{yz} \\ k_{zx} & k_{zy} & k_{zz} \end{bmatrix},$$

λ_{rj} is phase relative mobility defined as $\lambda_{rj} = \dfrac{k_{rj}}{\mu_j}$, and γ_j is specific gravity of phase *j*.

The Peng-Robinson EOS is used to calculate the physical properties and conduct the phase stability test. Appendix A presents the PR-EOS parameters and the calculation of the physical properties.

The modified Corey model is used to calculate relative permeability (Corey 1954, UTCOPM) of phases which is described in Appendix B.

3.3.3 Equality of Components Fugacity

In the three-phase model, there are three phases in equilibrium and therefore there are two fugacity equations. Phase equilibrium equations are given by

$$\begin{aligned} f_i^{oil} - f_i^{gas} &= 0 \qquad i = 1 \ldots n_c \\ f_i^{oil} - f_i^{L_2} &= 0 \qquad i = 1 \ldots n_c \end{aligned} \tag{3.3.3}$$

In the above equations, L_2 is the second liquid phase and the oil phase is considered the reference phase. For the case where water is treated as a component, a similar equation should be written for water.

3.3.4 Pore Volume Constraint

The pore volume constraint, also known as the saturation constraint, is used as an independent equation and is given by

$$\sum_{j=1}^{n_p}\left[\frac{N_j}{\xi_j}\right]=1.0 \tag{3.3.4}$$

where N_j is the number of moles of phase *j* per pore volume and ξ_j is the molar density of phase *j*.

The total fluid volume is a function of overall mole or composition of each component, temperature, and pressure as defined by the EOS. There are $3n_c+2$ number of equations, with n_c+1 mass conservation equations, $2n_c$ fugacity equations, and one pore volume constraint equation, to solve in the new feature of GPAS.

3.3.5 Phase Equilibrium Calculation

To solve the governing equations at each time-step, the number of hydrocarbon phases, the phase mole ratios, and the composition of each phase are calculated. The phase equilibrium calculation algorithm used in this simulator was developed by Perschke *et al*. (1989). In order to determine the number of phases, two-phase stability analysis, stationary point location, and Gibbs free energy minimization are used in this algorithm. For flash calculation and calculation of phase mole ratios and phase compositions, accelerated successive substitution (ACSS) and Gibbs free energy minimization are applied in this algorithm. Therefore, to show equilibrium between the phases, the phase fugacity equation has been solved with other governing equations in this simulator.

The procedure of the algorithm is the sequential application of stability test and flash calculation (Michelsen, 1982; Nghiem and Li, 1984; Trangenstein, 1987). First, from the overall mole fraction, the stability test determines how many phases can exist at the prevailing condition using the two mentioned methods. If the mixture is unstable, another phase is added and flash calculation computes the phase mole ratios and compositions of each phase. Then, the stability test is applied to one of two hydrocarbon phases. If that phase is stable, there are a maximum of two phases in equilibrium; but if the phase is not stable, another phase is added and three-phase flash calculation is conducted. We then determine the equilibrium composition of phases. After initialization during simulations, the equilibrium fugacity equations will be used with other governing equations of fluid flow in porous media. In four-phase model, water phase number is considered as one and the hydrocarbon phase numbers are from phase two to phase four. Thus, in the following sections, phase numbers for phase behavior calculations are from two to four.

3.3.6 Phase Stability Analysis

The stability test for a specific overall composition $\vec{z}$ is done via a search for a trial phase with any composition $\vec{y}$ from the whole mixture, which compared to the rest of the mixture, can give a value of Gibbs free energy lower than the value for single-phase mixture with overall composition $\vec{z}$. This condition is given by

$$\Delta G = \sum_{i=1}^{n_c} y_i [\mu_i(\vec{y}) - \mu_i(\vec{z})] \tag{3.3.5}$$

where μ_i is the chemical potential of the component *i*.

If for any set of mole fractions, the value of ΔG at constant temperature and pressure is greater than zero, the phase will be stable. If a set of mole fraction can be found for which $\Delta G < 0$, the phase is unstable.

In the algorithm, there are two methods for stability test. One of them is the search for stationary points of the ΔG equation so that phase stability is determined by the analysis of those points (Michelsen, 1982). The other is minimization of ΔG with respect to trial phase composition $\vec{y}$ (Trangenstein, 1987).

3.3.6.1 Stationary Point Location Method

The following set of nonlinear equations is solved to locate the stationary points for variable $\vec{Y}$:

$$LnY_i + Ln\varphi_i(\vec{y}) - h_i = 0 \qquad i = 1...n_c \tag{3.3.6}$$

$$y_i = \frac{Y_i}{\sum_{k=1}^{n_c} Y_k} \qquad i = 1...n_c \tag{3.3.7}$$

$$h_i = Lnz_i + Ln\varphi_i(\vec{z}) \qquad i = 1...n_c \tag{3.3.8}$$

Stability of the phase is checked by the summation of variable $\vec{Y}$ in Eq. (3.3.6). If the sum is greater than one, the phase is unstable; otherwise it is stable.

Successive substitution and Newton-Raphson methods are used to solve the Eq. (3.3.6). Since the initial guess for the Newton-Raphson method should be close to the solution, successive substitution is used first to provide reasonably good initial guess.

In the successive substitution, the following equation is used to update the variable $\vec{Y}$:

$$Y_i^{k+1} = \exp[h_i - Ln\varphi_i(\vec{y})] \qquad i = 1...n_c \tag{3.3.9}$$

The residual equation for the Newton-Raphson procedure is

$$R_i = LnY_i + Ln\varphi_i(\vec{y}) - h_i \qquad i = 1...n_c \tag{3.3.10}$$

The equation updating variable $\vec{Y}$ in the last equation is given by

$$\vec{Y}^{k+1} = \vec{Y}^k - (\vec{\vec{J}})^{-1}\vec{R} \tag{3.3.11}$$

where $\vec{\vec{J}}$ is the Jacobian matrix of size n_c with following elements

$$j_{ip} = \left(\frac{\partial R_i}{\partial Y_p}\right)_{Y_{m(m\neq p)}} = \frac{1}{\sum_{q=1}^{n_c} Y_q} + \frac{\partial\left[Ln(y_i\varphi_i(\vec{y}))\right]_{Y_{m(m\neq p)}}}{\partial Y_p} \tag{3.3.12}$$

The calculation procedure is as follows:

1. Calculate h_i from Eq. (3.3.8)
2. Estimate values of $\vec{Y}$
3. Calculate $\varphi_i(\vec{y})$ by calculation of y_i from Eq. (3.3.7)
4. Check the convergence for the successive substitution method given by

$$Max\left|R_i\right| \le Tol \qquad i = 1...n_c \tag{3.3.13}$$

5. If no convergence is achieved, check the criteria for switching to Newton-Raphson method

$$Max\left|R_i\right| \le Tol_{swi} \qquad i = 1...n_c \tag{3.3.14}$$

6. If the condition in step 5 is satisfied, go to step 7; if not, update the variable $\vec{Y}$ using Eq. (3.3.9) and continue successive substitution and go to step 3
7. Calculate the partial derivative for Eq.(3.3.11), elements of Jacobian matrix with Eq. (3.3.12)
8. Update variable $\vec{Y}$ from Eq. (3.3.11)
9. Calculate the residual equation from Eq. (3.3.10) and check for convergence with Eq. (3.3.13) or (3.3.14)
10. If the condition in step 9 is not satisfied, go to step 7

When stability analysis has converged, the solution should be different from the trivial solution. It means the variable $\vec{y}$ should not be the same as $\vec{z}$ (trivial solution). The following equation has to be satisfied for a nontrivial solution

$$\left[\sum_{i=1}^{n_c}(y_i - z_i)^2\right]^{1/2} \ge \frac{Tol_{tri}}{n_c} \tag{3.3.15}$$

If the above condition did not satisfy within a specific number of iterations, another set of estimates of $\vec{Y}$ should be tried. If the condition of Eq. (3.3.15) is not satisfied for the entire initial estimate, the phase is stable. If the condition of Eq. (3.3.15) is satisfied, the second condition should be checked to determine stability. The phase is unstable if the following equation is satisfied.

$$\left(\sum_{i=1}^{n_c} y_i\right) - 1 \ge Tol_{stab} \tag{3.3.16}$$

If the condition for nontrivial solution is satisfied, but the condition for the stability test is not, another estimate for $\vec{Y}$ should be used. If the criteria for stability, Eq. (3.3.16), are not met for the entire initial estimate, the phase is considered a stable phase. To check for convergence with nontrivial solution, Eq. (3.3.16) is tested to find a $\vec{Y}$ with the condition of $\Delta G < 0$.

To test overall composition for the single-phase, two initial estimates are used. The estimate equations are as follows:

$$Y_i = z_i K_i \qquad i = 1...n_c \tag{3.3.17}$$

$$Y_i = \frac{z_i}{K_i} \qquad i = 1...n_c \tag{3.3.18}$$

The *K*-values are computed using the Wilson (1969) correlation

$$K_i = \frac{P_{ci}}{P}\exp[5.37(1+w_i)(1-\frac{T_{ci}}{T})] \qquad i = 1...n_c \tag{3.3.19}$$

For the stability test of the two-phase mixture, the composition of one of the phases is used instead of overall composition as for the single phase stability test. There are four different sets of initial estimates to use:

$$Y_i = \frac{1}{2}(x_{i2} + x_{i3}) \qquad i = 1...n_c \tag{3.3.20}$$

$$Y_1 = 0.999 \; and \; Y_i = \frac{0.001}{n_c - 1} \qquad i = 2...n_c \tag{3.3.21}$$

$$Y_{n_c} = 0.999 \; and \; Y_i = \frac{0.001}{n_c - 1} \qquad i = 1...n_c - 1 \tag{3.3.22}$$

$$Y_i = \exp h_i \qquad i = 1...n_c \tag{3.3.23}$$

To test for trivial solution, Eq. (3.3.15) should be checked for the composition of two phases.

3.3.6.2 Minimization Method

The second method for stability test is minimization of Eq. (3.3.5) with respect to trial phase mole fraction. The partial derivative of the equation with respect to mole fraction is as follows:

$$\frac{\partial(\Delta G)}{\partial y_i} = \mu_i(\vec{y}) - \mu_i(\vec{z}) - \mu_{n_c}(\vec{y}) + \mu_{n_c}(\vec{z}) \qquad for \; i = 1...n_c - 1 \tag{3.3.24}$$

For a local minimum, the above equation should be zero when $\vec{y}$ is evaluated. The second partial derivatives, elements of Hessian matrix, should be positive definite. The Hessian matrix elements are as follows:

$$H_{ip} = \frac{\partial\left(\frac{\partial(\Delta G)}{\partial y_i}\right)}{\partial y_p} = \frac{\partial \mu_i(\vec{y})}{\partial y_p} - \frac{\partial \mu_{nc}(\vec{y})}{\partial y_p} - \frac{\partial \mu_i(\vec{y})}{\partial y_{nc}} + \frac{\partial \mu_{nc}(\vec{y})}{\partial y_{nc}} \qquad for \; i, p = 1...n_c - 1 \tag{3.3.25}$$

The composition constraint equation is another equation $\sum_{i=1}^{n_c} y_i = 1$. First, the entire Hessian matrix for $y_i = z_i$ should be calculated. The first partial derivative at this point

should be zero. If the Hessian matrix is not positive definite, the mixture cannot locate the local minimum of the ΔG equation. In this case, the ΔG function is minimized with respect to $\vec{y}$ and a descent step from the point can give a value of $\Delta G < 0$, which shows the phase to be unstable. If the Hessian matrix is positive definite, a local minimum of ΔG function does exist for the mixture. The global minimization method (Goldstein and Price, 1971) can be used to search for a local minimum value lower than the obtained value for the local minimum point. The following new objective function should be minimized for this calculation:

$$G1 = \frac{\Delta G}{R} \tag{3.3.26}$$

where

$$R = \frac{1}{2}\sum_{m=1}^{n_c}\sum_{n=1}^{n_c-1}\Delta y_m \Delta y_n H_{nm}(\vec{z}) \tag{3.3.27}$$

and

$$y_i = z_i + \Delta y_i \quad for\, i = 1...n_c \tag{3.3.28}$$

A value of G1, or ΔG, less than zero shows the phase is unstable. The minimization method combines modified Newton steps with line search. The H matrix is decomposed into LDL^T by using the Cholesky decomposition algorithm (Gill and Murray, 1974). When minimizing the ΔG function, the decomposition algorithm is used to determine the direction of negative curvature as a decent direction (Perschke, 1988).

The following procedure is applied for the minimization method:

1. Calculate of h_i from Eq. (3.3.9)
2. Calculate the first partial derivative of the objective function
3. Calculate the elements of Hessian matrix
4. Decompose the Hessian matrix
5. Check for the convergence
6. If the convergence criteria is not satisfied, calculate a descent direction
7. Calculate the step length by using the line search method
8. Update the variables
9. Repeat the algorithm from step 2

There are two criteria for convergence. One is that the maximum of the gradient element should be less than a specific tolerance and the other is that the maximum of variable changes must be less than a tolerance. If one of them is satisfied, the convergence has been achieved and these conditions are checks to ascertain a positive definite Hessian matrix.

The first and second (Hessian matrix) partial derivatives of the objective function $G1$ are as follows:

$$\frac{\partial G1}{\partial y_i} = \frac{1}{R}\left[\frac{\partial(\Delta G)}{\partial y_i} - G1\frac{\partial R}{\partial y_i}\right] \quad for\ i = 1...n_c - 1 \tag{3.3.29}$$

$$\frac{\partial^2 G1}{\partial y_m \partial y_n} = \frac{1}{R}\left[\frac{\partial^2(\Delta G)}{\partial y_m \partial y_n} - \frac{\partial G1}{\partial y_m}\frac{\partial R}{\partial y_n} - G1\frac{\partial^2 R}{\partial y_m \partial y_n} - \frac{\partial R}{\partial y_m}\frac{\partial G1}{\partial y_n}\right] \quad (3.3.30)$$

$$for\ m = 1...n_c - 1\ and\ n = 1...n_c - 1$$

where m and n define the elements of the Hessian matrix,

$$\frac{\partial R}{\partial y_i} = \sum_{m=1}^{nc-1} \Delta y_m H_{mi}(\vec{z}) \quad (3.3.31)$$

$$\frac{\partial^2 R}{\partial y_n \partial y_i} = H_{im}(\vec{z}) \quad (3.3.32)$$

The overall composition ($\vec{z}$) is used as an initial value for minimization of ΔG. The initial value for the minimization of G1 is $\vec{Y}$ calculated with two initial estimate equations, Eq. (3.3.17) or (3.3.18), whichever gives the smaller value of ΔG. For two-phase mixture stability test, the procedure is same as the single-phase stability test, but one of the phase compositions is used instead of the overall composition.

If the Hessian of ΔG is positive definite at the phase composition, the new minimization function G2 is minimized by the Goldstein and Price (1971) method.

$$G2 = \frac{S_1 \Delta G}{S T} \quad (3.3.33)$$

$$S = \frac{1}{2}\sum_{n=1}^{nc-1}\sum_{m=1}^{nc-1} \Delta y_{m2} \Delta y_{n2} H_{mn}(\vec{x}_2) \quad (3.3.34)$$

$$T = \frac{1}{2}\sum_{n=1}^{nc-1}\sum_{m=1}^{nc-1} \Delta y_{m3} \Delta y_{n3} H_{mn}(\vec{x}_3) \quad (3.3.35)$$

$$S_1 = \frac{1}{2}\sum_{n=1}^{nc-1}\sum_{m=1}^{nc-1}(x_{m2} - x_{m3})(x_{n2} - x_{n3})H_{mn}(\vec{x}_2) \tag{3.3.36}$$

with

$$y_{m2} = x_{m2} + \Delta y_{m2} \qquad for\ m = 1...n_c \tag{3.3.37}$$

$$y_{m3} = x_{m3} + \Delta y_{m3} \qquad for\ m = 1...n_c \tag{3.3.38}$$

The first and second derivatives (derivatives which ultimately form the Hessian matrix elements) of the objective function G2 are as follows:

$$\frac{\partial G2}{\partial y_i} = \frac{1}{ST}\left[S_1\frac{\partial(\Delta G)}{\partial y_i} - G1\left(T\frac{\partial S}{\partial y_i} + S\frac{\partial T}{\partial y_i}\right)\right] \qquad for\ i = 1...n_c - 1 \tag{3.3.39}$$

$$\begin{aligned}\frac{\partial^2 G2}{\partial y_k \partial y_i} = \frac{1}{ST}\Bigg[&S_1\frac{\partial^2(\Delta G)}{\partial y_k \partial y_i} - \frac{\partial G2}{\partial y_k}\left(T\frac{\partial S}{\partial y_i} + S\frac{\partial T}{\partial y_i}\right)\\ &-G2\left[\frac{\partial T}{\partial y_k}\frac{\partial S}{\partial y_i} + T\frac{\partial^2 S}{\partial y_k \partial y_i} + \frac{\partial S}{\partial y_k}\frac{\partial T}{\partial y_i} + S\frac{\partial^2 T}{\partial y_k \partial y_i}\right]\\ &- \frac{\partial G2}{\partial y_i}\left(T\frac{\partial S}{\partial y_k} + S\frac{\partial T}{\partial y_k}\right)\Bigg] \qquad for\ i\ and\ k = 1...n_c - 1\end{aligned} \tag{3.3.40}$$

Where

$$\frac{\partial S}{\partial y_i} = \sum_{n=1}^{nc-1}\Delta y_{n2}H_{ni}(\vec{x}_2) \tag{3.3.41}$$

$$\frac{\partial T}{\partial y_i} = \sum_{n=1}^{nc-1} \Delta y_{n3} H_{ni}(\vec{x}_3) \tag{3.3.42}$$

$$\frac{\partial^2 S}{\partial y_k \partial y_i} = H_{ik}(\vec{x}_2) \tag{3.3.43}$$

$$\frac{\partial^2 T}{\partial y_k \partial y_i} = H_{ik}(\vec{x}_3) \tag{3.3.44}$$

3.3.7 Flash Calculation

There are two different methods for flash calculation in GPAS: accelerated successive substitution method (ACSS) (Mehra *et al*., 1983) and minimization of the Gibbs free energy using the method presented by Trangenstein (1987), which is implementation of the reduced gradient approach (Perschke, 1988).

The alternative two-phase flash calculation which uses Michelsen and Mollerup approach (2004), has been described in Appendix A.

3.3.7.1 Accelerated Successive Substitution Method (ACSS)

The following equation is a modification of the Mehra *et al*. (1983) method for accelerated successive substitution method

$$K_{ij}^{k+1} = K_{ij}^{k} \exp(-\lambda^{k+1} \frac{f_{ij}}{f_{i2}}) \tag{3.3.45}$$

where λ^{k+1} is an acceleration factor.

The *K*-values are ratios of component mole fractions in a phase with respect to those of the reference phase

$$K_{ij} = \frac{x_{ij}}{x_{i2}} \qquad for\ i = 1...n_c \ \ and \ \ j = 3...n_p \tag{3.3.46}$$

where x_{i2}, is used as the reference phase mole fractions.

The acceleration factor is calculated by the following equation:

$$\lambda^{k+1} = \frac{\lambda^k \sum_{j=3}^{n_p}\sum_{i=1}^{n_c}(r_{ij}^k)^2}{\left|\sum_{j=3}^{n_p}\sum_{i=1}^{n_c}(r_{ij}^{k-1}r_{ij}^k) - \sum_{j=3}^{n_p}\sum_{i=1}^{n_c}(r_{ij}^k)^2\right|},\ r_{ij} = Ln(\frac{f_{i2}}{f_{ij}}) \quad for\ i = 1...n_c \ \ and \ \ j = 3...n_p \tag{3.3.47}$$

The acceleration factor is within the range of $1 \le \lambda^{k+1} \le 3$ and for *k=0*, λ^1 is equal to 1. The amount of non-reference phases can be calculated from the overall composition and the estimated *K*-values. The flash equation, which can be derived by the material balance of the components and by using the K-values, is as follows:

$$g_j(L_3...L_{n_p}) = \sum_{i=1}^{n_c} \frac{z_i(K_{ij} - 1)}{1 + \sum_{\beta=3}^{n_p} L_\beta(K_{i\beta} - 1)} \tag{3.3.48}$$

The above equations can be solved to calculate phase mole ratios ($L_3...L_{n_p}$) where L_j is defined as the ratio of moles in phase *j* to total moles of mixture. The mole ratio of the reference phase is calculated as follows:

$$L_2 = 1 - \sum_{j=3}^{n_p} L_j \tag{3.3.49}$$

Phase mole fractions of the reference phase and other phases are calculated as follows:

$$x_{i2} = \frac{z_i}{1 + \sum_{\beta=3}^{n_p} L_\beta (K_{i\beta} - 1)} \qquad for\ i = 1...n_c \tag{3.3.50}$$

$$x_{ij} = \frac{z_i K_{ij}}{1 + \sum_{\beta=3}^{n_p} L_\beta (K_{i\beta} - 1)} \qquad for\ i = 1...n_c \ \ and \ \ j = 3...n_p \tag{3.3.51}$$

In solving Eq. (3.3.47), in order to obtain the phase mole ratios, the Newton's method can be used. The variable L_j is updated by the following equation:

$$L_j^{k+1} = L_j^{k+1} - (\vec{\vec{J}})^{-1} \vec{g} \tag{3.3.52}$$

where $\vec{g}$ is the vector with the element of Eq. (3.3.48).

The elements of the Jacobian matrix $\vec{\vec{J}}$ are calculated by the following equation:

$$j_{mn} = -\sum_{i=1}^{n_c} \frac{z_i (K_{im} - 1)(K_{in} - 1)}{[1 + \sum_{\beta=3}^{n_p} L_\beta (K_{i\beta} - 1)]^2} \qquad for\ m, n = 3...n_p \tag{3.3.53}$$

Convergence criteria for solving the equations are the following equations:

$$Max\left|g_j\right| \le Tol_{con.} \quad for\ j = 3...n_p \tag{3.3.54}$$

$$Max\left|L_j^{k+1} - L_j^k\right| \le Tol_{con.} \quad for\ \ j = 3...n_p \tag{3.3.55}$$

The following procedure is applied for ACSS method:

1. Estimate *K*-values
2. Calculate phase mole ratios from Eqs. (3.3.48) and (3.3.49)
3. Calculate phase composition from Eqs. (3.3.50) and (3.3.51)
4. Calculate component fugacities for each phase
5. Calculate the acceleration factor from Eq. (3.3.47)
6. Update the K-values from Eq. (3.3.45)
7. Check for the convergence of the component fugacities which is

$$Max\left|r_{ij}\right| \le Tol_{con.} \quad for\ i = 1...n_c\ and\ \ j = 3...n_p \tag{3.3.56}$$

8. If convergence has not achieved, go to step 2 for new iteration

After initialization in GPAS, step 7 checks for all governing equations at each gridblock.

3.3.7.2 Gibbs Free Energy Minimization Method

In this method, the following function is minimized:

$$\frac{G}{RT} = \sum_{j=3}^{n_p}\sum_{i=1}^{n_c} n_{ij} Lnf_{ij} + \sum_{i=1}^{n_c} n_{i2} Lnf_{i2} \tag{3.3.57}$$

Independent variables for minimization are n_{ij}, for i=1…n_c and j=2…n_p. At the local minimum, the first partial derivatives of the equation with respect to the independent

variables should be zero and also the Hessian matrix should be positive definite. The first partial derivatives of the equation are as follows:

$$\frac{\partial}{\partial n_{ij}}\left(\frac{G}{RT}\right) = Lnf_{ij} - Lnf_{i2} \quad for\ i = 1...n_c\ \ and\ \ for\ \ j = 1...n_p \tag{3.3.58}$$

The Hessian matrix for the three-phase mixture is

$$\vec{\vec{G}} = \begin{bmatrix} \frac{\partial Ln\vec{f}_2}{\partial \vec{n}_2} + \frac{\partial Ln\vec{f}_3}{\partial \vec{n}_3} & \frac{\partial Ln\vec{f}_2}{\partial \vec{n}_2} \\ \frac{\partial Ln\vec{f}_2}{\partial \vec{n}_2} & \frac{\partial Ln\vec{f}_2}{\partial \vec{n}_2} + \frac{\partial Ln\vec{f}_4}{\partial \vec{n}_4} \end{bmatrix} \tag{3.3.59}$$

The elements of the matrix, for example $\frac{\partial Ln\vec{f}_2}{\partial \vec{n}_2}$, are determined by $\frac{\partial Lnf_{i2}}{\partial n_{k2}}$. The procedure for minimization of Eq. (3.3.57) is the same as the procedure for minimization in stability test calculation.

1. Estimate values for independent mole numbers, n_{ij}
2. Calculate n_{i2} for i=1…n_c from the equation

$$n_{i2} = N_i - \sum_{j=3}^{n_p} n_{ij} \quad for\ i = 1...n_c \tag{3.3.60}$$

3. Evaluate first partial derivatives, Eq. (3.3.58)
4. Calculate elements of the Hessian matrix
5. Decompose the Hessian matrix by using modified Cholesky decomposition algorithm

6. Check for convergence by satisfying one of the following criteria when the Hessian matrix is positive definite

$$Max\left|Lnf_{ij} - Lnf_{i2}\right| \le Tol._{con}.\ \ for\ i = 1...n_c\ \ and\ \ j = 3...n_p \tag{3.3.61}$$

$$Max\left|\frac{\Delta n_{ij}^{k}}{n_{ij}^{k}}\right| \le Tol._{con}.\ \ for\ i = 1...n_c\ \ and\ \ j = 3...n_p \tag{3.3.62}$$

7. Calculate the descent direction in case of no convergence
8. Calculate the step length from the line search algorithm
9. Update relevant variables and phase mole numbers
10. For the next iteration, go to step 2

The minimization method needs an initial estimate very close to the solution. First ACSS is used; then the procedure is switched to the minimization method. The criteria to switch is

$$Max\left|Lnf_{ij} - Lnf_{i2}\right| \le Tol._{swi}.\ \ for\ i = 1...n_c\ \ and\ \ j = 3...n_p \tag{3.3.63}$$

3.3.8 Primary Variables and Solution Procedure

The component-mass balance equation is discretized using the one-point upstream weighting scheme for the transmissibility terms. The discretized component mass-balance equation with the volume constraint equation and the fugacity equations were linearized in terms of independent or primary variables. There are different sets of primary variables found in the literature. The selected primary variables in GPAS are as follows (in order to make the fugacity equations much more linear, as stated earlier):

The two-phase model GPAS primary variables are

$$LnK_1,\ LnK_2, LnK_3\ \ldots\ LnK_{nc}, N_1, N_2, N_3 \ldots N_{nc}, P_w, N_w$$

In the new model, because of the additional phase in equilibrium, nc number of primary variables are added upon which the new primary variables are

$$LnK_{1,1},\ LnK_{1,2}, LnK_{1,3}\ \ldots\ LnK_{1,nc}, LnK_{2,1},\ LnK_{2,2}, LnK_{2,3}\ \ldots\ LnK_{2,nc}, N_1, N_2, N_3 \ldots N_{nc}, P_w, N_w$$

of which $LnK_{1,i}$ and $LnK_{2,i}$ are the first and the second set of LnK for component *i,* respectively. The $K_{1,i}$ is the composition ratio of component *i* in gas phase with respect to oil phase and $K_{2,i}$ is the composition ratio of component *i* in the second liquid phase with respect to the oil phase.

GPAS is a fully implicit simulator. Therefore, to solve the system of equations, it is necessary to have the residual function from the previous time-step and thus construct the Jacobian matrix.

$$\delta \mathrm{P} = \mathrm{P}^{n+1} - \mathrm{P}^{n} = -\vec{\vec{J}}^{-1} R^{n} \tag{3.3.64}$$

P is the primary variable and the R is the residual of the equations. Both the residual of the governing equations and the construction of the Jacobian matrix are presented below.

$$\begin{pmatrix} J_{1,1} & J_{1,2} & \cdots & J_{1,n_b} \\ J_{2,1} & J_{2,2} & \cdots & J_{2,n_b} \\ \vdots & & & \vdots \\ J_{n_b,1} & J_{n_b,2} & \cdots & J_{n_b,n_b} \end{pmatrix} \begin{pmatrix} \Delta\vec{x}_1 \\ \Delta\vec{x}_2 \\ \vdots \\ \Delta\vec{x}_{n_b} \end{pmatrix} = - \begin{pmatrix} \vec{R}_1 \\ \vec{R}_2 \\ \vdots \\ \vec{R}_{n_b} \end{pmatrix}$$

$$\mathrm{J}_{I,J} = \begin{bmatrix} \frac{\partial \mathrm{R}_{\mathrm{F1},1}|_{\mathrm{I}}}{\partial \mathrm{LnK}_{1,1}|_{\mathrm{J}}} & \cdots & \frac{\partial \mathrm{R}_{\mathrm{F1},1}|_{\mathrm{I}}}{\partial \mathrm{LnK}_{1,\mathrm{nc}}|_{\mathrm{J}}} & \frac{\partial \mathrm{R}_{\mathrm{F1},1}|_{\mathrm{I}}}{\partial \mathrm{LnK}_{2,1}|_{\mathrm{J}}} & \cdots & \frac{\partial \mathrm{R}_{\mathrm{F1},1}|_{\mathrm{I}}}{\partial \mathrm{LnK}_{2,\mathrm{nc}}|_{\mathrm{J}}} & \frac{\partial \mathrm{R}_{\mathrm{F1},1}|_{\mathrm{I}}}{\partial \mathrm{N}_{1}|_{\mathrm{J}}} & \cdots & \frac{\partial \mathrm{R}_{\mathrm{F1},1}|_{\mathrm{I}}}{\partial \mathrm{N}_{\mathrm{nc+1}}|_{\mathrm{J}}} & \frac{\partial \mathrm{R}_{\mathrm{F1},1}|_{\mathrm{I}}}{\partial \mathrm{P}|_{\mathrm{J}}} \\ \vdots & \vdots & \vdots & \vdots & \vdots & \vdots & \vdots & \vdots & \vdots & \vdots \\ \frac{\partial \mathrm{R}_{\mathrm{F1,nc}}|_{\mathrm{I}}}{\partial \mathrm{LnK}_{1,1}|_{\mathrm{J}}} & \cdots & \frac{\partial \mathrm{R}_{\mathrm{F1,nc}}|_{\mathrm{I}}}{\partial \mathrm{LnK}_{1,\mathrm{nc}}|_{\mathrm{J}}} & \frac{\partial \mathrm{R}_{\mathrm{F1,nc}}|_{\mathrm{I}}}{\partial \mathrm{LnK}_{2,1}|_{\mathrm{J}}} & \cdots & \frac{\partial \mathrm{R}_{\mathrm{F1,nc}}|_{\mathrm{I}}}{\partial \mathrm{LnK}_{2,\mathrm{nc}}|_{\mathrm{J}}} & \frac{\partial \mathrm{R}_{\mathrm{F1,nc+1}}|_{\mathrm{I}}}{\partial \mathrm{N}_{1}|_{\mathrm{J}}} & \cdots & \frac{\partial \mathrm{R}_{\mathrm{F1,nc+1}}|_{\mathrm{I}}}{\partial \mathrm{N}_{\mathrm{nc+1}}|_{\mathrm{J}}} & \frac{\partial \mathrm{R}_{\mathrm{F1,nc+1}}|_{\mathrm{I}}}{\partial \mathrm{P}|_{\mathrm{J}}} \\ \frac{\partial \mathrm{R}_{\mathrm{F2},1}|_{\mathrm{I}}}{\partial \mathrm{LnK}_{1,1}|_{\mathrm{J}}} & \cdots & \frac{\partial \mathrm{R}_{\mathrm{F2},1}|_{\mathrm{I}}}{\partial \mathrm{LnK}_{1,\mathrm{nc}}|_{\mathrm{J}}} & \frac{\partial \mathrm{R}_{\mathrm{F2},1}|_{\mathrm{I}}}{\partial \mathrm{LnK}_{2,1}|_{\mathrm{J}}} & \cdots & \frac{\partial \mathrm{R}_{\mathrm{F2},1}|_{\mathrm{I}}}{\partial \mathrm{LnK}_{2,\mathrm{nc}}|_{\mathrm{J}}} & \frac{\partial \mathrm{R}_{\mathrm{F2},1}|_{\mathrm{I}}}{\partial \mathrm{N}_{1}|_{\mathrm{J}}} & \cdots & \frac{\partial \mathrm{R}_{\mathrm{F2},1}|_{\mathrm{I}}}{\partial \mathrm{N}_{\mathrm{nc+1}}|_{\mathrm{J}}} & \frac{\partial \mathrm{R}_{\mathrm{F2},1}|_{\mathrm{I}}}{\partial \mathrm{P}|_{\mathrm{J}}} \\ \vdots & \vdots & \vdots & \vdots & \vdots & \vdots & \vdots & \vdots & \vdots & \vdots \\ \frac{\partial \mathrm{R}_{\mathrm{F2,nc}}|_{\mathrm{I}}}{\partial \mathrm{LnK}_{1,1}|_{\mathrm{J}}} & \cdots & \frac{\partial \mathrm{R}_{\mathrm{F2,nc}}|_{\mathrm{I}}}{\partial \mathrm{LnK}_{1,\mathrm{nc}}|_{\mathrm{J}}} & \frac{\partial \mathrm{R}_{\mathrm{F2,nc}}|_{\mathrm{I}}}{\partial \mathrm{LnK}_{2,1}|_{\mathrm{J}}} & \cdots & \frac{\partial \mathrm{R}_{\mathrm{F2,nc}}|_{\mathrm{I}}}{\partial \mathrm{LnK}_{2,\mathrm{nc}}|_{\mathrm{J}}} & \frac{\partial \mathrm{R}_{\mathrm{F2,nc+1}}|_{\mathrm{I}}}{\partial \mathrm{N}_{1}|_{\mathrm{J}}} & \cdots & \frac{\partial \mathrm{R}_{\mathrm{F2,nc+1}}|_{\mathrm{I}}}{\partial \mathrm{N}_{\mathrm{nc+1}}|_{\mathrm{J}}} & \frac{\partial \mathrm{R}_{\mathrm{F2,nc+1}}|_{\mathrm{I}}}{\partial \mathrm{P}|_{\mathrm{J}}} \\ \frac{\partial \mathrm{R}_{\mathrm{v}}|_{\mathrm{I}}}{\partial \mathrm{LnK}_{1,\mathrm{nc}}|_{\mathrm{J}}} & \cdots & \frac{\partial \mathrm{R}_{\mathrm{v}}|_{\mathrm{I}}}{\partial \mathrm{LnK}_{1,\mathrm{nc}}|_{\mathrm{J}}} & \frac{\partial \mathrm{R}_{\mathrm{v}}|_{\mathrm{I}}}{\partial \mathrm{LnK}_{2,1}|_{\mathrm{J}}} & \cdots & \frac{\partial \mathrm{R}_{\mathrm{v}}|_{\mathrm{I}}}{\partial \mathrm{LnK}_{2,\mathrm{nc}}|_{\mathrm{J}}} & \frac{\partial \mathrm{R}_{\mathrm{v}}|_{\mathrm{I}}}{\partial \mathrm{N}_{1}|_{\mathrm{J}}} & \cdots & \frac{\partial \mathrm{R}_{\mathrm{v}}|_{\mathrm{I}}}{\partial \mathrm{N}_{\mathrm{nc+1}}|_{\mathrm{J}}} & \frac{\partial \mathrm{R}_{\mathrm{v}}|_{\mathrm{I}}}{\partial \mathrm{P}|_{\mathrm{J}}} \\ \frac{\partial \mathrm{R}_{\mathrm{m},1}|_{\mathrm{I}}}{\partial \mathrm{LnK}_{1,1}|_{\mathrm{J}}} & \cdots & \frac{\partial \mathrm{R}_{\mathrm{m},1}|_{\mathrm{I}}}{\partial \mathrm{LnK}_{1,\mathrm{nc}}|_{\mathrm{J}}} & \frac{\partial \mathrm{R}_{\mathrm{m},1}|_{\mathrm{I}}}{\partial \mathrm{LnK}_{2,1}|_{\mathrm{J}}} & \cdots & \frac{\partial \mathrm{R}_{\mathrm{m},1}|_{\mathrm{I}}}{\partial \mathrm{LnK}_{2,\mathrm{nc}}|_{\mathrm{J}}} & \frac{\partial \mathrm{R}_{\mathrm{m},1}|_{\mathrm{I}}}{\partial \mathrm{N}_{1}|_{\mathrm{J}}} & \cdots & \frac{\partial \mathrm{R}_{\mathrm{m},1}|_{\mathrm{I}}}{\partial \mathrm{N}_{\mathrm{nc+1}}|_{\mathrm{J}}} & \frac{\partial \mathrm{R}_{\mathrm{m},1}|_{\mathrm{I}}}{\partial \mathrm{P}|_{\mathrm{J}}} \\ \vdots & \vdots & \vdots & \vdots & \vdots & \vdots & \vdots & \vdots & \vdots & \vdots \\ \frac{\partial \mathrm{R}_{\mathrm{m,nc+1}}|_{\mathrm{I}}}{\partial \mathrm{LnK}_{1,1}|_{\mathrm{J}}} & \cdots & \frac{\partial \mathrm{R}_{\mathrm{m,nc+1}}|_{\mathrm{I}}}{\partial \mathrm{LnK}_{1,\mathrm{nc}}|_{\mathrm{J}}} & \frac{\partial \mathrm{R}_{\mathrm{m,nc+1}}|_{\mathrm{I}}}{\partial \mathrm{LnK}_{2,1}|_{\mathrm{J}}} & \cdots & \frac{\partial \mathrm{R}_{\mathrm{m,nc}}|_{\mathrm{I}}}{\partial \mathrm{LnK}_{2,\mathrm{nc}}|_{\mathrm{J}}} & \frac{\partial \mathrm{R}_{\mathrm{m,nc+1}}|_{\mathrm{I}}}{\partial \mathrm{N}_{1}|_{\mathrm{J}}} & \cdots & \frac{\partial \mathrm{R}_{\mathrm{m,nc+1}}|_{\mathrm{I}}}{\partial \mathrm{N}_{\mathrm{nc+1}}|_{\mathrm{J}}} & \frac{\partial \mathrm{R}_{\mathrm{m,nc+1}}|_{\mathrm{I}}}{\partial \mathrm{P}|_{\mathrm{J}}} \end{bmatrix}$$

The flowchart for this model is presented in Figure 3.1.

3.3.8.1 Residuals of the Governing Equations

In this section, the residuals of the equations are described.

3.3.8.1.1 Residual of Equilibrium Equations

Two equilibrium equations are needed to show a maximum of three phases in equilibrium at each gridblock. In the previous version of GPAS, the maximum number of phases in equilibrium was two. In the initialization step, after the stability test, the batch flash calculation is performed to calculate mole ratios of the phases, the composition of the phases, the phase saturation and the initial amount of the phases in place. Next, the equilibrium equations are solved along with other governing equations. Equilibrium equations for each component α, considering the liquid phase (oil phase or second liquid phase) as the base phase are as follows:

$$R_{F_{1,\alpha,i,j,k}} = f_{g,\alpha,i,j,k} - f_{o,\alpha,i,j,k} = 0 = Lny_{\alpha,i,j,k}\phi_{g,\alpha,i,j,k} - Lnx_{\alpha,i,j,k}\phi_{o,\alpha,i,j,k} = 0 \tag{3.3.65}$$

$$R_{F_{2,,\alpha,i,j,k}} = f_{L2,,\alpha,i,j,k} - f_{o,\alpha,i,j,k} = 0 = Lnx_{2,\alpha,i,j,k}\phi_{L2,\alpha,i,j,k} - Lnx_{\alpha,i,j,k}\phi_{o,\alpha,i,j,k} = 0 \tag{3.3.66}$$

$$LnK_{1,\alpha,i,j,k} + Ln\phi_{g,\alpha,i,j,k} - Ln\phi_{o,\alpha,i,j,k} = 0 \tag{3.3.67}$$

$$LnK_{2,\alpha,i,j,k} + Ln\phi_{L2,\alpha,i,j,k} - Ln\phi_{o,\alpha,i,j,k} = 0 \tag{3.3.68}$$

3.3.8.1.2 Residual of Volume Constraint Equation

The volume constraint equation for each gridblock is as follows:

$$R_{V,i,j,k} = \sum_{\beta=1}^{n_p} \tilde{V}_{\beta,i,j,k} \sum_{\alpha=1}^{n_c+1} N_{\beta,\alpha,i,j,k} - 1 = 0 \tag{3.3.69}$$

where

$$\sum_{\beta=1}^{n_p} N_{\beta,i,j,k} = N_{T,i,j,k} = N_{L1,i,j,k} + N_{g,i,j,k} + N_{L2,i,j,k} \tag{3.3.70}$$

with

$$N_{L1,i,j,k} = \sum_{\alpha=1}^{n_c} n_{L1,\alpha,i,j,k} \tag{3.3.71}$$

$$N_{g,i,j,k} = \sum_{\alpha=1}^{n_c} n_{g,\alpha,i,j,k} \tag{3.3.72}$$

$$N_{L2,i,j,k} = \sum_{\alpha=1}^{n_c} n_{L2,\alpha,i,j,k} \tag{3.3.73}$$

3.3.8.1.3 Residual of Component Mass Conservation Equation

For each gridblock, flow can be across of the faces of that gridblock. For three-dimensional problems, the conservation of mass for each component can be written as follows:

$$\begin{aligned}
&R_{M_\alpha} = M_{\alpha,acc} - (M_{\alpha,in} - M_{\alpha,out}) + (q_{\alpha,win} - q_{\alpha,wout}) \\
&= \frac{V_{bi,j,k}\phi_{i,j,k}}{\Delta t}\left(N^{n+1}_{\alpha_{i,j,k}} - N^{n}_{\alpha_{i,j,k}}\right) + \\
&\left\{\left(F_{\alpha_{i+\frac{1}{2},j,k}} - F_{\alpha_{i-\frac{1}{2},j,k}}\right)^{n+1} + \left(F_{\alpha_{i,j+\frac{1}{2},k}} - F_{\alpha_{i,j-\frac{1}{2},k}}\right)^{n+1}\right. \\
&\left. + \left(F_{\alpha_{i,j,k+\frac{1}{2}}} - F_{\alpha_{i,j,k-\frac{1}{2}}}\right)^{n+1}\right\} - q_{\alpha_{i,j,k}} \\
&= Macc_{\alpha,i,j,k} + Mflux_{\alpha,i,j,k} - Msource_{\alpha,i,j,k} = 0
\end{aligned} \tag{3.3.74}$$

$$N_{\alpha i,j,k} = \sum_{\beta=1}^{n_p} \xi_{\beta i,j,k} S_{\beta i,j,k} x_{\alpha\beta i,j,k} \tag{3.3.75}$$

$Macc_{\alpha,i,j,k}$, $Mflux_{\alpha,i,j,k}$ and $Msource_{\alpha,i,j,k}$ are accumulation, flux, and source terms for a grid cell, respectively. In the notation, *i* is used for grid index, α for component index, and β for phase index.

$$F_{\alpha,i+1/2} = -\sum_{\beta=1}^{n_P} T_{\alpha,\beta,i+1/2} V_{\beta,i+1/2} \tag{3.3.76}$$

$$F_{\alpha,i-1/2} = -\sum_{\beta=1}^{n_P} T_{\alpha,\beta,i-1/2} V_{\beta,i-1/2} \tag{3.3.77}$$

where

$$V_{\beta,i+1/2} = -\tilde{K}_{i+1}\left(\Phi_{\beta,i+1} - \Phi_{\beta,i}\right) \tag{3.3.78}$$

$$V_{\beta,i-1/2} = -\tilde{K}_{i}\left(\Phi_{\beta,i} - \Phi_{\beta,i-1}\right) \tag{3.3.79}$$

In Eqs. (3.3.78) and (3.3.79), $\tilde{K}$ is the harmonic mean of permeability on a Cartesian grid with

$$\tilde{K}_{i+1} = \Delta y_i \Delta z_i 2K_i K_{i+1} / (\Delta x_{i+1} K_{i+1} + \Delta x_i K_i) \tag{3.3.80}$$

$$\tilde{K}_{i} = \Delta y_i \Delta z_i 2K_i K_{i-1} / (\Delta x_{i-1} K_{i-1} + \Delta x_i K_i) \tag{3.3.81}$$

Φ_β is the potential of phase β given by

$$\Phi_{\beta,i} = P_i + Pc_i - \gamma_{\beta,i} D_{x,i} \tag{3.3.82}$$

For one-point upstream weighting, we have

$$F_{\alpha,i+1/2} = \sum_{\beta=1}^{n_P} T_{\alpha,\beta,i+1} K_{i+1} (\Phi_{\beta,i+1} - \Phi_{\beta,i}) \quad if \quad \Phi_{\beta,i+1} > \Phi_{\beta,i} \tag{3.3.83}$$

$$F_{\alpha,i+1/2} = \sum_{\beta=1}^{n_P} T_{\alpha,\beta,i} K_{i+1} (\Phi_{\beta,i} - \Phi_{\beta,i+1}) \qquad if \quad \Phi_{\beta,i+1} < \Phi_{\beta,i} \tag{3.3.84}$$

$$F_{\alpha,i-1/2} = \sum_{\beta=1}^{n_P} T_{\alpha,\beta,i-1} K_i (\Phi_{\beta,i-1} - \Phi_{\beta,i}) \qquad if \quad \Phi_{\beta,i-1} > \Phi_{\beta,i} \tag{3.3.85}$$

$$F_{\alpha,i-1/2} = \sum_{\beta=1}^{n_P} T_{\alpha,\beta,i} K_i (\Phi_{\beta,i} - \Phi_{\beta,i-1}) \qquad if \quad \Phi_{\beta,i-1} < \Phi_{\beta,i} \tag{3.3.86}$$

There are four scenarios for the convection term

1. $\Phi_{\beta,i+1} < \Phi_{\beta,i} \quad and \quad \Phi_{\beta,i} < \Phi_{\beta,i-1}$ (3.3.87)

$$F_{\alpha,i+1/2} - F_{\alpha,i-1/2} = \sum_{\beta=1}^{n_P} T_{\alpha,\beta,i} K_{i+1} (\Phi_{\beta,i} - \Phi_{\beta,i+1}) - \sum_{\beta=1}^{n_P} T_{\alpha,\beta,i-1} K_i (\Phi_{\beta,i-1} - \Phi_{\beta,i})$$

2. $\Phi_{\beta,i+1} > \Phi_{\beta,i} \quad and \quad \Phi_{\beta,i} > \Phi_{\beta,i-1}$ (3.3.88)

$$F_{\alpha,i+1/2} - F_{\alpha,i-1/2} = -\sum_{\beta=1}^{n_P} T_{\alpha,\beta,i+1} K_{i+1} (\Phi_{\beta,i+1} - \Phi_{\beta,i}) + \sum_{\beta=1}^{n_P} T_{\alpha,\beta,i} K_i (\Phi_{\beta,i} - \Phi_{\beta,i-1})$$

3. $\Phi_{\beta,i+1} > \Phi_{\beta,i} \quad and \quad \Phi_{\beta,i} < \Phi_{\beta,i-1}$ (3.3.89)

$$F_{\alpha,i+1/2} - F_{\alpha,i-1/2} = -\sum_{\beta=1}^{n_P} T_{\alpha,\beta,i+1} K_{i+1} (\Phi_{\beta,i+1} - \Phi_{\beta,i}) - \sum_{\beta=1}^{n_P} T_{\alpha,\beta,i-1} K_i (\Phi_{\beta,i-1} - \Phi_{\beta,i})$$

4. $\Phi_{\beta,i+1} < \Phi_{\beta,i} \quad and \quad \Phi_{\beta,i} > \Phi_{\beta,i-1}$ (3.3.90)

$$F_{\alpha,i+1/2} - F_{\alpha,i-1/2} = \sum_{\beta=1}^{n_P} T_{\alpha,\beta,i} K_{i+1} (\Phi_{\beta,i} - \Phi_{\beta,i+1}) + \sum_{\beta=1}^{n_P} T_{\alpha,\beta,i} K_i (\Phi_{\beta,i} - \Phi_{\beta,i-1})$$

The equation of mass conservation of water is the same as of other components, but water can be considered both a separate phase and also a component, the same as other components.

3.3.8.2 Jacobian Matrix for Governing Equations

General equation of the elements of Jacobian matrix is described in this section.

3.3.8.2.1 Derivatives of Equilibrium Equations with Respect to Primary Variables

The derivatives of the residual of the equilibrium equations with respect to primary variable P in general are as follows:

$$\frac{\partial R_{F_{1,\alpha,i,j,k}}}{\partial \mathrm{P}_{i,j,k}} = \frac{\partial\, LnK_{1,\alpha,i,j,k}}{\partial \mathrm{P}_{i,j,k}} + \frac{\partial\, Ln\phi_{g,\alpha,i,j,k}}{\partial \mathrm{P}_{i,j,k}} - \frac{\partial Ln\phi_{o,\alpha,i,j,k}}{\partial \mathrm{P}_{i,j,k}} \tag{3.3.91}$$

$$\frac{R_{F_{2,,\alpha,i,j,k}}}{\partial \mathrm{P}_{i,j,k}} = \frac{\partial LnK_{2,\alpha,i,j,k}}{\partial \mathrm{P}_{i,j,k}} + \frac{\partial Ln\phi_{L2,\alpha,i,j,k}}{\partial \mathrm{P}_{i,j,k}} - \frac{\partial Ln\phi_{o,\alpha,i,j,k}}{\partial \mathrm{P}_{i,j,k}} \tag{3.3.92}$$

Entire derivatives with respect to each variable and the related derivatives with respect to phase behavior calculations are described in Appendix B.

3.3.8.2.2 Derivatives of Volume Constraint Equation with Respect to Primary Variables

The derivatives of the residual of the pore volume equation with respect to the primary variable P, in general are as follows. Eq. (3.3.69) can be written in the following form:

$$R_{V,i,j,k} = (\tilde{V}_w N_w)_{i,j,k} + (\tilde{V}_{L1} N_{L1})_{i,j,k} + (\tilde{V}_g N_g)_{i,j,k} + (\tilde{V}_{L2} N_{L2})_{i,j,k} - 1 = 0 \tag{3.3.93}$$

By taking the derivative of the above equation, we obtain the following expression:

$$\frac{\partial R_{v,i,j,k}}{\partial \mathrm{P}_{i,j,k}} = \frac{\partial \left(\tilde{V}_w N_w\right)_{i,j,k}}{\partial \mathrm{P}_{i,j,k}} + \frac{\partial \left(\tilde{V}_{L1} N_{L1}\right)_{i,j,k}}{\partial \mathrm{P}_{i,j,k}} + \frac{\partial \left(\tilde{V}_g N_g\right)_{i,j,k}}{\partial \mathrm{P}_{i,j,k}} + \frac{\partial \left(\tilde{V}_{L2} N_{L2}\right)_{i,j,k}}{\partial \mathrm{P}_{i,j,k}} \tag{3.3.94}$$

Appendix C presents all the derivatives of the pore volume equation.

3.3.8.2.3 Derivatives of Components Material Balance Equations with Respect to Primary Variables

The derivatives are for on-diagonal and off-diagonal terms. There are three sets of equations for derivatives, one for on-diagonal and two for off-diagonal in each direction. Therefore, the derivatives of the residual for the material balance equation for component α_1 with respect to primary variable P, for the *k*-direction are as follows:

For the diagonal terms:

$$\frac{\partial R_{M,\alpha_1,K}}{\partial \mathrm{P}_{\mathrm{K}}} = -\frac{\partial M_{accum,\alpha_1,\mathrm{K}}}{\partial \mathrm{P}_{\mathrm{K}}} + \frac{\partial M_{conv,\alpha_1,\mathrm{K}}}{\partial \mathrm{P}_{\mathrm{K}}} + \frac{\partial M_{source,\alpha_1,\mathrm{K}}}{\partial \mathrm{P}_{\mathrm{K}}} \tag{3.3.95}$$

and for the off-diagonal terms:

$$\frac{\partial R_{M,\alpha_1,\mathrm{K}}}{\partial \mathrm{P}_{\mathrm{K}\pm1}} = -\frac{\partial M_{accum,\alpha_1,\mathrm{K}}}{\partial \mathrm{P}_{\mathrm{K}\pm1}} + \frac{\partial M_{conv,\alpha_1,\mathrm{K}}}{\partial \mathrm{P}_{\mathrm{K}\pm1}} + \frac{\partial M_{source,\alpha_1,\mathrm{K}}}{\partial \mathrm{P}_{\mathrm{K}\pm1}} \tag{3.3.96}$$

The derivative expressions in their entirety for the above equations are given in Appendix D. The reaction term and related derivatives are presented in Appendix E.

3.4 CASE STUDIES AND EXAMPLES OF FOUR PHASE MODEL

In this section, the examples of two- and three-phase flash calculation and three- and four-phase models are presented.

Case 1: Validation of Two- and Three-Phase Flash Calculation Routine. To validate the flash calculation routine, the results of two- and three-phase flash calculations were compared to the flash calculation routine of CMG-WinProp. Two different mixtures were used for this comparison. The pressure and temperature for two-phase flash calculation are 500 psia and 140°F and the three-phase flash calculation was performed at a pressure of 200 psia and a temperature of 200°F. Tables 3.1 and 3.2 show the data and the results for the two-phase flash calculation, respectively. The input data for three-phase flash calculation is given in Table 3.3 and the results of this example are presented in Table 3.4. The agreement between the phase behavior calculation of GPAS and WinProp is excellent.

Case 2: Comparison of Three- and Four-Phase Model with Six Component Mixture. This case was designed to test the four-phase model with the original three-phase model of GPAS. The input data are given in Table 3.5 and the component properties and their initial compositions are shown in Table 3.6. The reservoir in this example is a 3D quarter of five spot with the size of 560×560×100 ft^3. The initial pressure and temperature of the reservoir are 1400 psia and 160˚F and the reservoir fluid mixture consists of six components. Initial water saturation is 0.17, porosity is 0.35, and permeability is 10 md. The relative permeability data are given in Table 3.7. The number of gridblocks is 7×7×3. The process is gas injection with an injection rate of 1000 Mscf/day and the production well condition is 1300 psia. The simulation time is 365 days. Oil and gas rates are shown in Figures 3.2 and 3.3. These results show that there is good agreement between three-phase and two-phase

models. In this case, the number of hydrocarbon phases was two and the new implementation gives the same result as the previous model, which was a three-phase model with two-phase flash calculation.

Case 3: Comparison of Four-Phase Model with Twelve Component Mixture. The two-dimensional reservoir in x-z cross-section was used to simulate the CO_2/NGL (natural gas liquid) with the two- and three-phase models. The reservoir size is 1000×50×55 ft^3 and the reservoir fluid is a twelve-component mixture. The initial pressure and temperature of the reservoir are 1750 psia and 86˚F. Initial water saturation is 0.4, porosity is 0.28, horizontal permeability is 180 md, and vertical permeability is 10 percent of horizontal permeability. The reservoir is divided into 25×1×11 gridblocks. The well condition for the injection well is 1800 psia pressure and production bottomhole pressure is 800 psia. Table 3.8 gives the reservoir input data. Table 3.9 presents component properties, initial reservoir and injected fluid compositions. The relative permeability data for this case are shown in Table 3.10. As discussed in Chapter 3, in CO_2 injection process, when temperature is low, three hydrocarbon phases may exist in the reservoir along with water. Figures 3.4 and 3.5 show the oil and gas rates. Results show that the four-phase model predicts higher oil and gas rates compared to the three-phase model. In this process, four phases exist in the reservoir; the three-phase model with two-phase flash calculation can not obviously address three hydrocarbon phases in equilibrium. In the four-phase model, the stability test shows the fluid to be unstable; three-phase flash calculation is used to determine the phase behavior of three hydrocarbon phases. Therefore, results for these models are different; it is expected that the four-phase model is more accurate because of its focus on three hydrocarbon regions in the reservoir.

Table 3.1 Component mole fractions for validation of two-phase flash calculation (Case1)

Component Name	Overall Mole%	Phase 1, Mole%		Phase 2, Mole%	
		GPAS	WinProp	GPAS	WinProp
C6	10.0	16.636	16.636	0.0	0.0
C10	20.0	33.272	33.273	0.0	0.0
C15	30.0	49.908	49.909	0.0	0.0
H_2O	40.0	0.184	0.1809	100.0	100.0

Table 3.2 Phase mole ratios and enthalpies for validation of two-phase flash calculation

Phase	Mole %		$\Delta H_{EOS(BTU/Lbmol)} \times 10^{-3}$	
	GPAS	WinProp	GPAS	WinProp
Phase 1	60.111	60.1087	-23.045	-23.049
Phase 2	39.889	39.8913	-18.934	-18.929

Table 3.3 Component mole fractions for validation of three-phase flash calculation (Case1)

Component name	Overall Mole%	Phase 1, Mole%		Phase 2, Mole%		Phase 3, Mole%	
		GPAS	WinProp	GPAS	WinProp	GPAS	WinProp
C1	10.0	3.984	3.976	91.174	91.1904	0.00019	0.00019
C6	10.0	13.374	13.375	2.8763	2.8793	0.0	0.0
C10	20.0	27.331	27.333	0.2779	0.27700	0.0	0.0
C15	40.0	54.718	54.724	0.0119	0.0119	0.0	0.0
H_2O	20.0	0.593	0.592	5.6599	5.6414	99.99981	99.99981

Table 3.4 Phase mole ratios and enthalpies for validation of three-phase flash calculation (Case1)

Phase	Mole %		$\Delta H_{EOS(BTU/Lbmol)} \times 10^{-3}$	
	GPAS	WinProp	GPAS	WinProp
Phase 1	73.0996	73.0915	-22.205	-22.149
Phase 2	7.7738	7.7796	-97.343×10^{-3}	-97.18×10^{-3}
Phase 3	19.1266	19.1289	-18.263	-18.261

Table 3.5 Summary of input data for comparison of three- and four-phase model with six component mixture (Case2)

Parameter	Value
Number of gridblocks	7×7×3
Gridblock size	80×80×20, 30, 50 ft^3
Initial temperature	160 °F
Initial pressure	1400 psia
Reservoir porosity	0.35
Permeability	10 md
Initial water saturation	0.17
Water viscosity	1 cp
Injection rate	1000 Mscf/day
Bottomhole production pressure	1300 psia

Table 3.6 Initial composition and properties of the components for comparison of three- and four-phase model with six component mixture (Case2)

Properties	C_1	C_3	C_6	C_{10}	C_{15}	C_{20}
Tc (°R)	343.0	665.7	913.4	1111.8	1270.0	1380.0
Pc (psia)	667.8	616.3	439.9	304.0	200.0	162.0
Vc(ft^3/Lb-mol)	1.599	3.211	5.923	10.087	16.696	21.484
MW	16.0	44.1	86.2	142.3	206.0	282.0
Acentric factor	0.013	0.152	0.301	0.488	0.650	0.850
Initial composition	0.5	0.03	0.07	0.20	0.15	0.05
Injected gas composition	0.77	0.2	0.01	0.01	0.005	0.005

Table 3.7 Relative permeability data for comparison of three- and four-phase model with six component mixture (Case2)

	Water	Oil	Gas
Endpoint	0.4	0.9	0.9
Residual saturation	0.3	0.1	0.0
Exponent	3.0	2.0	2.0

Table 3.8 Summary of input data for comparison of four-phase model with twelve component mixture (Case3)

Parameter	Value
Number of gridblocks	25×1×11
Gridblock size	40×50×5 ft^3
Initial temperature	86 °F
Initial pressure	1750 psia
Reservoir porosity	0.28
Horizontal Permeability	180 md
Vertical Permeability	18 md
Initial water saturation	0.4
Water viscosity	1 cp
Injection pressure	1800 psia
Bottomhole production pressure	800 psia

Table 3.9 Properties and initial composition of the components for comparison of four-phase model with twelve component mixture (Case3)

Properties	CO_2	C1	C2	C3	C4	C5	C6	C7-10	C11-14	C15-20	C21-32	$C33^+$
Tc (°R)	547.57	343.04	549.76	665.68	765.32	845.37	923.0	1040.3	1199.64	1346.56	1532.74	845.36
Pc (psia)	1071.6	667.8	707.8	616.3	550.7	488.6	483.77	415.41	225.39	203.91	158.03	94.80
Vc(ft^3/Lb-mol)	0.416	1.602	2.451	3.3	4.088	4.946	5.294	8.553	13.11	23.07	33.253	83.571
MW	44.01	16.04	30.07	44.10	58.12	72.15	84.00	145.16	223.26	353.51	554.55	1052.00
Acentric factor	0.225	0.013	0.0986	0.1524	0.2010	0.2539	0.2583	0.3165	0.4255	0.5768	0.7659	1.1313
Initial composition %	0.0436	27.215	0.4128	1.0484	2.123	2.002	2.256	9.875	10.053	14.514	16.4162	14.041
Injected gas composition %	81.5	0.0	0.0	0.0	0.43	7.98	5.22	2.67	2.2	0.0	0.0	0.0

Table 3.10 Relative permeability data for comparison of four-phase model with twelve component mixture (Case3)

	Water	Oil	Gas	2^{nd} Liquid
Endpoint	0.2	0.7	1.0	0.7
Residual saturation	0.25	0.2	0.05	0.2
Exponent	1.5	2.5	2.5	2.5

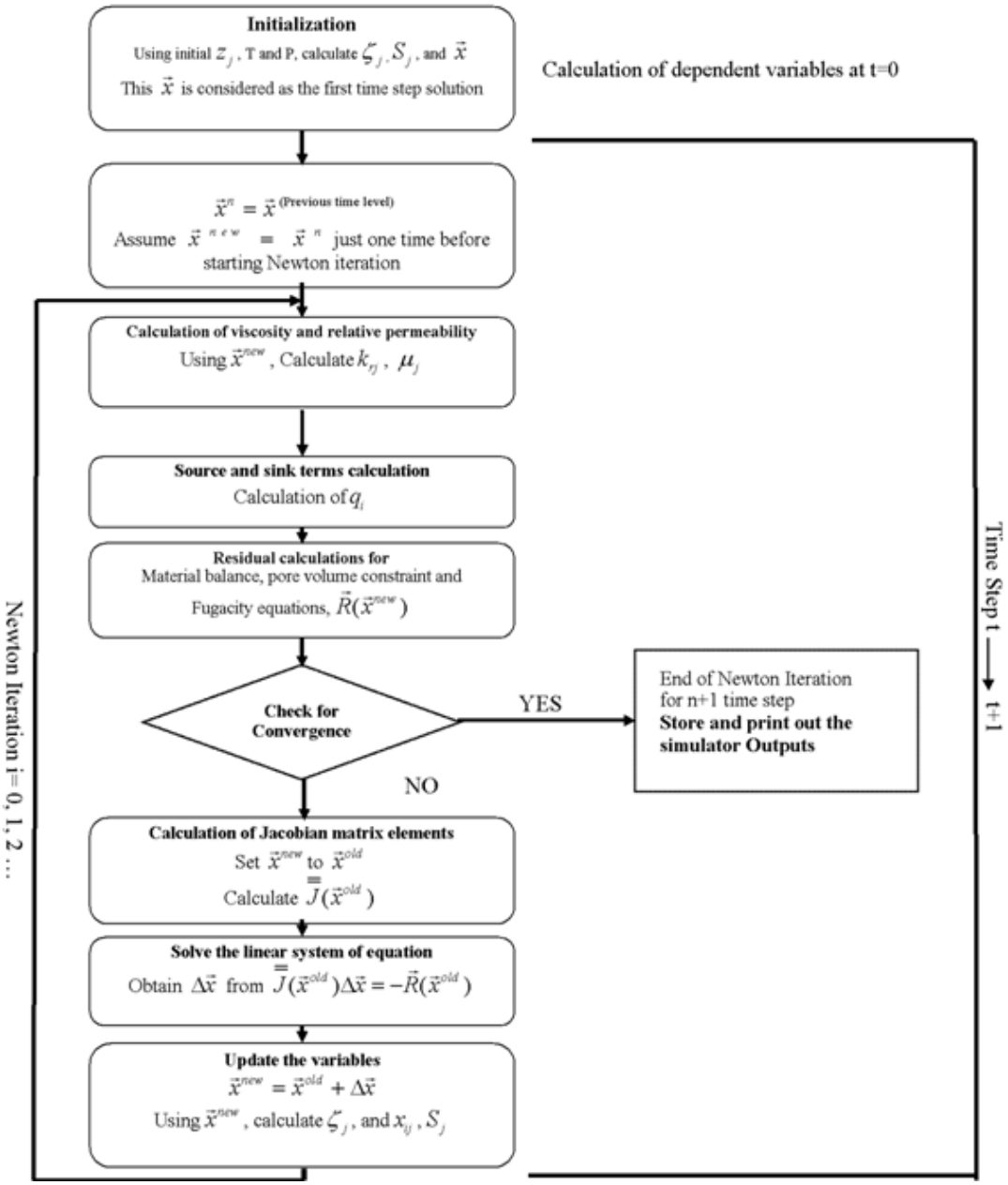

Figure 3.1 Computational flow chart for the four-phase model

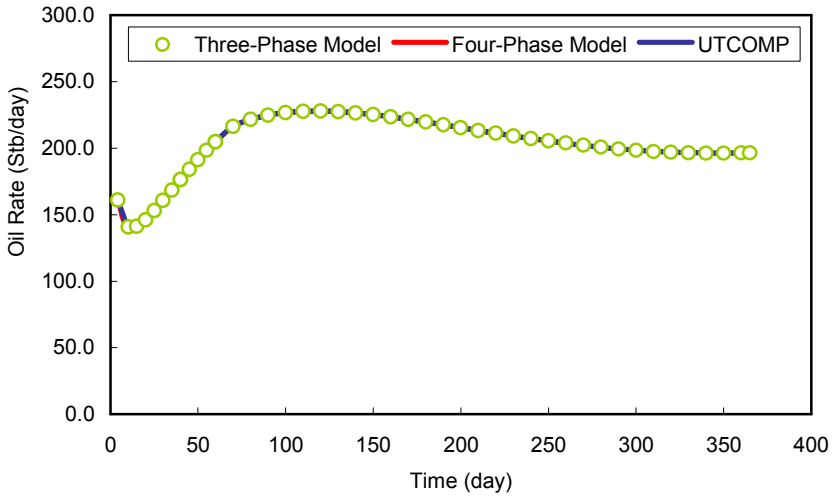

Figure 3.2 Comparison of oil rates using three-phase, four-phase model, and UTCOMP in the case of having maximum three phases in reservoir (Case 2)

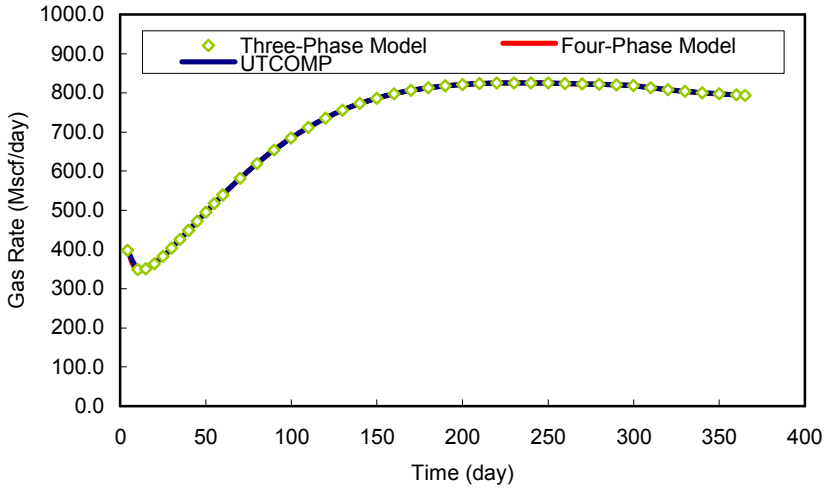

Figure 3.3 Comparison of gas rates using three-phase, four-phase model, and UTCOMP in the case of having maximum three phases in reservoir (Case 2)

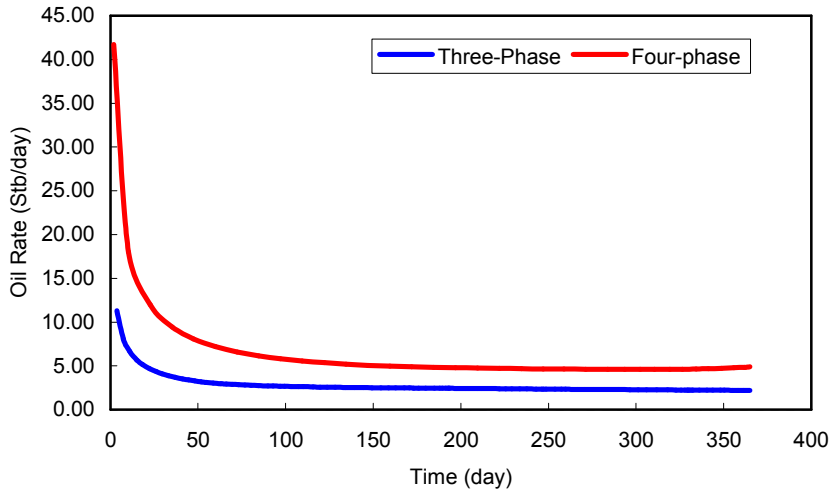

Figure 3.4 Comparison of oil rates for three-phase and four-phase models in the case of having maximum four-phase (Case 3)

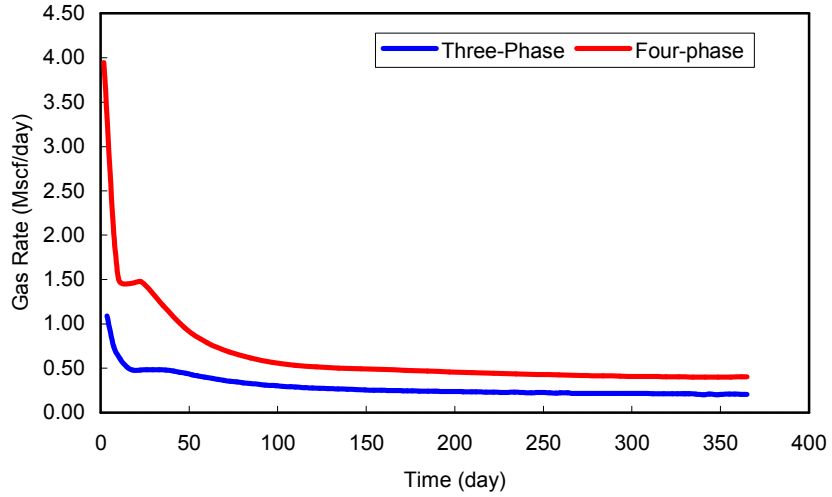

Figure 3.5 Comparison of gas rates for three-phase and four-phase models in the case of having maximum four-phase (Case 3)

Chapter 4: General Purpose Adaptive Compositional Reservoir Simulator (GPAS), Thermal Model

After the implementation of the four-phase model with three phase-flash calculation, thermal compositional reservoir simulation in GPAS was implemented. In this model, all phases (oil, gas, and aqueous) are in equilibrium, and an EOS is used for determining equilibrium between the phases. K-value approach was not used in this model. Physical properties of the phases and the components are calculated with the EOS. It is not necessary to use any steam-table to find water/steam properties, (Varavei and Sepehrnoori, 2009).

4.1 EOS-Based Thermal Model and K-Value Approach Thermal Model

The difference between the K-value approach and the EOS-based thermal models lies in the fact that the K-value is not a function of composition of the phases. The models, which use the K-value method, do not consider the solubility of hydrocarbon components in the water or aqueous phase and the solubility of water in the hydrocarbon liquid phase.

Conventional reservoir simulators for steam simulators ignore the solubility of the hydrocarbon in water phase and the solubility of water in oil phase. However, as the temperature increases, the solubility of the hydrocarbon components in water phase and also the solubility of the water phase in hydrocarbon liquid phase are significantly increased. Figures 4.1 through 4.4, which are from experimental data for C_1/n-C_4/Water in the three-phase region, have been shown by McKetta and Katz (1948). They show the solubility of

water in hydrocarbon-rich liquid and vapor phases and solubility of hydrocarbon in the aqueous phase.

Wang and Chao (1990) showed that the solubility of water in hydrocarbon-rich liquid can climb up to 50.0 % at high temperatures. Solubilities of 16.18 mole % water in 54.3° API naphtha at 431.6°F; 34.97 mole % water in 54.3°API kerosene at 507.2°F; and 43.44 mole % water in 29.3° API oil at 537.8°F have been reported by Griswold and Kasch (1942). Heidman (1985) showed the solubility of water in liquid C_8 at 500.0°F in liquid C_8. Glandt and Chapman (1995) presented the dissolution of water in crude oil up to 33.3 weight %.

These solubility values change viscosity, density, and other properties and may affect the production performance.

4.2 NEW DEVELOPMENTS

The following new features were incorporated into the thermal model for compositional reservoir simulation:

1. Implementation of three phase flash.
2. Implementation of the energy equation.
3. Implementation of two thermal flooding processes: steam injection and electrical heating models.
4. Effect of temperature on viscosity.
5. Effect of temperature on interfacial tension.
6. Effect of temperature on surfactant phase behavior.
7. Effect of temperature on geo-mechanics.
8. Electrical heating model.

4.3 GOVERNING EQUATIONS

Governing equations for the thermal model are equilibrium equations, mass conservation equations for each component, pore volume constraint, and energy equations. All of the equations, except the energy equation, were presented in Chapter 3. In the following, the energy equation and other auxiliary equations are described.

4.4 ENERGY BALANCE EQUATION

The energy balance equation for the simulator is as follows:

$$V_b \frac{\partial U^T}{\partial t} + V_b \nabla \cdot \sum_{j=a,v,o} (\zeta_j h_j \vec{v}_j) - V_b \nabla.(\lambda_T \nabla T) = -\dot{Q}_L + \dot{q}_H + \hat{H}_r \tag{4.1}$$

where U^T is the sum of rock and total fluid internal energy per bulk volume;

$$U^T = (1-\phi)\zeta_r u_r + \phi \sum_{j=a,v,o} \zeta_j S_j u_j \tag{4.2}$$

Here h_j is the phase molar enthalpy, λ_T is the effective conductivity coefficient, ζ_j is the phase fluid density, ζ_r is the rock density, ϕ is the porosity, T is the temperature, u_j and u_r are the internal energy of phase and rock, respectively. S_j is phase saturation, $\vec{v}_j$ is phase flux, Q_L is the heat losses, q_H is the enthalpy of injection fluid, and $\hat{H}_r$ is heat of reaction; the dot in the equation means rate.

4.5 HEAT LOSS TERM

The heat loss from overburden and underburden is calculated by the Vinsome and Westerveld (1980) method. It assumed the temperature in the base and caprock is function

of time and vertical distance from the reservoir boundary. Vinsome and Westerveld assumed a temperature profile in the form of

$$T(t,z)=(\theta-\theta^0+b_1 z+b_2 z^2)\,\exp(-z/d)+\theta^0 \tag{4.3}$$

where *T(t,z)* is overburden/underburden temperature at time *t* at a distance of *z* from the reservoir boundary; the interface between the reservoir and the cap- and base-rock is defined to be at *z*=0. Here, b_1 and b_2 are time-dependent parameters. θ is temperature in gridblock, θ^0 is initial temperature in gridblock, Δt is the time step size, and n is the notation for time. Moreover, *d* is a diffusion length, defined as follows:

$d=\frac{1}{2}\sqrt{\eta t}$, and η is the thermal diffusivity $\eta=\frac{\lambda_r}{c_r\xi_r}$

λ_r is thermal conductivity of the rock and c_r is rock heat capacity.

The following expressions are for b_1 and b_2:

$$b_1^{n+1}=\frac{\frac{\eta\Delta t(\theta^{n+1}-\theta^0)}{d^{n+1}}+\tau^n-\frac{(d^{n+1})^3(\theta^{n+1}-\theta^n)}{\eta\Delta t}}{3(d^{n+1})^2+\eta\Delta t} \tag{4.4}$$

$$b_2^{n+1}=\frac{2b_1^{n+1}(d^{n+1})-(\theta^{n+1}-\theta^0)+\frac{(d^{n+1})^2(\theta^{n+1}-\theta^n)}{\eta\Delta t}}{2(d^{n+1})^2} \tag{4.5}$$

$$\tau^n=\left[\left(\theta-\theta^0\right)d+b_1 d^2+2b_2 d^3\right]^n \tag{4.6}$$

$$Q_{loss}=\lambda_r A\left[\frac{(\theta^{n+1}-\theta^0)}{d^{n+1}}-b_1^{n+1}\right] \tag{4.7}$$

A is the cross-sectional area for heat loss to overburden and underburden.

4.6 RESIDUAL OF ENERGY EQUATION

The residual form of the energy equation is as follows:

$$R_E = E_{acc} - (E_{in} - E_{out}) - (qe_{win} - qe_{wout}) = \frac{1}{\Delta t}\left(U^{n+1}_{\alpha_{i,j,k}} - U^{n}_{\alpha_{i,j,k}}\right) +$$
$$\left\{\left(E_{conv,\alpha_{i+\frac{1}{2},j,k}} - E_{conv,\alpha_{i-\frac{1}{2},j,k}}\right)^{n+1} + \left(E_{conv,\alpha_{i,j+\frac{1}{2},k}} - E_{conv,\alpha_{i,j-\frac{1}{2},k}}\right)^{n+1}\right.$$
$$\left. + \left(E_{conv,\alpha_{i,j,k+\frac{1}{2}}} - E_{conv,\alpha_{i,j,k-\frac{1}{2}}}\right)^{n+1}\right\} +$$
$$\left\{\left(E_{cond,\alpha_{i+\frac{1}{2},j,k}} - E_{cond,\alpha_{i-\frac{1}{2},j,k}}\right)^{n+1} + \left(E_{cond,\alpha_{i,j+\frac{1}{2},k}} - E_{cond,\alpha_{i,j-\frac{1}{2},k}}\right)^{n+1}\right.$$
$$\left. + \left(E_{cond,\alpha_{i,j,k+\frac{1}{2}}} - E_{cond,\alpha_{i,j,k-\frac{1}{2}}}\right)^{n+1}\right\} - qe_{\alpha_{i,j,k}} + Q_{loss}$$
$$= E_{\alpha i,j,kaccum} + E_{\alpha i,j,kconv} + E_{\alpha i,j,kcond} - E_{\alpha i,j,ksource} + E_{loss} = 0 \qquad (4.8)$$

The convection terms for energy equation, the same as the material balance equation, have four scenarios. Their four set of equations by using one-point upstream are as follows:

$$E_{conv,\alpha i+1/2} = \sum_{\beta=1}^{n_P} T_{\alpha\beta i+1} H_{\beta i+1} K_{i+1} (\Phi_{\beta i+1} - \Phi_{\beta i}) \quad if \quad \Phi_{\beta i+1} > \Phi_{\beta i} \qquad (4.9)$$

$$E_{conv,\alpha i+1/2} = \sum_{\beta=1}^{n_P} T_{\alpha\beta i} H_{\beta i} K_{i+1} (\Phi_{\beta i} - \Phi_{\beta i+1}) \qquad if \quad \Phi_{\beta i+1} < \Phi_{\beta i} \qquad (4.10)$$

$$E_{convec,\alpha i-1/2} = \sum_{\beta=1}^{n_P} T_{\alpha\beta i-1} H_{\beta i-1} K_i (\Phi_{\beta i-1} - \Phi_{\beta i}) \quad if \quad \Phi_{\beta i-1} > \Phi_{\beta i} \qquad (4.11)$$

$$E_{convec,\alpha i-1/2} = \sum_{\beta=1}^{n_P} T_{\alpha\beta i} H_{\beta i} K_i (\Phi_{\beta i} - \Phi_{\beta i-1}) \qquad if \quad \Phi_{\beta i-1} < \Phi_{\beta i} \tag{4.12}$$

Hence, there are four scenarios for the convection term

1. $\Phi_{\beta i+1} < \Phi_{\beta i} \quad and \quad \Phi_{\beta i} < \Phi_{\beta i-1}$

$$E_{convec,\alpha i+1/2} - E_{convec,\alpha i-1/2} = \sum_{\beta=1}^{n_P} T_{\alpha\beta i} H_{\beta i} K_{i+1} (\Phi_{\beta i} - \Phi_{\beta i+1}) - \sum_{\beta=1}^{n_P} T_{\alpha\beta i-1} H_{\beta i-1} K_i (\Phi_{\beta i-1} - \Phi_{\beta i}) \tag{4.13}$$

2. $\Phi_{\beta i+1} > \Phi_{\beta i} \quad and \quad \Phi_{\beta i} > \Phi_{\beta i-1}$

$$E_{convec,\alpha i+1/2} - E_{convec,\alpha i-1/2} =$$
$$-\sum_{\beta=1}^{n_P} T_{\alpha\beta i+1} H_{\beta i+1} K_{i+1} (\Phi_{\beta i+1} - \Phi_{\beta i}) + \sum_{\beta=1}^{n_P} T_{\alpha\beta i} H_{\beta i} K_i (\Phi_{\beta i} - \Phi_{\beta i-1}) \tag{4.14}$$

3. $\Phi_{\beta_{i+1}} > \Phi_{\beta_i}$ and $\Phi_{\beta_i} < \Phi_{\beta_{i-1}}$

$$E_{convec,\alpha i+1/2} - E_{convec,\alpha i-1/2} =$$
$$-\sum_{\beta=1}^{n_P} T_{\alpha\beta i+1} H_{\beta i+1} K_{i+1} (\Phi_{\beta i+1} - \Phi_{\beta i}) - \sum_{\beta=1}^{n_P} T_{\alpha\beta i-1} H_{\beta i-1} K_i (\Phi_{\beta i-1} - \Phi_{\beta i}) \tag{4.15}$$

4. $\Phi_{\beta_{i+1}} < \Phi_{\beta_i}$ and $\Phi_{\beta_i} > \Phi_{\beta_{i-1}}$

$$E_{convec,\alpha i+1/2} - E_{convec,\alpha i-1/2} =$$
$$\sum_{\beta=1}^{n_P} T_{\alpha\beta i} H_{\beta i} K_{i+1} (\Phi_{\beta i} - \Phi_{\beta i+1}) + \sum_{\beta=1}^{n_P} T_{\alpha\beta i} H_{\beta i} K_i (\Phi_{\beta i} - \Phi_{\beta i-1}) \tag{4.16}$$

The conduction term is described in Appendix E.

Physical Properties

The simulator is EOS-based and the Peng-Robinson EOS (PR-EOS) is used in this simulator.

Evaluation of the Rock, Fluid-Rock and Fluid Properties

The following describes the calculation of rock and fluid properties.

Porosity. Porosity is defined as pore volume divided by bulk volume and is estimated from

$$\phi = \phi_r (1 + c_f (P - P_r^\circ)) \tag{4.17}$$

Heat Conductivity and Heat Capacity. The heat conductivity can be selected as a constant value and also as a function of fluid and rock for each gridblock using the Somerton *et al*. (1974) model. The equation is presented in Appendix E.

Molar Density. Subsequent to the calculation of Z-factor from EOS, the molar density is calculated from the following equation

$$\zeta_\beta = \frac{P}{Z_\beta RT} \tag{4.18}$$

where ζ_β .and Z_β are the density and compressibility factor of phase β .

Fugacity Coefficient, Enthalpy and Internal Energy. The fugacity coefficient, enthalpy, and internal energy are calculated from the EOS and they are described in Appendix A.

Viscosity. The viscosity of the hydrocarbon phases is determined by Lohrenz's correlation (Lohrenz *et al*., 1964). Tables of phase viscosities as a function of temperature can also be

used. The Andrade equation (1934) can also be used to calculate the pure-component oleic phase and aqueous phase viscosities as follows:

$$Ln\mu_i = a_i + \frac{b_i}{T} \tag{4.19}$$

where T is in Kelvin and a and b are pure-component coefficients estimated from experimental data. Figures 4.5 shows the viscosity of water and C_{17} as function of temperature using the Andrade equation (1934), and Figure 4.6 shows the effect of water solubility on viscosity.

Lohrenz *et al*. Correlation

The Lohrenz *et al*. (1964) correlation combines several viscosity correlations as described below. The steps involved in calculating the phase viscosity are given below.

The low-pressure, pure-component viscosity is calculated as follows:

$$\hat{\mu}_i = \frac{0.00034T_{ri}^{0.94}}{\zeta_i}, \quad T_{ri} \le 1.5 \tag{4.20}$$

or

$$\hat{\mu}_i = \frac{0.0001776(4.58T_{ri} - 1.67)^{5/8}}{\zeta_i}, \; T_{ri} > 1.5 \tag{4.21}$$

Where

$$\zeta_i = \frac{5.44T_{ci}^{1/6}}{MW_i^{1/2}P_{ci}^{2/3}} \tag{4.22}$$

The low pressure viscosity is calculated by the following equation:

$$\mu_j^* = \frac{\sum_{i=1}^{n_c} x_{ij} \hat{\mu}_i \sqrt{MW_i}}{\sum_{i=1}^{n_c} x_{ij} \sqrt{MW_i}} \tag{4.23}$$

Following equation gives the reduced phase molar density calculation.

$$\zeta_{jr} = \zeta_j \sum_{i=1}^{n_c} x_{ij} V_{ci} \tag{4.24}$$

$$\eta_j = \frac{5.44 \left[\sum_{i=1}^{n_c} x_{ij} T_{ci} \right]^{1/6}}{\left[\sum_{i=1}^{n_c} x_{ij} MW_i \right]^{1/2} \left[\sum_{i=1}^{n_c} x_{ij} P_{ci} \right]^{2/3}} \tag{4.25}$$

The phase viscosity calculation at the desired pressure is as follows:

$$\mu_j = \mu_j^* + 0.000205 \frac{\zeta_{jr}}{\eta_j}, \ \zeta_{jr} \le 0.18 \tag{4.26}$$

$$\mu_j = \frac{\mu_j^* + (\chi_j^4 - 1)}{10^4 \eta_j}, \ \zeta_{jr} > 0.18 \tag{4.27}$$

where

$$\chi_j = 1.023 + 0.23364 \zeta_{jr} + 0.58533 \zeta_{jr}^2 - 0.40758 \zeta_{jr}^3 + 0.093324 \zeta_{jr}^4 \tag{4.28}$$

4.7 PRIMARY VARIABLES

The primary variables for the thermal model are as follows: there are $3N_C+5$ of them for each gridblock in the case of three phases in equilibrium:

$$LnK_{1,1},\ LnK_{1,2}, LnK_{1,3}\ \ldots\ LnK_{1,nc+1}, LnK_{2,1},\ LnK_{2,2}, LnK_{2,3}\ \ldots\ LnK_{2,nc+1},$$
$$N_1, N_2, N_3 \ldots N_{nc+1}, P_w, T.$$

4.8 SOLUTION PROCEDURE

To solve the system of equations, it is necessary to have the residual from the previous time-step and construct the Jacobian matrix.

$$\delta \mathrm{P} = \mathrm{P}^{n+1} - \mathrm{P}^{n} = -\vec{\vec{J}}^{-1}.R^{n} \tag{4.29}$$

P is the primary variable and R is the residual of the equations. The residual of the governing equations, and also construction of the Jacobian matrix, is presented as given below:

$$\begin{pmatrix} J_{1,1} & J_{1,2} & \ldots & J_{1,n_b} \\ J_{2,1} & J_{2,2} & \ldots & J_{2,n_b} \\ \vdots & & & \vdots \\ J_{n_b,1} & J_{n_b,2} & \ldots & J_{n_b,n_b} \end{pmatrix} \begin{pmatrix} \Delta\vec{x}_1 \\ \Delta\vec{x}_2 \\ \vdots \\ \Delta\vec{x}_{n_b} \end{pmatrix} = - \begin{pmatrix} \vec{R}_1 \\ \vec{R}_2 \\ \vdots \\ \vec{R}_{n_b} \end{pmatrix}$$

$$
J_{I,J}=\begin{bmatrix}
\frac{\partial R_{F1,1}|_I}{\partial LnK_{1,1}|_J} & \cdots & \frac{\partial R_{F1,1}|_I}{\partial LnK_{1,nc+1}|_J} & \frac{\partial R_{F1,1}|_I}{\partial LnK_{2,1}|_J} & \cdots & \frac{\partial R_{F1,1}|_I}{\partial LnK_{2,nc+1}|_J} & \frac{\partial R_{F1,1}|_I}{\partial N_1|_J} & \cdots & \frac{\partial R_{F1,1}|_I}{\partial N_{nc+1}|_J} & \frac{\partial R_{F1,1}|_I}{\partial P|_J} & \frac{\partial R_{F1,1}|_I}{\partial T|_J} \\
\vdots & \vdots & \vdots & \vdots & \vdots & \vdots & \vdots & \vdots & \vdots & \vdots & \vdots \\
\frac{\partial R_{F1,nc+1}|_I}{\partial LnK_{1,1}|_J} & \cdots & \frac{\partial R_{F1,nc+1}|_I}{\partial LnK_{1,nc+1}|_J} & \frac{\partial R_{F1,nc+1}|_I}{\partial LnK_{2,1}|_J} & \cdots & \frac{\partial R_{F1,nc+1}|_I}{\partial LnK_{2,nc+1}|_J} & \frac{\partial R_{F1,nc+1}|_I}{\partial N_1|_J} & \cdots & \frac{\partial R_{F1,nc+1}|_I}{\partial N_{nc+1}|_J} & \frac{\partial R_{F1,nc+1}|_I}{\partial P|_J} & \frac{\partial R_{F1,nc+1}|_I}{\partial T|_J} \\
\frac{\partial R_{F2,1}|_I}{\partial LnK_{1,1}|_J} & \cdots & \frac{\partial R_{F2,1}|_I}{\partial LnK_{1,nc+1}|_J} & \frac{\partial R_{F2,1}|_I}{\partial LnK_{2,1}|_J} & \cdots & \frac{\partial R_{F2,1}|_I}{\partial LnK_{2,nc+1}|_J} & \frac{\partial R_{F2,1}|_I}{\partial N_1|_J} & \cdots & \frac{\partial R_{F2,1}|_I}{\partial N_{nc+1}|_J} & \frac{\partial R_{F2,1}|_I}{\partial P|_J} & \frac{\partial R_{F2,1}|_I}{\partial T|_J} \\
\vdots & \vdots & \vdots & \vdots & \vdots & \vdots & \vdots & \vdots & \vdots & \vdots & \vdots \\
\frac{\partial R_{F2,nc+1}|_I}{\partial LnK_{1,1}|_J} & \cdots & \frac{\partial R_{F2,nc+1}|_I}{\partial LnK_{1,nc+1}|_J} & \frac{\partial R_{F2,nc+1}|_I}{\partial LnK_{2,1}|_J} & \cdots & \frac{\partial R_{F2,nc+1}|_I}{\partial LnK_{2,nc+1}|_J} & \frac{\partial R_{F2,nc+1}|_I}{\partial N_1|_J} & \cdots & \frac{\partial R_{F2,nc+1}|_I}{\partial N_{nc+1}|_J} & \frac{\partial R_{F2,nc+1}|_I}{\partial P|_J} & \frac{\partial R_{F2,nc+1}|_I}{\partial T|_J} \\
\frac{\partial R_{v}|_I}{\partial LnK_{1,nc}|_J} & \cdots & \frac{\partial R_{v}|_I}{\partial LnK_{1,nc+1}|_J} & \frac{\partial R_{v}|_I}{\partial LnK_{2,1}|_J} & \cdots & \frac{\partial R_{v}|_I}{\partial LnK_{2,nc+1}|_J} & \frac{\partial R_{v}|_I}{\partial N_1|_J} & \cdots & \frac{\partial R_{v}|_I}{\partial N_{nc+1}|_J} & \frac{\partial R_{v}|_I}{\partial P|_J} & \frac{\partial R_{v}|_I}{\partial T|_J} \\
\frac{\partial R_{m,1}|_I}{\partial LnK_{1,1}|_J} & \cdots & \frac{\partial R_{m,1}|_I}{\partial LnK_{1,nc+1}|_J} & \frac{\partial R_{m,1}|_I}{\partial LnK_{2,1}|_J} & \cdots & \frac{\partial R_{m,1}|_I}{\partial LnK_{2,nc+1}|_J} & \frac{\partial R_{m,1}|_I}{\partial N_1|_J} & \cdots & \frac{\partial R_{m,1}|_I}{\partial N_{nc+1}|_J} & \frac{\partial R_{m,1}|_I}{\partial P|_J} & \frac{\partial R_{m,1}|_I}{\partial T|_J} \\
\vdots & \cdots & \vdots & \vdots & \cdots & \vdots & \vdots & \cdots & \vdots & \vdots & \vdots \\
\frac{\partial R_{m,nc+1}|_I}{\partial LnK_{1,1}|_J} & \cdots & \frac{\partial R_{m,nc+1}|_I}{\partial LnK_{1,nc+1}|_J} & \frac{\partial R_{m,nc+1}|_I}{\partial LnK_{2,1}|_J} & \cdots & \frac{\partial R_{m,nc+1}|_I}{\partial LnK_{2,nc+1}|_J} & \frac{\partial R_{m,nc+1}|_I}{\partial N_1|_J} & \cdots & \frac{\partial R_{m,nc+1}|_I}{\partial N_{nc+1}|_J} & \frac{\partial R_{m,nc+1}|_I}{\partial P|_J} & \frac{\partial R_{m,nc+1}|_I}{\partial T|_J} \\
\frac{\partial R_{E}|_I}{\partial LnK_{1,1}|_J} & \cdots & \frac{\partial R_{E}|_I}{\partial LnK_{1,nc+1}|_J} & \frac{\partial R_{E}|_I}{\partial LnK_{2,1}|_J} & \cdots & \frac{\partial R_{E}|_I}{\partial LnK_{2,nc+1}|_J} & \frac{\partial R_{E}|_I}{\partial N_1|_J} & \cdots & \frac{\partial R_{E}|_I}{\partial N_{nc+1}|_J} & \frac{\partial R_{E}|_I}{\partial P|_J} & \frac{\partial R_{E}|_I}{\partial T|_J}
\end{bmatrix}
$$

The flowchart of this model is presented in Figure 4.7.

4.9 JACOBIAN MATRIX TO SOLVE THE GOVERNING EQUATIONS

The derivatives of the energy equation with respect to the primary variables are presented below:

$$\frac{\partial R_{E,K}}{\partial P_K}=-\frac{\partial E_{accum,K}}{\partial P_K}+\frac{\partial E_{conv,K}}{\partial P_K}+\frac{\partial E_{cond,K}}{\partial P_K}+\frac{\partial E_{source,K}}{\partial P_K}-\frac{\partial E_{loss,K}}{\partial P_K} \tag{4.30}$$

And for the off-diagonal terms are

$$\frac{\partial R_{E,K}}{\partial P_{K\pm1}}=-\frac{\partial E_{accum,K}}{\partial P_{K\pm1}}+\frac{\partial E_{conv,K}}{\partial P_{K\pm1}}+\frac{\partial E_{cond,K}}{\partial P_{K\pm1}}+\frac{\partial E_{source,K}}{\partial P_{K\pm1}}-\frac{\partial E_{loss,K}}{\partial P_{K\pm1}} \tag{4.31}$$

The entire derivatives with respect to each variable and also the related derivative with respect to phase behavior calculations are described in Appendix E.

4.10 CASE STUDIES OF THE THERMAL MODEL FOR HOT FLUID INJECTION

The case studies for the thermal model are presented in the following sections. The K-value approach method in some of case studies has been used from CMG-STARS (2006.10) commercial simulator. STARS is CMG's advanced processes reservoir simulator which contains several options such as chemical/polymer flooding, thermal applications, steam injection, horizontal wells, dual porosity/permeability, directional permeabilities, flexible grids, fireflood, and many other aspects.

Comparison with Analytical Solution

The heat loss into overburden and underburden are necessary to be included for any thermal simulator because these values are crucial in thermal recovery. The Vinsome and Westerveld's heat loss model (Vinsome and Westerveld, 1980) was implemented into the simulator. In this section, the Lauwerier's analytical solution is used to verify the heat loss model.

Lauwerier's solution (1955) presented one of the earliest analytical solutions for displacing the cold oil with hot water in porous media using the following assumptions:

1. Constant thickness, porosity and permeability
2. Constant specific heat of the rock and fluid
3. Constant thermal conductivity for reservoir and caprock in z direction
4. No heat conduction in flow direction (x direction) and there is no vertical temperature gradient
5. Instantaneous thermal equilibrium between the fluid and rock

6. Water is injected at constant rate and temperature

The energy balance is as follows:

$$h_t \rho_t C_t \left(\frac{\partial \theta_r}{\partial t} \right) + h_t V_f \rho_f C_f \left(\frac{\partial \theta_r}{\partial x} \right) - 2\lambda_s \left(\frac{\partial \theta_s}{\partial y} \right)_{y=h_t/2} = 0 \tag{4.32}$$

The heat conduction is as follows:

$$\rho_s C_s \left(\frac{\partial \theta_s}{\partial t} \right) - \lambda_s \left(\frac{\partial^2 \theta_s}{\partial y^2} \right) = 0 \tag{4.33}$$

where h_t is the thickness of the reservoir, V_f, ρ_f and C_f are volume of fluid, fluid density and fluid heat capacity, respectively, and λ_s is heat conductivity of surroundings. ρ_s and C_s are density and heat capacity of the surroundings.

The first term is heat accumulation term, the second term is convection energy, and the third term is heat loss values into below and above the reservoir. θ and $\rho_t C_t$, which is volumetric heat capacity, of the fluid and the rock are defined as follows:

$$\theta = \frac{T - T_{ini}}{T_{inj} - T_{ini}} \tag{4.34}$$

$$\rho_t C_t = (1-\phi)\rho_r C_r + \phi \rho_w C_w S_w + \phi \rho_o C_o S_o \tag{4.35}$$

where ρ, C and S are density, heat capacity, and saturation, respectively. The subscript *w, o* and *r* represent water, oil, and rock, respectively.

The following dimensionless parameters are defined as

$$x_D = \frac{4\lambda_s x}{h_t^2 V_f \rho_f C_f} \tag{4.36}$$

$$y_D = \frac{2y}{h_t} \tag{4.37}$$

$$t_D = \frac{4\lambda_s t}{h_t^2 \rho_t C_t} \tag{4.38}$$

$$\beta = \frac{\rho_t C_t}{\rho_s C_s} \tag{4.39}$$

Using the above dimensionless variables in Eq. (4.31) and Eq. (4.32) gives

$$\beta\left(\frac{\partial^2 \theta_s}{\partial y_D^2}\right) = \left(\frac{\partial \theta_s}{\partial t_D}\right) \quad \text{If } |y_D| > 1 \tag{4.40}$$

$$\left(\frac{\partial \theta_s}{\partial t_D}\right) + \left(\frac{\partial \theta_s}{\partial x_D}\right) - \left(\frac{\partial \theta_s}{\partial y_D}\right) = 0 \quad \text{And} \quad \theta_r = \theta_s \quad \text{If } |y_D| = 1 \tag{4.41}$$

$$\theta_r = \theta_s = \begin{cases} 1 \text{ if } x_D < 0 \\ 0 \text{ if } x_D > 0 \end{cases} \quad \text{If } t_D = 0 \tag{4.42}$$

The solution of the equations which gives the temperature profile as a function of time and location within the media by Lauwerier's method is as follows:

$$\theta_s = \begin{cases} 0 & \text{if } x_D \geq 0 \\ erfc\left(\dfrac{x_D + |y_D| - 1}{2\sqrt{\beta(t_D - x_D)}}\right) & \text{if } x_D < 0 \end{cases} \tag{4.43}$$

$$\theta_r = \begin{cases} 0 & \text{if } x_D \geq 0 \\ erfc\left(\dfrac{x_D}{2\sqrt{\beta(t_D - x_D)}}\right) & \text{if } x_D < 0 \end{cases} \tag{4.44}$$

The following equation gives the heat flow rate from surface of the reservoir.

$$
\begin{aligned}
Q_L &= \lambda_s \left(\frac{\partial \theta_s}{\partial y} \right)_{y=h_t/2} \\
&= \lambda_s \left(\frac{\partial \theta}{\partial y_D} \cdot \frac{\partial y_D}{\partial y} \cdot \frac{\partial \theta_s}{\partial \theta} \right)_{y_D=1} \\
&= -\lambda_s (T_{inj} - T_{ini}) \frac{4}{h_t \sqrt{\pi}} exp\left(\frac{-x_D}{4\beta(t_D - x_D)} \right)
\end{aligned}
\tag{4.45}
$$

Case 1: Comparison with Analytical Solution. To show the validity and the test the implementation of heat loss into the simulator, the result of simulator was compared with the analytical solution for this example. The input data are summarized in Table 4.1. The case is a 1D homogeneous reservoir of size 1000×10×10 ft^3 with permeability of 10,000 md and porosity of 0.35. Initial pressure and temperature of the reservoir are 1000 psia and 520°R; the heat capacity ratio of fluid to rock is one. The volumetric heat capacity is 35 Btu/ (ft^3-°R) and the thermal conductivity is 35 Btu/(ft-day-°R). The reservoir is divided into 200 gridblocks in the *x* direction. Hot water with a rate of 662 Lbmol/day with a temperature of 660°R is injected into the reservoir and the production bottomhole pressure is maintained at 1000 psia. Figure 4.8 shows the temperature profile for the numerical and the analytical solutions. As shown in Figure 4.8, there is good agreement between the analytical solution and the developed model.

Case 2: One-Dimensional Case with Four Component Fluid Mixture. This case was defined to test the simulator for one-dimensional problems with multi-component mixture and to compare the simulation result with a K-value approach STARS thermal simulator. The reservoir properties are listed in Table 4.2. The relative permeability data are given in Table 4.3 and the fluid properties and initial compositions are shown in Table 4.4. The

reservoir size is 2500×50×20 ft^3. Initial pressure and temperature are 500 psia and 550˚R. Porosity and permeability of the reservoir are 0.3 and 200 md, respectively. Reservoir fluid is a four-component mixture; initial phase saturations and compositions are calculated at the initialization step using flash calculation. The number of gridblocks is 50×1×1. Injected fluid is water with a rate of 300 Lbmole/day and a temperature of 800˚R and the state of water is calculated in the injection well at well pressure and temperature. Production bottomhole pressure is 500 psia. Figure 4.9 shows the oil rate for 600 days for both the simulator and the K-value approach method. As shown, the results of the simulators are different. The main reason for the discrepancy is the solubility of the water in hydrocarbon-rich phase and the solubility of hydrocarbons in water-rich phase. In other words, K-value of each component in the K-value approach is a function of temperature, and pressure, while the K-value of EOS is a function of temperature, pressure, and composition with different EOS parameters in different conditions. Therefore, from a thermodynamic point of view, the result of EOS is expected to be more realistic and more accurate.

Case 3: Two-Dimensional Case with Four Component Fluid Mixture. A two-dimensional reservoir with the size of 400×50×80 ft^3 was used to test the simulator for a *x*-*z* cross-sectional problem. Initial pressure and temperature of the reservoir are 600 psia and 550°R; four components were used to represent the reservoir fluid, the reservoir, surrounding thermal conductivities and rock heat capacity are the same as in Case 2. Table 4.5 lists the input data for this case and the relative permeability data are presented in Table 4.6. Table 4.7 lists the properties and the mole percent of components in the mixture. The enthalpies of all the fluid phases are calculated by Peng-Robinson EOS (PR-EOS). An 8×1×8 grid is used to inject water at 800°R and at a rate of 1000 Lbmole/day. The production pressure is 600 psia. Oil and water rates of the simulator and the K-value

approach are presented in Figure 4.10. Figure 4.11 presents the cumulative oil production for EOS and K-value methods. The simulation is performed for 1500 days and water is produced after 410 days in the EOS method. As explained in Case 2, because of different mole fraction ratios in two methods, EOS and K-value, the results are different. The breakthrough time of water in the K-value approach is earlier than the EOS method because of our consideration of solubility of water in hydrocarbon-rich phase and because of higher volume of water-rich phase in the K-value method. Therefore, the EOS method has soluble water in the oil phase and higher oil phase volume; moreover, the water breakthrough of EOS method takes place after the water breakthrough of K-value method. The distribution of pressure and temperature are shown in Figures 4.12 and 4.13, respectively.

Case 4: Three-Dimensional Case with Four Component Fluid Mixture. This case was designed to test the simulator for 3D problems with four-component reservoir fluids. The result of this example is compared with that of the K-value approach. For this case, a quarter of five spot reservoir with the volume of $320\times320\times30$ ft^3 is considered. The mixture compositions and the rest of the data are the same as in Case 3. The reservoir domain is discretized into $8\times8\times3$ blocks. The input data are listed in Table 4.8 and the relative permeability data are given in Table 4.9. The result is shown in Figure 4.14. This figure shows that the oil rate of the EOS method is higher than the K-value approach. As explained in two previous examples, the solubility of water component in oil phase can increase the oil rate due to increase of the hydrocarbon-rich liquid phase saturation. The equilibrium ratio from EOS performs these calculations; while in the K-value method, there is no dependence on composition in the correlation of the mole fraction ratios. In other words, from a thermodynamic point of view, the aqueous phase is involved in the equality of component chemical potential and minimization of Gibbs free energy. However, the

difference of solubilities between the EOS method and the K-value approach and the existence of all components in all phases in the EOS method will change the phase saturation, the relative permeability values, and the phase rates in the reservoir.

Case 5: One-Dimensional Case with Six Component Fluid Mixture. A 1D reservoir with the size of 40×40×40 ft^3 was used to test the simulator for a six-component reservoir fluid mixture. Initial phase compositions and saturations are computed by flash calculation. The summary of input data is listed in Tables 4.10 and the relative permeability data are shown in Table 4.11. The component properties are shown in Table 4.12. Initial pressure and temperature of the reservoir are 650 psia and 560°R. The rock specific heat is 35 Btu/(ft^3-°R) and thermal conductivity is 35 Btu/(ft-°R). The caprock thermal conductivity is 20.0 Btu/(ft-°R). Water is injected at a pressure of 700 psia and a temperature of 1000°R, the state of the water is calculated at the injection well condition. The production well condition maintained a pressure of 630 psia. Figure 4.15 shows the results of this case. As seen in the figure, there are two rates, oil and oleic. The oleic phase is oil which includes soluble water that gives the higher rates. Due to the solubility of water in the oil phase, and the increase of the hydrocarbon liquid-rich phase saturation, the rate of the oleic phase is increased. As a result, the pure oil production is increased compared to the methods that do not consider the role of water component interaction in phase behavior calculations. These differences lead to different phase properties and therefore different production efficiencies.

Case 6: Two-Dimensional Case with Six Component Fluid Mixture. The steam flooding in a 2D cross-sectional reservoir was used for this simulation. The reservoir volume is 800×40×30 ft^3. The fluid mixture has six components and the fluid properties are calculated by PR-EOS. The reservoir pressure and temperature are 650 psia and 560°R, respectively.

The rock and caprock thermal properties are the same as in Case 5. The porosity is 0.3 and the horizontal and vertical permeabilities are 250 and 100 md, respectively. The number of gridblocks is 20×1×3. The injected fluid is water at 800°R and 680 psia. The production well condition is constant BHP of 630 psia. The summarized input data are shown in Table 4.13 and the same mixture as Case 5 is used in this example. The relative permeability data are presented in Table 4.14. The oil rates are shown in Figure 4.16. As discussed in this chapter, the solubility of water in the oil and the solubility of hydrocarbon in water phase are crucial, for they can change the phase properties and the production history. Figure 4.16 shows two rates; one of them is oil and the other one is oleic, which has soluble water. Due to the solubility of water in the oil phase, the calculated oil production rate includes the water component (oleic phase); if we separate oil from this phase, we can determine the pure oil production rate. If this solubility is not taken into account, the results will be different. By employing this model, all of the solubilities are calculated in all of the phases.

Case 7: Three-Dimensional Case with Six Component Fluid Mixture. In this example, a quarter of a five spot simulation for a reservoir with the size 500×500×50 ft^3 using the properties listed in Table 4.15 is performed and the relative permeability data are given in Table 4.16. The mixture compositions are same as in Case 6. The number of gridblocks is 10×10×5. The permeability is 300 md. The injected fluid is water at 800°R and at a rate of 800 Lbmole/day. Both wells are perforated across all layers. The rest of the data are the same as in Case 6. The results are shown in Figure 4.17. The production rates include those of oleic and pure oil phases. These results show that the solubility of water in the reservoir can affect fluid properties, rates and production results. The rate profile in the figure shows that the breakthrough for different layers has happened at different times due to gravity

override. The first breakthrough is after 4,000 days and the last one occurred after 10,000 days.

Case 8: Three-Dimensional, Heterogeneous Case with Six Component Fluid Mixture. This case is heterogeneous reservoir of Case 7. Two different V_{DP} (Dykstra-Parsons coefficient) values, 0.5 and 0.8 are used to generate permeability of the reservoir using random numbers and average value of permeabilities in x, y, and z directions. The average value of the permeability in *x*, *y*, and *z* directions are, 100, 50, and 10 md, respectively. The permeability distributions for both V_{DP}s are shown in Figures 4.18 through 4.23. Figures 4.24 through 4.27 show oil rate and oil recoveries, water rates, oleic phase rate, and average reservoir pressures for simulations using these two V_{DP} values, respectively. The figures show that the oil recovery is higher in the more heterogeneous case. The pressure and saturation maps at V_{DP} of 0.8 for the bottom layer are given in Figures 4.28 through 4.33. The figures show these distributions for two simulation time values.

Parallel Thermal Reservoir Simulation

In this section, the performance of parallel processing mode of the thermal model is presented. The speedup calculation is one of the ways to show the parallel processing efficiency which is defined as follows:

$$Speedup = \frac{t_1}{t_n}$$

where t_1 is the execution time to run the case on single processor and t_n is the execution time on *n* processors. The ideal speed-up for parallel processing simulation with *n* processors is equal to number of processors, *n*. It means that the code runs *n* times faster than for single processor. But in reality, due to communications between the processors and

also memory contention, the speed-up is less than n when the program is running on n number of processors. Also, inefficient programming style can decrease the efficiency of parallel processing. The simulator uses the cluster of PCs at The University of Texas at Austin to perform parallel processing simulations. The formulation of a fully implicit, parallel, EOS compositional simulator was developed by Wang *et al*. (1997).

Case 9: Parallel Processing Example. To test the simulator in the parallel processing mode, a quarter of five-spot reservoir with the size 1280×1280×70 ft^3 was used. The fluid mixture has four components. The reservoir permeability is 250 md. Initial pressure and temperature are 600 psia and 590°R, respectively. The rock and caprock thermal conductivities are 30 Btu/(ft-day-°R). The volumetric rock heat capacity used in this example is 35 Btu/(ft^3-°R) and the porosity is 0.3. The number of grids used in the simulations to inject water with the rate of 2000 Lbmole/day is 64×64×7 and the well condition of production well is 570 psia. The summary of input data is listed in Table 4.17 and the relative permeability data are shown in Table 4.18. The component properties are shown in Table 4.19. The wells are perforated across all layers. The oil rate for this case is given in Figure 4.34. The execution time and speed-up curves are shown in Figures 4.35 and 4.36. The figures show that as the number of processors is increased, the execution times are decreased. The efficiency of the parallel mode is decreased by increasing the number of processors. With the increasing number of processors, the computational time for each processor becomes smaller. An overwhelming amount of time is spent in the message-passing between the processors.

Case 10: Corner Point Grid Option. This example, which is a quarter of five-spot reservoir, was devised to test the simulator capability using the corner-point grid option.

The reservoir size is 560×560×100 ft^3. The initial pressure and temperature of the reservoir are 500 psia and 560°R. The reservoir permeability is 100 md. The rock and caprock thermal conductivities are 35 and 10 Btu/(ft-day-°R). The volumetric rock heat capacity used in this example is 35 Btu/(ft^3-°R). The porosity is 0.3. The mixture is 70 mole percent oil and 30 mole percent water. The case is tested for two sets of gridblock numbers, 16×16×10 and 32×32×10, for both corner-point and Cartesian grid options. The injected fluid is water at 750°R and at a rate of 500 Lbmole/day. Both wells are perforated across all layers. Input data for simulating this reservoir are given in Table 4.20 and the relative permeability data are given in Table 4.21. The component properties are shown in Table 4.22. The results are shown in Figure 4.37. The results show good agreement between the two mesh used in the simulation.

Table 4.1 Summary of data for Lauwerier's problem (Case1)

Parameter	Value
Number of gridblocks	200×1×1
Gridblock size	5×10×10 ft^3
Initial temperature	520.0°R
Initial pressure	1000 psia
Reservoir porosity	0.35
Reservoir thermal conductivity	0 Btu/(ft-day-°R)
Caprock thermal conductivity	35 Btu/(ft-day-°R)
Rock heat capacity	35 Btu/ft^3-°R)
Injection temperature	660°R
Injection rate	662 Lbmole/day
Bottomhole production pressure	1000 psia

Table 4.2 Summary of input data for one-dimensional case with four component fluid mixture (Case2)

Parameter	Value
Number of gridblocks	50×1×1
Gridblock size	50×50×20 ft^3
Initial temperature	550°R
Initial pressure	500 psia
Reservoir porosity	0.3
Permeability	200 md
Reservoir thermal conductivity	35 Btu/(ft-day-°R)
Caprock thermal conductivity	25 Btu/(ft-day-°R)
Rock heat capacity	35 Btu/(ft^3-°R)
Injection temperature	800 °R
Injection rate	300 Lbmole/day
Bottomhole production pressure	500 psia

Table 4.3 Relative permeability data for one-dimensional case with four component fluid mixture (Case2)

	Water	Oil	Gas
Endpoint	0.4	0.7	0.5
Residual saturation	0.2	0.25	0.06
Exponent	2.5	2.0	1.5

Table 4.4 Composition and oil properties for one-dimensional case with four component fluid mixture (Case2)

Component name	MW	Tc (°R)	Pc (psia)	Mole percent
C_6	86.0	913.00	436.90	5.0
C_{10}	134.0	1120.11	367.647	15.0
C_{15}	206.0	1270.00	200.00	30.0
H_2O	18.0	1165.47	3198.72	50.0

Table 4.5 Composition and oil properties for two-dimensional case with four component fluid mixture (Case3)

Component name	MW	Tc (°R)	Pc (psia)	Feed mole percent
C_6	86.0	913.00	436.90	20.0
C_{10}	134.0	1120.11	367.647	20.0
C_{15}	206.0	1270.00	200.00	30.0
H_2O	18.0	1165.47	3198.72	30.0

Table 4.6 Relative permeability data for two-dimensional case with four component fluid mixture (Case3)

	Water	Oil	Gas
Endpoint	0.8	0.7	0.5
Residual saturation	0.25	0.15	0.06
Exponent	2.5	2.0	1.5

Table 4.7 Summary of input data for two-dimensional case with four component fluid mixture (Case3)

Parameter	Value
Number of gridblocks	8×1×8
Gridblock size	50×50×10 ft^3
Initial temperature	550 °R
Initial pressure	600 psia
Reservoir porosity	0.3
Permeability	100 md
Reservoir thermal conductivity	35 Btu/(ft-day-°R)
Caprock thermal conductivity	25 Btu/(ft-day-°R)
Rock heat capacity	35 Btu/(ft^3-°R)
Injection temperature	800°R
Injection rate	1000 Lbmole/day
Bottomhole production pressure	600 psia

Table 4.8 Summary of input data for three-dimensional case with four component fluid mixture (Case4)

Parameter	Value
Number of gridblocks	8×8×3
Gridblock size	40×40×10 ft^3
Initial temperature	590°R
Initial pressure	600 psia
Reservoir porosity	0.3
Permeability	100 md
Reservoir thermal conductivity	35 Btu/(ft-day-°R)
Caprock thermal conductivity	35 Btu/(ft-day-°R)
Rock heat capacity	35 Btu/(ft^3-°R)
Injection temperature	800°R
Injection rate	1000 Lbmole/day
Bottomhole production pressure	600 psia
C_6 mole percent	15
C_{10} mole percent	20
C_{15} mole percent	25
H_2O mole percent	40

Table 4.9 Relative permeability data for three-dimensional case with four component fluid mixture (Case4)

	Water	Oil	Gas
Endpoint	0.8	0.7	0.5
Residual saturation	0.25	0.15	0.06
Exponent	2.5	2.0	1.5

Table 4.10 Summary of input data for one-dimensional case with six component fluid mixture (Case5)

Parameter	Value
Number of gridblocks	50×1×1
Gridblock size	40×40×40 ft^3
Initial temperature	560°R
Initial pressure	650 psia
Reservoir porosity	0.3
Permeability	250 md
Reservoir thermal conductivity	35 Btu/(ft-day-°R)
Caprock thermal conductivity	20 Btu/ft-day-°R
Rock heat capacity	35 Btu/(ft^3-°R)
Injection temperature	1000 °R
Injection pressure	700 psia
Bottomhole production pressure	630 psia

Table 4.11 Relative permeability data for one-dimensional case with six component fluid mixture (Case5)

	Water	Oil	Gas
Endpoint	0.9	0.55	0.6
Residual saturation	0.12	0.2	0.06
Exponent	2.5	2.0	1.5

Table 4.12 Initial oil composition and oil properties for the cases with six component fluid mixture (Cases 5, 6, 7)

Component name	MW	Tc (°R)	Pc (psia)	Mole percent
C_{10}	134.0	1120.11	367.647	0.045
C_{15}	206.0	1270.0	200.00	0.091
C_{19}	263.0	1388.13	221.38	0.091
C_{25}	337.0	1499.19	174.05	0.227
C_{26}^{+}	450.0	1710.33	140.0	90.40
H_2O	18.0	1165.47	3198.72	9.146

Table 4.13 Summary of input data for two-dimensional case with six component fluid mixture (Case6)

Parameter	Value
Number of gridblocks	20×1×3
Gridblock size	40×40×10 ft^3
Permeability (K_h, K_v)	250 md, 100md
Initial temperature	560°R
Initial pressure	650 psia
Injection temperature	800°R
Injection pressure	680 psia
Bottomhole production pressure	630 psia

Table 4.14 Relative permeability data for two-dimensional case with six component fluid mixture (Case6)

	Water	Oil	Gas
Endpoint	0.9	0.55	0.6
Residual saturation	0.12	0.2	0.06
Exponent	2.5	2.0	1.5

Table 4.15 Summary of input data for three-dimensional case with six component fluid mixture (Case7)

Parameter	Value
Number of gridblocks	10×10×5
Gridblock size	50×50×10 ft^3
Initial temperature	560°R
Initial pressure	650 psia
Reservoir porosity	0.3
Permeability	300 md
Reservoir, Caprock thermal conductivity	35, 20 Btu/(ft-day-°R)
Rock heat capacity	35 Btu/(ft^3-°R)
Injection temperature	800 °R
Injection rate	950 Lbmole/day
Bottomhole production pressure	645 psia

Table 4.16 Relative permeability data for three-dimensional case with six component fluid mixture (Case7)

	Water	Oil	Gas
Endpoint	0.7	0.55	0.6
Residual saturation	0.1	0.2	0.06
Exponent	2.5	2.0	1.5

Table 4.17 Summary of input data for parallel processing example (Case9)

Parameter	Value
Number of gridblocks	64×64×7
Gridblock size	1280×1280×70 ft^3
Initial temperature	590°R
Initial pressure	600 psia
Reservoir porosity	0.3
Permeability	250 md
Reservoir thermal conductivity	35 Btu/(ft-day-°R)
Caprock thermal conductivity	30 Btu/ft-day-°R
Rock heat capacity	35 Btu/(ft^3-°R)
Injection temperature	850°R
Injection rate	2000 Lbmole/day
Bottomhole production pressure	570 psia

Table 4.18 Relative permeability data for parallel processing example (Case9)

	Water	Oil	Gas
Endpoint	0.78	0.65	0.6
Residual saturation	0.2	0.25	0.06
Exponent	2.5	2.0	1.5

Table 4.19 Initial oil composition and oil properties for parallel processing example (Case9)

Component name	MW	Tc (°R)	Pc (psia)	Mole percent
C_{10}	134.0	1120.11	367.647	0.04
C_{15}	206.0	1270.0	200.0	0.06
C_{27}^{+}	520.0	1750.2	137.0	9.9
H_2O	18.015	1165.47	3198.72	90.0

Table 4.20 Summary of input data for corner point option (Case10)

Parameter	Value
Number of gridblocks	16×16×10
Gridblock size	560×560×100 ft^3
Initial temperature	590°R
Initial pressure	500 psia
Reservoir porosity	0.3
Permeability	100 md
Reservoir thermal conductivity	35 Btu/(ft-day-°R)
Caprock thermal conductivity	10 Btu/ft-day-°R
Rock heat capacity	35 Btu/(ft^3-°R)
Injection temperature	750°R
Injection rate	500 Lbmole/day
Bottomhole production pressure	500 psia

Table 4.21 Relative permeability data for corner point option (Case10)

	Water	Oil	Gas
Endpoint	0.4	0.9	0.9
Residual saturation	0.3	0.1	0.0
Exponent	3.0	2.0	2.0

Table 4.22 Initial oil composition and oil properties for corner point option (Case10)

Component name	MW	Tc (°R)	Pc (psia)	Mole percent
C_{10}	134.0	1120.11	367.647	0.70
H_2O	18.0	1165.47	3198.72	0.30

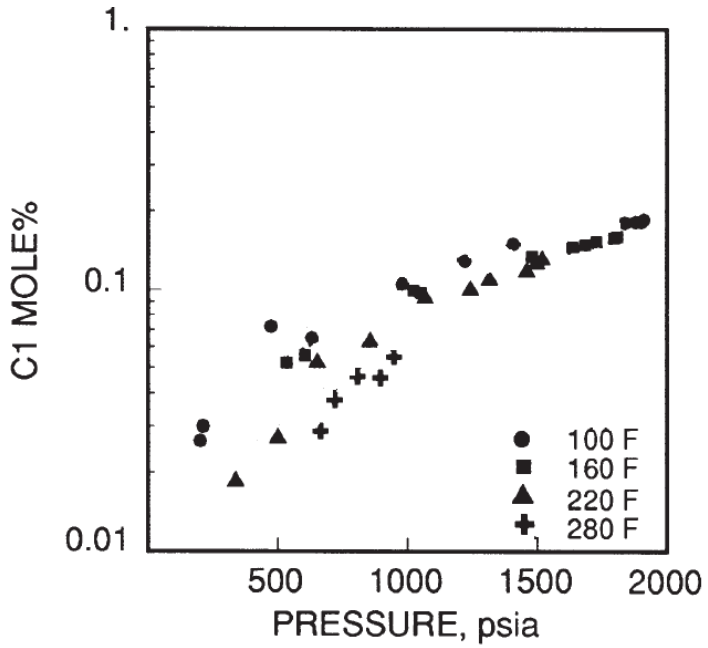

Figure 4.1 Solubility of C_1 in water-rich liquid phase of C_1/n-C_4/H_2O system, (McKetta and Katz, 1948)

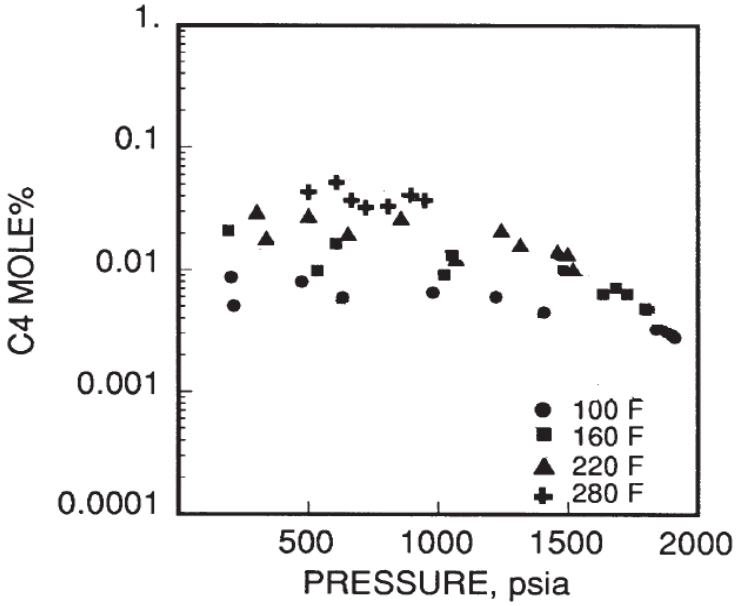

Figure 4.2 Solubility of C_4 in water-rich liquid phase of C_1/n-C_4/H_2O system (McKetta and Katz, 1948)

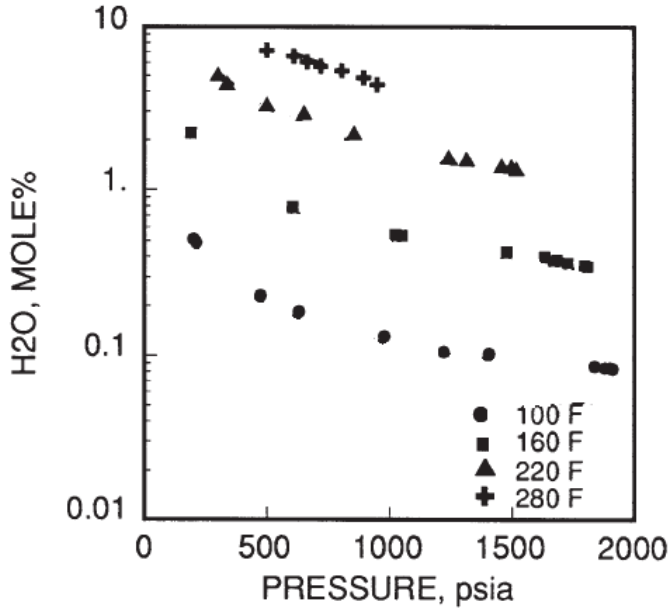

Figure 4.3 Solubility of H_2O in gas phase of C_1/n-C_4/H_2O system (McKetta and Katz, 1948)

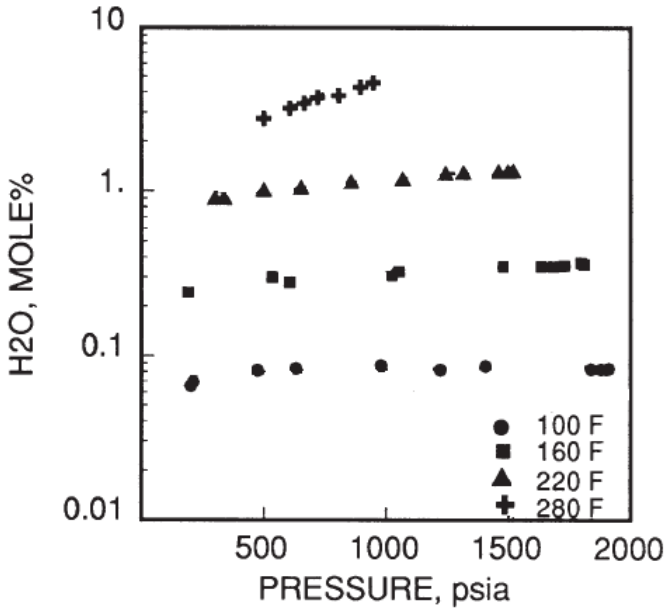

Figure 4.4 Solubility of H_2O in hydrocarbon-rich liquid phase of C1/n-C_4/H_2O system (McKetta and Katz, 1948)

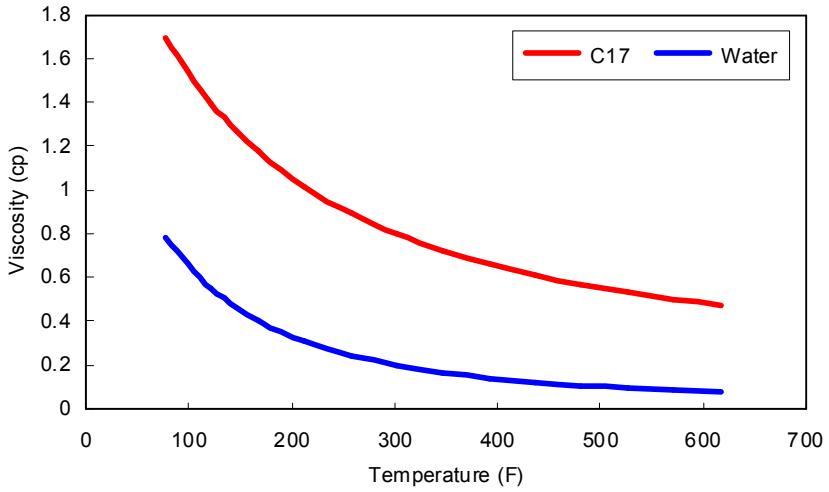

Figure 4.5 Viscosity of water and C_{17} versus temperature using Andrade's equation (1934)

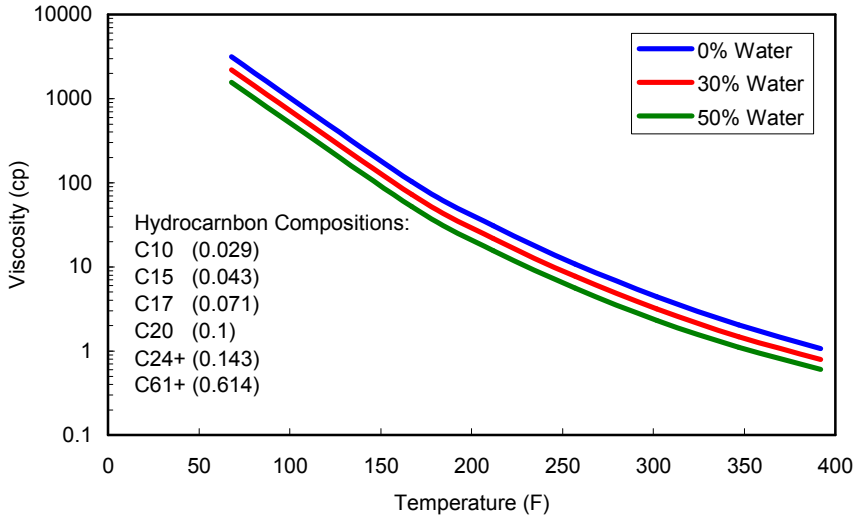

Figure 4.6 Effect of solubility of water on viscosity

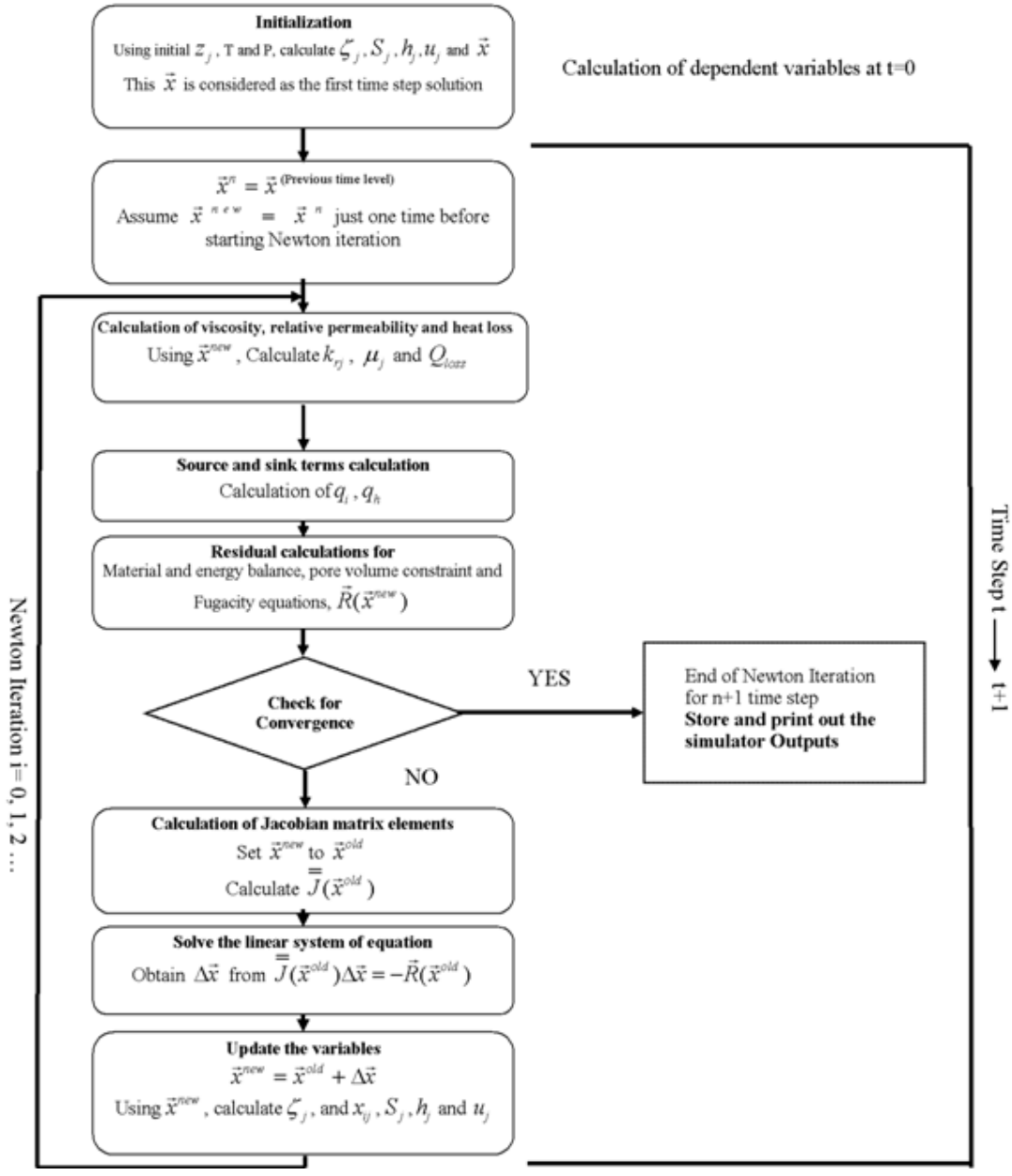

Figure 4.7 Computational flow chart for the hot fluid injection model

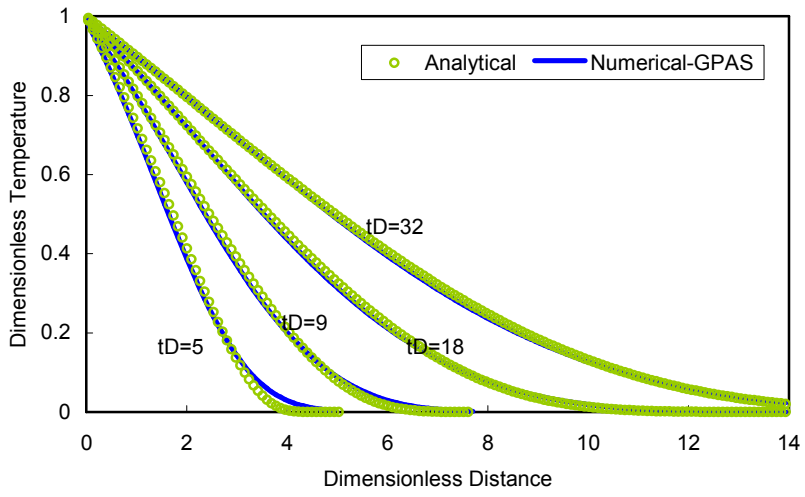

Figure 4.8 Comparison of temperature distribution using GPAS and analytical solution for compositional thermal model (Case 1)

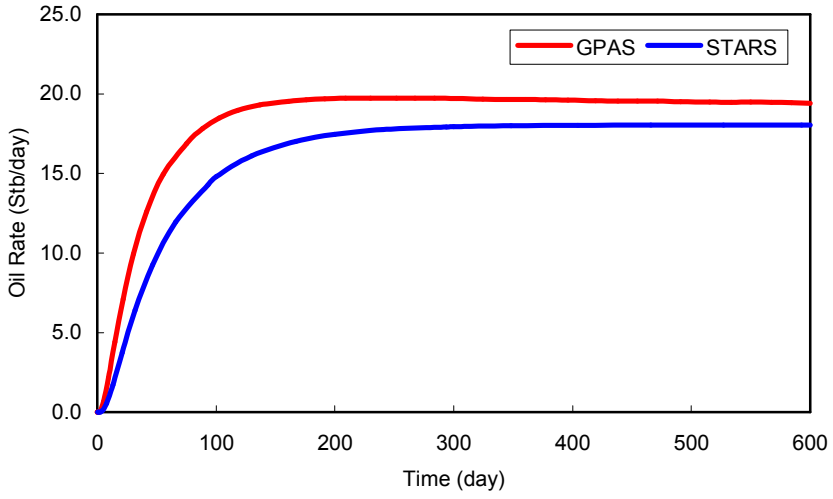

Figure 4.9 Comparison of oil rate between GPAS and K-value approach method for one-dimensional case with four component fluid mixture (Case 2)

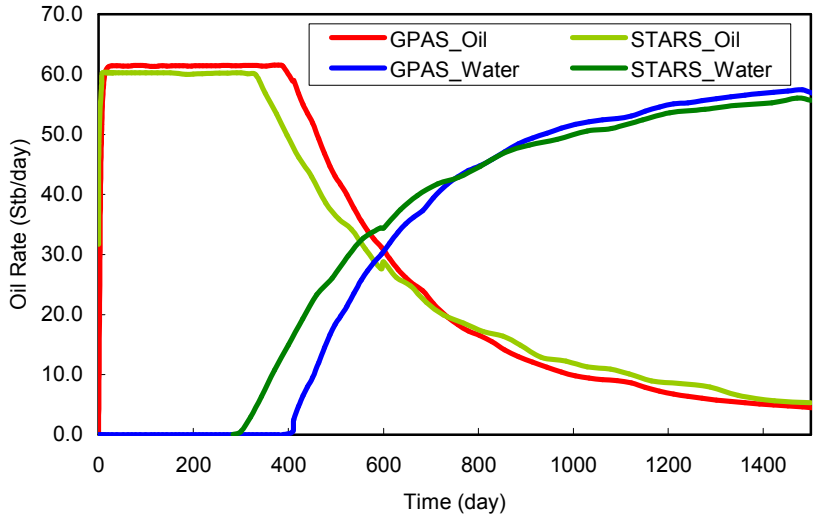

Figure 4.10 Comparison of oil and water rate of GPAS and K-value approach method for two-dimensional with four component fluid mixture (Case 3)

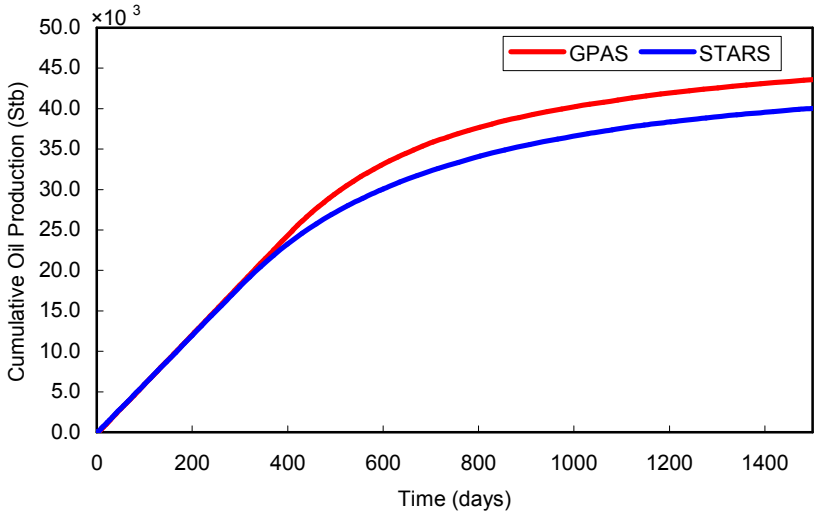

Figure 4.11 Comparison of cumulative oil production for GPAS and K-value approach method for two-dimensional with four component fluid mixture (Case 3)

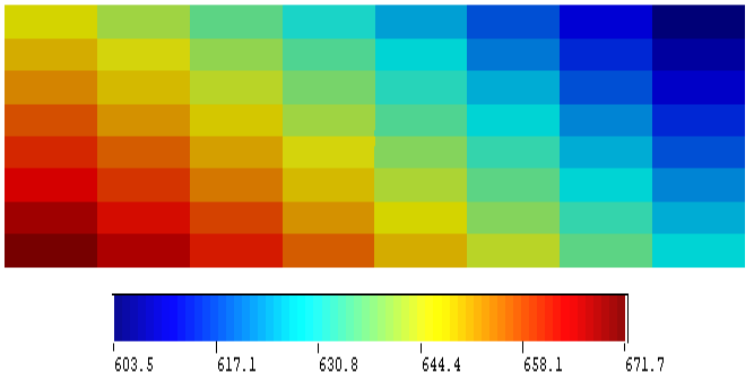

Figure 4.12 Pressure (Psia) distribution at the end of simulation for two-dimensional with four component fluid mixture (Case 3)

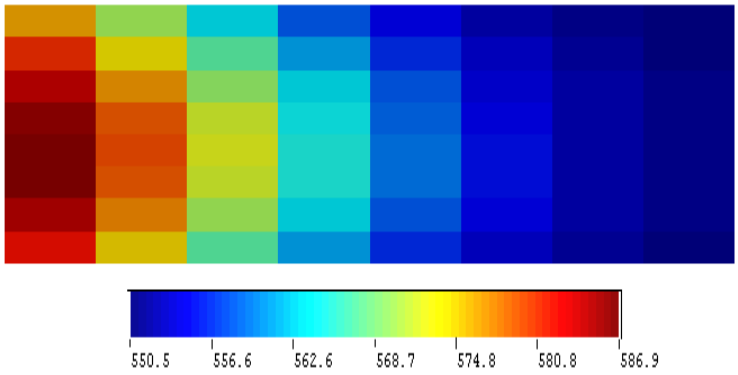

Figure 4.13 Temperature (°R) distribution at the end of simulation for two-dimensional with four component fluid mixture (Case 3)

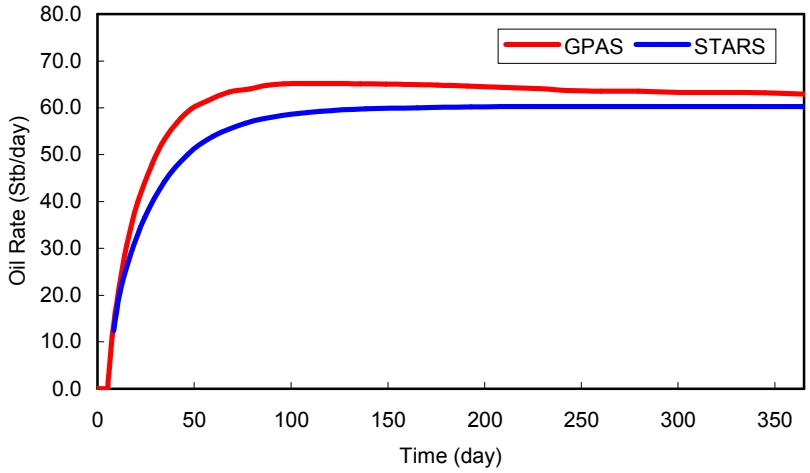

Figure 4.14 Comparison of oil rate of GPAS and K-value approach method for three-dimensional case study with four component fluid mixture (Case 4)

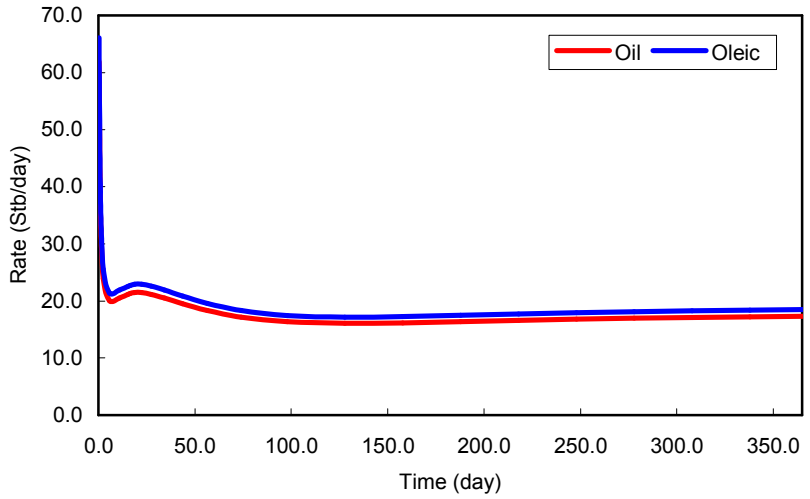

Figure 4.15 Oil and oleic rates for one-dimensional case study with six component fluid mixture (Case 5)

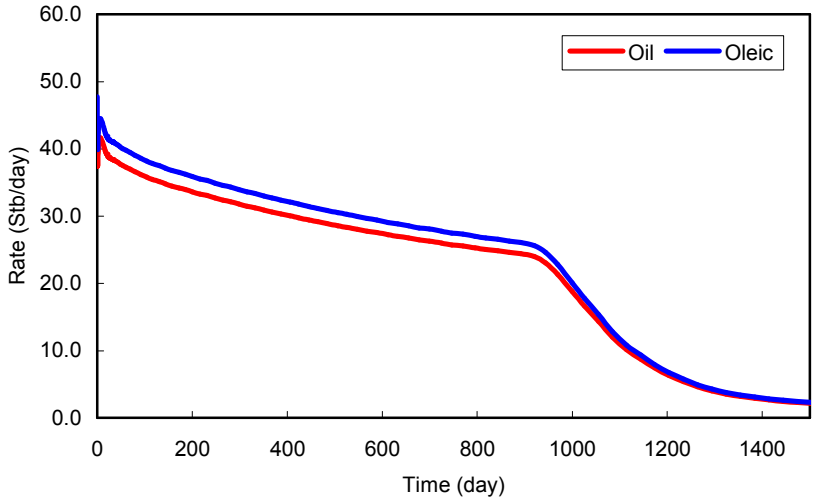

Figure 4.16 Oil and oleic rates for two-dimensional case study with six component fluid mixture (Case 6)

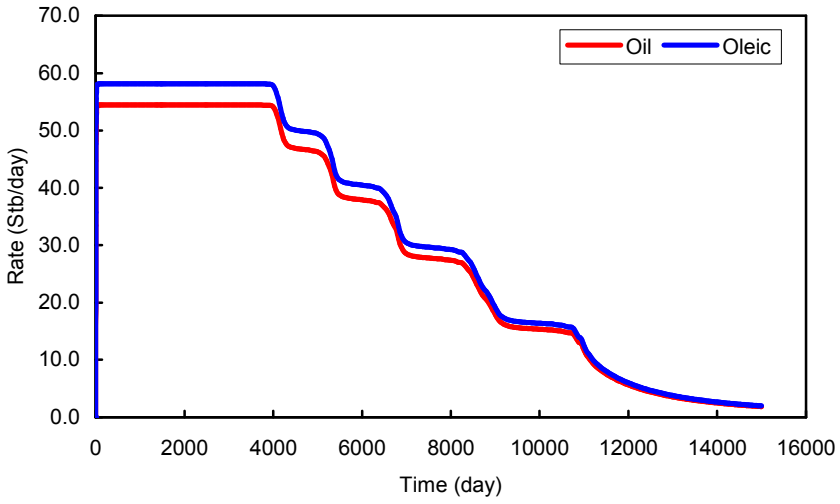

Figure 4.17 Oil and oleic rates for three-dimensional case study with six component fluid mixture (Case 7)

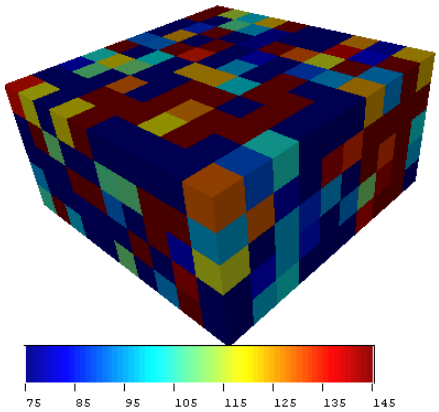

Figure 4.18 Permeability (md) in *x* direction for V_{DP} of 0.5

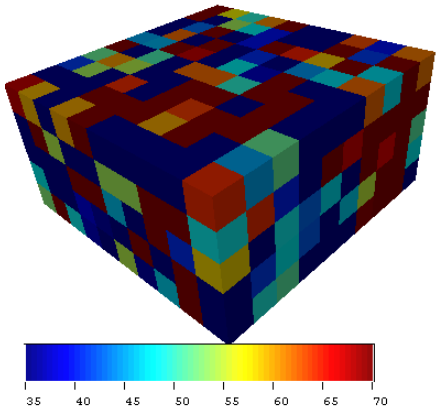

Figure 4.19 Permeability (md) in *y* direction for V_{DP} of 0.5

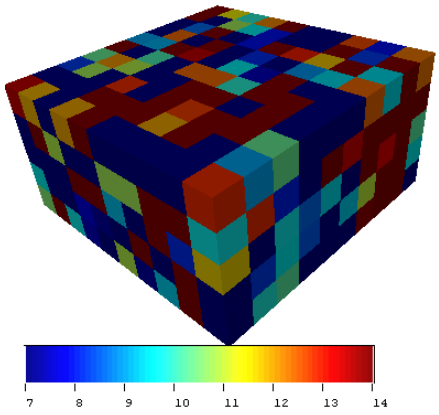

Figure 4.20 Permeability (md) in z direction for V_{DP} of 0.5

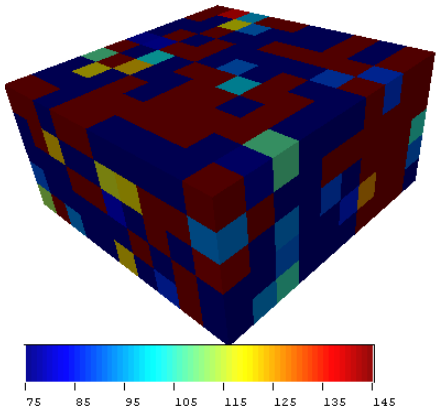

Figure 4.21 Permeability (md) in *x* direction for V_{DP} of 0.8

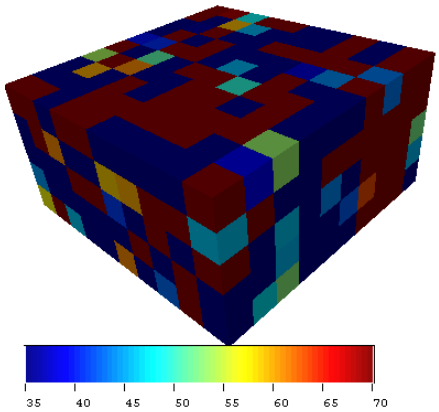

Figure 4.22 Permeability (md) in *y* direction for V_{DP} of 0.8

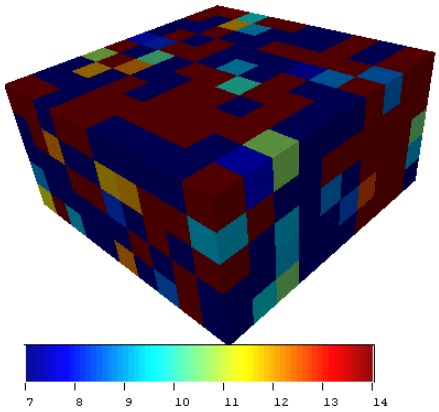

Figure 4.23 Permeability (md) in *z* direction for V_{DP} of 0.8

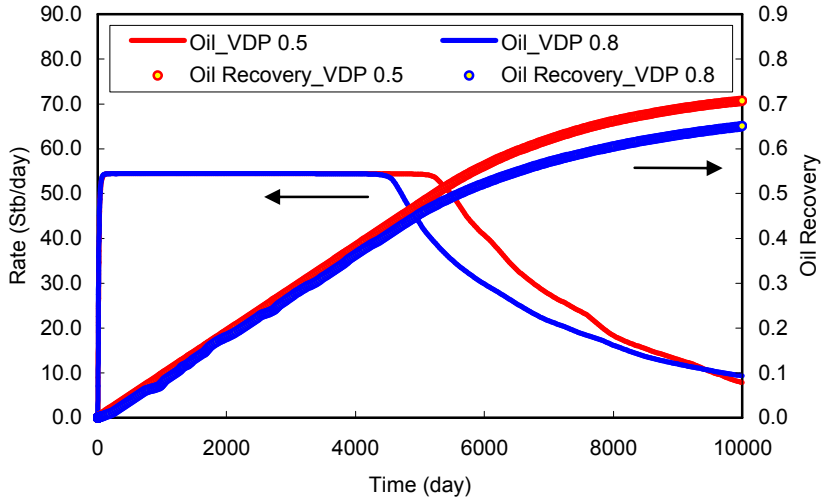

Figure 4.24 Oil rates and oil recoveries of V_{DP} 0.5 and 0.8 for three-dimensional, heterogeneous case with six component fluid mixture (Case 8)

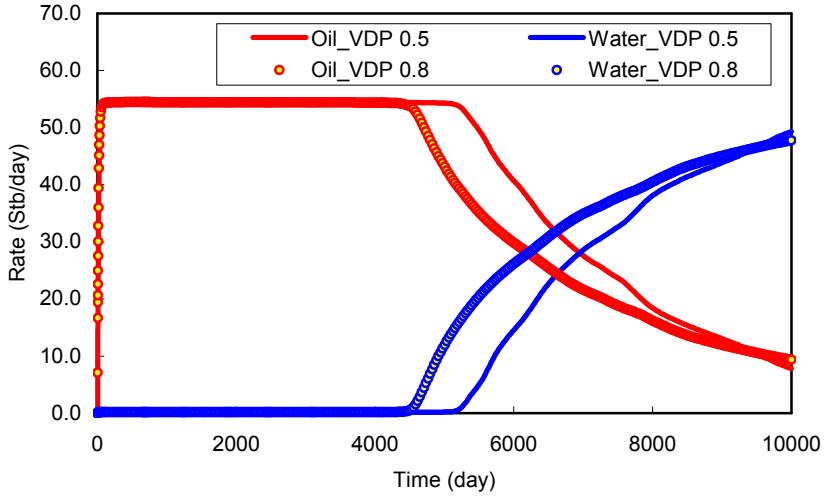

Figure 4.25 Oil and water rates of V_{DP} 0.5 and 0.8 for three-dimensional, heterogeneous case with six component fluid mixture (Case 8)

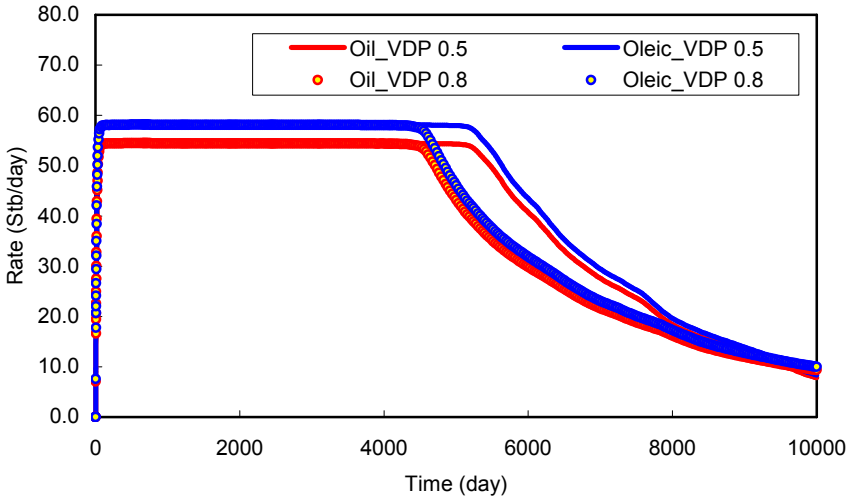

Figure 4.26 Oil, oleic rates of V_{DP} 0.5 and 0.8 for three-dimensional, heterogeneous case with six component fluid mixture (Case 8)

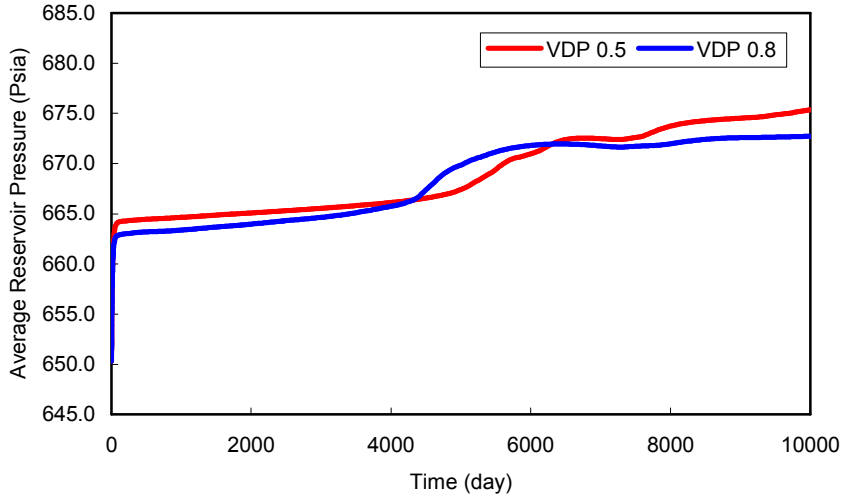

Figure 4.27 Average reservoir pressure at V_{DP} 0.5 and 0.8 for three-dimensional, heterogeneous case with six component fluid mixture (Case 8)

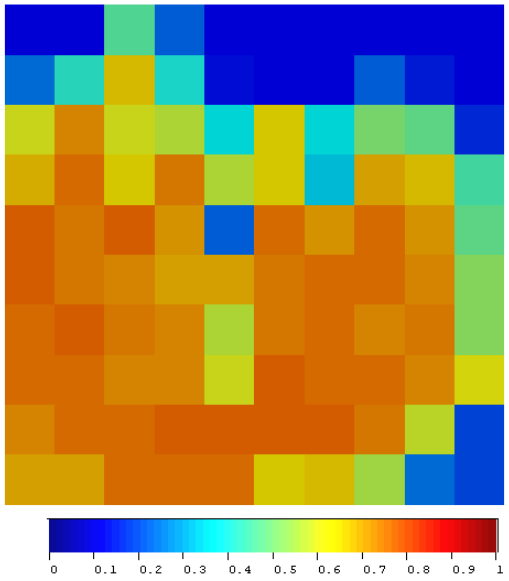

Figure 4.28 Aqueous phase saturation after 3800 days for V_{DP} 0.8 of three-dimensional, heterogeneous case with six component fluid mixture

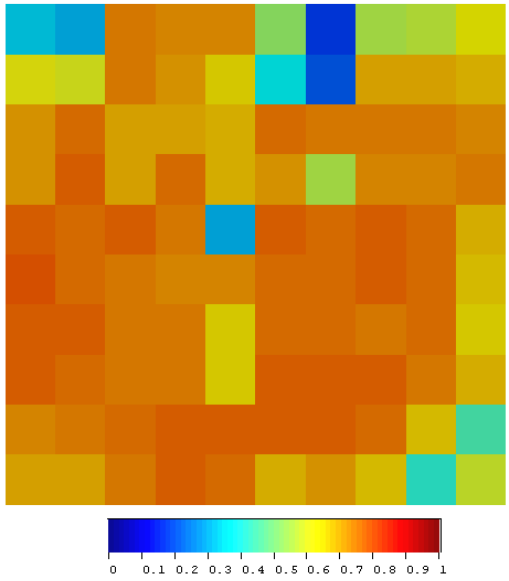

Figure 4.29 Aqueous phase saturation after 4180 days for V_{DP} 0.8 of three-dimensional, heterogeneous case with six component fluid mixture

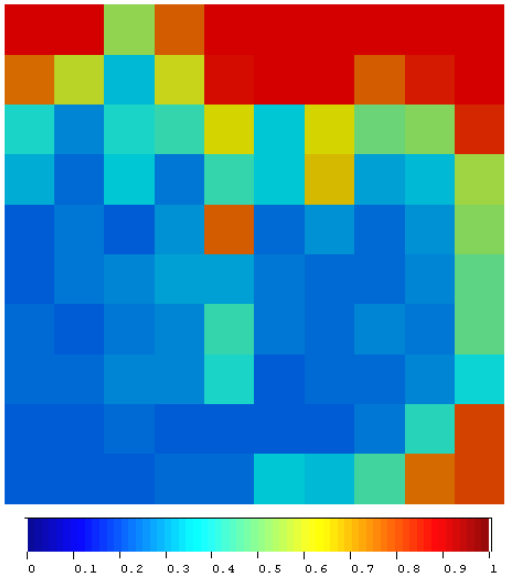

Figure 4.30 Oil phase saturation after 3800 days for V_{DP} 0.8 of three-dimensional, heterogeneous case with six component fluid mixture

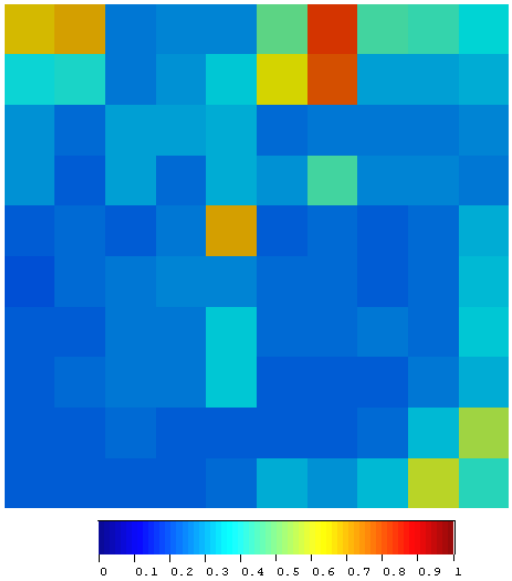

Figure 4.31 Oil phase saturation after 4180 days for V_{DP} 0.8 of three-dimensional, heterogeneous case with six component fluid mixture

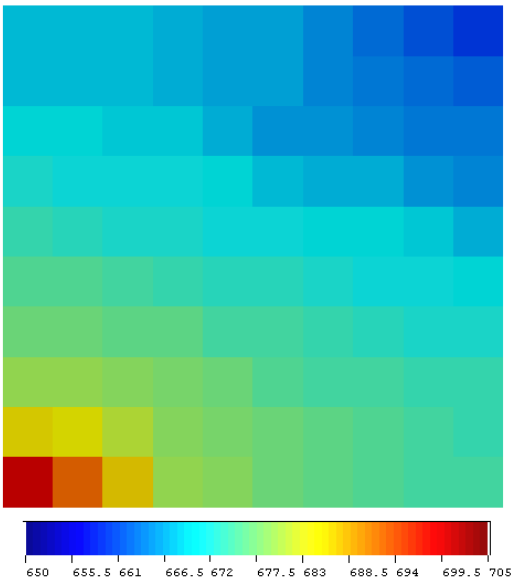

Figure 4.32 Pressure distributions after 3800 days for V_{DP} 0.8 of three-dimensional, heterogeneous case with six component fluid mixture

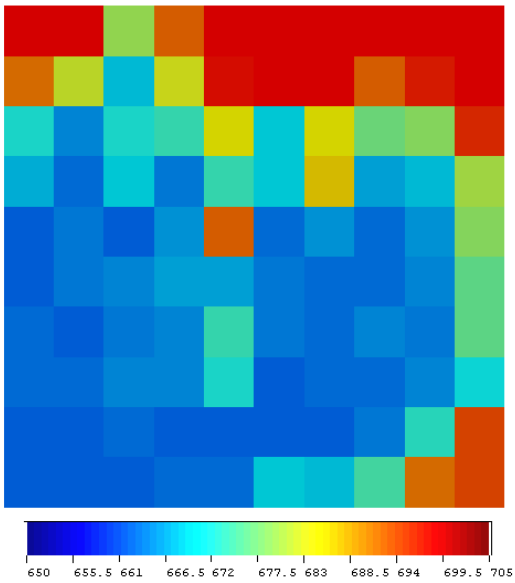

Figure 4.33 Pressure distributions after 4180 days for V_{DP} 0.8 three-dimensional, heterogeneous case with six component fluid mixture

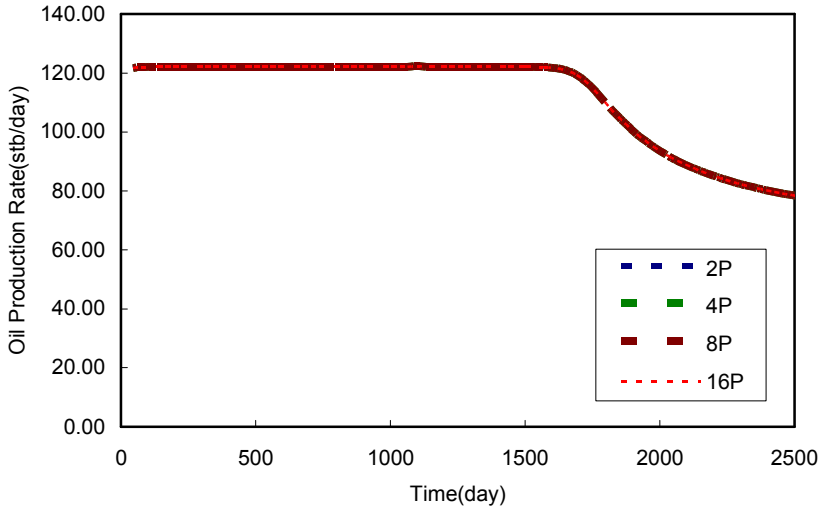

Figure 4.34 Oil rate for parallel processing example (Case 9)

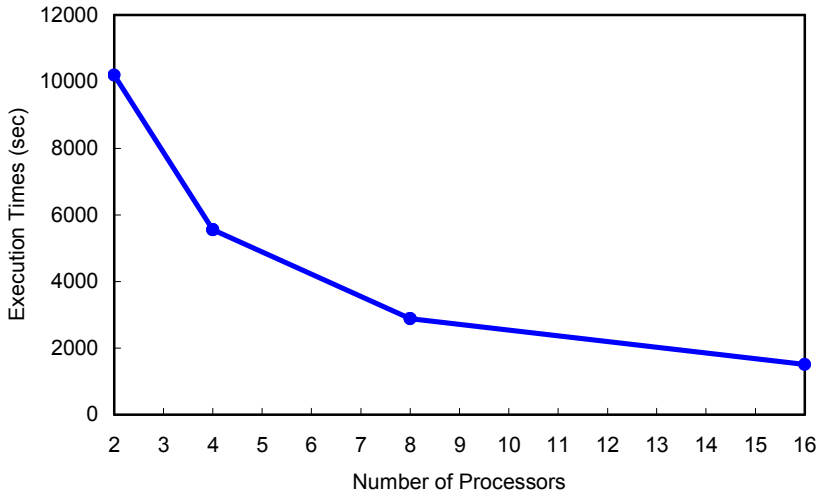

Figure 4.35 Execution time for parallel processing example (Case 9)

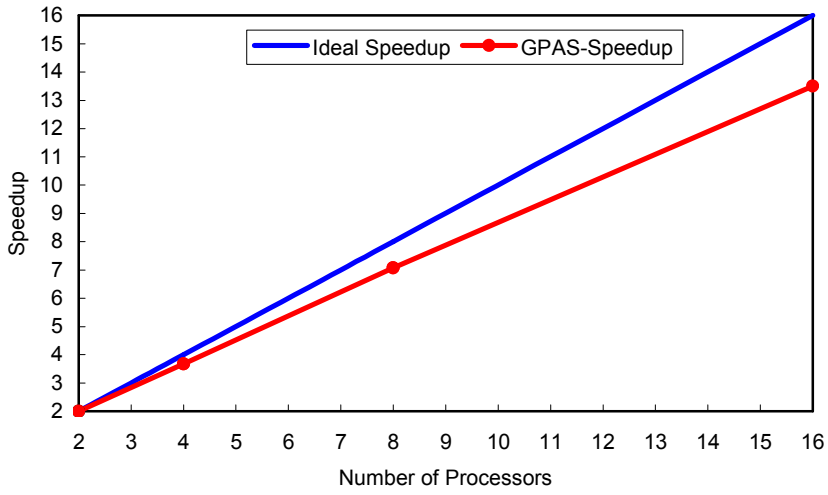

Figure 4.36 Speedup for parallel processing example (Case 9)

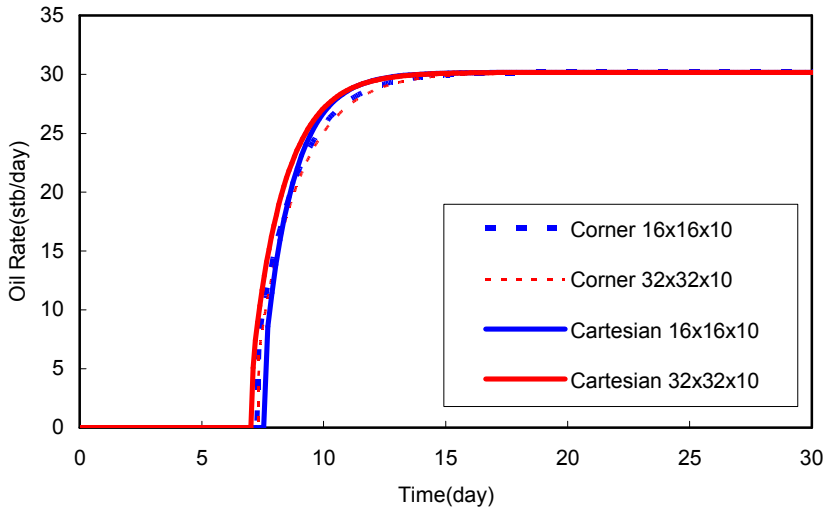

Figure 4.37 Oil rate for corner point option (Case 10)

Chapter 5: Electrical Heating Model

After the implementation of the thermal compositional reservoir simulation for GPAS, another thermal recovery process, the electrical heating was incorporated. This recovery method can be used for heavy oil reservoirs with thin pay zone of less than 10 m. Due to the heat loss from the reservoir, especially to overburden, steam injection and other thermal recovery methods for this kind of reservoirs may not be economical. Electromagnetic heating can introduce heat to the reservoir more efficiently. The modeling of the heating process can be done by the current continuity equation, petrochemical properties, and heat rate equation pertaining to electrical conduction.

The Maxwell's equations are solved using defined boundary conditions to find the electrical field. The assumptions of the model are mentioned in next sentences. The principle axis of conductivity tensor is parallel to the coordinate axis. The electrical properties do not depend on the electrical fields. The produced electrical field by charging the magnetic field is neglected by considering quasi-static approximations. Boundary conditions are defined as gridbblock voltage, and electrical current flows through the reservoir due to the potential difference between the adjacent gridblocks. The voltage difference between the adjacent gridblocks leads to have electrical current flow with definition of geometric term and resistances. The electrical field is expressed in term of scalar electrical potential. Finally, imaginary part of potential is zero.

5.1 GOVERNING EQUATION

There are two main equations in this model: The current continuity equation and the heat generation by Ohm's law (STARS, 2006.10).

5.1.1 Current Continuity Equation

The differential of the current continuity equation is as follows:

$$\nabla \cdot (\sigma \nabla \psi) = 0 \tag{5.1}$$

with σ and ψ, the diagonal tensor of electrical conductivity and the real scalar electrical potential, respectively.

In the case of three-dimensional Cartesian grids, the above equation becomes

$$\frac{\partial}{\partial x}\left[\sigma_x \frac{\partial \psi}{\partial x}\right] + \frac{\partial}{\partial y}\left[\sigma_y \frac{\partial \psi}{\partial y}\right] + \frac{\partial}{\partial z}\left[\sigma_z \frac{\partial \psi}{\partial z}\right] = 0 \tag{5.2}$$

5.1.2 Heat Generation

Heat generation due to potential difference and current can be determined by the following equation:

$$Q = \sigma_x \left[\frac{\partial \psi}{\partial x}\right]^2 + \sigma_y \left[\frac{\partial \psi}{\partial y}\right]^2 + \sigma_z \left[\frac{\partial \psi}{\partial z}\right]^2 \tag{5.3}$$

5.2 RESIDUAL EQUATION OF THE ELECTRICAL CURRENT EQUATION AND RELATED DERIVATIVES

The resistances between the gridblocks and also the current equation in three-dimensional model are described in this section.

5.2.1 Geometric Factor and Resistance in *x* Direction

There are two separate resistances between gridblock *i* and *i*+1 for current flow between two grids, from center block *i* to common block face *i*+1/2 and from block faces *i*+1/2 and *i*+1. The calculations of the resistances are as follows:

Cross-sectional area = $\Delta y. \Delta z$

Distance from *i* to *i*+1/2 = $\Delta x/2$

Geometric factor is $T_i = \Delta x/2/ (\Delta y. \Delta z)$

Resistance from *i* to *i*+1/2 is $R_i = T_i/\sigma_i$

Resistance from *i*+1/2 to *i*+1 is $R_{i+1} = T_{i+1}/\sigma_{i+1}$

5.2.2 Geometric Factor and Resistance in *y* Direction

There are two separate resistances between gridblock *j* and *j*+1 for current flow between two grids, from center block *j* to common block face *j*+1/2 and from block face *j*+1/2 and *j*+1. The calculations of the resistances are as follows:

Cross-sectional area = $\Delta x. \Delta z$

Distance from *j* to *j*+1/2 = $\Delta x/2$

Geometric factor is $T_j = \Delta y/2/ (\Delta x. \Delta z)$

Resistance from *j* to *j*+1/2 is $R_j = T_j/\sigma_j$

Resistance from *j*+1/2 to j+1 is $R_{j+1} = T_{j+1}/\sigma_{j+1}$

5.2.3. Geometric Factor and Resistance in *z* Direction

There are two separate resistances between gridblock *k* and *k*+1 for current flow between two grids, from center block *k* to common block face *k*+1/2 and from block face *k*+1/2 and *k*+1. The calculations of the resistances are as follows:

Cross-sectional area = $\Delta x. \Delta y$

Distance from k to k+1/2 = $\Delta z/2$

Geometric factor is $T_k = \Delta z/2/ (\Delta x. \Delta y)$

Resistance from k to k+1/2 is $R_k = T_k/\sigma_k$

Resistance from k+1/2 to k+1 is $R_{k+1} = T_{k+1}/\sigma_{k+1}$

5.2.4 Residual Equation

For the current from gridblock i to i+1 we have

$$I_{i-1\to i,j,k} - I_{i\to i+1,j,k} = 0 \tag{5.4}$$

$$I_{i,j-1\to j,k} - I_{i,j\to j+1,k} = 0 \tag{5.5}$$

$$I_{i,j,k-1\to k} - I_{i,j,k\to k+1} = 0 \tag{5.6}$$

The residual equation for each direction is as follows:

$$R_{ix} = I_{i-1\to i,j,k} - I_{i\to i+1,j,k} \tag{5.7}$$

$$R_{iy} = I_{i,j-1\to j,k} - I_{i,j\to j+1,k} \tag{5.8}$$

$$R_{iz} = I_{i,j,k-1\to k} - I_{i,j,k\to k+1} \tag{5.9}$$

$$R_I = I_{i-1\to i,j,k} - I_{i\to i+1,j,k} + I_{i,j-1\to j,k} - I_{i,j\to j+1,k} + I_{i,j,k-1\to k} - I_{i,j,k\to k+1} \tag{5.10}$$

$$R_I = \frac{V_{i-1,j,k} - V_{i,j,k}}{R_{i-1,j,k} + R_{i,j,k}} - \frac{V_{i,j,k} - V_{i+1,j,k}}{R_{i,j,k} + R_{i+1,j,k}} + \frac{V_{i,j-1,k} - V_{i,j,k}}{R_{i,j-1,k} + R_{i,j,k}} - \frac{V_{i,j,k} - V_{i,j+1,k}}{R_{i,j,k} + R_{i,j+1,k}} + \frac{V_{i,j,k-1} - V_{i,j,k}}{R_{i,j,k-1} + R_{i,j,k}} - \frac{V_{i,j,k} - V_{i,j,k+1}}{R_{i,j,k} + R_{i,j,k+1}} \tag{5.11}$$

The resistance factor from i to i+1/2

$$R_p = T_p \ / \sigma_p \ , p = i, j, k \tag{5.12}$$

5.2.5 Electrical Conductivity

The electrical conductivity for aqueous phase $\sigma_{aq,p}(T)$, oil phase $\sigma_{o,p}(T)$, gas phase $\sigma_{g,p}(T)$, solid phase $\sigma_{s,p}(T)$, and rock $\sigma_{r,p}(T)$ are provided by the user.

$$\sigma_{aq_i,p}(T) = \sum_i w_i . \sigma_{aq,i,p}(T) \tag{5.13}$$

where w_i, $\sigma_{aq,i,p}(T)$ are the mole fraction and the electrical conductivity of the aqueous phase components.

The water phase conductivity, which also depends on fluid porosity and water saturation, is calculated by Archie's equation (STARS, 2006.10):

$$\sigma_{aq,p}(T, \phi_f, S_w) = \sigma_{aq_i,p}(T) \left[\phi_f^{1.7} \, S_{aq}^2 / 0.88 \right], \quad p = i, j, k \tag{5.14}$$

$$\phi_f = 1 - \frac{Solid\ phase\ volume}{Pore\ Volume} \tag{5.15}$$

$$\phi_v = \frac{Pore\ volume}{Bulk\ Volume} \tag{5.16}$$

$$\sigma_{s,p}(T) = \sum_i (c_i / c_s)\sigma_{s,i,p}(T) \tag{5.17}$$

where c_i, c_s *and* $\sigma_{s,i,p}(T)$ are the concentration of component *i* in solid phase, the sum of the concentration of component *i* in solid phase, and the electrical conductivity of component *i* in solid phase, respectively.

Therefore, the bulk electrical conductivity is calculated as follows:

$$\sigma_p = \sigma_{w,p}(T, \phi_f, S_w) + \sigma_{r,p}(T)(1-\phi_v) + \sigma_{s,p}(T)(\phi_v - \phi_f) + \sigma_{o,p}(T)\phi_f S_o,\ p = i, j, k \tag{5.18}$$

5.3 HEAT GENERATION

The heat generation is the sum of heat rates for each gridblock corresponding to currents flowing into that gridblock.

If we consider current flow from grid block i to gridblock *i*+1

$$I_{i \to i+1} = \frac{V_i - V_{i+1}}{R_i + R_{i+1}} \tag{5.19}$$

$$Q_i = (I_{i \to i+1})^2 R_i \tag{5.20}$$

$$Q_{i+1} = (I_{i \to i+1})^2 R_{i+1} \tag{5.21}$$

The net heat generation for this gridblock is

$$\begin{aligned} Q_{gen\_i} &= (I_{i-1\to i,j,k})^2 R_{i-1/2\to i,j,k} + (I_{i\to i+1,j,k})^2 R_{i\to i+1/2,j,k} \\ &+ (I_{i,j-1\to j,k})^2 R_{i,j-1/2\to j,k} + (I_{i,j\to j+1,k})^2 R_{i,j\to j+1/2,k} \\ &+ (I_{i,j,k-1\to k})^2 R_{i,j,k-1/2\to k} + (I_{i,j,k\to k+1})^2 R_{i,j,k\to k+1/2} \end{aligned} \tag{5.22}$$

5.4 DERIVATIVES FOR ELECTRICAL HEATING MODEL

The derivatives of current residual equation and the related derivatives for the electrical heating model are presented in Appendix F.

Solution Procedure

To solve the system of equations, it is necessary to have the residual from the previous time-step and to construct the Jacobian matrix.

$$\delta \mathrm{P} = \mathrm{P}^{n+1} - \mathrm{P}^{n} = -\vec{\vec{J}}^{-1} R^{n} \tag{5.23}$$

P is the primary variable and the R is the residual of the equations. The residual of the governing equations and also the construction of the Jacobian matrix are given as follows:

$$\begin{pmatrix} J_{1,1} & J_{1,2} & \cdots & J_{1,n_b} \\ J_{2,1} & J_{2,2} & \cdots & J_{2,n_b} \\ \vdots & & & \vdots \\ J_{n_b,1} & J_{n_b,2} & \cdots & J_{n_b,n_b} \end{pmatrix} \begin{pmatrix} \Delta\vec{x}_1 \\ \Delta\vec{x}_2 \\ \vdots \\ \Delta\vec{x}_{n_b} \end{pmatrix} = - \begin{pmatrix} \vec{R}_1 \\ \vec{R}_2 \\ \vdots \\ \vec{R}_{n_b} \end{pmatrix}$$

$$
J_{I,J} = \begin{bmatrix}
\frac{\partial R_{F1,1}|_I}{\partial LnK_{1,1}|_J} & \cdots & \frac{\partial R_{F1,1}|_I}{\partial LnK_{1,nc+1}|_J} & \frac{\partial R_{F1,1}|_I}{\partial LnK_{2,1}|_J} & \cdots & \frac{\partial R_{F1,1}|_I}{\partial LnK_{2,nc+1}|_J} & \frac{\partial R_{F1,1}|_I}{\partial N_1|_J} & \cdots & \frac{\partial R_{F1,1}|_I}{\partial N_{nc+1}|_J} & \frac{\partial R_{F1,1}|_I}{\partial P|_J} & \frac{\partial R_{F1,1}|_I}{\partial T|_J} & 0 \\
\vdots & \vdots & \vdots & \vdots & \vdots & \vdots & \vdots & \vdots & \vdots & \vdots & \vdots & \vdots \\
\frac{\partial R_{F1,nc+1}|_I}{\partial LnK_{1,1}|_J} & \cdots & \frac{\partial R_{F1,nc+1}|_I}{\partial LnK_{1,nc+1}|_J} & \frac{\partial R_{F1,nc+1}|_I}{\partial LnK_{2,1}|_J} & \cdots & \frac{\partial R_{F1,nc+1}|_I}{\partial LnK_{2,nc+1}|_J} & \frac{\partial R_{F1,nc+1}|_I}{\partial N_1|_J} & \cdots & \frac{\partial R_{F1,nc+1}|_I}{\partial N_{nc+1}|_J} & \frac{\partial R_{F1,nc+1}|_I}{\partial P|_J} & \frac{\partial R_{F1,nc+1}|_I}{\partial T|_J} & 0 \\
\frac{\partial R_{F2,1}|_I}{\partial LnK_{1,1}|_J} & \cdots & \frac{\partial R_{F2,1}|_I}{\partial LnK_{1,nc+1}|_J} & \frac{\partial R_{F2,1}|_I}{\partial LnK_{2,1}|_J} & \cdots & \frac{\partial R_{F2,1}|_I}{\partial LnK_{2,nc+1}|_J} & \frac{\partial R_{F2,1}|_I}{\partial N_1|_J} & \cdots & \frac{\partial R_{F2,1}|_I}{\partial N_{nc+1}|_J} & \frac{\partial R_{F2,1}|_I}{\partial P|_J} & \frac{\partial R_{F2,1}|_I}{\partial T|_J} & 0 \\
\vdots & \vdots & \vdots & \vdots & \vdots & \vdots & \vdots & \vdots & \vdots & \vdots & \vdots & \vdots \\
\frac{\partial R_{F2,nc+1}|_I}{\partial LnK_{1,1}|_J} & \cdots & \frac{\partial R_{F2,nc+1}|_I}{\partial LnK_{1,nc+1}|_J} & \frac{\partial R_{F2,nc+1}|_I}{\partial LnK_{2,1}|_J} & \cdots & \frac{\partial R_{F2,nc+1}|_I}{\partial LnK_{2,nc+1}|_J} & \frac{\partial R_{F2,nc+1}|_I}{\partial N_1|_J} & \cdots & \frac{\partial R_{F2,nc+1}|_I}{\partial N_{nc+1}|_J} & \frac{\partial R_{F2,nc+1}|_I}{\partial P|_J} & \frac{\partial R_{F2,nc+1}|_I}{\partial T|_J} & 0 \\
\frac{\partial R_{v}|_I}{\partial LnK_{1,1}|_J} & \cdots & \frac{\partial R_{v}|_I}{\partial LnK_{1,nc+1}|_J} & \frac{\partial R_{v}|_I}{\partial LnK_{2,1}|_J} & \cdots & \frac{\partial R_{v}|_I}{\partial LnK_{2,nc+1}|_J} & \frac{\partial R_{v}|_I}{\partial N_1|_J} & \cdots & \frac{\partial R_{v}|_I}{\partial N_{nc+1}|_J} & \frac{\partial R_{v}|_I}{\partial P|_J} & \frac{\partial R_{v}|_I}{\partial T|_J} & 0 \\
\frac{\partial R_{m,1}|_I}{\partial LnK_{1,1}|_J} & \cdots & \frac{\partial R_{m,1}|_I}{\partial LnK_{1,nc+1}|_J} & \frac{\partial R_{m,1}|_I}{\partial LnK_{2,1}|_J} & \cdots & \frac{\partial R_{m,1}|_I}{\partial LnK_{2,nc+1}|_J} & \frac{\partial R_{m,1}|_I}{\partial N_1|_J} & \cdots & \frac{\partial R_{m,1}|_I}{\partial N_{nc+1}|_J} & \frac{\partial R_{m,1}|_I}{\partial P|_J} & \frac{\partial R_{m,1}|_I}{\partial T|_J} & 0 \\
\vdots & \vdots & \vdots & \vdots & \vdots & \vdots & \vdots & \vdots & \vdots & \vdots & \vdots & \vdots \\
\frac{\partial R_{m,nc+1}|_I}{\partial LnK_{1,1}|_J} & \cdots & \frac{\partial R_{m,nc+1}|_I}{\partial LnK_{1,nc+1}|_J} & \frac{\partial R_{m,nc+1}|_I}{\partial LnK_{2,1}|_J} & \cdots & \frac{\partial R_{m,nc+1}|_I}{\partial LnK_{2,nc+1}|_J} & \frac{\partial R_{m,nc+1}|_I}{\partial N_1|_J} & \cdots & \frac{\partial R_{m,nc+1}|_I}{\partial N_{nc+1}|_J} & \frac{\partial R_{m,nc+1}|_I}{\partial P|_J} & \frac{\partial R_{m,nc+1}|_I}{\partial T|_J} & \vdots \\
\frac{\partial R_{E}|_I}{\partial LnK_{1,1}|_J} & \cdots & \frac{\partial R_{E}|_I}{\partial LnK_{1,nc+1}|_J} & \frac{\partial R_{E}|_I}{\partial LnK_{2,1}|_J} & \cdots & \frac{\partial R_{E}|_I}{\partial LnK_{2,nc+1}|_J} & \frac{\partial R_{E}|_I}{\partial N_1|_J} & \cdots & \frac{\partial R_{E}|_I}{\partial N_{nc+1}|_J} & \frac{\partial R_{E}|_I}{\partial P|_J} & \frac{\partial R_{E}|_I}{\partial T|_J} & \frac{\partial R_{E}|_I}{\partial V|_J} \\
\frac{\partial R_{I}|_I}{\partial LnK_{1,1}|_J} & \cdots & \frac{\partial R_{I}|_I}{\partial LnK_{1,nc+1}|_J} & \frac{\partial R_{I}|_I}{\partial LnK_{2,1}|_J} & \cdots & \frac{\partial R_{I}|_I}{\partial LnK_{2,nc+1}|_J} & \frac{\partial R_{I}|_I}{\partial N_1|_J} & \cdots & \frac{\partial R_{I}|_I}{\partial N_{nc+1}|_J} & \frac{\partial R_{I}|_I}{\partial P|_J} & \frac{\partial R_{I}|_I}{\partial T|_J} & \frac{\partial R_{I}|_I}{\partial V|_J}
\end{bmatrix}
$$

The flowchart of this model is presented in Figure 5.1.

5.5 CASE STUDIES OF ELECTRICAL HEATING MODEL

The validation of the electrical current equation and cases studies of the electrical heating model are presented in this section. The keywords of the input file and also a sample input file are presented in Appendix G.

Case 1: One-Dimensional Case with Single Phase Fluid. To verify the electrical heating model, results of the model were compared with the CMG-STARS simulator. In this case study, the reservoir is one-dimensional with 1500 ft length, 10 ft width, and 10 ft thickness. The input data for this case are listed in Table 5.1. The water saturation is unity and the porosity and the permeability of the reservoir are 0.3 and 200 md, respectively. Initial pressure and temperature are 300 psia and 560˚R and the conductivity of water is considered to be 0.8 siemens/m. The number of gridblocks used to simulation case is 50×1×1. The well conditions are constant injection rate of 30 Lbmole/day and constant production pressure of 300 psia. Thermal conductivity of the reservoir and caprock is 35 Btu/(ft-day-°R) and the volumetric heat capacity of the rock is 35 Btu/(ft^3-°R). The simulation time is 20 days. The voltages are zero in the injection well and 100 volt in the production well location. Figure 5.2 shows the results for this example.

Case 2: One-Dimensional Case with Six Component Fluid Mixture. In order to test the thermal model with electrical heating option in 1D problem, this case was developed. The summarized input data are presented in Table 5.2. The reservoir fluid is a six-component mixture with the properties given in Table 5.3. The saturation of the phases is calculated at the beginning of the simulation. The permeability and porosity are 250 md and 0.3, respectively. Initial pressure and temperature are 650 psia and 560˚R. The volumetric heat

capacity of the rock is 35 Btu/(ft^3-°R). Thermal conductivity of the reservoir rock and caprock are 35 and 20 Btu/(ft-day-°R), respectively. The reservoir is divided into 50 gridblocks of size of 40×40×40 ft^3 in the *x* direction. The well conditions for injection and production wells are constant pressures of 900 and 650 psia, respectively. The electrical potential in the injection well is 200 volt and zero volt in the production well. Electrical conductivity of water is 0.8 siemens/m. Figure 5.3 gives the results of this case. The figure shows that water is produced after 1100 days. It shows oil and oleic phase rates, which are pure oil and the oil including water, respectively. As a result, an inclusion of water in the phase behavior calculation can change the phase properties and finally change the production history compared to methods that treat water as an entirely separate phase. This phase behavior calculation, which includes water as a mixture component, is thermodynamically consistent and more accurate in comparison to K-value methods.

Case 3: Two-Dimensional Case with Six Component Fluid Mixture. In this example, a 2D cross-sectional reservoir was used to test the electrical heating thermal module. The reservoir fluid is the same as in Case 2. Specifications of this case are given in Table 5.4. The horizontal permeability is 200 md and vertical permeability is 100 md and the porosity is 0.3. Initial pressure and temperature are 650 psia and 560˚R. There are 20 gridblocks in *x*, one in *y*, and three in *z* direction. Reservoir dimensions are 800 ft in length, 40 ft in width, and 30 ft in thickness. The electrical potentials are set in two locations of the reservoir, zero volt in the injection well and 200 volt in the production well. The wells are entirely perforated and are located at two ends of the reservoir in the *x* direction. The injection well condition is 700 psia and production well condition is 635 psia. The water electrical conductivity is 0.8 siemens/m. The properties of the reservoir rock and caprock are the same as in the previous example. The results of this case are presented in Figure 5.4.

The figure shows the water, oil, and oileic phase rates. As discussed in the previous case, the hydrocarbon-rich liquid phase in the calculations is the oleic phase and it includes water. In the reservoir condition, the concentration of water in the oil phase and the concentration of hydrocarbons in the water rich phase are not negligible. Hence, it is expected that the consideration of these concentrations will give more accurate results compared to methods that consider water as a separate component/phase with a separate phase calculation.

Case 4: Three-Dimensional Case with Six Component Fluid Mixture. In this case, a quarter of five-spot reservoir with the dimension of 500×500×50 ft^3 was used to illustrate the 3D example of electrical heating option in the EOS thermal module. Table 5.5 gives the data of this case. The reservoir fluid is the same as in Case 2. The reservoir is homogeneous with permeability of 100 md and porosity of 0.3. Initial pressure and temperature are 650 psia and 560˚R. The injection well condition is 750 psia and the production well condition is 650 psia. The reservoir is discretized into 20×20×5 gridblocks. The electrical potential is 300 volt in the injection well and zero volt in the production well. The water electrical conductivity is 8.0 siemens/m. Reservoir rock and caprock thermal properties are the same as in the previous example. Figure 5.5 presents the results of this case study. The figure shows the water, oil, and oleic phase rates with water-breakthrough taking place after 2000 days. In this case, as in the previous cases, oil phase in the calculations includes water; the phase is oleic at reservoir conditions and pure oil at the surface condition.

Case 5: Effect of Water Saturation on Electrical Conductivity. In this example, another 2D cross-sectional reservoir was used to show the importance of the water saturation in electrical heating process. The data are the same as in Case 3, but the number of gridblocks

is 8×8×1 with each grid having a size of 50×50×25 ft^3. The injected fluid is water and the injection well condition is a rate of 1000 Lbmole/day and the production well condition is maintenance of 650 psia. There are two locations for voltage maintenance: zero volt at the injection well and 1000 volt at the production well. Figure 5.6 shows oil, oleic, water rates, and the average reservoir pressure for this case. Voltage, temperature, and water-rich phase saturation after 2206 days are presented in Figures 5.7 through 5.9. Because water has a higher electrical conductivity and the water electrical conductivity is a function of water saturation, temperature is increased when water saturation rises. Therefore, as we see in the figures, temperature at the vicinity of the injection well is higher than the rest of the reservoir.

Case 6: Parallel Processing Case. This case was made to test and show the capability of the electrical heating model in the parallel mode. The reservoir in this case is 3D and a quarter of a five-spot reservoir with the size 1280×1280×50 ft^3. The fluid mixture has four components. The reservoir permeability is 100 md. Initial pressure and temperature are 650 psia and 560°R, respectively. The rock and caprock thermal conductivities are 35, 20 Btu/(ft-day-°R), respectively. The volumetric rock heat capacity used in this example is 35 Btu/(ft^3-°R) and the porosity is 0.3. The number of gridblocks is 64×64×5. The injection fluid is water with the rate of 1500 Lbmole/day and the well condition of the production well is a pressure of 500 psia. Two electrodes with 300 volt and zero volt are located at the injection and the production well locations, respectively. The water electrical conductivity is considered to have a constant value of 8.0 Siemens/m. The properties and the initial reservoir compositions are given in Table 5.6. The permeability data which are the same for all cases are shown in Table 5.7. Both wells are entirely perforated. The oil rates for different number of processors are given in Figure 5.10. The execution time and speed-up

curves are shown in Figure 5.11 and 5.12. Figure 5.11 shows that as the number of processors is increased the execution times are decreased. Good speedups were achieved using two through eight processors. As larger numbers of processors were used to carry out the simulations, the performance of parallel computations was decreased. The reason for the drop in the performance is that as we use larger numbers of processors, the problem size to be solved for each processor becomes smaller and hence the communication times between processors become more dominant. This results in decrease in speedups for the parallel computations.

Table 5.1 Summary of input data for one-dimensional case with single phase fluid (Case1)

Parameter	Value
Reservoir dimension	1500×10×10 ft^3
Gridblock size	30×10×10 ft^3
Initial temperature	560°R
Initial pressure	300 psia
Porosity	0.3
Permeability	200 md
Reservoir, Caprock thermal conductivity	35 Btu/(ft-day-°R)
Rock heat capacity	35 Btu/(ft^3-°R)
Injection rate	30 Lbmole/day
Bottomhole production pressure	300 psia
Water electrical conductivity	0.8 siemens/m

Table 5.2 Summary of input data for one-dimensional case with six component fluid mixture (Case2)

Parameter	Value
Reservoir dimension	2000×40×40 ft^3
Gridblock size	40×40×40 ft^3
Initial temperature	560°R
Initial pressure	650 psia
Porosity	0.3
Permeability	250 md
Reservoir thermal conductivity	35 Btu/(ft-day-°R)
Caprock thermal conductivity	20 Btu/ft-day-°R
Rock heat capacity	35 Btu/(ft^3-°R)
Injection pressure	900 psia
Bottomhole production pressure	650 psia
Water electrical conductivity	0.8 siemens/m

Table 5.3 Initial fluid composition and properties for cases 1, 2, 3, 4, and 5

Component name	MW	Tc (°R)	Pc (psia)	Mole percent
C_{10}	134.0	1120.11	367.647	0.01
C_{15}	206.0	1270.0	200.00	0.02
C_{19}	263.0	1388.13	221.38	0.02
C_{25}	337.0	1499,19	174.05	0.05
C_{26}^{+}	450.0	1710.33	140.0	19.90
H_2O	18.0	1165.47	3198.72	80.00

Table 5.4 Summary of input data for two-dimensional case with six component fluid mixture (Case3)

Parameter	Value
Reservoir dimension	800×40×30 ft^3
Gridblock size	40×40×10 ft^3
Initial temperature	560°R
Initial pressure	650 psia
Porosity	0.3
Permeability (K_h, K_v)	200 md, 100 md
Reservoir, Caprock thermal conductivities	35 Btu/(ft-day-°R)
Rock heat capacity	20 Btu/(ft^3-°R)
Injection pressure	700 psia
Bottomhole production pressure	635 psia
Water electrical conductivity	0.8 siemens/m

Table 5.5 Summary of input data for three-dimensional case with six component fluid mixture (Case4)

Parameter	Value
Reservoir dimension	500×500×50 ft^3
Gridblock size	25×25×10 ft^3
Initial temperature	560°R
Initial pressure	650 psia
Reservoir porosity	0.3
Permeability	100 md
Reservoir, Caprock thermal conductivities	35, 20 Btu/(ft-day-°R)
Rock heat capacity	35 Btu/(ft^3-°R)
Injection pressure	750 psia
Bottomhole production pressure	650 psia
Water electrical conductivity	0.8 siemens/m

Table 5.6 Initial fluid composition and properties for parallel processing case (Case6)

Component name	MW	Tc (°R)	Pc (psia)	Mole percent
C_{10}	134.0	1120.11	367.647	15.0
C_{15}	206.0	1270.0	200.0	13.0
C_{26}^{+}	450.0	1710.33	140.0	12.0
H_2O	18.0	1165.47	3198.72	60.0

Table 5.7 Relative permeability data for cases 1 through 6

	Water	Oil	Gas
Endpoint	0.9	0.55	0.6
Residual saturation	0.12	0.2	0.06
Exponent	2.5	2.0	1.5

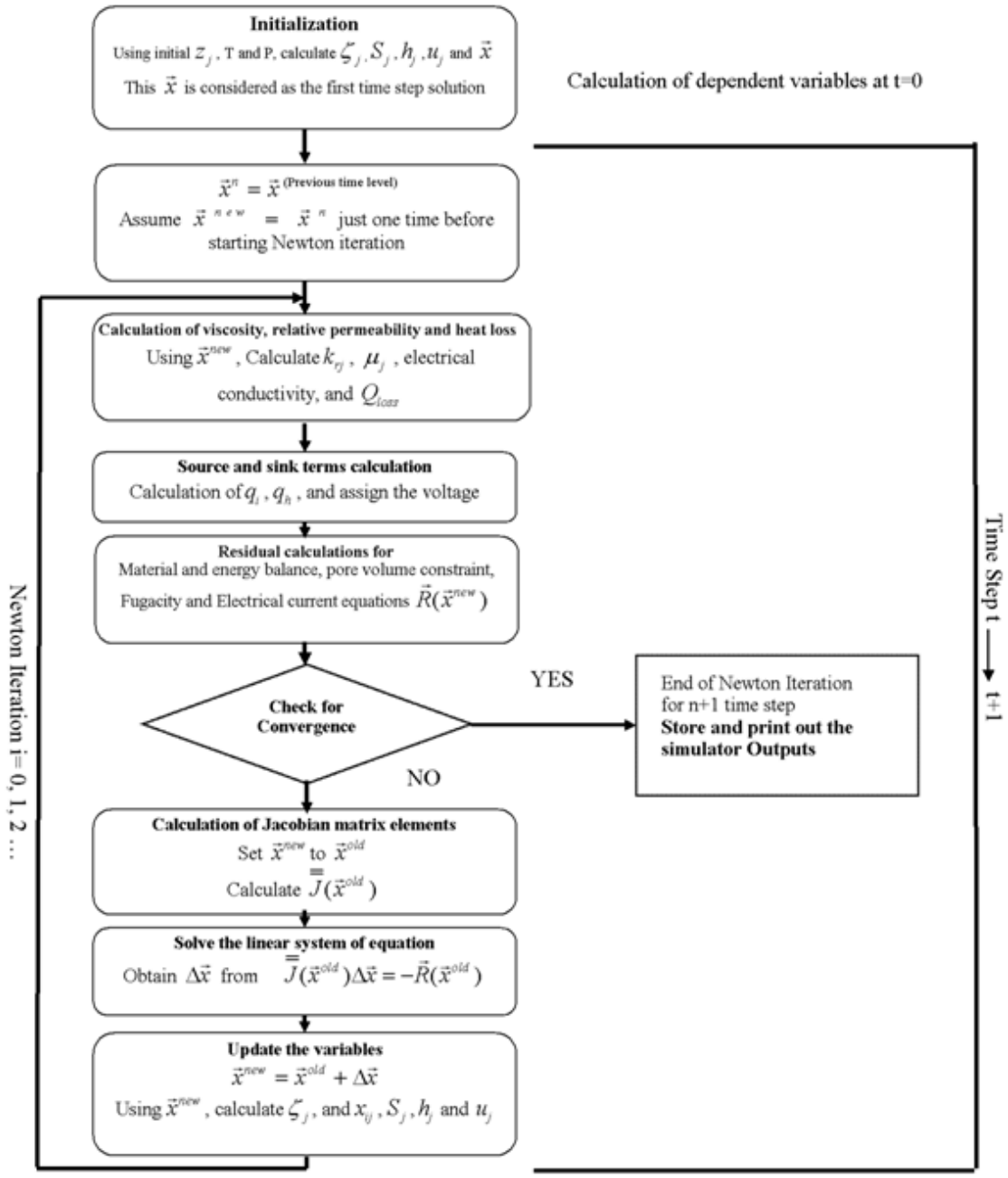

Figure 5.1 Computational flow chart of electrical heating model

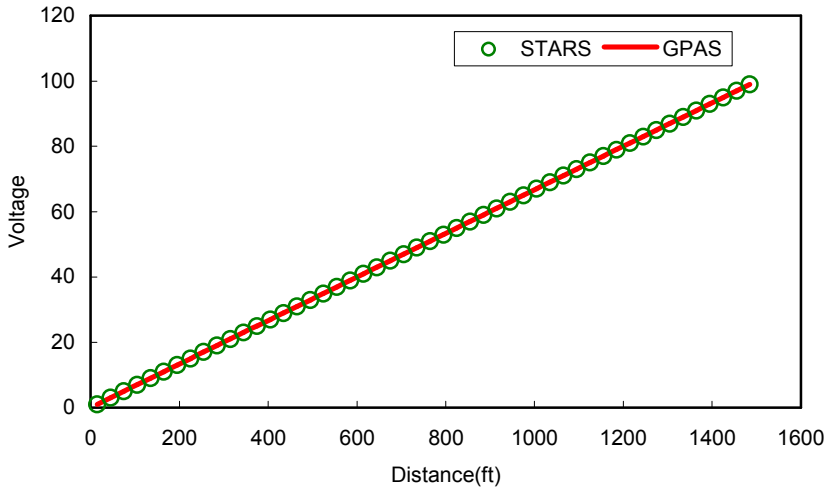

Figure 5.2 Comparison of voltage versus distance for validation of electrical heating model using CMG-STARS and GPAS (Case 1)

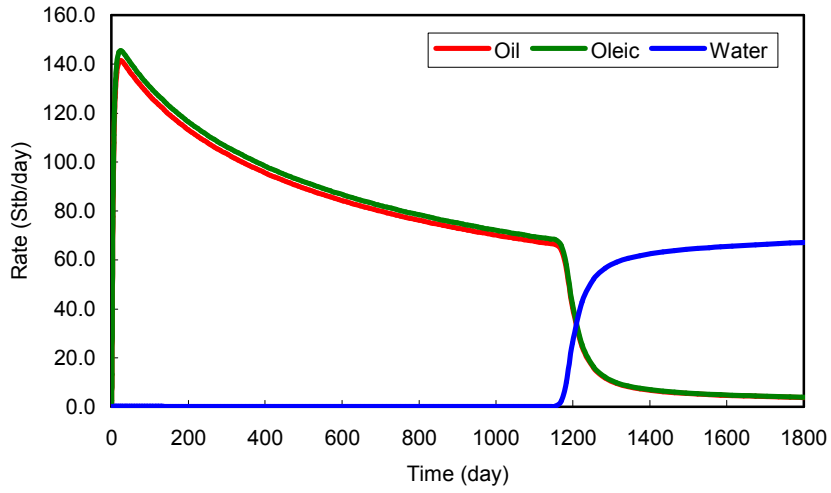

Figure 5.3 Oil rate and water rate for one-dimensional case with six component fluid mixture (Case 2)

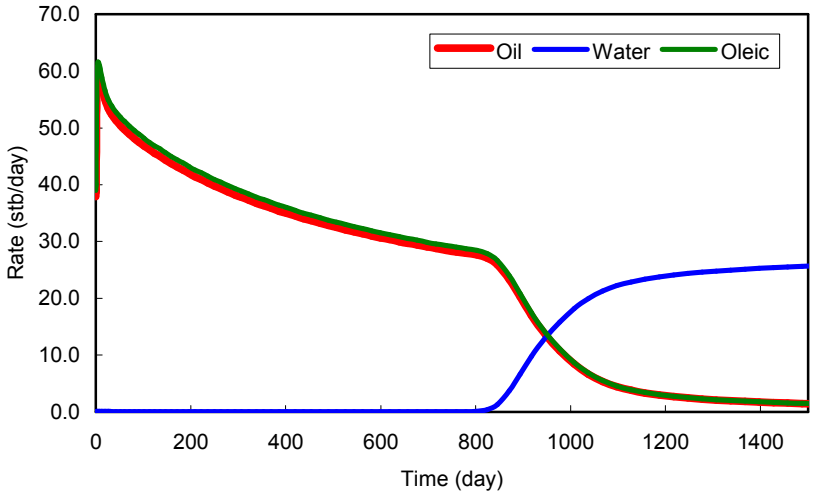

Figure 5.4 Oil rate and water rate for two-dimensional case with six component fluid mixture (Case 3)

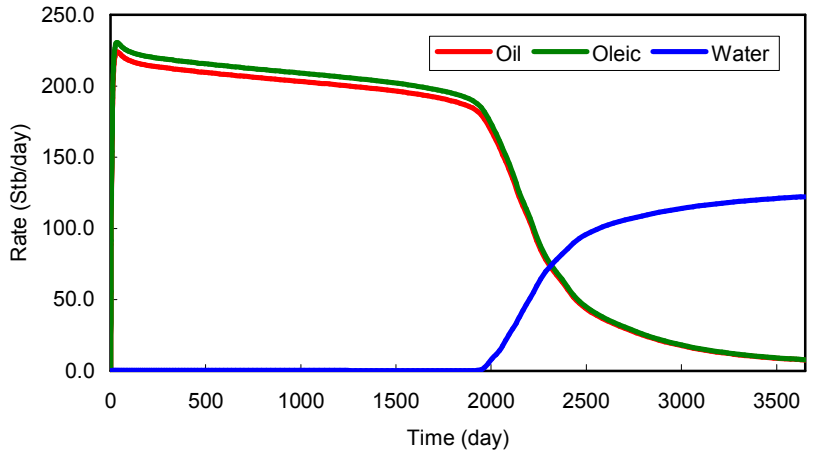

Figure 5.5 Oil rate and water rate for three-dimensional case with six component fluid mixture (Case 4)

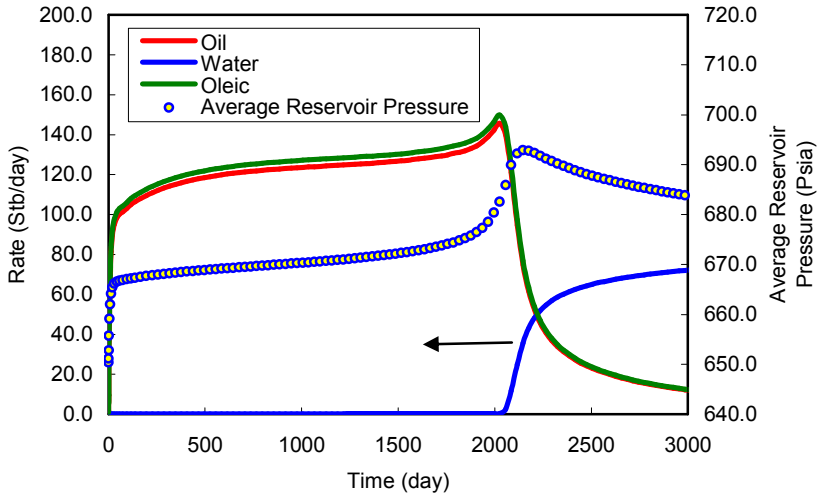

Figure 5.6 Fluids rates and average reservoir pressure for effect of water saturation on electrical conductivity (Case 5)

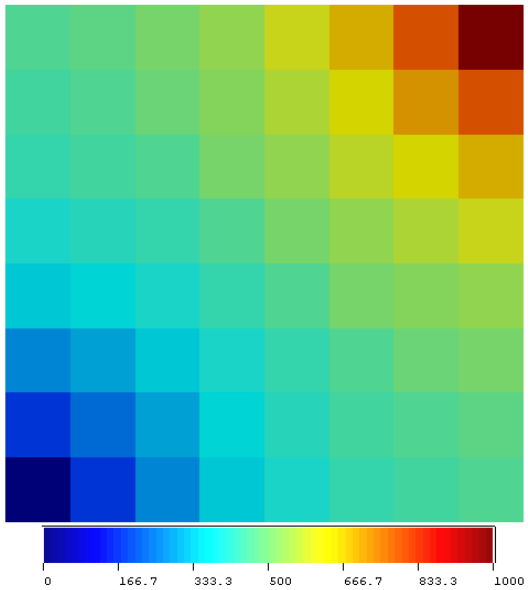

Figure 5.7 Voltage distributions after 2206 days for effect of water saturation on electrical conductivity

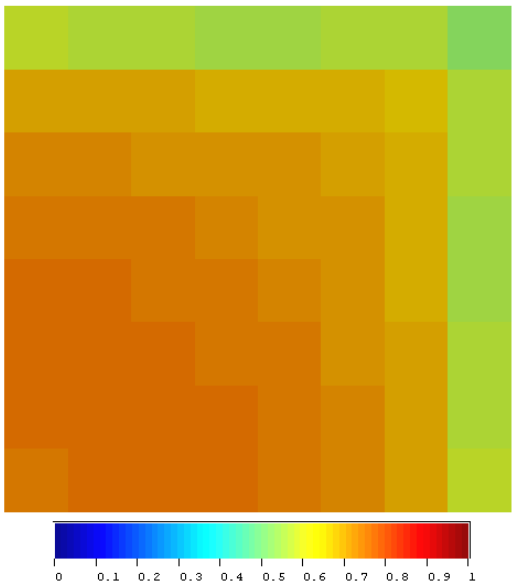

Figure 5.8 Water saturation after 2206 days for effect of water saturation on electrical conductivity

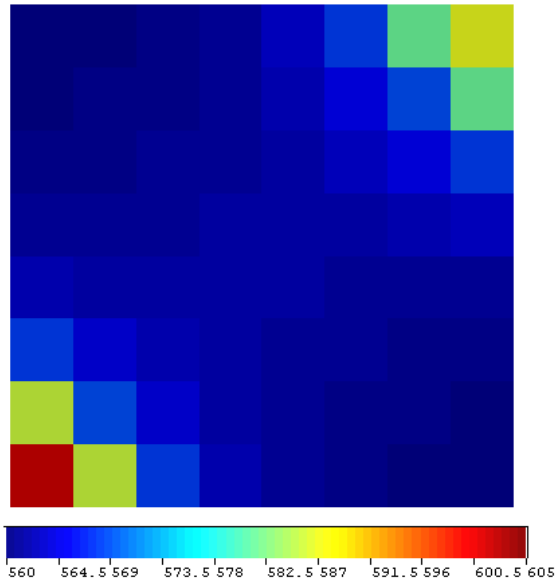

Figure 5.9 Temperature (ºR) distributions after 2206 days for effect of water saturation on electrical conductivity

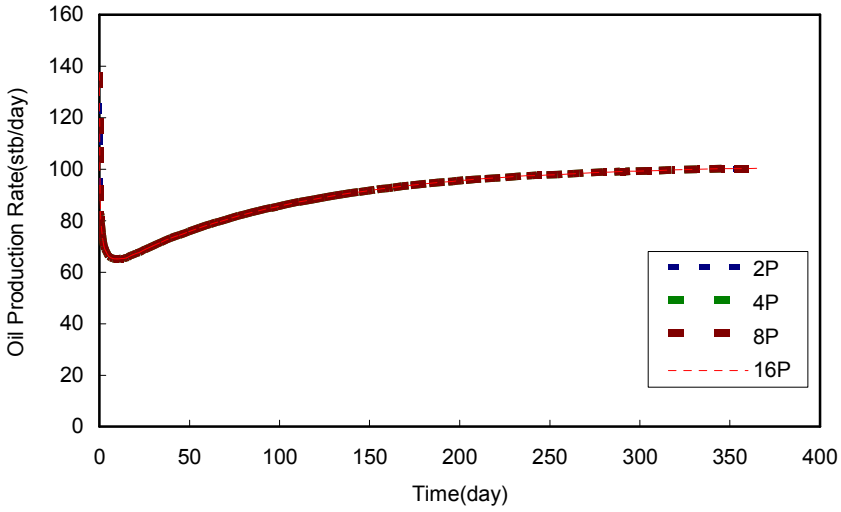

Figure 5.10 Oil rate for parallel processing case (Case 6)

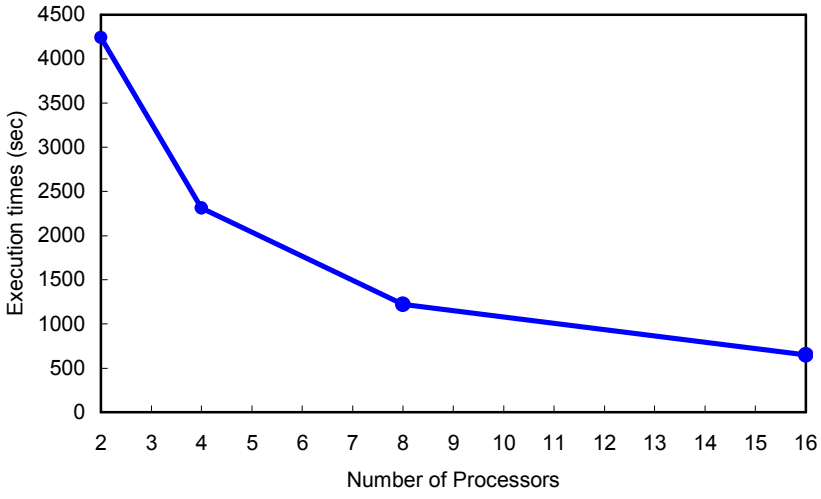

Figure 5.11 Execution time for parallel processing case (Case 6)

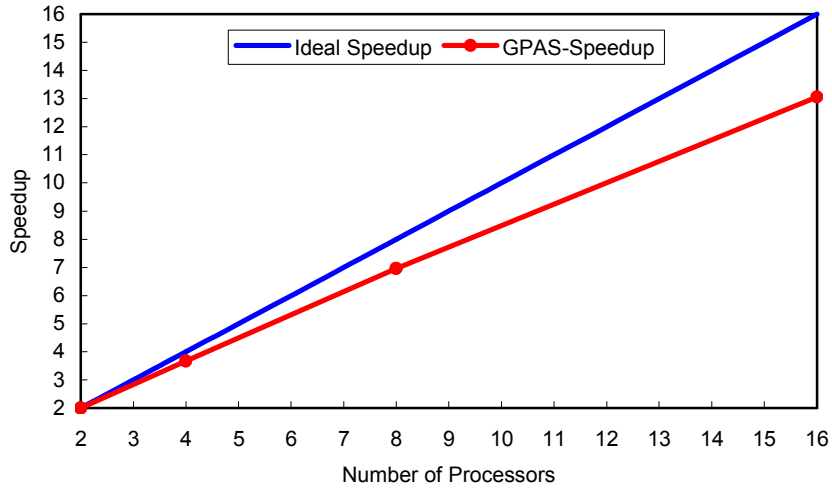

Figure 5.12 Speedup for parallel processing case (Case 6)

Chapter 6: Hot Chemical Flooding Model

The chemical flooding model was implemented into GPAS by Han *et al.* (2005). In this chapter, the implementation of temperature effect for the phase behavior model and other properties of the chemical flooding model are described.

Chemical flooding and hot chemical flooding are two ways to increase oil recovery. Surfactants have been found that both reduce interfacial tension and change wettability. Both of these effects can be beneficial in both sandstone and carbonate oil reservoirs, but the change from oil wet to water wet is of special interest to carbonate reservoir since most of them are oil wet. The effect of temperature on different parameters in chemical flooding has been investigated (Fathi, 2009). In this chapter, the effect of temperature on chemical flooding parameters has been studied and implemented into the GPAS chemical flooding model. Parameters of the chemical flooding model affected by temperature are summarized in the following sections.

6.1 PHASE TRANSITION

The microemulsion phase is defined as a thermodynamically stable phase where oil, water, and surfactant coexist in micellar form. There are three different microemulsion phase definitions

a. Type II(-), or lower phase microemulsion
b. Type II(+) or upper phase microemulsion
c. Type III or middle phase microemulsion

When the microemulsion phase is in equilibrium with excess oil, it is called Type II(-); when microemulsion phase in equilibrium with an excess water it is called Type II(+); and Type III is defined for the case when the microemulsion phase is in equilibrium with both excess oil and water. Figure 6.1 shows all three types of phase behavior.

When temperature is increased, the anionic surfactant has less soluble-oil and more soluble-water; thus, the phase equilibrium of anionic surfactant solution is changed to lower phase microemulsion types. As we see in Figure 6.2, which is given by Novosad (1982), an increase in temperature changes the middle phase microemulsion of the anionic surfactant (PDM 337) to a lower phase microemulsion. But all of these depend on the surfactant type and the trends can go either way.

6.2 SOLUBILIZATION PARAMETERS

Healy and Reed (1976) showed that an increase in temperature decreases the solubilization of oil in the microemulsion phase and increases the solubilization of water in the microemulsion phase at constant salinity. Novosad (1982) demonstrated, as we saw in the previous section, that Type III is changed to Type II(-) when the temperature is increased. Healy and Reed (1976) showed the effect of temperature on solubility ratios for two different temperatures; Figure 6.3 shows this effect. As we see, the oil solubility ratio is decreased with increasing temperature. Puetro and Reed (1983) showed that the optimum solubilization decreases with increasing temperature. Aoudia and Wade (1995), as given in Figure 6.4, showed the decrease in optimum solubilization with increasing temperature. They used propoxylated C_{14} alcohol sodium sulfates in their study. Austad and Skule (1996) demonstrated the same trend, which is given in Figure 6.5, as others had, of declining optimum solubilization with increasing temperature. Dwarakanath and Pope (2000) showed that optimum salinity increases with temperature. They also showed that the solubilization

ratio in different ranges of temperature versus normalized salinity (salinity divided by optimum salinity) remains constant; Figure 6.6 shows the volume fraction diagram at different temperatures. But all of the data are for particular surfactants and are not general. The surfactant behavior does depend on temperature but not always the same way.

6.3 INTERFACIAL TENSION

The interfacial tension between microemulsion/oil and microemulsion/water is increased with increasing temperature. Healy and Reed (1967) and Ziegler (1988) showed the effect of temperature on interfacial tensions at constant salinity; see Figures 6.7 and 6.8.

6.4 OPTIMUM SALINITY

The optimum salinity is increased with increasing temperature. Figure 6.9 shows the results of different references which document optimum salinity increase with increasing temperature.

6.5 SURFACTANT RETENTION

The retention and adsorption of surfactant is decreased with increasing temperature. Novsad (1982) studied this effect for two anionic surfactants in Berea cores. This study showed that increasing temperature can decrease the surfactant concentration in trapped oil phase, whereupon surfactant retention is decreased.

6.6 EFFECTIVE SALINITY

The effective salinity is the concentration of the anions when NaCl is the only salt present in the system. Then, this concentration is adjusted for the effect of cations, cation-

exchange with clays and surfactant micelles, and temperature. The effective salinity decreases as temperature increases for anionic surfactants and increases as temperature increases for nonionic surfactants. The following equation can be considered for anionic surfactant (UTCHEM-9.82):

$$C_{SE} = \frac{C_{51}}{1+\beta_T (T - T_{ref})} \tag{6.1}$$

This equation is non-linear; but as we see in Figures 6.10 and 6.11, some of the data have a linear trend (Healy and Reed, 1976). In GPAS, two equations, Equation (6.1) and following equation have been used.

$$C_{SE} = C_{51}\left[1+\beta_T^{'} (T - T_{ref})\right] \tag{6.2}$$

Equation (6.2) well fits with the experimental data produced by Healy and Reed (1976); Equation (6.1) fits well with the data given by Ziegler (1988). Both equations fit the data for Aoudia and Wade (1995). Equation (6.2) is a better fit for Dwarakanath and Pope's data. The equations should be used to calculate lower and upper limit effective salinities (C_{SEL} and C_{SEU}) at which three equilibrium phases can form or disappear.

The optimum effective salinity, C_{SEOP}, is the arithmetic average of C_{SEL} and C_{SEU}.

6.7 HEIGHT OF BINODAL CURVE

The following equation has been implemented into the code to calculate the height of the binodal curve (UTCHEM-9.82):

$$C_{3,\max} = H_{BNC,m} + H_{BNC,m}(T - T_{ref}) \quad m = 0,1, \text{ and } 2 \tag{6.3}$$

where m = 0, 1, and 2 correspond to low, optimal, and high salinities; $H_{BNC,m}$ and $H_{BNT,m}$ are the height of the binodal curve at a reference temperature and the slope of the binodal versus temperature curve respectively. Heights of the binodal curve at three reference salinities are input to the simulator. They are estimated based on phase behavior laboratory experiments.

6.8 CRITICAL MICELLE CONCENTRATION

Noll (1991) showed critical micelle concentration (CMC) measurements for three commercial sulfonate surfactants commonly used for producing foam. He showed that the CMC increased with temperature. Bourrel and Schechter (1988) presented some of the Flokhart data on temperature dependency of the CMC of the dodecyl sulfate. They showed that the CMC is a linear function of temperature. Figure 6.12 shows the results.

The following equation was implemented to calculate CMC

$$CMC = CMC_{ref} + S_{CMC}(T - T_{ref}) \tag{6.4}$$

where CMC, CMC_{ref} and S_{CMC} are CMC at elevated temperature, the slope of CMC as a function of temperature and CMC at reference temperature denoted as T_{ref}, respectively.

6.9 VISCOSITY AND DENSITY

As discussed in Chapter 4, the viscosity of the hydrocarbon phases is determined by Lohrenz's correlation (Lohrenz *et al.,* 1964) and Andrade equation (1934), and for water phase Grabowski function (1979) and the Andrade equation (1934) can be used. Tables of phase viscosities as a function of temperature can also be used. The Andrade equation can

also be used to calculate the pure-component oleic phase viscosities. The Grabowski function is as follow:

$$\mu_w = \frac{1}{A_w + B_w T + C_w T^2} \tag{6.5}$$

where μ_w is water density in cp, the temperature, T is in $^\circ C$ and the coefficients are A_w=0.1323, B_w=0.03333, C_w=7.643×10^{-6}. Figure 6.13 shows this function.

The water density is calculated by Trangenstein's modification of Kell's (1975) correlation

$$\zeta_w = \frac{E_0 + E_1 T + E_2 T^2 + E_3 T^3 + E_4 T^4 + E_5 T^5}{1 + E_6 T} e^{C_{pw}(P - E_7)} \tag{6.6}$$

where ζ_w is water density in terms of kg/m^3, the temperature, T is in $^\circ C$, the pressure is in Mpa, and C_{pw} is water compressibility in MPa^{-1}. The coefficients are

E_0 = 999.83952, E_1 = 16.955176, E_2 = -7.987×10^{-3}, E_3 = -46.170461×10^{-6},

E_4 = 105.56302×10^{-9}, E_5 =-280.54353×10^{-12}, E_6= 16.87985×10^{-3}, E_7=10.2

The water density as function of temperature is given the Figure 6.14.

6.10 GOVERNING EQUATION AND SOLUTION PROCEDURE

The governing equations of the hot chemical flooding model are pore volume constraint, material balance equation of the components, and conservation of the energy. They should be solved with a fully implicit method. Therefore, to solve the system of equations, it is necessary to have the residual function from the previous time-step and thus construct the Jacobian matrix.

$$\delta \mathrm{P} = \mathrm{P}^{n+1} - \mathrm{P}^{n} = -\vec{\vec{J}}^{-1} R^{n} \tag{6.7}$$

P is the primary variable and the R is the residual of the equations. Both the residual of the governing equations and the construction of the Jacobian matrix are presented below.

$$\begin{pmatrix} J_{1,1} & J_{1,2} & \cdots & J_{1,n_b} \\ J_{2,1} & J_{2,2} & \cdots & J_{2,n_b} \\ \vdots & & & \vdots \\ J_{n_b,1} & J_{n_b,2} & \cdots & J_{n_b,n_b} \end{pmatrix} \begin{pmatrix} \Delta\vec{x}_1 \\ \Delta\vec{x}_2 \\ \vdots \\ \Delta\vec{x}_{n_b} \end{pmatrix} = - \begin{pmatrix} \vec{R}_1 \\ \vec{R}_2 \\ \vdots \\ \vec{R}_{n_b} \end{pmatrix}$$

$$\mathrm{J}_{\mathrm{I,J}} = \begin{bmatrix} \frac{\partial \mathrm{R}_{\mathrm{v}}\big|_{\mathrm{I}}}{\partial \mathrm{N}_{1}\big|_{\mathrm{J}}} & \cdots & \frac{\partial \mathrm{R}_{\mathrm{v}}\big|_{\mathrm{I}}}{\partial \mathrm{N}_{\mathrm{n_C+n_A+1}}\big|_{\mathrm{J}}} & \frac{\partial \mathrm{R}_{\mathrm{v}}\big|_{\mathrm{I}}}{\partial \mathrm{P}\big|_{\mathrm{J}}} & \frac{\partial \mathrm{R}_{\mathrm{v}}\big|_{\mathrm{I}}}{\partial \mathrm{T}\big|_{\mathrm{J}}} \\ \frac{\partial \mathrm{R}_{\mathrm{m,1}}\big|_{\mathrm{I}}}{\partial \mathrm{N}_{1}\big|_{\mathrm{J}}} & \cdots & \frac{\partial \mathrm{R}_{\mathrm{m,1}}\big|_{\mathrm{I}}}{\partial \mathrm{N}_{\mathrm{n_C+n_A+1}}\big|_{\mathrm{J}}} & \frac{\partial \mathrm{R}_{\mathrm{m,1}}\big|_{\mathrm{I}}}{\partial \mathrm{P}\big|_{\mathrm{J}}} & \frac{\partial \mathrm{R}_{\mathrm{m,1}}\big|_{\mathrm{I}}}{\partial \mathrm{T}\big|_{\mathrm{J}}} \\ \vdots & \cdots & \cdots & \vdots & \vdots \\ \frac{\partial \mathrm{R}_{\mathrm{m,n_C+n_A+1}}\big|_{\mathrm{I}}}{\partial \mathrm{N}_{1}\big|_{\mathrm{J}}} & \cdots & \frac{\partial \mathrm{R}_{\mathrm{m,n_C+n_A+1}}\big|_{\mathrm{I}}}{\partial \mathrm{N}_{\mathrm{n_C+n_A+1}}\big|_{\mathrm{J}}} & \frac{\partial \mathrm{R}_{\mathrm{m,n_C+n_A+1}}\big|_{\mathrm{I}}}{\partial \mathrm{P}\big|_{\mathrm{J}}} & \frac{\partial \mathrm{R}_{\mathrm{m,n_C+n_A+1}}\big|_{\mathrm{I}}}{\partial \mathrm{T}\big|_{\mathrm{J}}} \\ \frac{\partial \mathrm{R}_{\mathrm{E}}\big|_{\mathrm{I}}}{\partial \mathrm{N}_{1}\big|_{\mathrm{J}}} & \cdots & \frac{\partial \mathrm{R}_{\mathrm{E}}\big|_{\mathrm{I}}}{\partial \mathrm{N}_{\mathrm{n_C+n_A+1}}\big|_{\mathrm{J}}} & \frac{\partial \mathrm{R}_{\mathrm{E}}\big|_{\mathrm{I}}}{\partial \mathrm{P}\big|_{\mathrm{J}}} & \frac{\partial \mathrm{R}_{\mathrm{E}}\big|_{\mathrm{I}}}{\partial \mathrm{T}\big|_{\mathrm{J}}} \end{bmatrix}$$

Figure 6.16 gives the computational flowchart for this model

6.11 CASE STUDIES OF THE THERMAL CHEMICAL MODEL

The model was tested using analytical solution and also was compared with the UTCHEM simulator. In this section, four examples are presented: one comparison with

analytical solution and rest of them comparisons with UTCHEM simulator for one-, two-, and three-dimensional reservoirs.

Case 1: Comparison with Analytical Solution. The thermal chemical model was tested using the Lauwerier's problem described in section 4.10. The input data for this case are summarized in Table 6.1. The case is a 1D homogeneous reservoir of size 1000×10×10 ft^3 with a permeability of 10,000 md and a porosity of 0.35. The initial pressure and temperature of the reservoir are 1000 psia and 520°R, and the water saturation is 1.0, the heat capacity ratio for fluid and rock is 1. The volumetric heat capacity is 35 Btu/(ft^3-°R) and the thermal conductivity is 35 Btu/(ft-day-°R). The reservoir is divided into 200 gridblocks. Hot water at a rate of 40 Stb/day and at a temperature of 660°R is injected into the reservoir; production bottomhole pressure is 1000 psia. Figure 6.16 shows the temperature profile for the numerical and analytical solutions. The figure shows that the result of the simulator has excellent agreement with analytical solution.

Case 2: One-Dimensional Case. To validate the model for one-dimensional problems, the result of the simulator was compared with UTCHEM simulator. A homogeneous reservoir with size of 2000×20×20 ft^3 was used in this example. The summarized data for cases 2 through 4 are listed in Table 6.2, 6.3 and 6.4. The reservoir pressure is 20 psia and initial water saturation is 0.7. The number of gridblocks is 100×1×1. There are constant production pressures of 20 psia and constant injection rate of 100 Stb/day and the injection is carried out for 365 days. A chemical slug is injected with a 0.01 volume fraction of surfactant concentration and a polymer concentration of 0.05wt% with 0.17 meq/ml of salt. After injection of the surfactant slug for 64 days, polymer is injected for 301 days. The oil has one component. The viscosity functions of water and oil for two simulators were fixed

to have same viscosity profile. Figures 6.17 and 6.18 show the results of GPAS and UTCHEM. The case was run in GPAS for different values of maximum time step (Dt_{max} in the figures) to see the effect of time step on the results. The results in these figures show that there is good agreement between the two simulators. The run time for this case for UTCHEM was 5.64 sec and for GPAS the run time was 157.731 sec for Dt_{max} of 0.4 day.

Case 3: Two-Dimensional Case. A 2D quarter of five-spot homogeneous reservoir with the size of 320×320×20 ft^3 was used to test and compare the result of the simulator with UTCHEM simulator. The properties of the reservoir and fluid are same as for Case 2. The number of gridblocks is 8×8×1 in this example. The injection rate is 200 Stb/day and the chemical slug is injected for 64 days; subsequently, polymer is injected into the reservoir for 301 days. Figures 6.19 and 6.20 show the results of GPAS and UTCHEM; they display good match. Figures 6.21, 6.22, and 6.23 show the temperature profile of GPAS, UTCHEM, and relative temperature difference between GPAS and UTCHEM respectively. The run time for this case for UTCHEM was 4.953 sec and for GPAS the run time was 51.238 sec for Dt_{max} of 1.0 day.

Case 4: Three-Dimensional Case. To verify the simulator for 3D problems, this case was made to compare the result of implemented model with UTCHEM simulator. A 3D quarter of five-spot homogeneous reservoir was used in this manner. The reservoir size is 320×320×20 ft^3 and the gridblock size is 40×40×5 ft^3. The injection rate is 200 Stb/day and the chemical slug is injected for 64 days; again subsequently, polymer is injected into the reservoir for 301 days. The properties of the reservoir and the fluid are same as for Case 2. Figures 6.24 and 6.25 show a remarkable agreement between the results of both simulators.

The run time for this case for UTCHEM was 27.312 sec and for GPAS the run time was 122.245 sec for Dt_{max} of 3.0 days.

Table 6.1 Summary of input data for Lauwerier's problem (1955) for chemical thermal model (Case1)

Parameter	Value
Reservoir dimension	$1000\times10\times10 ft^3$
Gridblock size	$5\times10\times10\ ft^3$
Initial temperature	520°R
Initial pressure	1000 psia
Porosity	0.35
Permeability	10,000 md
Reservoir thermal conductivity	0.0 Btu/(ft-day-°R)
Caprock thermal conductivity	35 Btu/(ft-day-°R)
Rock heat capacity	35 Btu/(ft^3-°R)
Injection temperature	660°R
Injection rate	40 STB/day
Bottomhole production pressure	1000 psia

Table 6.2 Summary of input data for case studies 2, 3, and 4

Parameter	Value
Initial temperature	520°R
Initial pressure	20 psia
Porosity	0.2
Permeability	500 md
Reservoir thermal conductivity	25 Btu/(ft-day-°R)
Caprock thermal conductivity	25 Btu/(ft-day-°R)
Rock heat capacity	35 Btu/(ft^3-°R)
Fluid heat capacities	1.0, 0.5, 1 Btu/(Lbm-°R)
Initial water saturation	0.7
Polymer viscosity parameters	81, 2700, 2500
Height of binodal curve	0.07, 04 vol. fraction
Salinity limit	0.177, 0.25 meq./ml
CMC	0.0001
Slope of CMC verses. Temperature	0.0
Surfactant adsorption parameters	1.5, 0.5, 1000
IFT correlation parameters	9, 0.2
Slope of height of bimodal curve versus temperature	
Zero salinity	0.00017
Optimum salinity	0.00017
Temperature parameter for salinity	0.00415

Table 6.3 Injection specification for case studies 2, 3, and 4

Parameter	Value
Injection temperature	660°R
Bottomhole production pressure	20 psia
Chemical slug composition	
Salt	0.17 meq/ml
Surfactant	0.01 volume fraction
Polymer	0.05 wt%
Polymer drive composition	0.17 meq/ml salt, 0.05 wt% polymer
Chemical slug injection time	64 days
Polymer slug injection time	301 days

Table 6.4 Relative permeability data for case studies 2, 3, and 4

Parameter	Value
Residual saturation at low trapping number	0.14, 0.25, 0.14
Residual saturation at high trapping number	0.0, 0.0, 0.0
End points at low trapping number	0.106, 0.08, 0.106
End points at high trapping number	1.0, 1.0, 1.0
Exponents at low trapping number	2.1, 1.7, 2.1
Exponents at high trapping number	0.48, 1.5, 0.48
Trapping number parameters	364, 59074, 364; 1,1,1

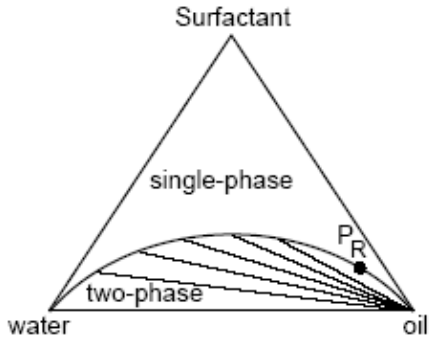

a) Type II(-)

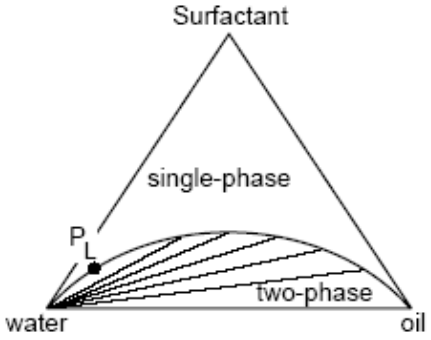

b) Type II (+)

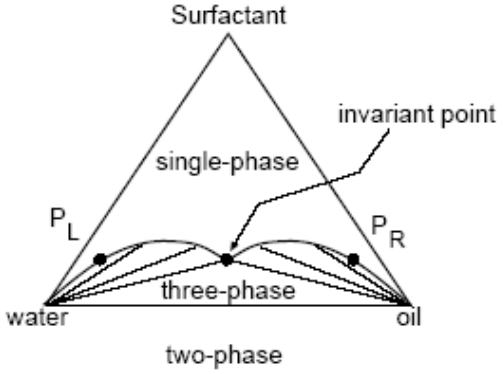

c) Type III

Figure 6.1 Schematic representations of a) Type II (-), b) Type II (+), and c) Type III

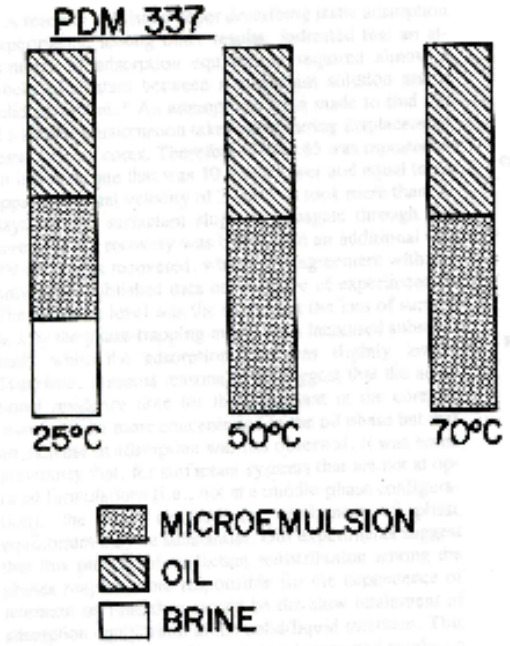

Figure 6.2 Effect of temperature on phase transition of an anionic surfactant (Novosad, 1982)

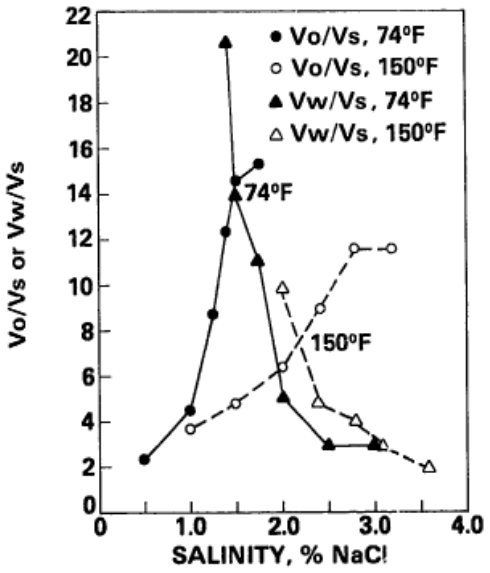

Figure 6.3 Effect of temperature on solubilization ratio of an anionic surfactant (Healy and Reed, 1976)

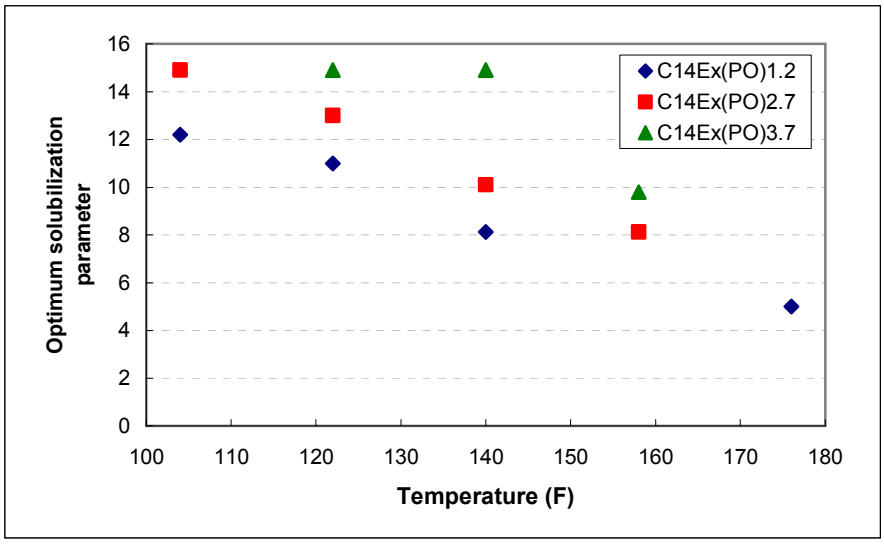

Figure 6.4 Effect of temperature on optimum solubilization ratio of three different anionic surfactants and octane (Aoudia and Wade, 1995)

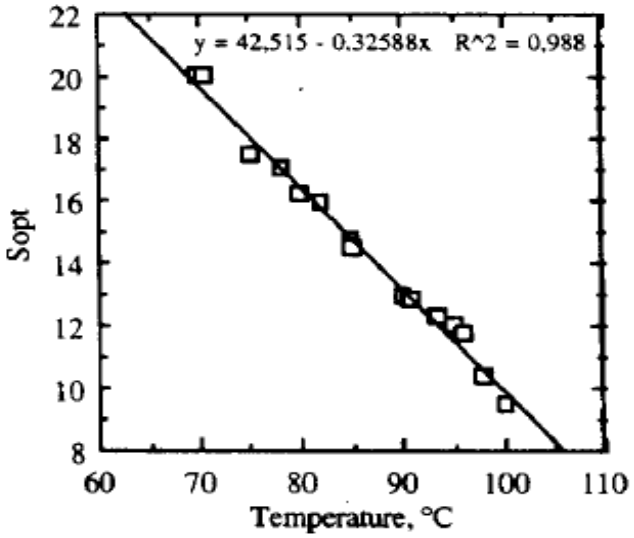

Figure 6.5 Effect of temperature on optimum solubilization ratio for C_{12}-O-xylene sulfonate and live crude oil (Austad and Skule, 1996)

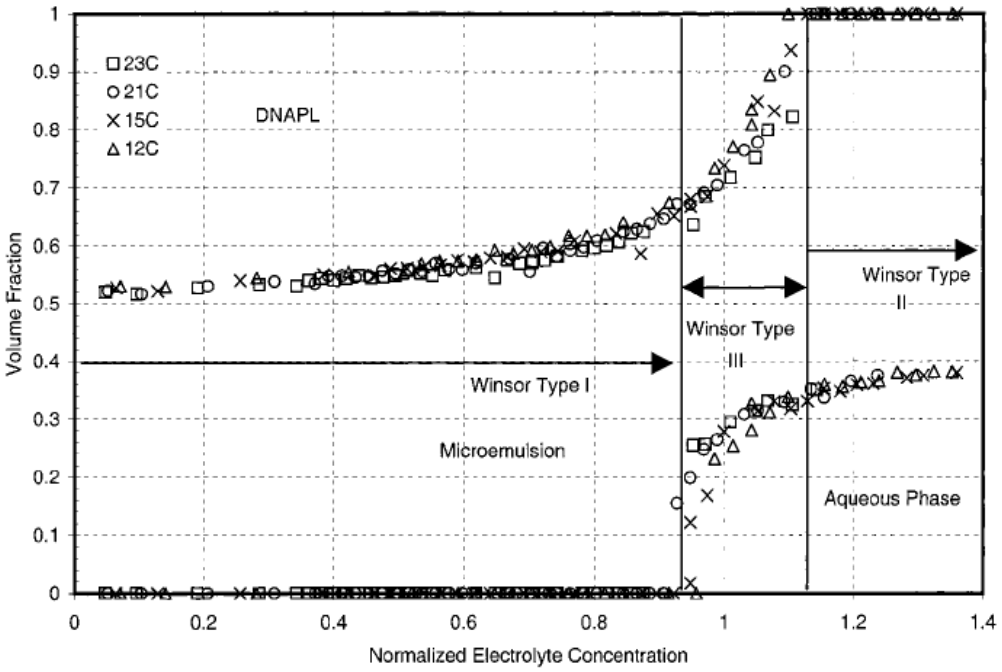

Figure 6.6 Volume fraction diagram for a mixture of 2-propanol and sodium dihexyl sulfosuccinate at different temperatures (Dwarakanath and Pope, 2000)

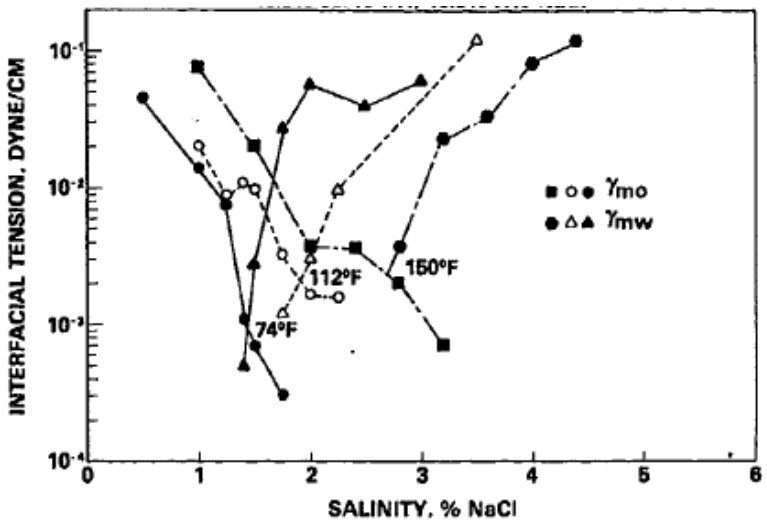

Figure 6.7 Effect of temperature on IFT of microemulsions created by anionic surfactants (Healy and Reed, 1976)

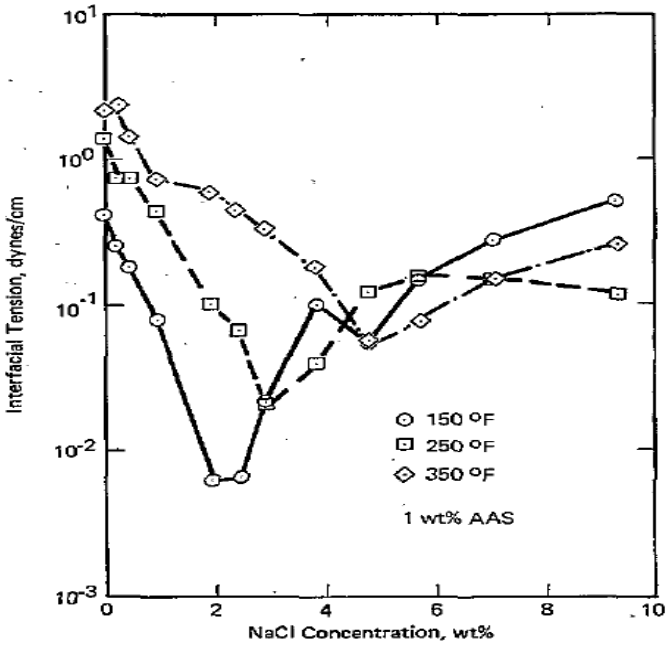

Figure 6.8 Effect of temperature on IFT of microemulsions created by anionic surfactants (Ziegler, 1988)

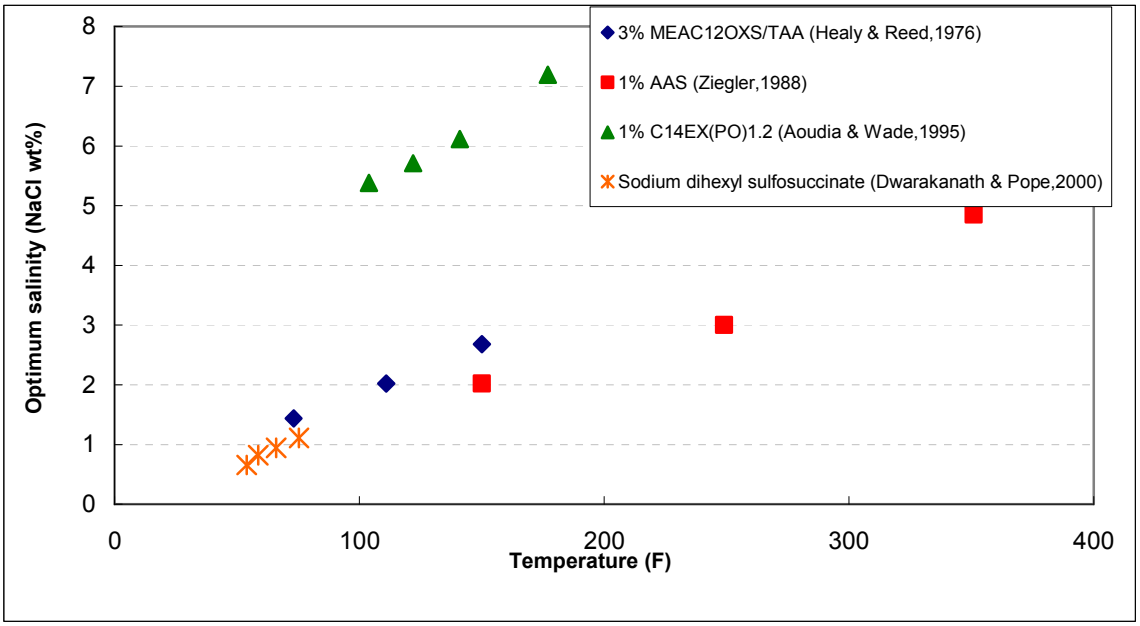

Figure 6.9 Effect of temperature on optimum salinity

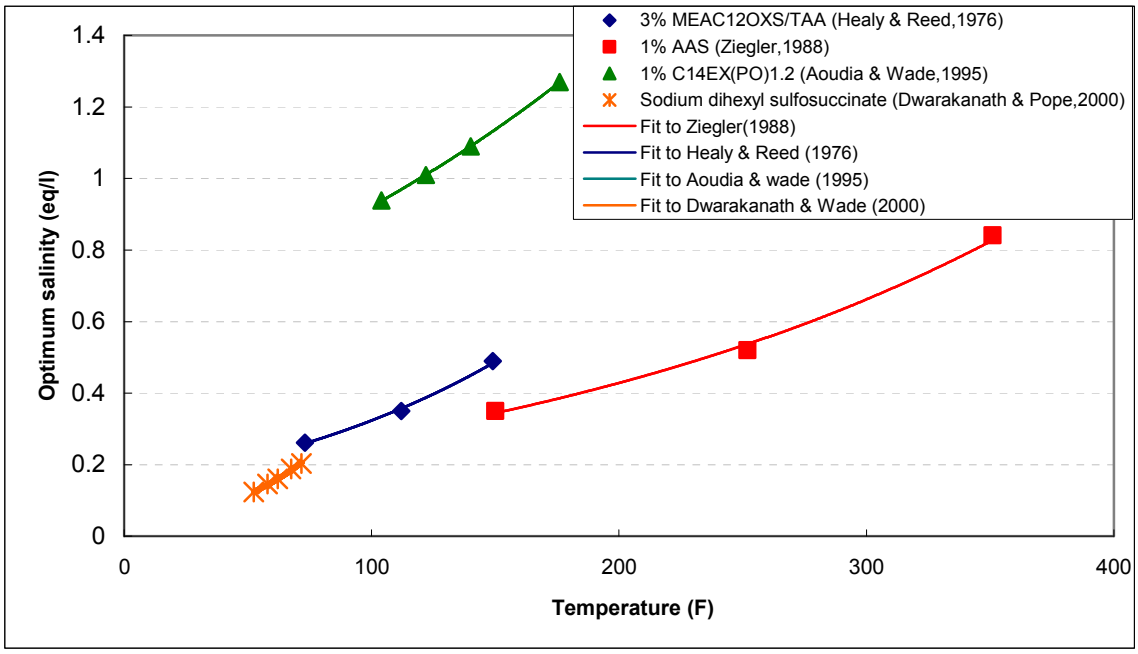

Figure 6.10 Effective salinity using Equation 6.1 to fit optimum salinity data found in the literature

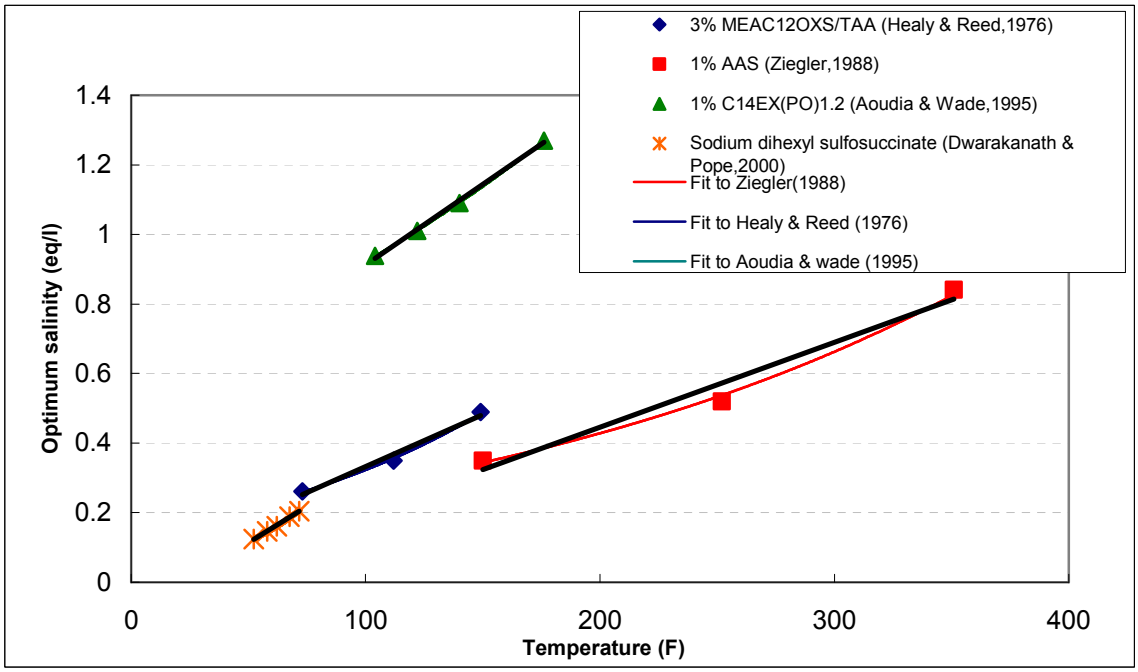

Figure 6.11 Comparing of Equation 6.1 and Equation 6.2 for effect of temperature on effective salinity

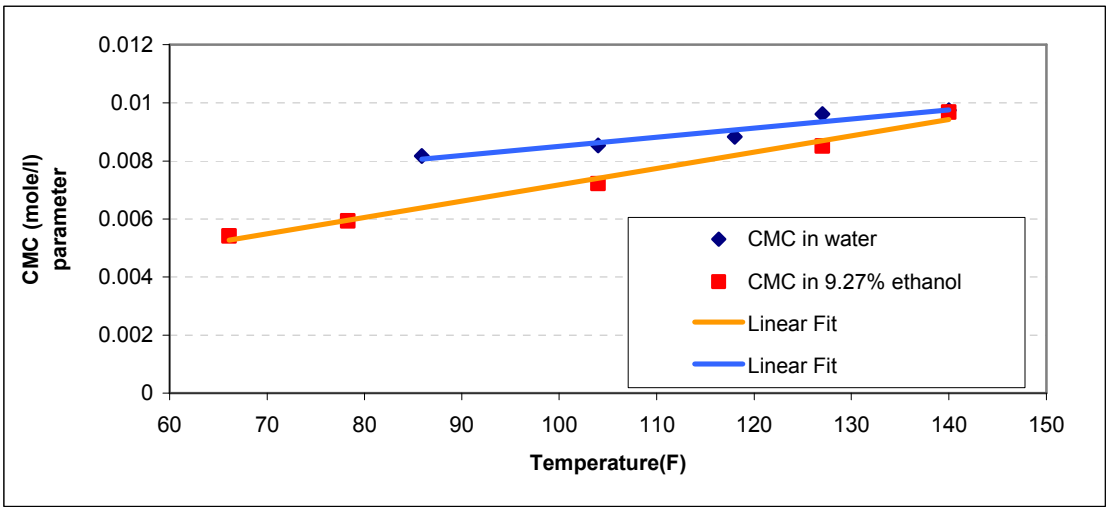

Figure 6.12 Effect of temperature on CMC for sodium dodecyl sulfate (Bourrel and Schechter, 1988)

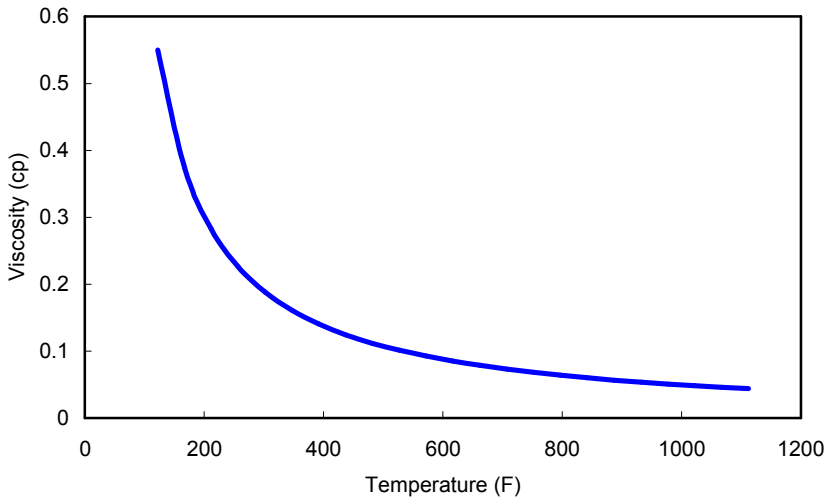

Figure 6.13 Water viscosity versus temperature from Grabowski's function (1979)

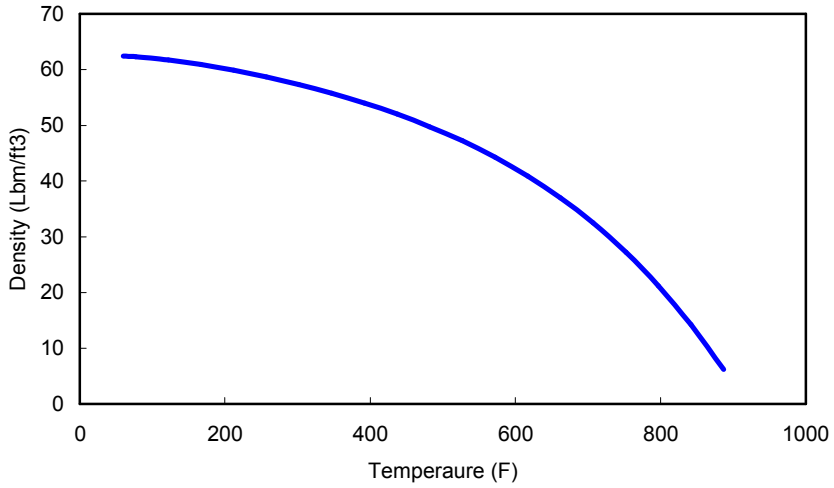

Figure 6.14 Water density versus temperature from Trangenstein's modification of Kell's correlation (1975)

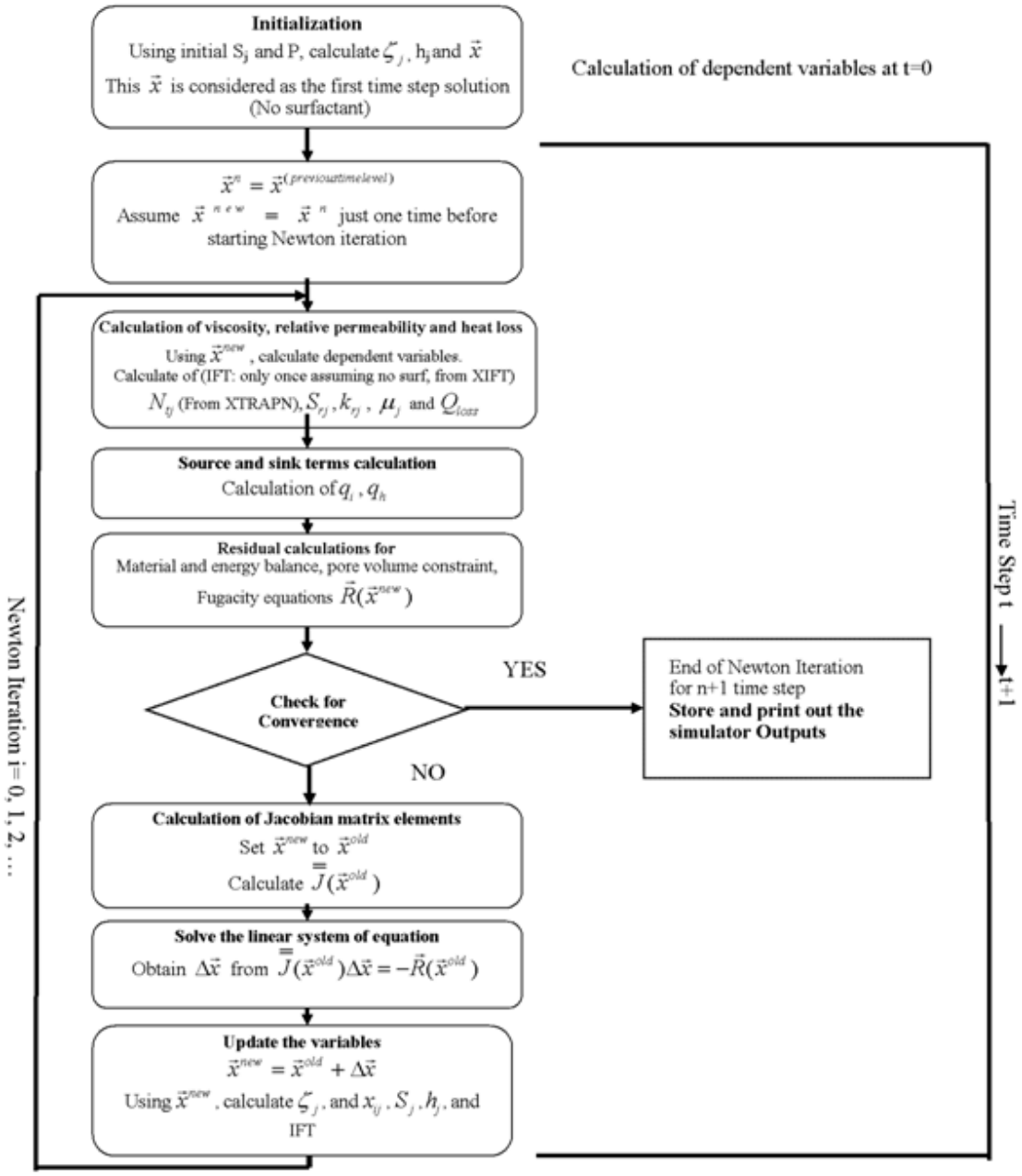

Figure 6.15 Computational flow chart for the hot chemical model

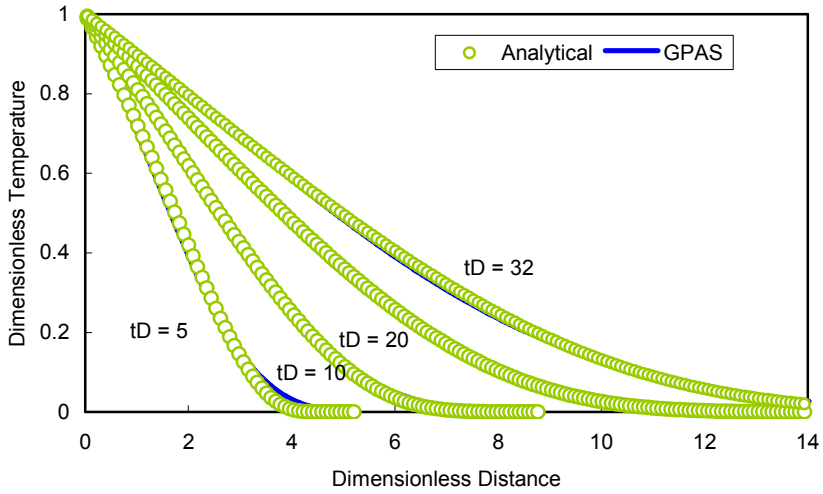

Figure 6.16 Comparison of the chemical thermal model with the analytical solution (Case1)

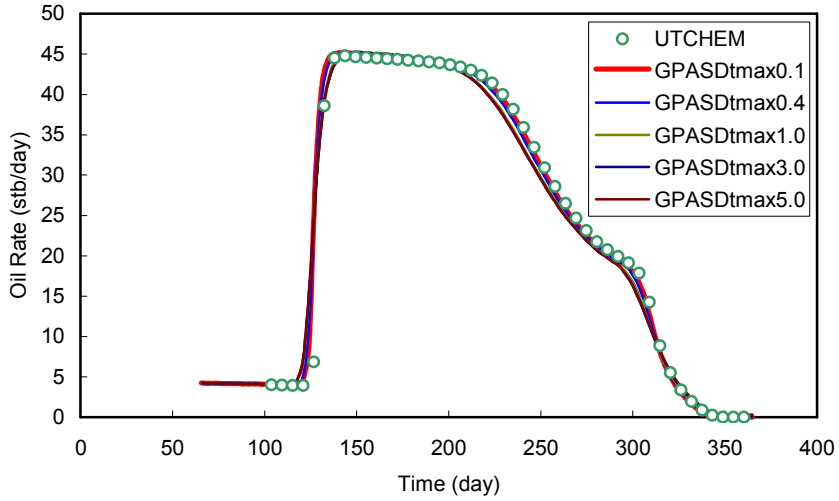

Figure 6.17 Oil production rate for one-dimensional case (Case 2)

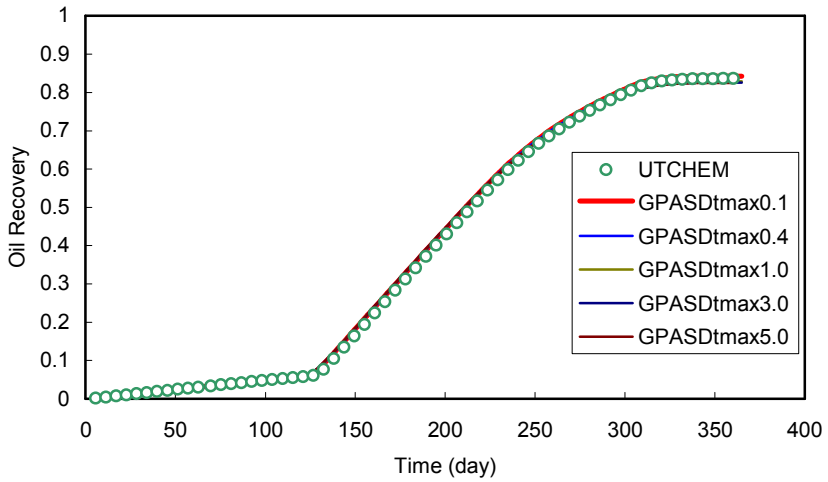

Figure 6.18 Oil recovery for one-dimensional case (Case 2)

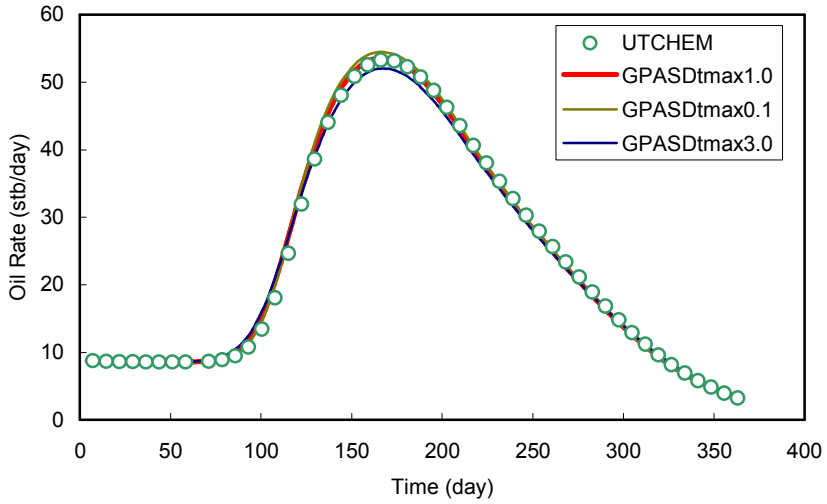

Figure 6.19 Oil production rate for two-dimensional case (Case 3)

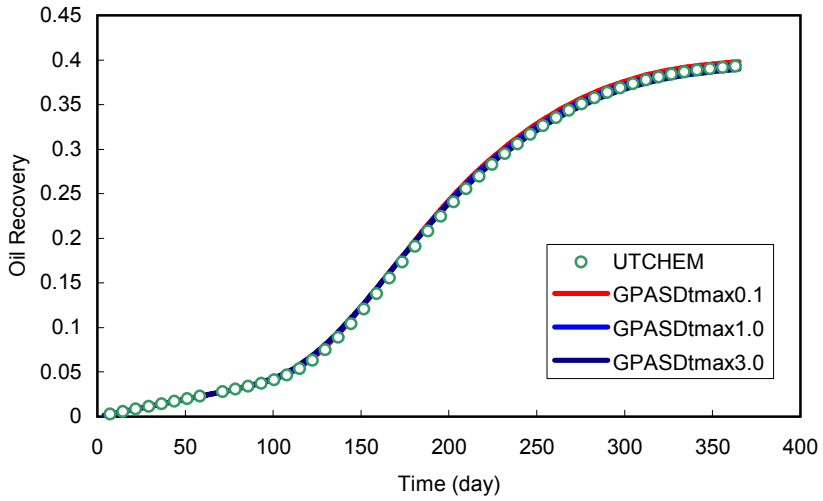

Figure 6.20 Oil recovery for two-dimensional case (Case 3)

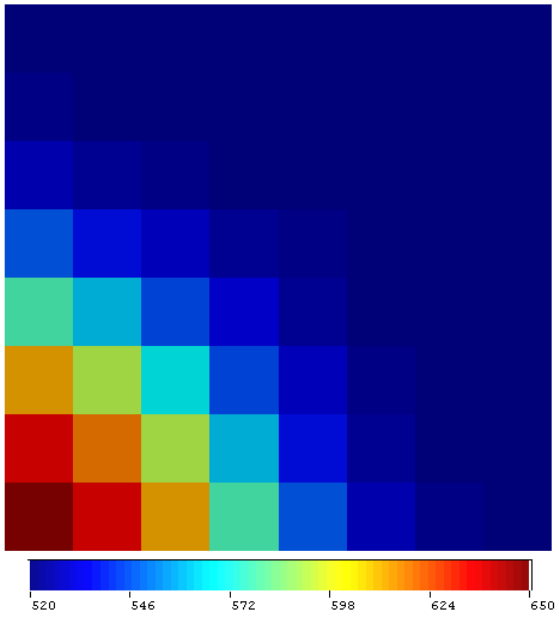

Figure 6.21 Temperature profile (°R) after 365 days of GPAS for two-dimensional case (Case 3)

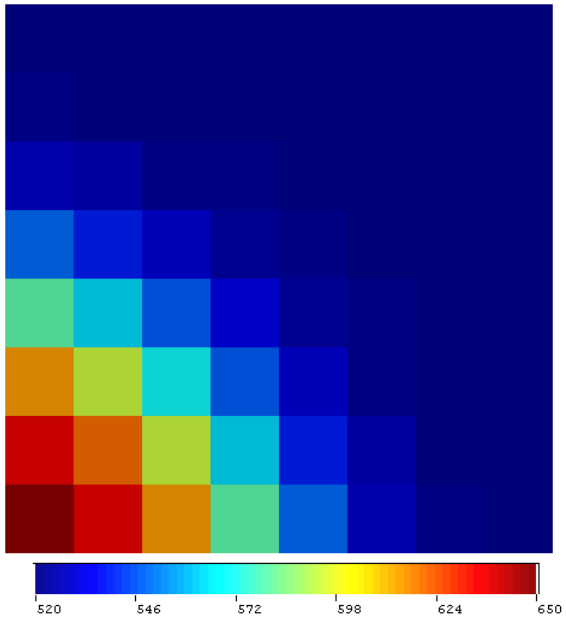

Figure 6.22 Temperature profile (°R) after 365 days of UTCHEM for two-dimensional case (Case 3)

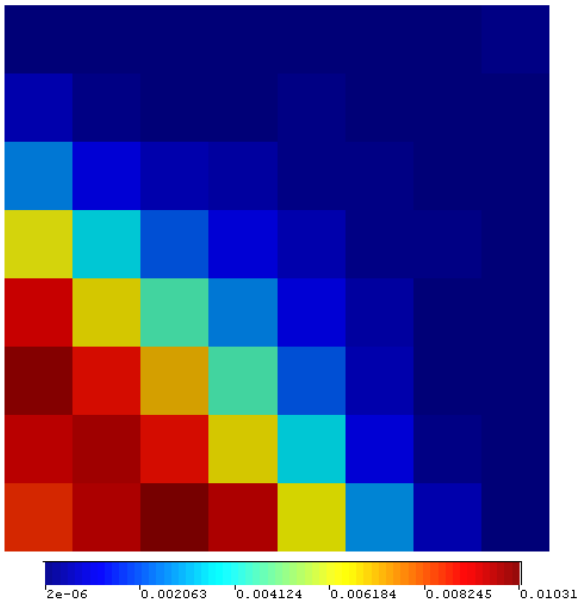

Figure 6.23 Relative temperature difference after 365 days between GPAS and UTCHEM for two-dimensional case (Case 3)

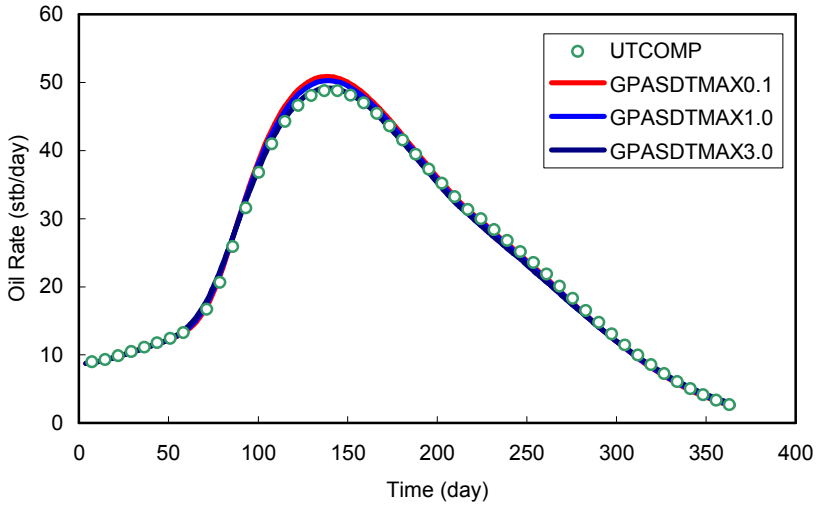

Figure 6.24 Oil production rate for three-dimensional case (Case 4)

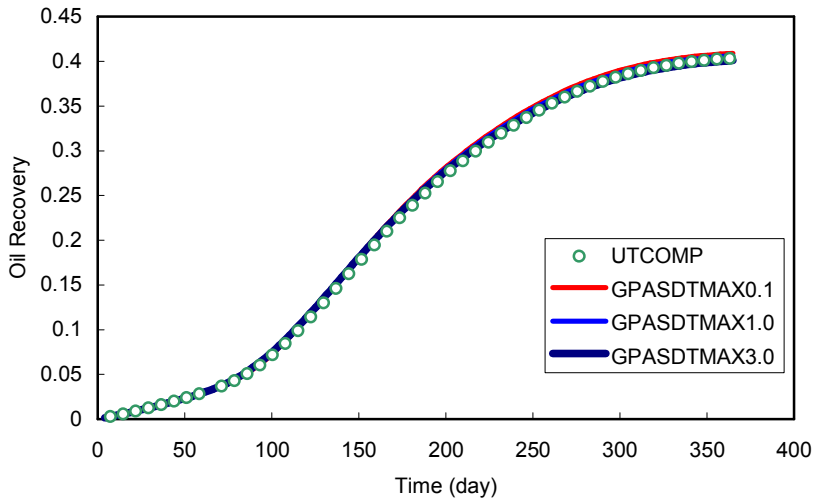

Figure 6.25 Oil recovery for three-dimensional case (Case 4)

Chapter 7: Summary, Conclusions, and Recommendations for future work

The *summary*, *conclusions* and the *recommendations* for future studies are presented in this chapter.

Summary

The following models were developed and incorporated into GPAS using a fully-implicit solution scheme.

1. A four-phase model, where three of the phases are in equilibrium, was developed and incorporated into the simulator that can be used for the following processes.
    - Miscible flooding, where miscible gases such as CO_2 are used at a low temperature
    - Recovery of very heavy oil with steam and solvents (i.e. VAPEX)
    - Solvent stimulation of gas condensate reservoirs
    - Asphaltene precipitation
    - Hydrate formation
2. A 3D EOS-based thermal model, which addresses three phases in equilibrium, was developed and incorporated into the simulator for
    - Hot fluid injection
    - Electrical heating
        i. Joule heating
        ii. In-situ thermal desorption

3. A hot chemical flooding model was implemented into the simulator
4. The models were compared with analytical solutions and other simulators and tested for different case studies

Conclusions

1. The multiple phase flash calculation routine was tested against WinProp and good agreements were obtained for various problems.
2. The four-phase model was tested and compared to three phase model for the case which was expected to have a second liquid phase with oil and gas phases. It gave accurate results due to having three phase in phase equilibrium routine.
3. The three-phase model, in which all of the phases are in equilibrium, was used for EOS-based thermal model.
4. The result of EOS-based thermal model was compared with Lauwerier problem, for hot water injection, to test the heat loss calculations and they had excellent agreement.
5. One outstanding feature of this thermal model is the incorporation of *mutual* solubilties of hydrocarbon components and water in hydrocarbon and aqueous phases. In thermal recovery processes, these solubilities command profound influences. Strikingly, this aspect was ignored in previous studies of all kinds of thermal recovery-related matters. In other words, the aqueous phase is a partner in Gibbs free energy minimization and in equality of component chemical potentials among phases. In this four-phase model, there can be simultaneous transport of four phases (gas, oil, second hydrocarbon liquid, and aqueous), but only three of these phases are in thermodynamic equilibrium. Subsequently, we developed a protocol to address all four

phases in equilibrium, which will offer a clearer and broader picture. Thus, this model successfully incorporates the role of *solubility*, which asserts itself more prominently should temperature increase. To the best of our knowledge, other published models do not address this important issue.

6. The EOS-thermal model was compared with K-value approach of CMG-STARS commercial simulator and different results were obtained. The equilibrium ratios of EOS- thermal model are a function of pressure, temperature, and phase compositions and they are thermodynamically consistent, while the K-values in K-value approaches are just function of pressure and temperature. Hence, the K-value approach is not as accurate as the EOS method.
7. In most of the K-value thermal model, the solubility of water in hydrocarbon rich liquid phase and hydrocarbon components in water rich phase are ignored. But in the developed thermal model all of the components can exist in all of the phases.
8. The EOS-thermal model was tested with different test cases such as one-two-and three-dimensional reservoirs, different number of component fluid mixtures, and heterogeneous reservoir.
9. The developed EOS-thermal model was tested in parallel mode. Good speedups were obtained using various case studies.
10. The developed thermal model has cartesian and corner-point options. The model was tested with corner-point option as well as Cartesian mesh option.
11. The EOS-electrical heating model was compared with the electrical heating model of STARS and good agreement was obtained.

12. The developed EOS-electrical heating model was tested for one-, two-, and three-dimensional reservoirs and different number of component fluid mixtures.
13. The electrical heating model was tested and showed that the existence of water is very important in order to maintain high electrical conductivity.
14. The electrical heating model was tested in parallel mode and good speedups were obtained.
15. The chemical-thermal model was tested using Lauwerier problem and good agreement between the simulation results and analytical solution was obtained.
16. The chemical-thermal model was tested in one-, two-, and three-dimensional reservoirs and was compared with the UTCHEM simulator with good agreement.

Recommendations

1. Development of the four-phase model, where four-phase flash calculation will be performed.
2. Development of a reduced flash calculation method, where by its outstanding features include a reduced set of functional variables and therefore is more computationally advantageous if larger reservoirs and higher-number-components fluids will be used, in lieu of conventional flash calculation, for the simulator during two-phase, three-phase, and four-phase flash calculations.

3. Development and implementation of algorithm for fugacity equations by using fully implicit partitioning computational method to improve the computational speed and convergence features of the simulator.
4. Modification and more accurate tuning of EOS parameters in water-hydrocarbon systems for EOS-thermal methods, i.e. binary interaction coefficients and volume shift parameters.
5. Implementation of wettability alteration into hot chemical flooding model as a function of temperature.
6. Further research to speed up the *linear solver* for the solution of linear systems of equations arising from discretization of governing partial differential equations representing the physical systems in the simulator.
7. Coupling thermal models with the geomechanics model to study the temperature effects on geomechanical parameters.
8. Extend the developed thermal models to include other models such as naturally fracture reservoir model.

Appendix A

Peng-Robinson Equation of State Parameters

A.1 PENG-ROBINSON EQUATION OF STATE

The main equations of the Peng-Robinson EOS (Peng and Robinson, 1976) are described in this appendix.

$$P = \frac{RT}{\bar{v} - b} - \frac{a}{\bar{v}(\bar{v} + b) + b(\bar{v} - b)} \tag{A.1}$$

The parameters *a* and *b* for a pure component are computed from

$$a = 0.45748 \frac{R^2 T_c^2}{P_c} \alpha(T) \tag{A.2}$$

$$b = 0.07780 \frac{RT_c}{P_c} \tag{A.3}$$

$$\sqrt{\alpha} = 1 + f_w \left(1 - \sqrt{\frac{T}{T_c}} \right) \tag{A.4}$$

$$f_w = \begin{cases} 0.37464 + 1.54226\omega - 0.26992\omega^2 & \omega < 0.49 \\ 0.379640 + 1.485030\ \omega - 0.164423\ \omega^2 + 0.016666\ \omega^3 & \omega \geq 0.49 \end{cases} \tag{A.5}$$

For component *i*

$$a_i = \frac{0.45748\, R^2\, T_{C_i}{}^2}{P_{C_i}} [1 + f_{w_i}(1 - \sqrt{T_{r_i}})]^2 \tag{A.6}$$

$$b_i = 0.07780 \frac{RT_{ci}}{P_{ci}} \tag{A.7}$$

For a multi-component mixture, the mixing rules for the two parameters are

$$a_{m,j} = \sum_{i=1}^{n_c} \sum_{k=1}^{n_c} x_{ij}\, x_{kj} a_{i,k} \quad \textit{for phase } j \tag{A.8}$$

$$a_{i,k} = \sqrt{(a_i a_k)}(1 - \delta_{ik}) \tag{A.9}$$

$$a_{m,j} = \sum_{i=1}^{n_c} \sum_{k=1}^{n_c} x_{ij}\, x_{kj} \sqrt{(a_i a_k)}(1 - \delta_{ik}) \quad \textit{for phase } j \tag{A.10}$$

$$b_{m,j} = \sum_{i=1}^{n_c} x_{ij} b_i \tag{A.11}$$

The constant δ_{ik} is called the binary interaction coefficient between components *i* and *k*.

The Peng-Robinson EOS for phase *j* can be written in the form

$$Z_j^3 + (B_j - 1)Z_j^2 + (A_j - 3B_j^2 - 2B_j)Z_j + (-A_j B_j + B_j^2 + B_j^3) = 0 \tag{A.12}$$

where $Z_j = \frac{P\overline{v}_j}{RT}$ is the compressibility factor.

$$A_j = \frac{a_{m,j} P}{(RT)^2} \tag{A.13}$$

$$B_j = \frac{b_{m,j} P}{RT} \tag{A.14}$$

By having the related parameters for each phase, the compressibility factor for that phase is calculated from the above EOS.

A.2 FUGACITY EQUATION FOR PENG-ROBINSON EQUATION OF STATE

The fugacity is calculated for each component in each phase as follows:

$$Ln\varphi_{ij} = \frac{b_i}{b}\left(Z_j - 1\right) - Ln\left(Z_j - B_j\right) - \frac{A_j}{2\sqrt{2}B_j}\left(\frac{2}{a_j}\sum_{m=1}^{n_c} x_{mj} a_{im} - \frac{b_i}{b_m}\right)$$
$$Ln\left[\frac{Z_j + \left(1+\sqrt{2}\right)B_j}{Z_j + \left(1-\sqrt{2}\right)B_j}\right] \tag{A.15}$$

A.3 ENTHALPY EQUATION FOR PENG-ROBINSON EQUATION OF STATE

The enthalpy for each phase with parameters of each phase can be calculated by

$$h_j = \frac{T\frac{\partial a_{m,j}}{\partial T} - a_{m,j}}{b_{m,j}} Ln\left(\frac{Z_j + (\sqrt{2}+1)B_j}{Z_j + (\sqrt{2}-1)B_j}\right) + RT(Z_j - 1) + h_j^{\circ} \tag{A.16}$$

$$h_j^{\circ} = \sum_{i=1}^{n_c} x_i h_i^{\circ} \tag{A.17}$$

$$h_i^{\circ} = Cp_{1,i}^{\circ}(T - T_{ref}) + \frac{Cp_{2,i}^{\circ}}{2}(T^2 - {T_{ref}}^2) + \frac{Cp_{3,i}^{\circ}}{3}(T^3 - {T_{ref}}^3) + \frac{Cp_{4,i}^{\circ}}{4}(T^4 - {T_{ref}}^4) \tag{A.18}$$

The parameters h_j° and h_i° are the reference enthalpy for phase *j* and component *i,* respectively. The reference state is an ideal gas for that component. The coefficient

$Cp^{\circ}_{1,i} \ldots Cp^{\circ}_{4,i}$ are the heat capacity coefficients for component *i* at the ideal gas condition, which is considered the reference state.

$$\frac{\partial a_{m,j}}{\partial T} = \frac{1}{2}\sum_{i=1}^{n_c}\sum_{k=1}^{n_c} x_{ij}\, x_{kj} (a_i a_k)^{-\frac{1}{2}} (a_i \frac{\partial a_k}{\partial T} + a_k \frac{\partial a_i}{\partial T})(1-\delta_{ik}) \tag{A.19}$$

$$\frac{\partial^2 a_{m,j}}{\partial T^2} = \sum_{i=1}^{n_c}\sum_{k=1}^{n_c} x_{ij}\, x_{kj} [-\frac{1}{4}(a_i a_k)^{-\frac{3}{2}} (a_i \frac{\partial a_k}{\partial T} + a_k \frac{\partial a_i}{\partial T}) +$$
$$\frac{1}{2}(a_i a_k)^{-\frac{1}{2}} (a_i \frac{\partial^2 a_k}{\partial T^2} + 2\frac{\partial a_i}{\partial T}\frac{\partial a_k}{\partial T} + a_k \frac{\partial^2 a_i}{\partial T^2})](1-\delta_{ik}) \tag{A.20}$$

$$\frac{\partial a_i}{\partial T} = -\frac{0.42748\, R^2\, {T_{C_i}}^2}{P_{C_i}} [f_{w_i} \frac{1}{{T_{C_i}}^{1.5}} (1-\sqrt{T_{r_i}})] \tag{A.21}$$

$$f_{w_i} = 0.48 + 1.574 w_i - 0.176 w_i^2 \tag{A.22}$$

A.4 INTERNAL ENERGY

The enthalpy for each phase with parameters of each phase is calculated by

$$u_j = h_j - p\overline{v}_i \tag{A.23}$$

A.5 ALTERNATIVE TWO-PHASE FLASH CALCULATION

The convergence analysis for constant pressure and temperature, two-phase flash calculation, was presented by Michelsen and Mollerup (2004). The method uses the components mole values in gas phase as primary variables instead of phase mole ratio, which is calculated by Rachrod-Rice equation) and K values (or *LnK*).

The objective function which is used in this method is derived as follow:

The equilibrium equations of the components are

$$R_i(\vec{v}) = Lnf_i^v - Lnf_i^l \tag{A.24}$$

The independent variables are components mole value in gas phase (v_i) and the amount of the components value in liquid phase per one mole of the mixture are calculated by

$$l_i = z_i - v_i \tag{A.25}$$

The solution of the equations (A.24) is as follow:

$$\vec{v}^{k+1} = \vec{v}^{k+1} + \Delta v = v^{k+1} - (\vec{J}^k)^{-1}\vec{R}^k \tag{A.26}$$

The Jacobian matrix for set of equations (A.24) is calculated by

$$J_{ij} = \frac{\partial R_i}{\partial v_i} = \frac{\partial Lnf_i^v}{\partial v_i} - \frac{\partial Lnf_i^l}{\partial v_i} = \frac{\partial Lnf_i^v}{\partial v_i} + \frac{\partial Lnf_i^l}{\partial l_i} \tag{A.27}$$

For the fugacity coefficient equation we have

$$Lnf_i^v = Lny_i + Ln\varphi_i^v + LnP = Ln\frac{v_i}{V} + Ln\varphi_i^v + LnP \tag{A.28}$$

where $V = \sum_{i=1}^{n_c} v_i$, and the derivatives of equation (A.28) is

$$\frac{\partial(Lnf_i^v)}{\partial v_i} = \frac{1}{v_i}\delta_{ij} - \frac{1}{V} + \frac{\partial(Ln\varphi_i^v)}{\partial v_i} = \frac{1}{V}\left(\frac{1}{y_i}\delta_{ij} - 1 + \bar{\Phi}_{ij}\right) \tag{A.29}$$

where

$$\delta_{ij} = \left(1\ if\ i = j, 0\ if\ i \neq j\right)$$

$$\bar{\Phi}_{ij} = n_T\left(\frac{\partial(Ln\varphi_i^v)}{\partial v_i}\right)_{T,P} \text{ and } n_T = \sum_{k=1}^{n_c} n_i$$

The liquid phase derivatives are similar to the gas phase derivatives. The equation (A.27) can be written in the following form

$$\begin{aligned} J_{ij} &= \frac{1}{V}\left(\frac{1}{y_i}\delta_{ij} - 1 + \bar{\Phi}^v_{ij}\right) + \frac{1}{1-V}\left(\frac{1}{x_i}\delta_{ij} - 1 + \bar{\Phi}^l_{ij}\right) \\ &= \frac{1}{V(1-V)}\left(\frac{z_i}{x_i y_i}\delta_{ij} - 1 + (1-V)\bar{\Phi}^v_{ij} + V\bar{\Phi}^l_{ij}\right) \end{aligned} \tag{A.30}$$

Michelsen and Mollerup (2004) presented that instead of using full-Jacobian matrix, the iterative sequence was used, which was based on the approximation in the successive substitution method, i.e. the fugacity coefficient are composition independent. The approximate expression of equation (A.30) is

$$J_{ij} = \frac{1}{V(1-V)}\left(\frac{z_i}{x_i y_i}\delta_{ij} - 1\right) \tag{A.31}$$

The expression to calculate amount of the components in vapor phase is

$$\delta v_i = V(1-V)s_i\left(\frac{\sum_j s_j R_j}{\sum_j s_j - 1} - R_j\right) \tag{A.32}$$

where $s_i = \frac{x_i y_i}{z_i}$

The following procedure was used for alternative flash calculation:

1. Initial guess for v_i
2. Calculate $l_i = z_i - v_i$
3. Calculate $V = \sum_{i=1}^{n_c} v_i$ and $y_i = \frac{v_i}{V}$
4. Calculate $L = \sum_{i=1}^{n_c} l_i$ and $x_i = \frac{l_i}{L}$
5. Calculate f_i^v and f_i^l
6. Check the following conditions $\left|f_i^v - f_i^l\right| < Tol_{.1}$ and $\left|v_i^k - v_i^{k+1}\right| \le Tol_{.2}$
7. If the conditions of step 6 are not achieved calculate the new values for v_i using equation (A.32) and repeat the steps from step 2.

The following examples show the difference between this method and conventional two-phase flash calculation. Tables A.1 through A.4 show the composition of the mixture and the comparison between the explained method and conventional flash calculations for six- and ten- component mixture, respectively.

Table A.1 Component mole fraction for six component mixture

Component	Mole fraction
C1	0.50
C3	0.03
C6	0.07
C10	0.2
C15	0.15
C20	0.05

Table A.2 Comparison of alternative two-phase flash and conventional flash calculations for six component mixture

T(°F)	P(Psia)	Gas mole ratio	Number of iterations for conventional flash calculations, Rachford-Rice plus fugacity equations	Number of iterations for new algorithm
60.0	14.7	0.53342	4	3
160.0	1400.0	0.21317	13	9
200.0	1000.0	0.335847	14	5

Table A.3 Component mole fraction for ten component mixture

Component	Mole fraction
CO_2	0.000492
C1	0.295064
C2	0.003934
C3	0.009835
C4	0.020881
C5	0.020654
C6	0.21638
C8	0.147532
C11	0.10819
C13	0.177038

Table A.4 Comparison of alternative two-phase flash and conventional flash calculations for ten component mixture

T(°F)	P(Psia)	Gas mole ratio	Number of iterations for conventional flash calculations, Rachford-Rice plus fugacity equations	Number of iterations for new algorithm
150.0	500.0	0.21317	10	4

Appendix B

Evaluation of Jacobian Elements for Fugacity Equations

B.1 Derivatives of Equilibrium Equations Residual with Respect to LnK_1, LnK_2

Since only one grid cell is involved in the derivatives, we can drop grid indices and use *i* and *j* for the component index. There are two fugacity equations when three phases are in equilibrium in the gridblocks. In the following equations, oil phase is considered the base phase; if oil phase does not exist in the gridblock, second hydrocarbon liquid phase will be the base phase. The relevant equations are as follows:

$$\frac{\partial R_{F_{1,\alpha,i,j,k}}}{\partial LnK_{1,i,j,k}} = \frac{\partial\ LnK_{1,\alpha,i,j,k}}{\partial LnK_{1,i,j,k}} + \frac{\partial\, Ln\varphi_{g,\alpha,i,j,k}}{\partial LnK_{1,i,j,k}} - \frac{\partial Ln\varphi_{o,\alpha,i,j,k}}{\partial LnK_{1,i,j,k}} \tag{B.1}$$

$$\frac{R_{F_{2,,\alpha i,j,k}}}{\partial LnK_{1,i,j,k}} = \frac{\partial LnK_{2,\alpha,i,j,k}}{\partial LnK_{1,i,j,k}} + \frac{\partial Ln\varphi_{L2,\alpha,i,j,k}}{\partial LnK_{1,i,j,k}} - \frac{\partial Ln\varphi_{o,\alpha,i,j,k}}{\partial LnK_{1,i,j,k}} \tag{B.2}$$

For LnK_2 the equations are as follows:

$$\frac{\partial R_{F_{1,\alpha,i,j,k}}}{\partial LnK_{2,i,j,k}} = \frac{\partial LnK_{1,\alpha,i,j,k}}{\partial LnK_{2,i,j,k}} + \frac{\partial Ln\varphi_{g,\alpha,i,j,k}}{\partial LnK_{2,i,j,k}} - \frac{\partial Ln\varphi_{o,\alpha,i,j,k}}{\partial LnK_{2,i,j,k}} \tag{B.3}$$

$$\frac{R_{F_{2,,\alpha,i,j,k}}}{\partial LnK_{2,i,j,k}} = \frac{\partial \ln K_{2,\alpha,i,j,k}}{\partial LnK_{2,i,j,k}} + \frac{\partial \ln \varphi_{L2,\alpha,i,j,k}}{\partial LnK_{2,i,j,k}} - \frac{\partial \ln \varphi_{o,\alpha,i,j,k}}{\partial LnK_{2,i,j,k}} \tag{B.4}$$

At constant pressure and temperature,

$$Ln\varphi_{i\beta} = f(\vec{K}_1, \vec{K}_2, \vec{N}, v, L_2) \tag{B.5}$$

where L_2 and v are the mole ratios of the second liquid phase and the gas phase, the oil mole ratio is

$L_1=1.0-(v+L_2)$

and

$\vec{K}_1=(K_{1,1},K_{1,2},...,K_{1,n_c})$, $\vec{K}_2=(K_{2,1},K_{2,2},...,K_{2,n_c})$

and $\vec{N}=(N_1,N_2,...,N_{n_c})$

Taking the total differential of Eq. (B.5), we have

$$dLn\varphi_{i\beta}=\sum_{j=1}^{n_c}\left(\frac{\partial\varphi_{i\beta}}{\partial LnK_{1,j}}\right)_{\vec{N},\vec{K}_m,\vec{K}_2,L_2,v}dLnK_{1,j}+\sum_{j=1}^{n_c}\left(\frac{\partial\varphi_{i\beta}}{\partial LnK_{2,j}}\right)_{\vec{N},\vec{K}_n,\vec{K}_1,L_2,v}dLnK_{2,j}$$

$$+\left(\frac{\partial\varphi_{i\beta}}{\partial v}\right)_{\vec{N},\vec{K}_1,\vec{K}_2,L_2}dv+\left(\frac{\partial\varphi_{i\beta}}{\partial L_2}\right)_{\vec{N},\vec{K}_1,\vec{K}_2,v}dL_2+\sum_{j=1}^{n_c}\left(\frac{\partial\varphi_{i\beta}}{\partial N_j}\right)_{\vec{N}_m,\vec{K}_1,\vec{K}_2,L_2,v}dN_j \qquad \text{(B.6)}$$

where $\vec{K}_m=(K_{1,1},K_{1,2},...,K_{1,j-1},K_{1,j+1},...,K_{1,n_c})$, $\vec{K}_n=(K_{2,1},K_{2,2},...,K_{2,j-1},K_{2,j+1},...,K_{2,n_c})$

and $\vec{N}_m=(N_1,N_2,...,N_{j-1},N_{j+1},...,N_{n_c})$

From Eq. (B.6), we can get

$$\left(\frac{\partial R_{F_{1,i}}}{\partial LnK_{1,j}}\right)_{\vec{N},\vec{K}_m,\vec{K}_2}=\begin{cases}\left(\dfrac{\partial Ln\varphi_{ig}}{\partial LnK_{1,j}}\right)_{\vec{N},\vec{K}_m,\vec{K}_2}-\left(\dfrac{\partial Ln\varphi_{io}}{\partial LnK_{1,j}}\right)_{\vec{N},\vec{K}_m,\vec{K}_2}+1 & if \quad i=j\\ \left(\dfrac{\partial Ln\varphi_{ig}}{\partial LnK_{1,j}}\right)_{\vec{N},\vec{K}_m,\vec{K}_2}-\left(\dfrac{\partial Ln\varphi_{io}}{\partial LnK_{1,j}}\right)_{\vec{N},\vec{K}_m,\vec{K}_2} & if \quad i\neq j\end{cases} \qquad \text{(B.7)}$$

$$\left(\frac{\partial R_{F_{1,i}}}{\partial LnK_{2,j}}\right)_{\vec{N},\vec{K}_1,\vec{K}_n} = \left(\frac{\partial Ln\varphi_{ig}}{\partial LnK_{2,j}}\right)_{\vec{N},\vec{K}_1,\vec{K}_n} - \left(\frac{\partial Ln\varphi_{io}}{\partial LnK_{2,j}}\right)_{\vec{N},\vec{K}_1,\vec{K}_n} \tag{B.8}$$

For the second fugacity equation

$$\left(\frac{\partial R_{F_{2,i}}}{\partial LnK_{2,j}}\right)_{\vec{N},\vec{K}_m,\vec{K}_2} = \begin{cases} \left(\frac{\partial Ln\varphi_{iL2}}{\partial LnK_{2,j}}\right)_{\vec{N},\vec{K}_1,\vec{K}_n} - \left(\frac{\partial Ln\varphi_{io}}{\partial LnK_{2,j}}\right)_{\vec{N},\vec{K}_1,\vec{K}_n} + 1 & if \quad i = j \\ \left(\frac{\partial Ln\varphi_{iL2}}{\partial LnK_{2,j}}\right)_{\vec{N},\vec{K}_1,\vec{K}_n} - \left(\frac{\partial Ln\varphi_{io}}{\partial LnK_{2,j}}\right)_{\vec{N},\vec{K}_1,\vec{K}_n} & if \quad i \neq j \end{cases} \tag{B.9}$$

$$\left(\frac{\partial R_{F_{2,i}}}{\partial LnK_{1,j}}\right)_{\vec{N},\vec{K}_1,\vec{K}_n} = \left(\frac{\partial Ln\varphi_{iL2}}{\partial LnK_{1,j}}\right)_{\vec{N},\vec{K}_1,\vec{K}_n} - \left(\frac{\partial Ln\varphi_{io}}{\partial LnK_{1,j}}\right)_{\vec{N},\vec{K}_m,\vec{K}_2} \tag{B.10}$$

Dividing Eq. (B.6) by $\partial LnK_{1,j}$, while holding $\vec{N}$, $\vec{K}_2$ and $\vec{K}_m$ constant, for the gas phase we have

$$\left(\frac{\partial Ln\varphi_{i\beta}}{\partial LnK_{1,j}}\right)_{\vec{N},\vec{K}_m,\vec{K}_2} = \left(\frac{\partial Ln\varphi_{i\beta}}{\partial LnK_{1,j}}\right)_{\vec{N},\vec{K}_m,\vec{K}_2,v,L_2} + \left(\frac{\partial Ln\varphi_{i\beta}}{\partial v}\right)_{\vec{N},\vec{K}_1,\vec{K}_2,L_2}\left(\frac{\partial v}{\partial LnK_{1,j}}\right)_{\vec{N},\vec{K}_m,\vec{K}_2} + \left(\frac{\partial Ln\varphi_{i\beta}}{\partial L_2}\right)_{\vec{N},\vec{K}_1,\vec{K}_2,v}\left(\frac{\partial L_2}{\partial LnK_{1,j}}\right)_{\vec{N},\vec{K}_m,\vec{K}_2} \tag{B.11}$$

Dividing Eq. (B.6) by $\partial LnK_{2,j}$ while holding $\vec{N}$, $\vec{K}_1$ and $\vec{K}_n$ constant, for the gas phase we have

$$\left(\frac{\partial Ln\varphi_{i\beta}}{\partial LnK_{2,j}}\right)_{\vec{N},\vec{K}_n,\vec{K}_1} = \left(\frac{\partial Ln\varphi_{i\beta}}{\partial LnK_{2,j}}\right)_{\vec{N},\vec{K}_n,\vec{K}_1,v,L_2} + \left(\frac{\partial Ln\varphi_{i\beta}}{\partial v}\right)_{\vec{N},\vec{K}_1,\vec{K}_2,L_2}\left(\frac{\partial v}{\partial LnK_{2,j}}\right)_{\vec{N},\vec{K}_n,\vec{K}_1} + \left(\frac{\partial Ln\varphi_{i\beta}}{\partial L_2}\right)_{\vec{N},\vec{K}_1,\vec{K}_2,v}\left(\frac{\partial L_2}{\partial LnK_{2,j}}\right)_{\vec{N},\vec{K}_n,\vec{K}_1} \tag{B.12}$$

The above equations are expanded as follows:

$$\left(\frac{\partial Ln\varphi_{i\beta}}{\partial LnK_{1,j}}\right)_{\vec{N},\vec{K}_m,\vec{K}_2} = \left(\frac{\partial Ln\varphi_{i\beta}}{\partial x_{j,\beta}}\right)_{\vec{N},\vec{K}_m,\vec{K}_2,v} \left(\frac{\partial x_{j,\beta}}{\partial LnK_{1,j}}\right)_{\vec{N},\vec{K}_m,\vec{K}_2,v,L_2} +$$

$$\left(\frac{\partial Ln\varphi_{i\beta}}{\partial v}\right)_{\vec{N},\vec{K}_1,\vec{K}_2} \frac{\left(\frac{\partial G2}{\partial LnK_{1,j}}\right)_{\vec{N},\vec{K}_m,\vec{K}_2,v}}{\left(\frac{\partial G2}{\partial v}\right)_{\vec{N},\vec{K}_1,\vec{K}_2}} + \left(\frac{\partial Ln\varphi_{i\beta}}{\partial L_2}\right)_{\vec{N},\vec{K}_1,\vec{K}_2} \frac{\left(\frac{\partial G3}{\partial LnK_{1,j}}\right)_{\vec{N},\vec{K}_m,\vec{K}_2,L_2}}{\left(\frac{\partial G3}{\partial L_2}\right)_{\vec{N},\vec{K}_1,\vec{K}_2}} \tag{B.13}$$

and the equation for the second set of equilibrium ratios K2 is as follows:

$$\left(\frac{\partial Ln\varphi_{i\beta}}{\partial LnK_{2,j}}\right)_{\vec{N},\vec{K}_n,\vec{K}_1} = \left(\frac{\partial Ln\varphi_{i\beta}}{\partial x_{j,\beta}}\right)_{\vec{N},\vec{K}_n,\vec{K}_1,v} \left(\frac{\partial x_{j,\beta}}{\partial LnK_{2,j}}\right)_{\vec{N},\vec{K}_n,\vec{K}_1,v,L_2} +$$

$$\left(\frac{\partial Ln\varphi_{i\beta}}{\partial v}\right)_{\vec{N},\vec{K}_1,\vec{K}_2} \frac{\left(\frac{\partial G2}{\partial LnK_{2,j}}\right)_{\vec{N},\vec{K}_n,\vec{K}_1,v}}{\left(\frac{\partial G2}{\partial v}\right)_{\vec{N},\vec{K}_1,\vec{K}_2}} + \left(\frac{\partial Ln\varphi_{i\beta}}{\partial L_2}\right)_{\vec{N},\vec{K}_1,\vec{K}_2} \frac{\left(\frac{\partial G3}{\partial LnK_{1,j}}\right)_{\vec{N},\vec{K}_n,\vec{K}_1,L_2}}{\left(\frac{\partial G3}{\partial L_2}\right)_{\vec{N},\vec{K}_1,\vec{K}_2}} \tag{B.14}$$

where $x_{j,\beta}$ is the mole fraction of component j in phase β.

B.2 DERIVATIVES OF EQUILIBRIUM EQUATIONS RESIDUAL WITH RESPECT TO COMPONENT MOLE NUMBER

Dividing Eq. (B.6) by ∂N_j while holding $\vec{K}_1$, $\vec{K}_2$ and $\vec{N}_m$ constant, we have

$$\left(\frac{\partial Ln\varphi_{i\beta}}{\partial N_j}\right)_{\vec{K}_1,\vec{K}_2,\vec{N}_m} = \left(\frac{\partial Ln\varphi_{i\beta}}{\partial N_j}\right)_{\vec{N}_m,\vec{K}_1,\vec{K}_2,L_2,v} + \left(\frac{\partial Ln\varphi_{i\beta}}{\partial v}\right)_{\vec{K}_1,\vec{K}_2,L_2,\vec{N}} \left(\frac{\partial v}{\partial N_j}\right)_{\vec{K}_1,\vec{K}_2,L_2,\vec{N}_m}$$

$$+\left(\frac{\partial Ln\varphi_{i\beta}}{\partial L_2}\right)_{\vec{K}_1,\vec{K}_2,v,\vec{N}}\left(\frac{\partial L_2}{\partial N_j}\right)_{\vec{K}_1,\vec{K}_2,v,\vec{N}_m} \tag{B.15}$$

$$\left(\frac{\partial Ln\varphi_{i\beta}}{\partial N_j}\right)_{\vec{K}_1,\vec{K}_2,\vec{N}_m}=\left(\frac{\partial Ln\varphi_{i\beta}}{\partial x_{j\beta}}\right)_{\vec{N}_m,\vec{K}_1,\vec{K}_2,L_2,v}\left(\frac{\partial x_{j\beta}}{\partial N_j}\right)_{\vec{N}_m,\vec{K}_1,\vec{K}_2,L_2,v}+$$

$$\left(\frac{\partial Ln\varphi_{i\beta}}{\partial v}\right)_{\vec{K}_1,\vec{K}_2,L_2,\vec{N}}\frac{\left(\frac{\partial G2}{\partial N_j}\right)_{\vec{K}_1,\vec{K}_2,L_2,\vec{N}_m}}{\left(\frac{\partial G2}{\partial v}\right)_{\vec{K}_1,\vec{K}_2,L_2,\vec{N}_m}}+\left(\frac{\partial Ln\varphi_{i\beta}}{\partial L_2}\right)_{\vec{K}_1,\vec{K}_2,v,\vec{N}}\frac{\left(\frac{\partial G3}{\partial N_j}\right)_{\vec{K}_1,\vec{K}_2,v,\vec{N}_m}}{\left(\frac{\partial G3}{\partial L_2}\right)_{\vec{K}_1,\vec{K}_2,v,\vec{N}_m}} \tag{B.16}$$

Hence, the derivatives of fugacity equations with respect to primary variable N_i are as follows:

$$\frac{\partial R_{F_{1,i}}}{\partial N_j}=\frac{\partial Ln\varphi_{ig}}{\partial N_j}-\frac{\partial Ln\varphi_{io}}{\partial N_j} \tag{B.17}$$

$$\frac{\partial R_{F_{2,i}}}{\partial N_j}=\frac{\partial Ln\varphi_{iL_2}}{\partial N_j}-\frac{\partial Ln\varphi_{io}}{\partial N_j} \tag{B.18}$$

B.3 DERIVATIVES OF EQUILIBRIUM EQUATIONS RESIDUAL WITH RESPECT TO P

The final forms of the equations are as follows:

$$\left(\frac{\partial R_{F_{1,i}}}{\partial P}\right)_{\vec{K}_1,\vec{K}_2,\vec{N}}=\frac{\partial Ln\varphi_{ig}}{\partial P}-\frac{\partial Ln\varphi_{io}}{\partial P} \tag{B.19}$$

$$\left(\frac{\partial R_{F_{2,i}}}{\partial P}\right)_{\vec{K}_1,\vec{K}_2,\vec{N}}=\frac{\partial Ln\varphi_{iL_2}}{\partial P}-\frac{\partial Ln\varphi_{io}}{\partial P} \tag{B.20}$$

$\frac{\partial Ln\varphi_{i\beta}}{\partial x_{i\beta}}$ and $\frac{\partial Ln\varphi_{i\beta}}{\partial P}$ are derived from Peng-Robinson EOS and are given in subsection B.4.2.

B.4 DERIVATIVES OF EQUILIBRIUM EQUATIONS RESIDUAL WITH RESPECT TO T

The derivatives of the fugacity equations with respect to temperature are as follows:

$$R_{F_{1,i}} = LnK_i^{og} + Ln\varphi_{ig} - Ln\varphi_{io} \tag{B.21}$$

$$R_{2,i} = LnK_i^{oL_2} + Ln\varphi_{iL_2} - Ln\varphi_{io} \tag{B.22}$$

$$\frac{\partial R_{F_{1,i}}}{\partial T} = \frac{\partial Ln\varphi_{ig}}{\partial T} - \frac{\partial Ln\varphi_{io}}{\partial T},\ \frac{\partial R_{F_{2,i}}}{\partial T} = \frac{\partial Ln\varphi_{iL_2}}{\partial T} - \frac{\partial Ln\varphi_{io}}{\partial T} \tag{B.23}$$

If total enthalpy is selected as the primary variable,

$$\frac{\partial R_{F_{1,i}}}{\partial H_t} = \frac{\partial Ln\varphi_{ig}}{\partial H_t} - \frac{\partial Ln\varphi_{io}}{\partial H_t},\ \frac{\partial R_{F_{2,i}}}{\partial H_t} = \frac{\partial Ln\varphi_{iL_2}}{\partial H_t} - \frac{\partial Ln\varphi_{io}}{\partial H_t} \tag{B.24}$$

B.5 DERIVATIVES OF PENG-ROBINSON EQUATION OF STATE PARAMETERS

The derivatives of the EOS parameters, compressibility factor, density, fugacity, enthalpy, and other parameters are presented in this section.

B.5.1 Derivatives of Compressibility Factor

The derivative of compressibility factor with respect to mole fraction $\frac{\partial Z}{\partial x_i}$ is

$$Z_j^{\,3} - \left(1 - B_j\right) Z_j^{\,2} + \left(A_j - 3B_j^{\,2} - 2B_j\right) Z_j - \left(A_j B_j - B_j^{\,2} - B_j^{\,3}\right) = 0 \tag{B.25}$$

$$A_j = \frac{a_{m,j} P}{(RT)^2},\ B_j = \frac{b_{m,j} P}{RT} \tag{B.26}$$

$$A_j = \frac{P}{(RT)^2}\sum_{i=1}^{n_c}\left(x_{ij}x_{1j}a_{i1} + x_{ij}x_{2j}a_{i2} + \cdots + x_{ij}x_{n_cj}a_{in_c}\right)$$

$$= \frac{P}{(RT)^2}\Big[\left(x_{1j}x_{1j}a_{11} + x_{1j}x_{2j}a_{12} + x_1x_{n_c}a_{1n_c}\right) + \left(x_{2j}x_{1j}a_{21} + x_{2j}x_{2j}a_{22} + \cdots + x_{2j}x_{n_cj}a_{2n_c}\right)$$

$$+ \cdots + \left(x_{n_cj}x_{1j}a_{n_c1} + x_{n_cj}x_{2j}a_{n_c2} + \cdots + x_{n_cj}x_{n_cj}a_{n_cn_c}\right)\ \Big] \qquad \text{(B.27)}$$

B.5.1.1 Derivatives of Compressibility Factor with Respect to Mole Fraction

The derivatives of the Z-factor are described below

$$\frac{\partial A_j}{\partial x_{ij}} = \frac{2P}{(RT)^2}\sum_{k=1}^{n_c}x_{kj}a_{ki} \qquad \text{(B.28)}$$

where $a_{ki} = \sqrt{(a_k a_i)}(1-\delta_{ki})$

$$\frac{\partial B_j}{\partial x_{ij}} = \frac{P}{RT}b_i \qquad \text{(B.29)}$$

$$3Z^2\frac{\partial Z_j}{\partial x_{ij}} - 2Z\left(1-B_j\right)\frac{\partial Z_j}{\partial x_{ij}} + \left(A_j - 3B_j^2 - 2B_j\right)\frac{\partial Z_j}{\partial x_{ij}}$$

$$+Z_j{}^2\frac{\partial B_j}{\partial x_{ij}} + Z\frac{\partial A_j}{\partial x_{ij}} - 6B_jZ_j\frac{\partial B_j}{\partial x_{ij}} - 2Z_j\frac{\partial B_j}{\partial x_{ij}} - B_j\frac{\partial A_j}{\partial x_{ij}} - A_j\frac{\partial B_j}{\partial x_{ij}} + 2B_j\frac{\partial B_j}{\partial x_{ij}}$$

$$+3B_j^2\frac{\partial B_j}{\partial x_{ij}} = 0 \qquad \text{(B.30)}$$

From the above equation, we can get

$$\frac{\partial Z_j}{\partial x_{ij}} = \frac{\left(B_j - Z_j\right)\frac{\partial A_j}{\partial x_i} + \left[A_j - 2B_j - 3B_j^2 + 2\left(3B_j + 1\right)Z_j - Z_j{}^2\right]\frac{\partial B_j}{\partial x_{ij}}}{\frac{\partial F}{\partial Z}} \tag{B.31}$$

$$\frac{\partial F}{\partial Z} = 3Z_j{}^2 - 2Z_j\left(1 - B_j\right) + \left(A_j - 3B_j^2 - 2B_j\right) \tag{B.32}$$

B.5.1.2 Derivatives of Compressibility Factor with Respect to Pressure

The derivative of the Z-factor with respect to pressure is

$$\frac{\partial Z}{\partial P} = \frac{1}{P}\frac{A_j\left(B_j - Z\right) + B_j\left(A_j - 2B_j - 3B_j^2 + 2\left(3B_j + 1\right)Z - Z^2\right)}{\frac{\partial F}{\partial Z}} \tag{B.33}$$

B.5.1.3 Derivatives of Compressibility Factor with Respect to Temperature

The derivative of the Z-factor with respect to temperature is outlined as below

$$A_j = \frac{a_{m,j}P}{(RT)^2} \tag{B.34}$$

$$B_j = \frac{b_{m,j}P}{RT} \tag{B.35}$$

$$\frac{\partial A_j}{\partial T} = \frac{\partial a_{m,j}}{\partial T}\frac{P}{(RT)^2} - 2A_j\frac{1}{T} \tag{B.36}$$

$$\frac{\partial B_j}{\partial T} = -B_j\frac{1}{T} \tag{B.37}$$

$$\frac{\partial Z}{\partial T}=\frac{\frac{\partial A_j}{\partial T}(B_j-Z)+\frac{\partial B_j}{\partial T}(A_j-2B_j-3B_j{}^2+2\left(3B_j+1\right)Z-Z^2)}{\frac{\partial F}{\partial Z}} \tag{B.38}$$

B.5.2 Derivatives of Fugacity Coefficient

The expression of the fugacity of Peng-Robinson equation of state is as follows:

$$Ln\varphi_{ij}=\frac{b_i}{b_{m,j}}\left(Z_j-1\right)-Ln\left(Z_j-B_j\right)-\frac{A_j}{2\sqrt{2}B_j}\left(\frac{2}{a_{m,j}}\sum_{m=1}^{n_c}x_{mj}a_{im}-\frac{b_i}{b_{m,j}}\right)$$

$$Ln\left[\frac{Z_j+\left(1+\sqrt{2}\right)B_j}{Z_j+\left(1-\sqrt{2}\right)B_j}\right] \tag{B.39}$$

$$=LnC_{ij}+D_{ij}+E_{ij}LnG_j$$

where

$$C_{ij}=\frac{1}{\left(Z_j-B_j\right)} \tag{B.40}$$

$$D_{ij}=\frac{b_i}{b_{m,j}}\left(Z_j-1\right) \tag{B.41}$$

$$E_{ij}=-\frac{A_j}{2\sqrt{2}B_j}\left(\frac{2}{a_{m,j}}\sum_{m=1}^{n_c}x_{mj}a_{im}-\frac{b_i}{b}\right) \tag{B.42}$$

$$G_j=\frac{Z_j+\left(1+\sqrt{2}\right)B_j}{Z_j+\left(1-\sqrt{2}\right)B_j} \tag{B.43}$$

B.5.2.1 Derivatives of Fugacity Coefficient with Respect to Mole Fraction

The derivative of the fugacity coefficient of component *i* with respect to mole fraction is as follows:

$$\frac{\partial Ln\varphi_{ij}}{\partial x_{kj}} = \frac{1}{C_{ij}}\frac{\partial C_{ij}}{\partial x_{kj}} + \frac{\partial D_{ij}}{\partial x_{kj}} + LnG_j\frac{\partial E_{ij}}{\partial x_{kj}} + \frac{E_{ij}}{G_j}\frac{\partial G_j}{\partial x_{kj}} \tag{B.44}$$

where

$$\frac{\partial C_{ij}}{\partial x_{kj}} = -\frac{\dfrac{\partial Z_j}{\partial x_{kj}} - \dfrac{\partial B_j}{\partial x_{kj}}}{\left(Z_j - B_j\right)^2} \tag{B.45}$$

$$\frac{\partial D_{ij}}{\partial x_{kj}} = \frac{b_i}{{b_{m,j}}^2}\left[b_{m,j}\frac{\partial Z_j}{\partial x_{kj}} - b_k\left(Z_j - 1\right)\right] \tag{B.46}$$

$$\frac{\partial E_{ij}}{\partial x_{kj}} = \frac{1}{2\sqrt{2}a_{m,j}b_{m,j}B_j}\left\{\frac{1}{B_j}\left(a_{m,j}b_i - 2b_{m,j}\sum_{m=1}^{n_c}x_{mi}a_{im}\right)\left(B_j\frac{\partial A_j}{\partial x_{kj}} - A_j\frac{\partial B_j}{\partial x_{kj}}\right)\right.$$

$$\left. - \frac{A_j}{a_{m,j}b_{m,j}}\left[4{b_{m,j}}^2\left(\sum_{m=1}^{n_c}x_{mj}a_{im}\right)\left(\sum_{m=1}^{n_c}x_{mj}a_{mk}\right) - 2a_{m,j}{b_{m,j}}^2a_{ik} - b_ib_k{a_{m,j}}^2\right]\right\} \tag{B.47}$$

and

$$\frac{\partial G}{\partial x_{kj}} = \frac{2\sqrt{2}}{\left[Z_j + \left(1-\sqrt{2}\right)B_j\right]^2}\left(Z_j\frac{\partial B_j}{\partial x_{kj}} - B_j\frac{\partial Z_j}{\partial x_{kj}}\right) \tag{B.48}$$

with

$$\frac{\partial A_j}{\partial x_{kj}} = \frac{2P}{\left(RT\right)^2}\sum_{m=1}^{n_c}x_{mj}a_{mk} \tag{B.49}$$

and

$$\frac{\partial B_j}{\partial x_{kj}} = \frac{Pb_k}{RT} \tag{B.50}$$

B.5.2.2 Derivatives of Fugacity Coefficient with Respect to Pressure

The derivative of the fugacity coefficient of component *i* with respect to pressure is as follows:

$$\frac{\partial Ln\varphi_{ij}}{\partial P} = \frac{1}{C_{ij}}\frac{\partial C_{ij}}{\partial P} + \frac{\partial D_{ij}}{\partial P} + \frac{E_{ij}}{G_j}\frac{\partial G_j}{\partial P} \tag{B.51}$$

where

$$\frac{\partial C_{ij}}{\partial P} = -\frac{\left(\frac{\partial Z_j}{\partial P} - \frac{\partial B_j}{\partial P}\right)}{\left(Z_j - B_j\right)^2} \tag{B.52}$$

$$\frac{\partial D_{ij}}{\partial P} = \frac{b_i}{b_j}\frac{\partial Z_j}{\partial P} \tag{B.53}$$

and

$$\frac{\partial G_j}{\partial P} = \frac{2\sqrt{2}}{\left[Z_j + \left(1-\sqrt{2}\right)B_j\right]^2}\left(Z_j\frac{\partial B_j}{\partial P} - B_j\frac{\partial Z_j}{\partial P}\right) \tag{B.54}$$

with

$$\frac{\partial B_j}{\partial P} = \frac{b_{m,j}}{RT} \tag{B.55}$$

B.5.2.3 Derivatives of Fugacity Coefficient with Respect to Temperature

The derivative of the fugacity coefficient of component *i* with respect to temperature is as follows:

$$Ln\varphi_{ij} = LnC_{ij} + D_{ij} + E_{ij}LnG_i \tag{B.56}$$

$$\frac{\partial LnC_{ij}}{\partial T}=\frac{1}{C_{ij}}\frac{\partial C_{ij}}{\partial T}=-\frac{1}{C_{ij}}\frac{\left(\frac{\partial Z_j}{\partial T}-\frac{\partial B_j}{\partial T}\right)}{(Z_j-B_j)^2} \tag{B.57}$$

$$\frac{\partial D_{ij}}{\partial T}=\frac{b_i}{b_{m,j}}\frac{\partial Z_j}{\partial T} \tag{B.58}$$

$$\frac{\partial E_{ij}}{\partial T}=-[\frac{1}{2\sqrt{2}}(\frac{\frac{\partial A_j}{\partial T}}{B_j}-\frac{\frac{\partial B_j}{\partial T}A_j}{B_j^{\,2}})(\frac{2}{a_{m,j}}\sum_{k=1}^{n}x_{ij}a_{ik}-\frac{b_i}{b_{m,j}})]+$$
$$[\frac{A_j}{\sqrt{2}\,B_j}(\frac{-\frac{\partial a_{m,j}}{\partial T}}{a_{m,j}^{\,2}}\sum_{k=1}^{n}x_{ij}a_{ik}+\frac{1}{a_{m,j}}\sum_{k=1}^{n}\frac{\partial a_{k,j}}{\partial T})] \tag{B.59}$$

$$\frac{\partial LnG_j}{\partial T}=\frac{2\sqrt{2}\,(Z_j\frac{\partial B_j}{\partial T}-B_j\frac{\partial Z_j}{\partial T})}{(Z_j+(1+\sqrt{2})B_j)(Z_j+(1-\sqrt{2})B_j)} \tag{B.60}$$

$$\frac{\partial Ln\varphi_{ij}}{\partial T}=\frac{\partial D_{ij}}{\partial T}+\frac{\partial LnC_{ij}}{\partial T}+(\frac{\partial E_{ij}}{\partial T}LnG_j+E_{ij}\frac{\partial LnG_j}{\partial T}) \tag{B.61}$$

B.5.2.4 Derivatives of Fugacity Coefficient with Respect to Phase Mole Ratios

The derivative of fugacity coefficient can be calculated by the following expressions; L_2 and v are the phase mole ratios of the second liquid phase and the gas phase, respectively.

$$\left(\frac{\partial Ln\varphi_{i\beta}}{\partial v}\right)_{N,\vec{K}_1,\vec{K}_2,L_2}=\sum_{i=1}^{n_c}\left(\frac{\partial Ln\varphi_{i\beta}}{\partial x_{i\beta}}\frac{\partial x_{i\beta}}{\partial v}\right)_{N,\vec{K}_1,\vec{K}_2,L_2} \tag{B.62}$$

$$\left(\frac{\partial Ln\varphi_{i\beta}}{\partial L_2}\right)_{N,\vec{K}_1,\vec{K}_2,v}=\sum_{i=1}^{n_c}\left(\frac{\partial Ln\varphi_{i\beta}}{\partial x_{i\beta}}\frac{\partial x_{i\beta}}{\partial L_2}\right)_{N,\vec{K}_1,\vec{K}_2,v} \tag{B.63}$$

where $\frac{\partial Ln\varphi_{i\beta}}{\partial x_{i\beta}}$ and $\frac{\partial x_{i\beta}}{\partial L_2}$, $\frac{\partial x_{i\beta}}{\partial v}$, are described in sections B.4 and B.5, respectively.

B.5.3 Derivatives of Enthalpy Equation

The enthalpy expression which is the function of mole fraction, temperature, and pressure is

$$H_j = f(x_{ij}, T, P) \tag{B.64}$$

$$H_j = \frac{T\frac{\partial a_{m,j}}{\partial T} - a_{m,j}}{b_{m,j}} Ln\left(\frac{Z_j + (\sqrt{2}+1)B_j}{Z_j + (\sqrt{2}-1)B_j}\right) + RT(Z_j - 1) + H_j^{\circ} \tag{B.65}$$

$$H_j = \sum_{i=1}^{n} x_i h_i^{\circ} \tag{B.66}$$

$$h_i^{\circ} = Cp_{1,i}^{\circ}(T - T_{ref}) + \frac{Cp_{2,i}^{\circ}}{2}(T^2 - {T_{ref}}^2) + \frac{Cp_{3,i}^{\circ}}{3}(T^3 - {T_{ref}}^3) + \frac{Cp_{4,i}^{\circ}}{4}(T^4 - {T_{ref}}^4) \tag{B.67}$$

B.5.3.1 Derivatives of Enthalpy with Respect to Mole Fraction

The derivative of the enthalpy expression for phase *j* with respect to mole of component *i* is

$$\frac{\partial H_j}{\partial x_{ij}} = \frac{[T\frac{\partial(\frac{\partial a_{m,j}}{\partial T})}{\partial x_{ij}} - \frac{\partial a_{m,j}}{\partial x_{ij}}]b_{m,j} - [\frac{\partial b_{m,j}}{\partial x_{ij}}(T\frac{\partial a_{m,j}}{\partial T} - a_{m,j})]}{{b_{m,j}}^2} Ln(\frac{Z_j}{Z_j + B_j}) +$$
$$\frac{T\frac{\partial a_{m,j}}{\partial T} - a_{m,j}}{b_{m,j}} \frac{2\sqrt{2}(Z_j\frac{\partial B_j}{\partial x_{ij}} - B_j\frac{\partial Z_j}{\partial x_{ij}})}{(Z_j + (\sqrt{2}-1)B_j)(Z_j + (\sqrt{2}+1)B_j)} + R[(Z_j - 1) + T\frac{\partial Z_j}{\partial x_{ij}}] + \frac{\partial H_j^{\circ}}{\partial x_{ij}} \tag{B.68}$$

$$\frac{\partial H_j^{\circ}}{\partial x_{ij}} = Cp_{1,i}^{\circ}(T - T_{ref}) + \frac{Cp_{2,i}^{\circ}}{2}(T^2 - T_{ref}{}^2) + \frac{Cp_{3,i}^{\circ}}{3}(T^3 - T_{ref}{}^3) + \frac{Cp_{4,i}^{\circ}}{4}(T^4 - T_{ref}{}^4) \tag{B.69}$$

where

$$\frac{\partial(\frac{\partial a_{m,j}}{\partial T})}{\partial x_{ij}} = \sum_{k=1}^{n} x_{kj}(a_i a_k)^{-\frac{1}{2}}(a_i \frac{\partial a_k}{\partial T} + a_k \frac{\partial a_i}{\partial T})(1-\delta_{ik}) \tag{B.70}$$

$$\frac{\partial b_{m,j}}{\partial x_{i,j}} = b_i \tag{B.71}$$

$$\frac{\partial a_{m,j}}{\partial x_{i,j}} = 2\sum_{k=1}^{n} x_{kj}\sqrt{a_i a_k}(1-\delta_{ik}) \tag{B.72}$$

$$\frac{\partial B_j}{\partial x_{i,j}} = \frac{P}{RT} b_i \tag{B.73}$$

B.5.3.2 Derivatives of Enthalpy with Respect to Pressure

The derivative of the enthalpy expression for phase *j* with respect to pressure is

$$\frac{\partial H_j}{\partial P} = \frac{T\frac{\partial a_{m,j}}{\partial T} - a_{m,j}}{2\sqrt{2}b_{m,j}} \frac{2\sqrt{2}(Z_j \frac{b_{m,j}}{RT} - B_j \frac{\partial Z_j}{\partial P})}{(Z_j + (\sqrt{2}-1)B_j)(Z_j + (\sqrt{2}+1)B_j)} + RT\frac{\partial Z_j}{\partial P} \tag{B.74}$$

B.5.3.3 Derivatives of Enthalpy with Respect to Temperature

The derivative of the enthalpy expression for phase *j* with respect to temperature is

$$\frac{\partial H_j}{\partial T} = \frac{T\frac{\partial^2 a_{m,j}}{\partial T^2}}{2\sqrt{2}\, b_{m,j}} Ln\left(\frac{Z_j + (\sqrt{2}+1)B_j}{Z_j + (\sqrt{2}-1)B_j}\right) + \frac{T\frac{\partial a_{m,j}}{\partial T} - a_{m,j}}{2\sqrt{2}b_{m,j}} \frac{2\sqrt{2}\left(Z_j \frac{\partial B_j}{\partial T} - B_j \frac{\partial Z_j}{\partial T}\right)}{(Z_j + (\sqrt{2}-1)B_j)(Z_j + (\sqrt{2}+1)B_j)}$$

$$+R[(Z_j-1)+T\frac{\partial Z_j}{\partial T}]+\frac{\partial H_j^{\circ}}{\partial T} \tag{B.75}$$

$$\frac{\partial a_{m,j}}{\partial T}=\frac{1}{2}\sum_{i=1}^{n}\sum_{k=1}^{n}x_{ij}\,x_{kj}(a_i a_k)^{-\frac{1}{2}}(a_i\frac{\partial a_k}{\partial T}+a_k\frac{\partial a_i}{\partial T})(1-\delta_{ik}) \tag{B.76}$$

$$\frac{\partial a_i}{\partial T}=-\frac{0.42748\,R^2\,T_{C_i}{}^2}{P_{C_i}}[f_{w_i}\frac{1}{T_{C_i}{}^{1.5}}(1-\sqrt{T_{r_i}})] \tag{B.77}$$

$$\frac{\partial^2 a_{m,j}}{\partial T^2}=\sum_{i=1}^{n}\sum_{k=1}^{n}x_{ij}\,x_{kj}[-\frac{1}{4}(a_i a_k)^{-\frac{3}{2}}(a_i\frac{\partial a_k}{\partial T}+a_k\frac{\partial a_i}{\partial T})+$$
$$\frac{1}{2}(a_i a_j)^{-\frac{1}{2}}(a_i\frac{\partial^2 a_k}{\partial T^2}+2\frac{\partial a_i}{\partial T}\frac{\partial a_k}{\partial T}+a_k\frac{\partial^2 a_i}{\partial T^2})](1-\delta_{ik}) \tag{B.78}$$

$$\frac{\partial^2 a_i}{\partial T^2}=\frac{0.42748\,R^2\,T_{C_i}}{P_{C_i}}[\frac{1}{2}f_{w_i}\frac{1}{T_{r_i}{}^{1.5}}] \tag{B.79}$$

$$\frac{\partial H_j^{\circ}}{\partial T}=\sum_{i=1}^{n}x_{ij}\,[Cp_{1,i}^{\circ}+Cp_{2,i}^{\circ}T+Cp_{3,i}^{\circ}T^2+Cp_{4,i}^{\circ}T^3] \tag{B.80}$$

B.6 DERIVATIVES OF FLASH EQUATIONS AND MOLE FRACTIONS

The equations related to flash calculation and the derivates are described in the following sections.

B.6.1 Derivatives of Flash Equations

There are two flash equations for the case of three phases in equilibrium, called G2 and G3.

$$G2 = \sum_{i=1}^{nc} \frac{z_i (K_{1,i} - 1)}{1 + v(K_{1,i} - 1) + L_2 (k_{2,i} - 1)} \tag{B.81}$$

$$G3 = \sum_{i=1}^{nc} \frac{z_i (K_{2,i} - 1)}{1 + v(K_{1,i} - 1) + L_2 (k_{2,i} - 1)} \tag{B.82}$$

B.6.2 Derivatives of Flash Equations with Respect to Mole Ratios

The derivatives of flash equations, G2 and G3, with respect to the mole ratios, *v* and L_2, are

$$\frac{\partial G2}{\partial v} = -\sum_{i=1}^{nc} \frac{Z_i (K_{1,i} - 1)(K_{1,i} - 1)}{[1 + v(K_{1,i} - 1) + L_2 (k_{2,i} - 1)]^2} \tag{B.83}$$

$$\frac{\partial G2}{\partial L_2} = -\sum_{i=1}^{nc} \frac{Z_i (K_{1,i} - 1)(K_{2,i} - 1)}{[1 + v(K_{1,i} - 1) + L_2 (k_{2,i} - 1)]^2} \tag{B.84}$$

$$\frac{\partial G3}{\partial v} = -\sum_{i=1}^{nc} \frac{z_i (K_{2,i} - 1)(K_{1,i} - 1)}{[1 + v(K_{1,i} - 1) + L_2 (k_{2,i} - 1)]^2} \tag{B.85}$$

$$\frac{\partial G3}{\partial L_2} = -\sum_{i=1}^{nc} \frac{z_i (K_{2,i} - 1)(K_{2,i} - 1)}{[1 + v(K_{1,i} - 1) + L_2 (k_{2,i} - 1)]^2} \tag{B.86}$$

B.6.3 Derivatives of Flash Equations with Respect to LnK_1 and LnK_2

The following are the derivatives of the G2 and G3 with respect to the primary variables LnK_1 *and* LnK_2

$$\frac{\partial G2}{\partial LnK_{1,i}} = \frac{z_i K_{1,i} (1 + L_2 (K_{2,i} - 1))}{[1 + v(K_{1,i} - 1) + L_2 (K_{2,i} - 1)]^2} \tag{B.87}$$

$$\frac{\partial G2}{\partial LnK_{2,i}} = \frac{-z_i K_{1,i} L_2 (K_{1,i} - 1)}{[1 + v(K_{1,i} - 1) + L_2 (K_{2,i} - 1)]^2} \tag{B.88}$$

$$\frac{\partial G3}{\partial LnK_{1,i}} = \frac{-z_i K_{2,i} v(K_{2,i} - 1)}{[1 + v(K_{1,i} - 1) + L_2(K_{2,i} - 1)]^2} \tag{B.89}$$

$$\frac{\partial G3}{\partial LnK_{2,i}} = \frac{z_i K_{2,i} (1 + v(K_{1,i} - 1))}{[1 + v(K_{1,i} - 1) + L_2(K_{2,i} - 1)]^2} \tag{B.90}$$

B.6.4 Derivatives of Flash Equations with Respect to Component Mole Number

The following are the derivatives of the *G2* and *G3* with respect to the primary variable N_i

$$\frac{\partial G2}{\partial N_i} = \sum_{i=1}^{nc} \frac{\partial \left(\frac{z_i (K_{1,i} - 1)}{1 + v(K_{1,i} - 1) + L_2(k_{2,i} - 1)} \right)}{\partial N_i} =$$

$$\frac{1}{N_T} \frac{(K_{1,i} - 1)}{1 + v(K_{1,i} - 1) + L_2(K_{2,i} - 1)} - \frac{1}{N_T^2} \sum_{i=1}^{nc} \frac{z_i (K_{1,i} - 1)}{1 + v(K_{1,i} - 1) + L_2(K_{2,i} - 1)} =$$

$$\frac{1}{N_T} \left(\frac{(K_{1,i} - 1)}{1 + v(K_{1,i} - 1) + L_2(K_{2,i} - 1)} - G2 \right) \tag{B.91}$$

$$\frac{\partial G3}{\partial N_i} = \sum_{i=1}^{nc} \frac{\partial \left(\frac{z_i (K_{2,i} - 1)}{1 + v(K_{1,i} - 1) + L_2(K_{2,i} - 1)} \right)}{\partial N_i} =$$

$$\frac{1}{N_T} \frac{(K_{2,i} - 1)}{1 + v(K_{1,i} - 1) + L_2(K_{2,i} - 1)} - \frac{1}{N_T^2} \sum_{i=1}^{nc} \frac{z_i (K_{2,i} - 1)}{1 + v(K_{1,i} - 1) + L_2(K_{2,i} - 1)} =$$

$$\frac{1}{N_T} \left(\frac{(K_{2,i} - 1)}{1 + v(K_{1,i} - 1) + L_2(K_{2,i} - 1)} - G3 \right) \tag{B.92}$$

B.7 TOTAL DERIVATIVES OF MOLE FRACTIONS

For constant pressure and temperature, the derivative of the mole fraction with respect to the related variables, equilibrium ratios, number of moles, and mole ratios are as follows. The mole fraction of the component in each phase can be expressed as in the following equation in terms of related parameters:

$$x_{i,\beta} = f(K_{1,i}, K_{2,i}, N_i, v, L_2) \tag{B.93}$$

$$dx_{i,\beta} = \left(\frac{\partial x_{i,\beta}}{\partial LnK_{1,j}}\right)_{\vec{K}_m,\vec{K}_2,N,v,L_2} dLnK_{1,j} + \left(\frac{\partial x_{i,\beta}}{\partial LnK_{2,j}}\right)_{\vec{K}_1,\vec{K}_n,N,v,L_2} dLnK_{2,j} + \left(\frac{\partial x_{i,\beta}}{\partial v}\right)_{\vec{K}_1,\vec{K}_2,N,L_2} dv + \left(\frac{\partial x_{i,\beta}}{\partial L_2}\right)_{\vec{K}_1,\vec{K}_2,N,v} dL_2 + \left(\frac{\partial x_{i,\beta}}{\partial N_j}\right)_{\vec{K}_1,\vec{K}_2,v,L_2} dN_j \tag{B.94}$$

B.7.1 Derivative of Mole Fraction with Respect to LnK_1 and LnK_2

Equation (B.95) is divided into $Lnk_{1,i}$, $Lnk_{2,i}$ to determine the derivatives with respect to these variables.

$$\left(\frac{\partial x_{i,\beta}}{\partial LnK_{1,j}}\right) = \left(\frac{\partial x_{i,\beta}}{\partial LnK_{1,j}}\right)_{\vec{K}_m,\vec{K}_2,N,v,L_2} + \left(\frac{\partial x_{i,\beta}}{\partial v}\right)_{\vec{K}_1,\vec{K}_2,N,L_2} \left(\frac{\partial v}{\partial LnK_{1,j}}\right)_{\vec{K}_m,\vec{K}_2,N,L_2} + \left(\frac{\partial x_{i,\beta}}{\partial L_2}\right)_{\vec{K}_1,\vec{K}_2,N,v} \left(\frac{\partial L_2}{\partial LnK_{1,j}}\right)_{\vec{K}_m,\vec{K}_2,N,v} \tag{B.95}$$

$$\left(\frac{\partial x_{i,\beta}}{\partial LnK_{2,j}}\right) = \left(\frac{\partial x_{i,\beta}}{\partial LnK_{2,j}}\right)_{\vec{K}_1,\vec{K}_n,N,v,L_2} + \left(\frac{\partial x_{i,\beta}}{\partial v}\right)_{\vec{K}_1,\vec{K}_2,N,L_2} \left(\frac{\partial v}{\partial LnK_{2,j}}\right)_{\vec{K}_1,\vec{K}_n,N,L_2} + \left(\frac{\partial x_{i,\beta}}{\partial L_2}\right)_{\vec{K}_1,\vec{K}_2,N,v} \left(\frac{\partial L_2}{\partial LnK_{2,j}}\right)_{\vec{K}_1,\vec{K}_n,N,v} \tag{B.96}$$

$$\left(\frac{\partial x_{i,\beta}}{\partial LnK_{1,j}}\right)=\left(\frac{\partial x_{i,\beta}}{\partial LnK_{1,j}}\right)_{\vec{K}_m,\vec{K}_2,N,v,L_2}+\left(\frac{\partial x_{i,\beta}}{\partial v}\right)_{\vec{K}_1,\vec{K}_2,N,L_2}\frac{\left(\frac{\partial G2}{\partial LnK_{1,j}}\right)_{\vec{K}_m,\vec{K}_2,N,L_2,v}}{\left(\frac{\partial G2}{\partial v}\right)_{\vec{K}_1,\vec{K}_2,N,L_2}}+$$

$$\left(\frac{\partial x_{i,\beta}}{\partial L_2}\right)_{\vec{K}_1,\vec{K}_2,N,v}\frac{\left(\frac{\partial G3}{\partial LnK_{1,j}}\right)_{\vec{K}_m,\vec{K}_2,N,v,L_2}}{\left(\frac{\partial G3}{\partial L_2}\right)_{\vec{K}_1,\vec{K}_2,N,v}} \tag{B.97}$$

$$\left(\frac{\partial x_{i,\beta}}{\partial LnK_{2,j}}\right)=\left(\frac{\partial x_{i,\beta}}{\partial LnK_{2,j}}\right)_{\vec{K}_1,\vec{K}_n,N,v,L_2}+\left(\frac{\partial x_{i,\beta}}{\partial v}\right)_{\vec{K}_1,\vec{K}_2,N,L_2}\frac{\left(\frac{\partial G2}{\partial LnK_{2,j}}\right)_{\vec{K}_1,\vec{K}_n,N,L_2,v}}{\left(\frac{\partial G2}{\partial v}\right)_{\vec{K}_1,\vec{K}_2,N,L_2}}+$$

$$\left(\frac{\partial x_{i,\beta}}{\partial L_2}\right)_{\vec{K}_1,\vec{K}_2,N,v}\frac{\left(\frac{\partial G3}{\partial LnK_{2,j}}\right)_{\vec{K}_1,\vec{K}_n,N,v,L_2}}{\left(\frac{\partial G3}{\partial L_2}\right)_{\vec{K}_1,\vec{K}_2,N,v}} \tag{B.98}$$

In the above equation, if $i \neq j$ then

$$\left(\frac{\partial x_{i,\beta}}{\partial LnK_{1,j}}\right)_{\vec{K}_m,\vec{K}_2,N,v,L_2,i\neq j}=0 \; and \left(\frac{\partial x_{i,\beta}}{\partial LnK_{2,j}}\right)_{\vec{K}_1,K_2,N,v,L_2,i\neq j}=0 \tag{B.99}$$

B.7.2 Derivative of Mole Fraction with Respect to Component Mole Number

The derivatives of the mole fraction with respect to *Ni* can be calculated by the following equations:

$$dx_{i,\beta}=\left(\frac{\partial x_{i,\beta}}{\partial LnK_{1,j}}\right)_{\vec{K}_m,\vec{K}_2,N,v,L_2}dLnK_{1,j}+\left(\frac{\partial x_{i,\beta}}{\partial LnK_{2,j}}\right)_{\vec{K}_1,\vec{K}_n,N,v,L_2}dLnK_{2,j}+$$

$$\left(\frac{\partial x_{i,\beta}}{\partial v}\right)_{\vec{K}_1,\vec{K}_2,N,L_2} dv+\left(\frac{\partial x_{i,\beta}}{\partial L_2}\right)_{\vec{K}_1,\vec{K}_2,N,v} dL_2+\left(\frac{\partial x_{i,\beta}}{\partial N_j}\right)_{\vec{K}_1,\vec{K}_2,v,L_2} dN_j \tag{B.100}$$

$$\left(\frac{\partial x_{i,\beta}}{\partial N_j}\right)=\left(\frac{\partial x_{i,\beta}}{\partial N_j}\right)_{\vec{K}_1,\vec{K}_2,N_m,v,L_2}+\left(\frac{\partial x_{i,\beta}}{\partial v}\right)_{\vec{K}_1,\vec{K}_2,N,L_2}\left(\frac{\partial v}{\partial LnN_j}\right)_{\vec{K}_1,\vec{K}_2,N_m,L_2}+$$
$$\left(\frac{\partial x_{i,\beta}}{\partial N_j}\right)_{\vec{K}_1,\vec{K}_2,N,v}\left(\frac{\partial L_2}{\partial LnN_j}\right)_{\vec{K}_1,\vec{K}_2,N_m,v} \tag{B.101}$$

B.7.3 Derivative of Mole Fraction Equation of Flash Calculation

The derivatives of mole fraction equation of each phase with respect to different variables are described in the following sections.

B.7.3.1 Derivative of Mole Fraction with Respect to LnK_1 and LnK_2

The derivatives of the mole fractions of oil, gas, and second hydrocarbon liquid phase with respect to two sets of equilibrium ratios are

$$x_{1,i}=\frac{z_i}{1+v(K_{1,i}-1)+L_2(K_{2,i}-1)} \tag{B.102}$$

$$y_i=K_{1,i}\,x_{1,i}\ \ and\ \ x_{2,i}=K_{2,i}\,x_{1,i} \tag{B.103}$$

$$y_i=\frac{z_i K_{1,i}}{1+v(K_{1,i}-1)+L_2(K_{2,i}-1)} \tag{B.104}$$

$$\frac{\partial x_{1,i}}{\partial Lnk_{1,i}}=\frac{-z_i\,v\,K_{1,i}}{(1+v(K_{1,i}-1)+L_2(K_{2,i}-1))^2} \tag{B.105}$$

$$\frac{\partial y_i}{\partial Lnk_{1,i}}=\frac{z_i K_{1,i}(1-v+L_2(K_{2,i}-1))}{(1+v(K_{1,i}-1)+L_2(K_{2,i}-1))^2} \tag{B.106}$$

$$\frac{\partial x_{2,i}}{\partial Lnk_{1,i}} = \frac{-z_i K_{1,i} K_{2,i} v}{(1+v(K_{1,i}-1)+L_2(K_{2,i}-1))^2} \tag{B.107}$$

$$\frac{\partial x_{1,i}}{\partial Lnk_{2,i}} = \frac{-z_i v K_{2,i}}{(1+v(K_{1,i}-1)+L_2(K_{2,i}-1))^2} \tag{B.108}$$

$$\frac{\partial y_i}{\partial Lnk_{2,i}} = \frac{-z_i K_{1,i} K_{2,i} v}{(1+v(K_{1,i}-1)+L_2(K_{2,i}-1))^2} \tag{B.109}$$

$$\frac{\partial x_{2,i}}{\partial Lnk_{2,i}} = \frac{z_i K_{2,i} (1-v+v(K_{1,i}-1))}{(1+v(K_{1,i}-1)+L_2(K_{2,i}-1))^2} \tag{B.110}$$

B.7.3.2 Derivative of Mole Fraction with Respect to Component Mole Number

The derivatives of the mole fractions of oil, gas and second liquid hydrocarbon phase with respect to total component mole number per pore volume are as follows:

for $i = j$

$$\left(\frac{\partial x_{1,j}}{\partial N_j}\right)_{\vec{K}_1,\vec{K}_2,\vec{N}_m,v,L_2} = \frac{\partial\left(\frac{z_j}{1+v\left(K_{1,j}-1\right)+L_2\left(K_{2,j}-1\right)}\right)}{\partial N_j} =$$

$$\frac{1}{1+v\left(K_{1,j}-1\right)+L_2\left(K_{2,j}-1\right)}\frac{\partial\left(\frac{N_j}{N_T}\right)}{\partial N_j} = \frac{1}{1+v\left(K_{1,j}-1\right)+L_2\left(K_{2,j}-1\right)}\left(\frac{N_T-N_j}{N_T^2}\right) =$$

$$\frac{1}{1+v\left(K_{1,j}-1\right)+L_2\left(K_{2,j}-1\right)}\left(\frac{1-z_j}{N_T}\right) \tag{B.111}$$

and for $i \neq j$

$$\left(\frac{\partial x_{1,j}}{\partial N_j}\right)_{\vec{K}_1,\vec{K}_2,\vec{N}_m,v,L_2} = \frac{1}{1+v\left(K_{1,j}-1\right)+L_2\left(K_{2,j}-1\right)}\left(\frac{-N_j}{N_T^2}\right) =$$

$$\frac{1}{1+v\left(K_{1,j}-1\right)+L_2\left(K_{2,j}-1\right)}\left(\frac{-z_j}{N_T}\right) \tag{B.112}$$

for i = j

$$\left(\frac{\partial y_j}{\partial N_j}\right)_{\vec{K}_1,\vec{K}_2,,\vec{N}_m,v,L_2}=\frac{\partial\left(\frac{z_j K_{1,j}}{1+v\left(K_{1,j}-1\right)+L_2\left(K_{2,j}-1\right)}\right)}{\partial N_j}=$$

$$\frac{K_{1,j}}{1+v\left(K_{1,j}-1\right)+L_2\left(K_{2,j}-1\right)}\frac{\partial\left(\frac{N_j}{N_T}\right)}{\partial N_j}=\frac{K_{1,j}}{1+v\left(K_{1,j}-1\right)+L_2\left(K_{2,j}-1\right)}\left(\frac{N_T-N_j}{N_T^2}\right)=$$

$$\frac{K_{1,j}}{1+v\left(K_{1,j}-1\right)+L_2\left(K_{2,j}-1\right))}\left(\frac{1-z_j}{N_T}\right) \tag{B.113}$$

and for i ≠ j

$$\left(\frac{\partial y_j}{\partial N_j}\right)_{\vec{K}_1,\vec{K}_2,\vec{N}_m,v,L_2}=\frac{K_{1,j}}{1+v\left(K_{1,j}-1\right)+L_2\left(K_{2,j}-1\right)}\left(\frac{-N_j}{N_T^2}\right)=$$

$$\frac{K_{1,j}}{1+v\left(K_{1,j}-1\right)+L_2\left(K_{2,j}-1\right)}\left(\frac{-z_j}{N_T}\right) \tag{B.114}$$

for i = j

$$\left(\frac{\partial x_{2,j}}{\partial N_j}\right)_{\vec{K}_1,\vec{K}_2,\vec{N}_m,v,L_2}=\frac{\partial\left(\frac{z_j K_{2,j}}{1+v\left(K_{1,j}-1\right)+L_2\left(K_{2,j}-1\right)}\right)}{\partial N_j}=$$

$$\frac{K_{2,j}}{1+v\left(K_{1,j}-1\right)+L_2\left(K_{2,j}-1\right)}\frac{\partial\left(\frac{N_j}{N_T}\right)}{\partial N_j}=\frac{K_{2,j}}{1+v\left(K_{1,j}-1\right)+L_2\left(K_{2,j}-1\right)}\left(\frac{N_T-N_j}{N_T^2}\right)=$$

$$\frac{K_{2,j}}{1+v\left(K_{1,j}-1\right)+L_2\left(K_{2,j}-1\right)}\left(\frac{1-z_j}{N_T}\right) \tag{B.115}$$

and for $i \neq j$

$$\left(\frac{\partial x_{2,j}}{\partial N_j}\right)_{\vec{K}_1,\vec{K}_2,\vec{N}_m,v,L_2} = \frac{K_{2,j}}{1+v\left(K_{1,j}-1\right)+L_2\left(K_{2,j}-1\right)}\left(\frac{-N_j}{N_T^2}\right) = \frac{K_{2,j}}{1+v\left(K_{1,j}-1\right)+L_2\left(K_{2,j}-1\right)}\left(\frac{-z_j}{N_T}\right) \tag{B.116}$$

B.7.3.3 Derivative of Mole Fraction with Respect to Phase Mole Ratios

The derivatives of the mole fractions with respect to the mole ratios, v, and L_2, can be calculated by the following expressions:

$$\frac{\partial x_{1,i}}{\partial v} = \frac{\partial\left(\frac{z_i}{1+v\left(K_{1,i}-1\right)+L_2\left(K_{2,i}-1\right)}\right)}{\partial v} = -z_i\frac{\left(K_{1,i}-1\right)}{\left[1+v\left(K_{1,i}-1\right)+L_2\left(K_{2,i}-1\right)\right]^2} \tag{B.117}$$

$$\frac{\partial y_i}{\partial v} = \frac{\partial\left(\frac{z_i K_{1,i}}{1+v\left(K_{1,i}-1\right)+L_2\left(K_{2,i}-1\right)}\right)}{\partial v} = -z_i K_{1,i}\frac{\left(K_{1,i}-1\right)}{\left[1+v\left(K_{1,i}-1\right)+L_2\left(K_{2,i}-1\right)\right]^2} \tag{B.118}$$

$$\frac{\partial x_{2,i}}{\partial v} = \frac{\partial\left(\frac{z_i K_{2,i}}{1+v\left(K_{1,i}-1\right)+L_2\left(K_{2,i}-1\right)}\right)}{\partial v} = -z_i K_{2,i}\frac{\left(K_{1,i}-1\right)}{\left[1+v\left(K_{1,i}-1\right)+L_2\left(K_{2,i}-1\right)\right]^2} \tag{B.119}$$

$$\frac{\partial x_{1,i}}{\partial L_2} = \frac{\partial\left(\frac{z_i}{1+v\left(K_{1,i}-1\right)+L_2\left(K_{2,i}-1\right)}\right)}{\partial L_2} = -z_i \frac{\left(K_{2,i}-1\right)}{\left[1+v\left(K_{1,i}-1\right)+L_2\left(K_{2,i}-1\right)\right]^2} \tag{B.120}$$

$$\frac{\partial y_i}{\partial L_2} = \frac{\partial\left(\frac{z_i K_{2,i}}{1+v\left(K_{1,i}-1\right)+L_2\left(K_{2,i}-1\right)}\right)}{\partial L_2} = -z_i K_{1,i} \frac{\left(K_{2,i}-1\right)}{\left[1+v\left(K_{1,i}-1\right)+L_2\left(K_{2,i}-1\right)\right]^2} \tag{B.121}$$

$$\frac{\partial x_{2,i}}{\partial L_2} = \frac{\partial\left(\frac{z_i K_{2,i}}{1+v\left(K_{1,i}-1\right)+L_2\left(K_{2,i}-1\right)}\right)}{\partial L_2} = -z_i K_{2,i} \frac{\left(K_{2,i}-1\right)}{\left[1+v\left(K_{1,i}-1\right)+L_2\left(K_{2,i}-1\right)\right]^2} \tag{B.122}$$

B.7.4 Total Derivatives of Compressibility Factor

The phase compressibility factor function can be written as follows:

$$Z = f(x_1, x_2 \ldots x_{nc}, P, T) \tag{B.123}$$

By taking the total differentiation of the above equation

$$dZ = \sum_{i=1}^{n_c} \frac{\partial Z}{\partial x_i} dx_i + \frac{\partial Z}{\partial P} dP + \frac{\partial Z}{\partial T} dT \tag{B.124}$$

Dividing the above equation by $LnK_{1,j}$ ($LnK_{2,j}$), while holding *P,* $\vec{N}$, and $\vec{K}_m$ ($\vec{K}_n$) constant, we have

$$\frac{\partial Z}{\partial LnK_{1,j}} = \sum_{i=1}^{n_c} \frac{\partial Z}{\partial x_i} \frac{\partial x_i}{\partial LnK_{1,j}} \tag{B.125}$$

$$\frac{\partial Z}{\partial LnK_{2,j}} = \sum_{i=1}^{n_c} \frac{\partial Z}{\partial x_i} \frac{\partial x_i}{\partial LnK_{2,j}} \tag{B.126}$$

and for N_j while holding *P,* K_1, K_2 and $\vec{N}_m$ constant, we have

$$\frac{\partial Z}{\partial N_j} = \sum_{i=1}^{n_c} \frac{\partial Z}{\partial x_i} \frac{\partial x_i}{\partial N_j} \tag{B.127}$$

To calculate the derivative with respect to phase mole ratios, i.e., *v*, while holding *P,* K_1, K_2, *and* $\vec{N}$ constant, we have

$$\frac{\partial Z}{\partial v} = \sum_{i=1}^{n_c} \frac{\partial Z}{\partial x_i} \frac{\partial x_i}{\partial v} \tag{B.128}$$

B.8 DERIVATIVES OF DENSITY

The derivative of the density with respect to mole fraction, LnK_1, LnK_2, number of mole, pressure, and temperature are as follows:

$$\frac{\partial \xi_\beta}{\partial x_{i\beta}} = -\frac{P_\beta}{RTZ_\beta{}^2} \frac{\partial Z_\beta}{\partial x_{i\beta}} \tag{B.129}$$

$$\frac{\partial \xi_\beta}{\partial LnK_{1,i}} = -\frac{P_\beta}{RTZ_\beta{}^2} \sum_{j=1}^{n_c} \frac{\partial Z_\beta}{\partial x_{j\beta}} \frac{\partial x_{j\beta}}{\partial LnK_{1,i}} \tag{B.130}$$

$$\frac{\partial \xi_\beta}{\partial LnK_{2,i}} = -\frac{P_\beta}{RTZ_\beta{}^2} \sum_{j=1}^{n_c} \frac{\partial Z_\beta}{\partial x_{j\beta}} \frac{\partial x_{j\beta}}{\partial LnK_{2,i}} \tag{B.131}$$

$$\frac{\partial \xi_\beta}{\partial N_i} = -\frac{P_\beta}{RTZ_\beta{}^2} \sum_{j=1}^{n_c} \frac{\partial Z_\beta}{\partial x_{j\beta}} \frac{\partial x_{j\beta}}{\partial N_i} \tag{B.132}$$

$$\frac{\partial \xi_\beta}{\partial P} = \frac{(-P_\beta \frac{\partial Z_\beta}{\partial P_\beta} + Z_\beta)}{RTZ_\beta{}^2} \tag{B.133}$$

$$\frac{\partial \xi_\beta}{\partial T} = \frac{-P_\beta (T \frac{\partial Z_\beta}{\partial T} + Z_\beta)}{RT^2 Z_\beta{}^2} \tag{B.134}$$

B.9 DERIVATIVES OF SATURATION

The derivative of the saturation with respect to mole fraction, LnK_1, LnK_2, number of mole, pressure, and temperature are as follows:

$$\begin{aligned}
&\frac{\partial S_\beta}{\partial LnK_{1,i}} = \frac{\partial \left(n_\beta \tilde{V}_\beta \right)}{\partial LnK_{1,i}} = N_T \frac{\partial \left(L_\beta \tilde{V}_\beta \right)}{\partial LnK_{1,i}} \\
&= N_T \left(\tilde{V}_\beta \frac{\partial L_\beta}{\partial LnK_{1,i}} + L_\beta \frac{\partial \tilde{V}_\beta}{\partial LnK_{1,i}} \right) = N_T \left[\frac{RTZ_\beta}{P_\beta} \frac{\partial L_\beta}{\partial LnK_{1,i}} + L_\beta \frac{RT}{P_\beta} \frac{\partial Z_\beta}{\partial LnK_{1,i}} \right] \\
&= \frac{N_T RT}{P_\beta} \left(L_\beta \frac{\partial Z_\beta}{\partial LnK_{1,i}} + Z_\beta \frac{\partial L_\beta}{\partial LnK_{1,i}} \right)
\end{aligned} \tag{B.135}$$

Same equation can be used for $LnK_{2,i}$

$$\frac{\partial S_\beta}{\partial N_i} = \frac{\partial \left(N_T L_\beta \tilde{V}_\beta \right)}{\partial N_i} = \left(L_\beta \tilde{V}_\beta + \tilde{V}_\beta \frac{\partial L_\beta}{\partial N_i} + L_\beta \frac{\partial \tilde{V}_\beta}{\partial N_i} \right)$$

$$= \frac{RT}{P_\beta}\left(L_\beta Z_\beta + N_T Z_\beta \frac{\partial L_\beta}{\partial N_i} + N_T L_\beta \frac{\partial Z_\beta}{\partial N_i} \right) \tag{B.136}$$

$$\frac{\partial S_\beta}{\partial P_\beta} = \frac{RTN_T}{P_\beta}\left(\frac{\partial Z_\beta}{\partial P} - \frac{Z_\beta}{P} \right) L_\beta \tag{B.137}$$

$$\frac{\partial S_\beta}{\partial T} = \frac{RN_T}{P}\left(T\frac{\partial Z_\beta}{\partial T} + Z_\beta \right) L_\beta \tag{B.138}$$

B.10 RELATIVE PERMEABILITY

The relative permeabilities are calculated using modified Corey model as follows:

$$k_{r1} = k^\circ_{r1}\left(S_{1e}\right)^{e_1} \tag{B.139}$$

$$k_{r2} = k^\circ_{r2}\left(S_{2e}\right)^2\left[1-(1-S_{2e})^{e_2}\right] \tag{B.140}$$

$$k_{r3} = k^\circ_{r3}\left(S_{3e}\right)^2\left[1-(1-S_{3e})^{e_3}\right] \tag{B.141}$$

where the effective saturations are

$$S_{1e} = \frac{S_1 - S_{1r}}{1 - S_{1r} - S_{2r}} \tag{B.142}$$

$$S_{2e} = \frac{S_2 - S_{2r}}{1 - S_{1r} - S_{2r}} \tag{B.143}$$

$$S_{3e} = \frac{S_3 - S_{3r}}{1 - S_{1r} - S_{2r} - S_{3r}} \tag{B.144}$$

For four-phase model with three-phase flash calculation, the relative permeability of second liquid is calculated as follow:

$$k_{r4} = k^{\circ}_{r4}\left(S_{4e}\right)^2\left[1-(1-S_{4e})^{e_4}\right] \tag{B.145}$$

where

$$S_{4e} = \frac{S_4 - S_{4r}}{1 - S_{1r} - S_{2r} - S_{4r}} \tag{B.146}$$

B.11 DERIVATIVES OF RELATIVE PERMEABILITY

The derivative of the relative permeability with respect to mole fraction, LnK_1, LnK_2, number of mole, pressure, and temperature are as follows:

$$k_{rw} = k_{rw}\left(S_w\right) \tag{B.147}$$

$$k_{rg} = k_{rg}\left(S_g\right) \tag{B.148}$$

$$k_{ro} = k_{ro}\left(S_w, S_g\right) \tag{B.149}$$

$$\frac{\partial S_w}{\partial LnK_{1,i}} = 0 \tag{B.150}$$

$$\frac{\partial k_{rw}}{\partial LnK_{1,i}} = \frac{\partial k_{rw}}{\partial S_w}\frac{\partial S_w}{\partial LnK_{1,i}} = 0 \tag{B.151}$$

$$\frac{\partial k_{rg}}{\partial LnK_{1,i}} = \frac{\partial k_{rg}}{\partial S_g}\frac{\partial S_g}{\partial LnK_{1,i}} \tag{B.152}$$

$$\frac{\partial k_{ro}}{\partial LnK_{1,i}} = \frac{\partial k_{rw}}{\partial S_w}\frac{\partial S_w}{\partial LnK_{1,i}} + \frac{\partial k_{ro}}{\partial S_g}\frac{\partial S_g}{\partial LnK_{1,i}} = \frac{\partial k_{ro}}{\partial S_g}\frac{\partial S_g}{\partial LnK_{1,i}} \tag{B.153}$$

Same equations can be used for $LnK_{2,i}$

$$\frac{\partial k_{rw}}{\partial N_i} = \begin{cases} \frac{\partial k_{rw}}{\partial S_w}\frac{\partial S_w}{\partial N_w} & i = w \\ 0 & i \neq w \end{cases} \tag{B.154}$$

$$\frac{\partial k_{rg}}{\partial N_i} = \frac{\partial k_{rg}}{\partial S_g}\frac{\partial S_g}{\partial N_i} \tag{B.155}$$

$$\frac{\partial k_{ro}}{\partial N_i} = \frac{\partial k_{rw}}{\partial S_w}\frac{\partial S_w}{\partial N_i} + \frac{\partial k_{ro}}{\partial S_g}\frac{\partial S_g}{\partial N_i} = \frac{\partial k_{ro}}{\partial S_g}\frac{\partial S_g}{\partial N_i} \tag{B.156}$$

$$\frac{\partial k_{rg}}{\partial P} = \frac{\partial k_{rg}}{\partial S_g}\frac{\partial S_g}{\partial P} \tag{B.157}$$

$$\frac{\partial k_{ro}}{\partial P} = \frac{\partial k_{ro}}{\partial S_g}\frac{\partial S_g}{\partial P} + \frac{\partial k_{ro}}{\partial S_w}\frac{\partial S_w}{\partial P} \tag{B.158}$$

$$\frac{\partial k_{rw}}{\partial P} = \frac{\partial k_{rw}}{\partial S_w}\frac{\partial S_w}{\partial P} \tag{B.159}$$

$$\frac{\partial k_{rg}}{\partial T} = \frac{\partial k_{rg}}{\partial S_g}\frac{\partial S_g}{\partial T} \tag{B.160}$$

$$\frac{\partial k_{ro}}{\partial T} = \frac{\partial k_{ro}}{\partial S_g}\frac{\partial S_g}{\partial T} + \frac{\partial k_{ro}}{\partial S_w}\frac{\partial S_w}{\partial T} \tag{B.161}$$

$$\frac{\partial k_{rw}}{\partial T} = \frac{\partial k_{rw}}{\partial S_w}\frac{\partial S_w}{\partial T} \tag{B.162}$$

Appendix C

Evaluation of Jacobian Elements for Volume Constraint Equation

In this appendix, derivatives of the pore-volume constraint equation with respect to primary variables of the four-phase model are described.

C.1 DERIVATIVES WITH RESPECT TO MOLE NUMBER

If water is considered a fluid component, there is no separate water equation. Water is considered the same as any other component in the mixture. However, if water is a separate phase, the aqueous phase is considered the same as any other phase, but without the chemical equilibrium with other phases.

In the case in which water prevailing as a separate phase, i.e., for isothermal option, we have

$$n_{wL1} = n_{wg} = n_{wL2} = 0,$$

$$\frac{\partial \tilde{V}_g}{\partial N_w} = \frac{\partial \tilde{V}_{L1}}{\partial N_w} = \frac{\partial \tilde{V}_{L2}}{\partial N_w} = 0 \tag{C.1}$$

$$\frac{\partial R_V}{\partial N_w} = \frac{\partial \tilde{V}_w}{\partial N_w} N_w + \tilde{V}_w \frac{\partial N_w}{\partial N_w} \tag{C.2}$$

$$\frac{\partial \tilde{V}_w}{\partial N_w} = \left[\partial \left(\frac{ZRT}{P} \right) / \partial N_w \right]_{P,T} = 0 \tag{C.3}$$

$$\frac{\partial R_V}{\partial N_w} = \tilde{V}_w \tag{C.4}$$

If we neglect the solubility of hydrocarbon components in the water phase, we have

$$\frac{\partial N_w}{\partial N_i\left(i \neq n_c+1\right)} = 0 \tag{C.5}$$

$$\frac{\partial \tilde{V}_w}{\partial N_i\left(i \neq n_c+1\right)} = 0 \tag{C.6}$$

Then

$$\frac{\partial R_V}{\partial N_i\left(i \neq n_c+1\right)} = N_{L1}\frac{\partial \tilde{V}_{L1}}{\partial N_i} + \hat{V}_{L1}\frac{\partial N_{L1}}{\partial N_i} + N_g\frac{\partial \tilde{V}_g}{\partial N_i} + \tilde{V}_g\frac{\partial N_g}{\partial N_i} + N_{L2}\frac{\partial \tilde{V}_{L2}}{\partial N_i} + \tilde{V}_{L2}\frac{\partial N_{L2}}{\partial N_i}$$

$$= \frac{RT}{P}\left(N_{L1}\frac{\partial Z_{L1}}{\partial N_i} + N_g\frac{\partial Z_g}{\partial N_i} + N_{L2}\frac{\partial Z_{L2}}{\partial N_i}\right) + \tilde{V}_{L1}\frac{\partial\left(L_1 N_T\right)}{\partial N_i} + \tilde{V}_g\frac{\partial\left(vN_T\right)}{\partial N_i} + \tilde{V}_{L2}\frac{\partial\left(L_2 N_T\right)}{\partial N_i}$$

$$= \frac{RTN_T}{P}\left(L_1\frac{\partial Z_{L1}}{\partial N_i} + v\frac{\partial Z_g}{\partial N_i} + L_2\frac{\partial Z_{L2}}{\partial N_i}\right) +$$

$$\tilde{V}_{L1}\left(L_1 + N_T\frac{\partial L_1}{\partial N_i}\right) + \tilde{V}_g\left(v + N_T\frac{\partial v}{\partial N_i}\right) + \tilde{V}_{L2}\left(L_2 + N_T\frac{\partial L_2}{\partial N_i}\right)$$

$$= \frac{RTN_T}{P}\left(L_1\frac{\partial Z_{L1}}{\partial N_i} + v\frac{\partial Z_g}{\partial N_i} + L_2\frac{\partial Z_{L2}}{\partial N_i}\right) +$$

$$\tilde{V}_{L1}L_1 + \tilde{V}_{L1}N_T\frac{\partial L_1}{\partial N_i} + \tilde{V}_g v + \tilde{V}_g N_T\frac{\partial v}{\partial N_i} + \tilde{V}_{L2}L_2 + \tilde{V}_{L2}N_T\frac{\partial L_2}{\partial N_i}$$

$$= \frac{RTN_T}{P}\left(L_1\frac{\partial Z_{l1}}{\partial N_i} + v\frac{\partial Z_g}{\partial N_i} + L_2\frac{\partial Z_{L2}}{\partial N_i}\right) +$$

$$\tilde{V}_{L1}L_1 + \tilde{V}_{L1}N_T\frac{\partial(1-v-L_2)}{\partial N_i} + \tilde{V}_g v + \tilde{V}_g N_T\frac{\partial v}{\partial N_i} + \tilde{V}_{L2}L_2 + \tilde{V}_{L2}N_T\frac{\partial L_2}{\partial N_i}$$

$$= \frac{RTN_T}{P}\left(L_1\frac{\partial Z_{L1}}{\partial N_i} + v\frac{\partial Z_g}{\partial N_i} + L_2\frac{\partial Z_{L2}}{\partial N_i}\right) +$$

$$\tilde{V}_{L1}L_1 + \tilde{V}_g v + \tilde{V}_{L2}L_2 + N_T(\tilde{V}_{L1} - \tilde{V}_g)\frac{\partial v}{\partial N_i} + N_T(\tilde{V}_{L1} - \tilde{V}_{L2})\frac{\partial L_2}{\partial N_i}$$

$$= \frac{RTN_T}{P}\left(L_1\frac{\partial Z_{L1}}{\partial N_i} + v\frac{\partial Z_g}{\partial N_i} + L_2\frac{\partial Z_{L2}}{\partial N_i}\right) +$$

$$\tilde{V}_{L1}L_1 + \tilde{V}_g v + \tilde{V}_{L2}L_2 + N_T(\tilde{V}_{L1} - \tilde{V}_g)\frac{\dfrac{\partial G2}{\partial N_i}}{\dfrac{\partial G2}{\partial v}} + N_T(\tilde{V}_{L1} - \tilde{V}_{L2})\frac{\dfrac{\partial G3}{\partial N_i}}{\dfrac{\partial G3}{\partial L_2}} \tag{C.7}$$

C.2 DERIVATIVES WITH RESPECT TO *LNK1, LNK2*

The derivative equations for primary variables LnK_1 and LnK_2 are as follows (liquid phases are labeled as L_1 and L_2):

$$\frac{\partial R_V}{\partial LnK_{1,i}} = N_w\frac{\partial \tilde{V}_w}{\partial LnK_{1,i}} + \tilde{V}_w\frac{\partial N_w}{\partial LnK_{1,i}} + N_{L1}\frac{\partial \tilde{V}_{L1}}{\partial LnK_{1,i}} + \tilde{V}_{L1}\frac{\partial N_{L1}}{\partial LnK_{1,i}} + N_g\frac{\partial \tilde{V}_g}{\partial LnK_{1,i}} + \tilde{V}_g\frac{\partial N_g}{\partial LnK_{1,i}}$$
$$+N_{L2}\frac{\partial \tilde{V}_{L2}}{\partial LnK_{1,i}} + \tilde{V}_{L2}\frac{\partial N_{L2}}{\partial LnK_{1,i}} \tag{C.8}$$

$$\frac{\partial \tilde{V}_w}{\partial LnK_{1,i}} = 0, \quad \frac{\partial \tilde{V}_w}{\partial LnK_{2,i}} = 0 \quad \text{and} \quad \frac{\partial N_w}{\partial LnK_{1,i}} = 0, \quad \frac{\partial N_w}{\partial LnK_{2,i}} = 0$$

$$\frac{\partial R_V}{\partial LnK_{1,i}} = N_T\left(L_1\frac{\partial \tilde{V}_{L1}}{\partial LnK_{1,i}} + v\frac{\partial \tilde{V}_g}{\partial LnK_{1,i}} + L_2\frac{\partial \tilde{V}_{L2}}{\partial LnK_{1,i}} + \right.$$
$$\left.\tilde{V}_{L_1}\frac{\partial L_1}{\partial LnK_{1,i}} + \tilde{V}_g\frac{\partial v_g}{\partial LnK_{1,i}} + \tilde{V}_{L_2}\frac{\partial L_2}{\partial LnK_{1,i}}\right) \tag{C.9}$$

$$\frac{\partial R_V}{\partial LnK_{1,i}} = N_T\frac{RT}{P}\left(L_1\frac{\partial Z_{L1}}{\partial LnK_{1,i}} + v\frac{\partial Z_g}{\partial LnK_{1,i}} + L_2\frac{\partial Z_{L2}}{\partial LnK_{1,i}}\right) -$$
$$N_T\left(\tilde{V}_{L1} - \tilde{V}_g\right)\frac{\dfrac{\partial G2}{\partial LnK_{1,i}}}{\dfrac{\partial G2}{\partial v}} - N_T\left(\tilde{V}_{L1} - \tilde{V}_{L2}\right)\frac{\dfrac{\partial G3}{\partial LnK_{1,i}}}{\dfrac{\partial G3}{\partial L_2}} \tag{C.10}$$

To have the derivative with respect to LnK_2, in the above equations LnK_1 can be replaced by LnK_2.

C.3 DERIVATIVES WITH RESPECT TO PRESSURE

The equation for derivatives with respect to pressure is

$$\frac{\partial R_V}{\partial P} = N_w \frac{\partial \tilde{V}_w}{\partial P} + \tilde{V}_w \frac{\partial N_w}{\partial P} + N_{L1} \frac{\partial \tilde{V}_{L1}}{\partial P} + \tilde{V}_{L1} \frac{\partial N_{L1}}{\partial P} + N_g \frac{\partial \tilde{V}_g}{\partial P} + \tilde{V}_g \frac{\partial N_g}{\partial P}$$
$$+ N_{L2} \frac{\partial \tilde{V}_{L2}}{\partial P} + \tilde{V}_{L2} \frac{\partial N_{L2}}{\partial P} \qquad \text{(C.11)}$$

$$\frac{\partial N_w}{\partial P} = 0 \quad and \quad \frac{\partial N_{L1}}{\partial P} = \frac{\partial N_g}{\partial P} = \frac{\partial N_{L2}}{\partial P} = 0$$

$$\frac{\partial R_V}{\partial P} = N_w \frac{\partial \tilde{V}_w}{\partial P} + N_T RT \sum_{j=2}^{4} v_j \frac{P \frac{\partial Z_j}{\partial P} - Z_j}{P^2} \qquad \text{(C.12)}$$

C.4 DERIVATIVES WITH RESPECT TO TEMPERATURE

The equation for derivatives with respect to temperature is

$$\frac{\partial R_V}{\partial T} = [N_w \frac{\partial \tilde{V}_w}{\partial T} + \frac{N_T R}{P} \sum_{j=2}^{n_p} v_j (T \frac{\partial Z_j}{\partial T} + Z_j)] \qquad \text{(C.13)}$$

If total enthalpy is selected as the primary variable,

$$\frac{\partial R_V}{\partial H_t} = [N_w \frac{\partial \tilde{V}_w}{\partial H_t} + \frac{N_T R}{P} \sum_{j=2}^{n_p} v_j (T \frac{\partial Z_j}{\partial H_t} + Z_j \frac{\partial T}{\partial H_t})] \qquad \text{(C.14)}$$

The derivatives of $\frac{\partial Z_j}{\partial T}$ and $\frac{\partial \tilde{V}_w}{\partial T}$ can be found in Appendix A.

Appendix D

Evaluation of Jacobian Elements for Material Balance Equations

In the following sections, the derivatives of the material balance equation with respect to primary variables are presented. The equations are written for *x* direction and are the same for other directions.

D.1 DERIVATIVES OF THE MATERIAL BALANCE WITH RESPECT TO LnK_1 AND LnK_2

By taking the derivative of material balance equation of each component (i.e.$\alpha 1$) with respect to *LnK1* and *LnK2* of another component (i.e.$\alpha 2$), we have the following expressions.

D.1.1 Derivatives for the Diagonal Elements of the Jacobian Matrix

The general equation is as follows:

$$\frac{\partial R_M}{\partial LnK_{1,\alpha 2i}} = -\frac{\partial M_{accum}}{\partial LnK_{1,\alpha 2i}} + \frac{\partial M_{conv}}{\partial LnK_{1,\alpha 2i}} + \frac{\partial M_{source}}{\partial LnK_{1,\alpha 2i}} \tag{D.1}$$

For the accumulation term, we have

$$\frac{\partial\left(\frac{V_{bi}\phi_i N_{\alpha 1i}}{\Delta t}\right)}{\partial LnK_{1,\alpha 2i}} = 0 \tag{D.2}$$

For the source term, we have

$$\frac{\partial q_{\alpha 1i}}{\partial LnK_{1,\alpha 2i}} = C\frac{\left[1-(f_w)_{inj}\right]}{\left[V(t)\right]_{inj}}\sum_{\beta=1}^{n_p}\left[\frac{\mu_{\beta i}\dfrac{\partial k_{r\beta i}}{\partial LnK_{1,\alpha 2i}} - k_{r\beta i}\dfrac{\partial \mu_{\beta i}}{\partial LnK_{1,\alpha 2i}}}{\mu_{\beta i^2}}\left(P_{wf}-P_{\beta i}\right)-\lambda_{\beta i}\right] \tag{D.3}$$

The term $\left[V(t)\right]_{inj}$ is total volume per mole of injected fluid.

For the convection term, neglecting the effect wrought by changes in $LnK_{1,\alpha}$ and $LnK_{2,\alpha}$ on capillary pressure, we have

$$\frac{\partial V_{\beta i}}{\partial LnK_{1,\alpha i}} = 0,\ \frac{\partial V_{\beta i}}{\partial LnK_{2,\alpha i}} = 0 \tag{D.4}$$

$$\frac{\partial T_{\alpha 1\beta i}}{\partial LnK_{1,\alpha 2i}} = \frac{\partial\left(x_{\alpha 1\beta i}\lambda_{\beta i}\xi_{\beta i}\right)}{\partial LnK_{1,\alpha 2i}} = \lambda_{\beta i}\xi_{\beta i}\frac{\partial x_{\alpha 1\beta i}}{\partial LnK_{1,\alpha 2i}}$$
$$+x_{\alpha 1\beta i}\xi_{\beta i}\frac{\partial \lambda_{\beta i}}{\partial LnK_{1,\alpha 2i}} + x_{\alpha 1\beta i}\lambda_{\beta i}\frac{\partial \xi_{\beta i}}{\partial LnK_{1,\alpha 2i}} \tag{D.5}$$

Then, the derivatives of convection term in terms of LnK_1 for the four scenarios (Section 3.3.8.1.3) are

1. $$\frac{\partial M_{conv}}{\partial LnK_{1,\alpha 2i}} = \frac{\partial(T_{\beta i}\tilde{K}_i(\Phi_{\beta i}-\Phi_{\beta i+1}) - T_{\beta i-1}\tilde{K}_i(\Phi_{\beta i-1}-\Phi_{\beta i}))}{\partial LnK_{1,\alpha 2i}}$$
$$= \tilde{K}_i(\Phi_{wi}-\Phi_{wi+1})\frac{\partial T_{wi}}{LnK_{1,\alpha 2i}} \tag{D.6}$$

2. $$\frac{\partial M_{conv}}{\partial LnK_{1,\alpha 2i}} = \frac{\partial(-T_{\beta i+1}\tilde{K}_{i+1}(\Phi_{\beta i+1}-\Phi_{\beta i}) + T_{wi}\tilde{K}_i(\Phi_{\beta i}-\Phi_{\beta i-1}))}{\partial LnK_{1,\alpha 2i}}$$
$$= \tilde{K}_i(\Phi_{\beta i}-\Phi_{\beta i+1})\frac{\partial T_{\beta i}}{\partial LnK_{1,\alpha 2i}} \tag{D.7}$$

3. $$\frac{\partial M_{conv}}{LnK_{1,\alpha 2i}} = \frac{\partial(-T_{\beta i+1}K_{i+1}(\Phi_{\beta i+1}-\Phi_{\beta i})-T_{\beta i-1}K_i(\Phi_{\beta i-1}-\Phi_{\beta i}))}{LnK_{1,\alpha 2i}}$$
$$= 0 \qquad \text{(D.8)}$$

4. $$\frac{\partial M_{conv}}{LnK_{1,\alpha 2i}} = \frac{\partial(T_{\beta i}K_{i+1}(\Phi_{\beta i}-\Phi_{\beta i+1})+T_{\beta i}K_i(\Phi_{\beta i}-\Phi_{\beta i-1}))}{LnK_{1,\alpha 2i}}$$

$$= K_{i+1}(\Phi_{\beta i}-\Phi_{\beta i+1})\frac{\partial T_{\beta i}}{LnK_{1,\alpha 2i}} + K_i(\Phi_{\beta i}-\Phi_{\beta i+1})\frac{\partial T_{\beta i}}{LnK_{1,\alpha 2i}} \qquad \text{(D.9)}$$

Then, the derivatives in terms of LnK_2 for the four scenarios are same as for LnK_1.

D.1.2 Derivatives for the Off-Diagonal Elements of the Jacobian Matrix

By taking the derivative of material balance equation of each component (i.e. $\alpha 1$) with respect to $LnK_{1,\alpha}$ and $LnK_{2,\alpha}$ of another component (i.e. $\alpha 2$) at the neighborhoods of the specific gridblock, we have

$$\frac{\partial R_M}{\partial LnK_{1,\alpha 2i\pm 1}} = -\frac{\partial M_{accum}}{\partial LnK_{1,\alpha 2i\pm 1}} + \frac{\partial M_{conv}}{\partial LnK_{1,\alpha 2i\pm 1}} + \frac{\partial M_{source}}{\partial LnK_{1,\alpha 2i\pm 1}} \qquad \text{(D.10)}$$

For the accumulation term, we have

$$\frac{\partial\left(\frac{V_{bi}\phi_i N_{\alpha 1i}}{\Delta t}\right)}{\partial LnK_{1,\alpha 2i\pm 1}} = 0, \quad \frac{\partial\left(\frac{V_{bi}\phi_i N_{\alpha 1i}}{\Delta t}\right)}{\partial LnK_{2,\alpha 2i\pm 1}} = 0 \qquad \text{(D.11)}$$

For the source term, we have

$$\frac{\partial q_{\alpha 1i}}{LnK_{1,\alpha 2i\pm 1}} = 0,\ \frac{\partial q_{\alpha 1i}}{LnK_{2,\alpha 2i\pm 1}} = 0 \tag{D.12}$$

The derivatives of the convection terms for the cell to the left side of diagonal in x direction the four scenarios (Section 3.3.8.1.3) are

$$1.\ \frac{\partial M_{conv}}{\partial LnK_{1,\alpha 2i-1}} = \frac{\partial (T_{\beta i}\tilde{K}_i(\Phi_{\beta i} - \Phi_{\beta i+1}) - T_{\beta i-1}\tilde{K}_i(\Phi_{\beta i-1} - \Phi_{\beta i}))}{\partial LnK_{1,\alpha 2i-1}}$$

$$= -\tilde{K}_i(\Phi_{\beta i-1} - \Phi_{\beta i})\left(\frac{\partial T_{\beta i-1}}{\partial LnK_{1,\alpha 2i-1}}\right) \tag{D.13}$$

$$2.\quad \frac{\partial M_{conv}}{\partial LnK_{1,\alpha 2i-1}} = 0 \tag{D.14}$$

$$3.\quad \frac{\partial M_{conv}}{\partial LnK_{1,\alpha 2i-1}} = \frac{\partial (T_{\beta i}\tilde{K}_i(\Phi_{\beta i} - \Phi_{\beta i+1}) - T_{\beta i-1}\tilde{K}_i(\Phi_{\beta i-1} - \Phi_{\beta i}))}{\partial LnK_{1,\alpha 2i-1}}$$

$$= -\tilde{K}_i(\Phi_{\beta i-1} - \Phi_{\beta i})\left(\frac{\partial T_{\beta i-1}}{LnK_{1,\alpha 2i-1}}\right) \tag{D.15}$$

$$4.\quad \frac{\partial M_{conv}}{\partial LnK_{1,\alpha 2i-1}} = 0 \tag{D.16}$$

Similarly, for the cell to the right side of diagonal in the x direction

$$1.\quad \frac{\partial M_{conv}}{\partial LnK_{1,\alpha 2i+1}} = 0 \tag{D.17}$$

2. $$\frac{\partial M_{conv}}{\partial LnK_{1,\alpha 2i+1}} = \frac{\partial(-T_{\beta i+1}\tilde{K}_{i+1}(\Phi_{\beta i+1}-\Phi_{\beta i})+T_{wi}\tilde{K}_i(\Phi_{\beta i}-\Phi_{\beta i+1}))}{\partial LnK_{1,\alpha 2i+1}}$$

$$= -\frac{\tilde{K}_{i+1}(\Phi_{\beta i+1}-\Phi_{\beta i})}{\mu_{wi+1}}\left(\frac{\partial T_{\beta i+1}}{\partial LnK_{1,\alpha 2i+1}}\right) \quad \text{(D.18)}$$

3. $$\frac{\partial M_{conv}}{\partial LnK_{1,\alpha 2i+1}} = \frac{\partial(-T_{wi+1}\tilde{K}_{i+1}(\Phi_{i+1}-\Phi_i)+T_{wi}\tilde{K}_i(\Phi_i-\Phi_{i+1}))}{\partial LnK_{1,\alpha 2i+1}}$$

$$= -\tilde{K}_{i+1}(\Phi_{i+1}-\Phi_i)\left(\frac{\partial T_{wi+1}}{\partial LnK_{1,\alpha 2i+1}}\right) \quad \text{(D.19)}$$

4. $$\frac{\partial M_{conv}}{\partial LnK_{1,\alpha 2i+1}} = 0 \quad \text{(D.20)}$$

The same equations as above can be written for LnK_2 and also for x and y directions.

D.2 Derivatives of the Material Balance with Respect to Component Mole Number

The derivative equations for the diagonal and off-diagonal elements with respect to N_i are the same for LnK_i by replacing of LnK_i by N_i.

D.3 Derivatives of the material balance with respect to Pressure

By taking the derivative of material balance equation of each component (i.e. $\alpha 1$) with respect to pressure, we can determine the following equation.

$$\frac{\partial R_M}{\partial P_{\alpha 2i}} = -\frac{\partial M_{accum}}{\partial P_{\alpha 2i}} + \frac{\partial M_{conv}}{\partial P_{\alpha 2i}} + \frac{\partial M_{source}}{\partial P_{\alpha 2i}} \quad \text{(D.21)}$$

D.3.1 Derivatives for the Diagonal Elements of the Jacobian Matrix

The derivative for each term is described as follows:

For the accumulation term, we have

$$\frac{\partial\left(\frac{V_{bi}\phi_i N_{\alpha i}}{\Delta t}\right)}{\partial P_i} = \frac{V_{bi}\phi_{0i} C_f N_{\alpha i}}{\Delta t} \tag{D.22}$$

For the source term, we have

$$\frac{\partial q_{\alpha i}}{\partial P_i} = C_i \frac{\left[1-\left(f_w\right)_{inj}\right]}{\left[V\left(t\right)\right]_{inj}} \sum_{\beta=1}^{n_p} \left[\frac{\mu_{\beta i}\frac{\partial k_{r\beta i}}{\partial P_i} - k_{r\beta i}\frac{\partial \mu_{\beta i}}{\partial P_i}}{\mu_{\beta i^2}} \left(P_{wf} - P_{\beta i}\right) - \lambda_\beta \right] \tag{D.23}$$

For the convection term, we have

$$\frac{\partial T_{\alpha\beta i}}{\partial P_i} = \frac{\partial\left(x_{\alpha\beta i}\lambda_{\beta i}\xi_{\beta i}\right)}{\partial P_i} = \lambda_{\beta i}\xi_{\beta i}\frac{\partial x_{\alpha\beta i}}{\partial P_i} + x_{\alpha\beta i}\xi_{\beta i}\frac{\partial \lambda_{\beta i}}{\partial P_i} + x_{\alpha\beta i}\lambda_{\beta i}\frac{\partial \xi_{\beta i}}{\partial P_i} \tag{D.24}$$

$$\begin{aligned}
\frac{\partial T_{\alpha\beta i}}{\partial P_i} &= x_{\alpha\beta i}\xi_{\beta i}\frac{\mu_{\beta i}\frac{\partial k_{r\beta i}}{\partial P_i} - k_{r\beta i}\frac{\partial \mu_{\beta i}}{\partial P_i}}{{\mu_{\beta i}}^2} + x_{\alpha\beta i}\frac{k_{r\beta i}}{\mu_{\beta i}}\frac{\partial \xi_{\beta i}}{\partial P_i} \\
&= \frac{1}{{\mu_{\beta i}}^2}\left(-x_{\alpha\beta i}\xi_{\beta i}k_{r\beta i}\frac{\partial \mu_{\beta i}}{\partial P_i} + x_{\alpha\beta i}k_{rwi}\mu_{\beta i}\frac{\partial \xi_{\beta i}}{\partial P_i} + x_{\alpha\beta i}\xi_{\beta i}\mu_{\beta i}\frac{\partial k_{r\beta i}}{\partial P_i}\right) \\
&= \frac{x_{\alpha\beta i}}{{\mu_{\beta i}}^2}\left[\mu_{\beta i}\left(k_{r\beta i}\frac{\partial \xi_{\beta i}}{\partial P_i} + \xi_{\beta i}\frac{\partial k_{r\beta i}}{\partial P_i}\right) - \xi_{\beta i}k_{r\beta i}\frac{\partial \mu_{\beta i}}{\partial P_i}\right]
\end{aligned} \tag{D.25}$$

For the four scenarios (section 3.3.8.1.3), we have

1. $$\frac{\partial M_{conv}}{\partial P_i} = \frac{\partial (T_{\beta i}\tilde{K}_i(\Phi_{\beta i} - \Phi_{\beta i+1}) - T_{\beta i-1}\tilde{K}_i(\Phi_{\beta i-1} - \Phi_{\beta i}))}{\partial P_i}$$

$$= \tilde{K}_i(\Phi_{\beta i} - \Phi_{\beta i+1})\frac{\partial T_{\beta i}}{\partial P_i} + \tilde{K}_{i+1}T_{\beta i} + \tilde{K}_i T_{\beta i-1} \quad \text{(D.26)}$$

2. $$\frac{\partial M_{conv}}{\partial P_i} = \frac{\partial (-T_{\beta i+1}\tilde{K}_{i+1}(\Phi_{\beta i+1} - \Phi_{\beta i}) + T_{\beta i}\tilde{K}_i(\Phi_{\beta i} - \Phi_{\beta i-1}))}{\partial P_i}$$

$$= T_{\beta i+1}\tilde{K}_{i+1} + \tilde{K}_i(\Phi_{\beta i} - \Phi_{\beta i+1})\frac{\partial T_{\beta i}}{\partial P} + T_{\beta i}\tilde{K}_i \quad \text{(D.27)}$$

3. $$\frac{\partial M_{conv}}{\partial P_i} = \frac{\partial (-T_{\beta i+1}K_{i+1}(\Phi_{\beta i+1} - \Phi_{\beta i}) - T_{\beta i-1}K_i(\Phi_{\beta i-1} - \Phi_{\beta i}))}{\partial P_i}$$

$$= T_{\beta i+1}K_{i+1} + T_{\beta i-1}K_i \quad \text{(D.28)}$$

4. $$\frac{\partial M_{conv}}{\partial P_i} = \frac{\partial (T_{\beta i}K_{i+1}(\Phi_{\beta i} - \Phi_{\beta i+1}) + T_{\beta i}K_i(\Phi_{\beta i} - \Phi_{\beta i-1}))}{\partial P_i}$$

$$= K_{i+1}(\Phi_{\beta i} - \Phi_{\beta i+1})\frac{\partial T_{\beta i}}{\partial P_i} + T_{\beta i}K_{i+1} + K_i(\Phi_{\beta i} - \Phi_{\beta i+1})\frac{\partial T_{\beta i}}{\partial P_i} + T_{\beta i}K_i \quad \text{(D.29)}$$

D.3.2 Derivatives for the Off-Diagonal Elements of the Jacobian Matrix

By taking the derivative of material balance equation of each component (i.e. *α1*) with respect to pressure of the neighborhoods of the specific gridblock, we have

$$\frac{\partial R_M}{\partial P_{2i\pm1}} = -\frac{\partial M_{accum}}{\partial P_{2i\pm1}} + \frac{\partial M_{conv}}{\partial P_{2i\pm1}} + \frac{\partial M_{source}}{\partial P_{2i\pm1}} \quad \text{(D.30)}$$

For the accumulation term,

$$\frac{\partial M_{accum}}{\partial P_{i\pm1}} = 0 \quad \text{(D.31)}$$

For the source term,

$$\frac{\partial M_{source}}{\partial P_{i\pm1}} = 0 \tag{D.32}$$

For the convection term, the derivatives in the case of four scenarios (section 3.3.8.1.3) as relevant to the cell to the left side of the diagonal in the *x* direction are

1. $$\frac{\partial M_{conv}}{\partial P_{i-1}} = \frac{\partial(T_{\beta i}\tilde{K}_i(\Phi_{\beta i} - \Phi_{\beta i+1}) - T_{\beta i-1}\tilde{K}_i(\Phi_{\beta i-1} - \Phi_{\beta i}))}{\partial P_{i-1}}$$
$$= -T_{\beta i-1}\tilde{K}_i - \tilde{K}_i(\Phi_{\beta i-1} - \Phi_{\beta i})\frac{\partial T_{\beta i-1}}{\partial P_{i-1}} \tag{D.33}$$

2. $$\frac{\partial M_{conv}}{\partial P_{i-1}} = \frac{\partial(-T_{\beta i+1}\tilde{K}_{i+1}(\Phi_{\beta i+1} - \Phi_{\beta i}) + T_{\beta i}\tilde{K}_i(\Phi_{\beta i} - \Phi_{\beta i-1}))}{\partial P_{i-1}}$$
$$= -T_{\beta i}\tilde{K}_i \tag{D.34}$$

3. $$\frac{\partial M_{conv}}{\partial P_{i-1}} = \frac{\partial(-T_{\beta i+1}K_{i+1}(\Phi_{\beta i+1} - \Phi_{\beta i}) - T_{\beta i-1}K_i(\Phi_{\beta i-1} - \Phi_{\beta i}))}{\partial P_{i-1}}$$
$$= -T_{\beta i-1}K_i - K_i(\Phi_{\beta i-1} - \Phi_{\beta i})\frac{\partial T_{\beta i-1}}{\partial P_{i-1}} \tag{D.35}$$

4. $$\frac{\partial M_{conv}}{\partial P_{i-1}} = \frac{\partial(T_{\beta i}K_{i+1}(\Phi_{\beta i} - \Phi_{\beta i+1}) + T_{\beta i}K_i(\Phi_{\beta i} - \Phi_{\beta i-1}))}{\partial P_{i-1}}$$
$$= -T_{\beta i}K_i \tag{D.36}$$

Similarly, for the cell to the right side of the diagonal in the *x* direction we have

1. $$\frac{\partial M_{conv}}{\partial P_{i+1}} = \frac{\partial(T_{\beta i}\tilde{K}_i(\Phi_{\beta i} - \Phi_{\beta i+1}) - T_{\beta i-1}\tilde{K}_i(\Phi_{\beta i-1} - \Phi_{\beta i}))}{\partial P_{i+1}}$$
$$= -T_{\beta i}\tilde{K}_i \tag{D.37}$$

2. $$\frac{\partial M_{conv}}{\partial P_{i+1}} = \frac{\partial(-T_{\beta i+1}\tilde{K}_{i+1}(\Phi_{\beta i+1}-\Phi_{\beta i}) + T_{\beta i}\tilde{K}_{i}(\Phi_{\beta i}-\Phi_{\beta i-1}))}{\partial P_{i+1}}$$

$$= -T_{wi+1}\tilde{K}_{i+1} - \tilde{K}_{i+1}(\Phi_{\beta i+1}-\Phi_{\beta i})\frac{\partial T_{\beta i+1}}{\partial P_{i+1}} \quad \text{(D.38)}$$

3. $$\frac{\partial M_{conv}}{\partial P_{i+1}} = \frac{\partial(-T_{\beta i+1}K_{i+1}(\Phi_{\beta i+1}-\Phi_{\beta i}) - T_{\beta i-1}K_{i}(\Phi_{\beta i-1}-\Phi_{\beta i}))}{\partial P_{i+1}}$$

$$= -T_{\beta i+1}K_{i+1} - K_{i+1}(\Phi_{\beta i+1}-\Phi_{\beta i})\frac{\partial T_{\beta i+1}}{\partial P_{i+1}} \quad \text{(D.39)}$$

4. $$\frac{\partial M_{conv}}{\partial P_{i+1}} = \frac{\partial(T_{\beta i}K_{i+1}(\Phi_{\beta i}-\Phi_{\beta i+1}) + T_{\beta i}K_{i}(\Phi_{\beta i}-\Phi_{\beta i-1}))}{\partial P_{i+1}}$$

$$= -T_{\beta i}K_{i+1} \quad \text{(D.40)}$$

D.4 DERIVATIVES OF THE MATERIAL BALANCE WITH RESPECT TO TEMPERATURE

By taking the derivative of material balance equation of each component (i.e. *α1*) with respect to temperature, we can determine the following equation. In the equations, H_t is indication of temperature.

$$\frac{\partial R_M}{\partial H_{t,i}} = -\frac{\partial M_{accum}}{\partial H_{t,i}} + \frac{\partial M_{conv}}{\partial H_{t,i}} + \frac{\partial M_{source}}{\partial H_{t,i}} \quad \text{(D.41)}$$

D.4.1 Derivatives for the Diagonal Elements of the Jacobian Matrix

The derivative of each term is determined by following equations.

For the accumulation term, we have

$$\frac{\partial\left(\frac{V_{bi}\phi_i N_{\alpha i}}{\Delta t}\right)}{\partial H_{t,i}} = 0 \tag{D.42}$$

For the source term, we have

$$\frac{\partial q_{\alpha i}}{\partial H_{t,i}} = C_i \frac{\left[1-\left(f_w\right)_{inj}\right]}{\left[V\left(t\right)\right]_{inj}} \sum_{\beta=1}^{n_p} \left[\frac{\mu_{\beta i}\frac{\partial k_{r\beta i}}{\partial H_{t,i}} - k_{r\beta i}\frac{\partial \mu_{\beta i}}{\partial H_{t,i}}}{\mu_{\beta i^2}} \left(P_{wf} - P_{\beta i}\right) \right] \tag{D.43}$$

For the convection term, we have

$$\frac{\partial T_{\alpha\beta i}}{\partial H_{t,i}} = \frac{\partial\left(x_{\alpha\beta i}\lambda_{\beta i}\xi_{\beta i}\right)}{\partial H_{t,i}} = \lambda_{\beta i}\xi_{\beta i}\frac{\partial x_{\alpha\beta i}}{\partial H_{t,i}} + x_{\alpha\beta i}\xi_{\beta i}\frac{\partial \lambda_{\beta i}}{\partial H_{t,i}} + x_{\alpha\beta i}\lambda_{\beta i}\frac{\partial \xi_{\beta i}}{\partial H_{t,i}} \tag{D.44}$$

$$\begin{aligned}
\frac{\partial T_{\alpha\beta i}}{\partial H_{t,i}} &= x_{\alpha\beta i}\xi_{\beta i}\frac{\mu_{\beta i}\frac{\partial k_{r\beta i}}{\partial H_{t,i}} - k_{r\beta i}\frac{\partial \mu_{\beta i}}{\partial H_{t,i}}}{{\mu_{\beta i}}^2} + x_{\alpha\beta i}\frac{k_{r\beta i}}{\mu_{\beta i}}\frac{\partial \xi_{\beta i}}{\partial H_{t,i}} \\
&= \frac{1}{{\mu_{\beta i}}^2}\left(-x_{\alpha\beta i}\xi_{\beta i}k_{r\beta i}\frac{\partial \mu_{\beta i}}{\partial H_{t,i}} + x_{\alpha\beta i}k_{r\beta i}\mu_{\beta i}\frac{\partial \xi_{\beta i}}{\partial H_{t,i}} + x_{\alpha\beta i}\xi_{\beta i}\mu_{\beta i}\frac{\partial k_{r\beta i}}{\partial H_{t,i}}\right) \\
&= \frac{x_{\alpha\beta i}}{{\mu_{\beta i}}^2}\left[\mu_{\beta i}\left(k_{r\beta i}\frac{\partial \xi_{\beta i}}{\partial H_{t,i}} + \xi_{\beta i}\frac{\partial k_{r\beta i}}{\partial H_{t,i}}\right) - \xi_{\beta i}k_{r\beta i}\frac{\partial \mu_{\beta i}}{\partial H_{t,i}}\right]
\end{aligned} \tag{D.45}$$

For the four scenarios (section 3.3.8.1.3), we have

1. $$\begin{aligned}
\frac{\partial M_{conv}}{\partial H_t} &= \frac{\partial(T_{\beta i}\tilde{K}_i(\Phi_{\beta i} - \Phi_{\beta i+1}) - T_{\beta i-1}\tilde{K}_i(\Phi_{\beta i-1} - \Phi_{\beta i}))}{\partial H_t} \\
&= \tilde{K}_i(\Phi_{wi} - \Phi_{wi+1})\frac{\partial T_{wi}}{\partial H_t}
\end{aligned} \tag{D.46}$$

2. $$\frac{\partial M_{conv}}{\partial H_t} = \frac{\partial(-T_{\beta i+1}\tilde{K}_{i+1}(\Phi_{\beta i+1} - \Phi_{\beta i}) + T_{wi}\tilde{K}_i(\Phi_{\beta i} - \Phi_{\beta i-1}))}{\partial H_t}$$

$$= \tilde{K}_i(\Phi_{\beta i} - \Phi_{\beta i+1})\frac{\partial T_{\beta i}}{\partial H_t} \tag{D.47}$$

3. $$\frac{\partial M_{conv}}{\partial H_t} = \frac{\partial(-T_{\beta i+1}K_{i+1}(\Phi_{\beta i+1} - \Phi_{\beta i}) - T_{\beta i-1}K_i(\Phi_{\beta i-1} - \Phi_{\beta i}))}{\partial H_t}$$

$$= 0 \tag{D.48}$$

4. $$\frac{\partial M_{conv}}{\partial H_t} = \frac{\partial(T_{\beta i}K_{i+1}(\Phi_{\beta i} - \Phi_{\beta i+1}) + T_{\beta i}K_i(\Phi_{\beta i} - \Phi_{\beta i-1}))}{\partial H_t}$$

$$= K_{i+1}(\Phi_{\beta i} - \Phi_{\beta i+1})\frac{\partial T_{\beta i}}{\partial H_t} + K_i(\Phi_{\beta i} - \Phi_{\beta i+1})\frac{\partial T_{\beta i}}{\partial H_t} \tag{D.49}$$

D.4.2 Derivatives for the Off-Diagonal Elements of the Jacobian Matrix

By taking the derivative of material balance equation of each component (i.e. *α1*) with respect to temperature of the neighborhoods of the specific gridblock, we have

$$\frac{\partial R_M}{\partial H_{t,i\pm1}} = -\frac{\partial M_{accum}}{\partial H_{t,i\pm1}} + \frac{\partial M_{conv}}{\partial H_{t,i\pm1}} + \frac{\partial M_{source}}{\partial H_{t,i\pm1}} \tag{D.50}$$

For the accumulation term, we have

$$\frac{\partial\left(\frac{V_{bi}\phi_i N_{\alpha 1 i}}{\Delta t}\right)}{\partial H_{t,i\pm1}} = 0 \tag{D.51}$$

For the source term, we have

$$\frac{\partial q_{\alpha 1 i}}{\partial H_{t,i\pm1}} = 0 \tag{D.52}$$

For the convection term, the derivatives in the case of the four scenarios (Section 3.3.8.1.3) pertinent to the cell to the left side of the diagonal in *x* direction

1. $$\frac{\partial M_{conv}}{\partial H_{t,i-1}} = \frac{\partial (T_{\beta i}\tilde{K}_i(\Phi_{\beta i} - \Phi_{\beta i+1}) - T_{\beta i-1}\tilde{K}_i(\Phi_{\beta i-1} - \Phi_{\beta i}))}{\partial H_{t,i-1}}$$

$$= -\tilde{K}_i(\Phi_{\beta i-1} - \Phi_{\beta i})\left(\frac{\partial T_{\beta i-1}}{\partial H_{t,i-1}}\right) \quad \text{(D.53)}$$

2. $$\frac{\partial M_{conv}}{\partial H_{t,i-1}} = 0 \quad \text{(D.54)}$$

3. $$\frac{\partial M_{conv}}{\partial H_{t,i-1}} = \frac{\partial (T_{\beta i}\tilde{K}_i(\Phi_{\beta i} - \Phi_{\beta i+1}) - T_{\beta i-1}\tilde{K}_i(\Phi_{\beta i-1} - \Phi_{\beta i}))}{\partial H_{t,i-1}}$$

$$= -\tilde{K}_i(\Phi_{\beta i-1} - \Phi_{\beta i})\left(\frac{\partial T_{\beta i-1}}{\partial H_{t,i-1}}\right) \quad \text{(D.55)}$$

4. $$\frac{\partial M_{conv}}{\partial H_{t,i-1}} = 0 \quad \text{(D.56)}$$

Similarly, for the cell to the right side of the diagonal in the *x* direction, we have

1. $$\frac{\partial M_{conv}}{\partial H_{t,i+1}} = 0 \quad \text{(D.57)}$$

2. $$\frac{\partial M_{conv}}{\partial H_{t,i+1}} = \frac{\partial (-T_{\beta i+1}\tilde{K}_{i+1}(\Phi_{\beta i+1} - \Phi_{\beta i}) + T_{wi}\tilde{K}_i(\Phi_{\beta i} - \Phi_{\beta i+1}))}{\partial H_{t,i+1}}$$

$$= -\frac{\tilde{K}_{i+1}(\Phi_{\beta i+1} - \Phi_{\beta i})}{\mu_{wi+1}}\left(\frac{\partial T_{\beta i+1}}{\partial H_{t,i+1}}\right) \quad \text{(D.58)}$$

3. $$\frac{\partial M_{conv}}{\partial H_{t,i+1}} = \frac{\partial (-T_{wi+1}\tilde{K}_{i+1}(\Phi_{i+1} - \Phi_i) + T_{wi}\tilde{K}_i(\Phi_i - \Phi_{i+1}))}{\partial H_{t,i+1}}$$

$$= -\tilde{K}_{i+1}(\Phi_{i+1} - \Phi_i)\left(\frac{\partial T_{wi+1}}{\partial H_{t,i+1}}\right) \quad \text{(D.59)}$$

4. $$\frac{\partial M_{conv}}{\partial H_{t,i+1}} = 0$$ (D.60)

Appendix E

Evaluation of Jacobian Elements for Energy Equations

The derivatives of the energy equation with respect to primary variables are described as follows; the equations are written for the *x* direction, the same equations can be written for other directions.

E.1 DERIVATIVES OF THE ENERGY EQUATION WITH RESPECT TO LNK_1 AND LNK_2

The equations have been written for LnK_1, by replacing the LnK_1 with LnK_2; we can have the same derivatives with respect to LnK_2.

E.1.1 Derivatives for the Diagonal Elements of the Jacobian Matrix

The Jacobian elements related to derivatives with respect to LnK_1 and LnK_2 are

$$\frac{\partial R_E}{\partial LnK_{1,\alpha i}} = -\frac{\partial E_{accum}}{\partial LnK_{1,\alpha i}} + \frac{\partial E_{conv}}{\partial LnK_{1,\alpha i}} + \frac{\partial E_{cond}}{\partial LnK_{1,\alpha i}} + \frac{\partial E_{source}}{\partial LnK_{1,\alpha i}} - \frac{\partial E_{loss}}{\partial LnK_{1,\alpha i}} \tag{E.1}$$

Accumulation Term

Let us consider the accumulation equation,

$$E_{Acc} = \frac{U^{n+1} - U^n}{\Delta t} \tag{E.2}$$

$$U = (1-\phi)\zeta_r U_r + \phi \zeta_f U_f \tag{E.3}$$

$$\frac{\partial E_{Acc}}{\partial LnK_{1,\alpha}} = \frac{1}{\Delta t}\,\phi\,(U_f \frac{\partial \zeta_f}{\partial LnK_{1,\alpha}} + \zeta_f \frac{\partial U_f}{\partial LnK_{1,\alpha}}) \tag{E.4}$$

The internal energy of the fluid and the rock are

$$U_f = H_f - \frac{P}{\zeta_f} \tag{E.5}$$

$$U_r = A_r(T - T_{ref}) + 0.5B_r\,(T^2 - T_{ref}{}^2) \tag{E.6}$$

$$\frac{\partial U_f}{\partial LnK_{1,\alpha i}} = \frac{\partial H_f}{\partial LnK_{1,\alpha i}} + \frac{P}{\zeta_f{}^2}\frac{\partial \zeta_f}{\partial LnK_{1,\alpha i}} \tag{E.7}$$

Source Term

The total injected heat rate is

$$\left(q_H\right)_z = \left(q_t H_t\right)_z \tag{E.8}$$

$$q_H\,|_z = \frac{\partial q_{\alpha i}}{\partial LnK_{1,\alpha i}} = C\frac{(H_t)_{inj}}{\left(V_t\right)_{inj}}\frac{\partial\left[\sum_{\beta=1}^{n_p}\lambda_{\beta i}\left(P_{wf} - P_{\beta i}\right)\right]}{\partial LnK_{1,\alpha i}} \tag{E.9}$$

$$q_H\,|_z = C\frac{(H_t)_{inj}}{\left(V_t\right)_{inj}}\sum_{\beta=1}^{n_p}\left[\left(\frac{\mu_{\beta i}\frac{\partial k_{r\beta i}}{\partial LnK_{1,\alpha i}} - k_{r\beta i}\frac{\partial \mu_{\beta i}}{\partial LnK_{1,\alpha i}}}{\mu_{\beta i^2}}\right)\left(P_{wf} - P_{\beta i}\right)\right]$$

$$= C_i\frac{(H_t)_{inj}}{\left(V_t\right)_{inj}}\sum_{\beta=1}^{n_p}\left(\frac{\mu_{\beta i}\frac{\partial k_{r\beta i}}{\partial S_{\beta i}}\frac{\partial S_{\beta i}}{\partial LnK_{1,\alpha i}} - k_{r\beta i}\frac{\partial \mu_{\beta i}}{\partial LnK_{1,\alpha i}}}{\mu_{\beta i}{}^2}\right)\left(P_{wf} - P_{\beta i}\right) \tag{E.10}$$

Convective Term

The convection term of the energy equation is given by

$$E_{conv} = V_b \nabla . \sum_{\beta=o,g,aq} (\zeta_\beta H_\beta \vec{v}_\beta) \tag{E.11}$$

where

$$\vec{v}_\beta = -\vec{\vec{K}} \lambda_{r\beta} (\nabla P_\beta - \gamma_\beta \nabla D) \tag{E.12}$$

$$TE_{\beta i} = \zeta_{\beta i} \lambda_{\beta i} H_{\beta i} \tag{E.13}$$

$$\frac{\partial TE_{\beta i}}{\partial LnK_{1,\alpha i}} = V_b \frac{\partial (\zeta_{\beta i} \lambda_{\beta i} H_{\beta i})}{\partial LnK_{1,\alpha i}} = V_b (\lambda_{\beta i} H_{\beta i} \frac{\partial \zeta_{\beta i}}{\partial LnK_{1,\alpha i}} +$$
$$\zeta_{\beta i} H_{\beta i} \frac{\partial \lambda_{\beta i}}{\partial LnK_{1,\alpha i}} + \zeta_{\beta i} \lambda_{\beta i} \frac{\partial H_{\beta i}}{\partial LnK_{1,\alpha i}}) \tag{E.14}$$

For the four scenarios (Section 4.6), we have

1. $$\frac{\partial E_{conv}}{\partial LnK_{1,\alpha}} = \frac{\partial (TE_{\beta i} \tilde{K}_{i+1} (\Phi_{\beta i} - \Phi_{\beta i+1}) - TE_{\beta i-1} \tilde{K}_i (\Phi_{\beta i-1} - \Phi_{\beta i}))}{\partial LnK_{1,\alpha}}$$
$$= \tilde{K}_i (\Phi_{\beta i} - \Phi_{\beta i+1}) \frac{\partial TE_{\beta i}}{\partial N_{\alpha 2i}} \tag{E.15}$$

2. $$\frac{\partial E_{conv}}{\partial LnK_{1,\alpha}} = \frac{\partial (-TE_{\beta i+1} \tilde{K}_{i+1} (\Phi_{\beta i+1} - \Phi_{\beta i}) + TE_{\beta i} \tilde{K}_i (\Phi_{\beta i} - \Phi_{\beta i-1}))}{\partial LnK_{1,\alpha}}$$
$$= \tilde{K}_i (\Phi_{\beta i} - \Phi_{\beta i+1}) \frac{\partial TE_{\beta i}}{\partial LnK_{1,\alpha}} \tag{E.16}$$

3. $$\frac{\partial E_{conv}}{\partial LnK_{1,\alpha}} = \frac{\partial (-TE_{\beta i+1} K_{i+1} (\Phi_{\beta i+1} - \Phi_{\beta i}) - TE_{\beta i-1} K_i (\Phi_{\beta i-1} - \Phi_{\beta i}))}{\partial LnK_{1,\alpha}}$$
$$= 0 \tag{E.17}$$

4. $$\frac{\partial E_{conv}}{\partial LnK_{1,\alpha}} = \frac{\partial(TE_{\beta i}\tilde{K}_{i+1}(\Phi_{\beta i} - \Phi_{\beta i+1}) + TE_{\beta i}\tilde{K}_{i}(\Phi_{\beta i} - \Phi_{\beta i-1}))}{\partial LnK_{1,\alpha}}$$

$$= \tilde{K}_{i+1}(\Phi_{\beta i} - \Phi_{\beta i+1})\frac{\partial TE_{\beta i}}{\partial LnK_{1,\alpha}} + \tilde{K}_{i}(\Phi_{\beta i} - \Phi_{\beta i+1})\frac{\partial TE_{\beta i}}{\partial LnK_{1,\alpha}} \quad \text{(E.18)}$$

Conduction Term

The thermal conductivity can be a constant or a variable using the model of Somerton *et al.,* (1974).

$$\lambda_{125} = 0.735 - 1.3C_f\phi_{ini} + 0.39\lambda_m\sqrt{S_{aq}} \quad \text{(E.19)}$$

$$\lambda_m = 4.45f_q + 1.65(1 - f_q) \quad \text{(E.20)}$$

$$\tilde{\lambda} = \lambda_{125} - 1.28\times10^{-3}(T - 125)(\lambda_{125} - 0.82) \quad \text{(E.21)}$$

$$\frac{\partial\lambda_{125i}}{\partial LnK_{1,\alpha i}} = 0.39\lambda_m\frac{1}{\sqrt{S_{aqi}}}\frac{\partial S_{aqi}}{\partial S_{\beta i}}\frac{\partial S_{\beta i}}{\partial LnK_{1,\alpha i}} \quad \text{(E.22)}$$

$$\frac{\partial\tilde{\lambda}}{\partial LnK_{1,\alpha i}} = \frac{\partial\lambda_{125i}}{\partial LnK_{1,\alpha i}}[1 - 1.28\times10^{-3}(T_i - 125)]$$

The following equations have been selected in *x* direction as examples (same scenarios apply for the other axes)

$$\tilde{\lambda}_{av}|_{i\to i+1} = \frac{(2\Delta y_i\,\Delta z_i\,\tilde{\lambda}_i\,\tilde{\lambda}_{i+1})}{(\Delta x_i\,\tilde{\lambda}_i + \Delta x_{i+1}\,\tilde{\lambda}_{i+1})} \quad \text{(E.23)}$$

$$\tilde{\lambda}_{av}|_{i-1\to i} = \frac{(2\Delta y_i\,\Delta z_i\,\tilde{\lambda}_{i-1}\,\tilde{\lambda}_i)}{(\Delta x_{i-1}\,\tilde{\lambda}_{i-1} + \Delta x_i\,\tilde{\lambda}_i)} \quad \text{(E.24)}$$

$$E_{cond,i+1/2} = \tilde{\lambda}_{av}|_{i\to i+1}(T_{i+1} - T_i) \quad if \quad T_{i+1} > T_i \quad \text{(E.25)}$$

$$E_{cond,i+1/2} = \tilde{\lambda}_{av}|_{i\to i+1}(T_i - T_{i+1}) \quad if \quad T_{i+1} < T_i \quad \text{(E.26)}$$

$$E_{cond,i-1/2} = \tilde{\lambda}_{av}\,|_{i-1\to i}\,(T_{i-1} - T_i) \quad if \quad T_{i-1} > T_i \tag{E.27}$$

$$E_{cond,i-1/2} = \tilde{\lambda}_{av}\,|_{i-1\to i}\,(T_i - T_{i-1}) \quad if \quad T_{i-1} < T_i \tag{E.28}$$

Obviously, there are four scenarios for the conduction term

1. $T_{i+1} < T_i \quad and \quad T_i < T_{i-1}$

$$E_{cond,i+1/2} - E_{cond,i-1/2} = \tilde{\lambda}_{av}\,|_{i\to i+1}\,(T_i - T_{i+1}) - \tilde{\lambda}_{av}\,|_{i-1\to i}\,(T_{i-1} - T_i) \tag{E.29}$$

2. $T_{i+1} > T_i \quad and \quad T_i > T_{i-1}$

$$E_{cond,i+1/2} - E_{cond,i-1/2} = -\tilde{\lambda}_{av}\,|_{i\to i+1}\,(T_{i+1} - T_i) + \tilde{\lambda}_{av}\,|_{i-1\to i}\,(T_i - T_{i-1}) \tag{E.30}$$

3. $T_{i+1} > T_i \quad and \quad T_i < T_{i-1}$

$$E_{cond,i+1/2} - E_{cond,i-1/2} = -\tilde{\lambda}_{av}\,|_{i\to i+1}\,(T_{i+1} - T_i) - \tilde{\lambda}_{av}\,|_{i-1\to i}\,(T_{i-1} - T_i) \tag{E.31}$$

4. $T_{i+1} < T_i \quad and \quad T_i > T_{i-1}$

$$E_{cond,i+1/2} - E_{cond,i-1/2} = \tilde{\lambda}_{av}\,|_{i\to i+1}\,(T_i - T_{i+1}) + \tilde{\lambda}_{av}\,|_{i-1\to i}\,(T_i - T_{i-1}) \tag{E.32}$$

$$\frac{\partial \tilde{\lambda}_{av}\,|_{i\to i+1}}{\partial LnK_{1,\alpha i}} = 2\frac{(\tilde{\lambda}_{i+1}\dfrac{\partial \tilde{\lambda}_i}{\partial LnK_{1,\alpha i}}(\,\Delta x_i\,\tilde{\lambda}_i + \Delta x_{i+1}\,\tilde{\lambda}_{i+1}) - \Delta x_i\,\tilde{\lambda}_i\,\tilde{\lambda}_{i+1}\dfrac{\partial \tilde{\lambda}_i}{\partial LnK_{1,\alpha i}})}{(\,\Delta x_i\,\tilde{\lambda}_i + \Delta x_{i+1}\,\tilde{\lambda}_{i+1})^2}$$

$$= 2\,\Delta y_i\,\Delta z_i\frac{(\Delta x_{i+1}\tilde{\lambda}_{i+1}^{\,2}\dfrac{\partial \tilde{\lambda}_i}{\partial LnK_{1,\alpha i}})}{(\,\Delta x_i\,\tilde{\lambda}_i + \Delta x_{i+1}\,\tilde{\lambda}_{i+1})^2} \tag{E.33}$$

$$\frac{\partial \tilde{\lambda}_{av}\,|_{i\to i+1}}{\partial LnK_{1,\alpha i+1}} = 2\,\Delta y_i\,\Delta z_i\frac{(\Delta x_i\tilde{\lambda}_i^{\,2}\dfrac{\partial \tilde{\lambda}_{i+1}}{\partial LnK_{1,\alpha i+1}})}{(\,\Delta x_i\,\tilde{\lambda}_i + \Delta x_{i+1}\,\tilde{\lambda}_{i+1})^2} \tag{E.34}$$

The derivatives of the four scenarios are as follows (derivatives are presented for the cases if H_t is selected as the primary variable and also if T is the primary variable)

1. $$\frac{\partial E_{cond}}{\partial LnK_{1,\alpha i}} = \frac{\partial\left(\tilde{\lambda}_{av}\mid_{i\to i+1}(T_i - T_{i+1}) - \tilde{\lambda}_{av}\mid_{i-1\to i}(T_{i-1} - T_i)\right)}{\partial LnK_{1,\alpha i}}$$

$$\frac{\partial E_{cond}}{\partial LnK_{1,\alpha i}} = (T_i - T_{i+1})\frac{\partial \tilde{\lambda}_{av}\mid_{i\to i+1}}{\partial LnK_{1,\alpha i}} + \tilde{\lambda}_{av}\mid_{i\to i+1}\frac{\partial T_i}{\partial LnK_{1,\alpha i}}$$

$$-(T_{i-1} - T_{i+1})\frac{\partial \tilde{\lambda}_{av}\mid_{i-1\to i}}{\partial LnK_{1,\alpha i}} + \tilde{\lambda}_{av}\mid_{i-1\to i}\frac{\partial T_i}{\partial LnK_{1,\alpha i}} \qquad \text{(E.35)}$$

when T is primary variable,

$$\frac{\partial E_{cond}}{\partial LnK_{1,\alpha i}} = (T_i - T_{i+1})\frac{\partial \tilde{\lambda}_{av}\mid_{i\to i+1}}{\partial LnK_{1,\alpha i}} - (T_{i-1} - T_{i+1})\frac{\partial \tilde{\lambda}_{av}\mid_{i-1\to i}}{\partial LnK_{1,\alpha i}} \qquad \text{(E.36)}$$

2. $$\frac{\partial E_{cond}}{\partial LnK_{1,\alpha i}} = \frac{\partial\left(-\tilde{\lambda}_{av}\mid_{i\to i+1}(T_{i+1} - T_i) + \tilde{\lambda}_{av}\mid_{i-1\to i}(T_i - T_{i-1})\right)}{\partial LnK_{1,\alpha i}}$$

$$\frac{\partial E_{cond}}{\partial LnK_{1,\alpha i}} = -\frac{\partial \tilde{\lambda}_{av}\mid_{i\to i+1}}{\partial LnK_{1,\alpha i}}(T_{i+1} - T_i) + \tilde{\lambda}_{av}\mid_{i\to i+1}\frac{\partial T_i}{\partial LnK_{1,\alpha i}}$$

$$+\frac{\partial \tilde{\lambda}_{av}\mid_{i-1\to i}}{\partial LnK_{1,\alpha i}}(T_i - T_{i-1}) + \tilde{\lambda}_{av}\mid_{i-1\to i}\frac{\partial T_i}{\partial LnK_{1,\alpha i}} \qquad \text{(E.37)}$$

when T is primary variable,

$$\frac{\partial E_{cond}}{\partial LnK_{1,\alpha i}} = -\frac{\partial \tilde{\lambda}_{av}\mid_{i\to i+1}}{\partial LnK_{1,\alpha i}}(T_{i+1} - T_i) + \frac{\partial \tilde{\lambda}_{av}\mid_{i-1\to i}}{\partial LnK_{1,\alpha i}}(T_i - T_{i-1}) \qquad \text{(E.38)}$$

3. $$\frac{\partial E_{cond}}{\partial LnK_{1,\alpha i}} = \frac{\partial\left(-\tilde{\lambda}_{av}\mid_{i\to i+1}(T_{i+1} - T_i) - \tilde{\lambda}_{av}\mid_{i-1\to i}(T_{i-1} - T_i)\right)}{\partial LnK_{1,\alpha i}}$$

$$\frac{\partial E_{cond}}{\partial LnK_{1,\alpha i}} = -(T_{i+1} - T_i)\frac{\partial \tilde{\lambda}_{av}\,|_{i\to i+1}}{\partial LnK_{1,\alpha i}} + \tilde{\lambda}_{av}\,|_{i\to i+1}\,\frac{\partial T_i}{\partial LnK_{1,\alpha i}}$$
$$-(T_{i-1} - T_i)\frac{\partial \tilde{\lambda}_{av}\,|_{i-1\to i}}{\partial LnK_{1,\alpha i}} + \tilde{\lambda}_{av}\,|_{i-1\to i}\,\frac{\partial T_i}{\partial LnK_{1,\alpha i}} \qquad \text{(E.39)}$$

when T is primary variable,

$$\frac{\partial E_{cond}}{\partial LnK_{1,\alpha i}} = -(T_{i+1} - T_i)\frac{\partial \tilde{\lambda}_{av}\,|_{i\to i+1}}{\partial LnK_{1,\alpha i}} - (T_{i-1} - T_i)\frac{\partial \tilde{\lambda}_{av}\,|_{i-1\to i}}{\partial LnK_{1,\alpha i}} \qquad \text{(E.40)}$$

4.
$$\frac{\partial E_{cond}}{\partial LnK_{1,\alpha i}} = \frac{\partial\left(\tilde{\lambda}_{av}\,|_{i\to i+1}\,(T_i - T_{i+1}) + \tilde{\lambda}_{av}\,|_{i-1\to i}\,(T_i - T_{i-1})\right)}{\partial LnK_{1,\alpha i}}$$
$$\frac{\partial E_{cond}}{\partial LnK_{1,\alpha i}} = (T_i - T_{i+1})\frac{\partial \tilde{\lambda}_{av}\,|_{i\to i+1}}{\partial LnK_{1,\alpha i}} + \tilde{\lambda}_{av}\,|_{i\to i+1}\,\frac{\partial T_i}{\partial LnK_{1,\alpha i}}$$
$$+(T_i - T_{i-1})\frac{\partial \tilde{\lambda}_{av}\,|_{i-1\to i}}{\partial LnK_{1,\alpha i}} + \tilde{\lambda}_{av}\,|_{i-1\to i}\,\frac{\partial T_i}{\partial LnK_{1,\alpha i}} \qquad \text{(E.41)}$$

when T is primary variable,

$$\frac{\partial E_{cond}}{\partial LnK_{1,\alpha i}} = (T_i - T_{i+1})\frac{\partial \tilde{\lambda}_{av}\,|_{i\to i+1}}{\partial LnK_{1,\alpha i}} + (T_i - T_{i-1})\frac{\partial \tilde{\lambda}_{av}\,|_{i-1\to i}}{\partial LnK_{1,\alpha i}} \qquad \text{(E.42)}$$

Heat Loss Term

The heat-loss term as described in Section 4.5 can be calculated by the following equations.

$$d = \frac{1}{2}\sqrt{\eta t} \qquad \text{(E.43)}$$

$$\eta = \frac{\lambda_r}{c_r \xi_r} \qquad \text{(E.44)}$$

$$T\,|_{under\ or\ underburden} = \theta$$

$$\tau^n = \left[\left(\theta - \theta^0\right)d + b_1 d^2 + 2b_2 d^3\right]^n \tag{E.45}$$

$$Q_{loss} = \lambda_r A\left[\frac{(\theta^{n+1} - \theta^0)}{d^{n+1}} - b_1^{n+1}\right] \tag{E.46}$$

The following equations describe the derivatives of the heat-loss parameters.

$$\frac{\partial d}{\partial LnK_{1,\alpha}}\,|_{under\ or\ underburden} = \frac{1}{2}\,t\,(\eta\,t)^{-\frac{1}{2}}\frac{\partial \eta}{\partial LnK_{1,\alpha}} \tag{E.47}$$

when T is used as the primary variable,

$$\frac{\partial \eta}{\partial LnK_{1,\alpha}} = \frac{C_r \zeta_r \dfrac{\partial \lambda_r}{\partial LnK_{1,\alpha}}}{(C_r \zeta_r)^2} \tag{E.48}$$

If H_t is used as the primary variable,

$$\frac{\partial \eta}{\partial LnK_{1,\alpha}} = \frac{C_r \zeta_r \dfrac{\partial \lambda_r}{\partial LnK_{1,\alpha}} - \lambda_r \zeta_r \dfrac{\partial C_r}{\partial LnK_{1,\alpha}}}{(C_r \zeta_r)^2} \tag{E.49}$$

$$C_r = A_r + B_r\theta\ ;\frac{\partial C_r}{\partial LnK_{1,\alpha}} = B_r\frac{\partial \theta}{\partial LnK_{1,\alpha}} \tag{E.50}$$

$$b_1^{n+1} = \frac{\dfrac{\eta\Delta t(\theta^{n+1}-\theta^0)}{d^{n+1}} + \tau^n - \dfrac{(d^{n+1})^3(\theta^{n+1}-\theta^n)}{\eta\Delta t}}{3(d^{n+1})^2 + \eta\Delta t} \tag{E.51}$$

$$Term1 = \frac{\partial\left(\dfrac{\eta\Delta t(\theta^{n+1}-\theta^0)}{d^{n+1}}\right)}{\partial LnK_{1,\alpha}} =$$

$$\frac{\left(\Delta t(\theta^{n+1}-\theta^0)\dfrac{\partial\eta}{\partial LnK_{1,\alpha}} + \eta\Delta t\dfrac{\partial\theta^{n+1}}{\partial LnK_{1,\alpha}}\right)d^{n+1} - \left(\eta\Delta t(\theta^{n+1}-\theta^0)\dfrac{\partial d^{n+1}}{\partial LnK_{1,\alpha}}\right)}{(d^{n+1})^2} \tag{E.52}$$

$$Term2 = \frac{\partial\tau^n}{\partial LnK_{1,\alpha}} = 0 \tag{E.53}$$

$$Term3 = \frac{\partial\left(\dfrac{(d^{n+1})^3(\theta^{n+1}-\theta^n)}{\eta\Delta t}\right)}{\partial LnK_{1,\alpha}} =$$

$$\frac{\left(3(d^{n+1})^2(\theta^{n+1}-\theta^0)\dfrac{\partial d^{n+1}}{\partial LnK_{1,\alpha}} + (d^{n+1})^3\dfrac{\partial\theta^{n+1}}{\partial LnK_{1,\alpha}}\right)\eta\Delta t - \Delta t(d^{n+1})^3(\theta^{n+1}-\theta^0)\dfrac{\partial\eta}{\partial LnK_{1,\alpha}}}{(\eta\Delta t)^2} \tag{E.54}$$

$$Term4 = \frac{\partial\left(3(d^{n+1})^2 + \eta\Delta t\right)}{\partial LnK_{1,\alpha}} = 6d^{n+1}\frac{\partial d^{n+1}}{\partial LnK_{1,\alpha}} + \Delta t\frac{\partial\eta}{\partial LnK_{1,\alpha}} \tag{E.55}$$

$$\frac{\partial b_1^{n+1}}{\partial LnK_{1,\alpha}} = \frac{(Term1 - Term3)(3(d^{n+1})^2 + \eta\Delta t) - (\dfrac{\eta\Delta t(\theta^{n+1}-\theta^0)}{d^{n+1}}}{(3(d^{n+1})^2 + \eta\Delta t)^2}$$

$$\frac{+\tau^n - \frac{(d^{n+1})^3(\theta^{n+1}-\theta^n)}{\eta\Delta t})Term4}{} \tag{E.56}$$

For T as the primary variable

$$Term1 = \frac{\partial\left(\frac{\eta\Delta t(\theta^{n+1}-\theta^0)}{d^{n+1}}\right)}{\partial LnK_{1,\alpha}} =$$

$$\frac{\left(\Delta t(\theta^{n+1}-\theta^0)\frac{\partial\eta}{\partial LnK_{1,\alpha}}\right)d^{n+1} - \left(\eta\Delta t(\theta^{n+1}-\theta^0)\frac{\partial d^{n+1}}{\partial LnK_{1,\alpha}}\right)}{(d^{n+1})^2} \tag{E.57}$$

$$Term2 = \frac{\partial\tau^n}{\partial LnK_{1,\alpha}} = 0 \tag{E.58}$$

$$Term3 = \frac{\partial\left(\frac{(d^{n+1})^3(\theta^{n+1}-\theta^n)}{\eta\Delta t}\right)}{\partial LnK_{1,\alpha}} =$$

$$\frac{\left(3(d^{n+1})^2(\theta^{n+1}-\theta^0)\frac{\partial d^{n+1}}{\partial LnK_{1,\alpha}}\right)\eta\Delta t - \Delta t(d^{n+1})^3(\theta^{n+1}-\theta^0)\frac{\partial\eta}{\partial LnK_{1,\alpha}}}{(\eta\Delta t)^2} \tag{E.59}$$

$$Term4 = \frac{\partial\left(3(d^{n+1})^2+\eta\Delta t\right)}{\partial LnK_{1,\alpha}} = 6d^{n+1}\frac{\partial d^{n+1}}{\partial LnK_{1,\alpha}} + \Delta t\frac{\partial\eta}{\partial LnK_{1,\alpha}} \tag{E.60}$$

$$\frac{\partial b_1^{n+1}}{\partial LnK_{1,\alpha}} = \frac{(Term1-Term3)(3(d^{n+1})^2+\eta\Delta t) - (\frac{\eta\Delta t(\theta^{n+1}-\theta^0)}{d^{n+1}}}{(3(d^{n+1})^2+\eta\Delta t)^2}$$

$$+\tau^n-\frac{(d^{n+1})^3(\theta^{n+1}-\theta^n)}{\eta\Delta t})Term4 \tag{E.61}$$

$$b_2^{n+1}=\frac{2b_1^{n+1}(d^{n+1})-(\theta^{n+1}-\theta^0)+\frac{(d^{n+1})^2(\theta^{n+1}-\theta^n)}{\eta\Delta t}}{2(d^{n+1})^2} \tag{E.62}$$

If H_t is the primary variable

$$Term5=\frac{\partial\left(2b_1^{n+1}(d^{n+1})\right)}{\partial LnK_{1,\alpha}}=2(d^{n+1}\frac{\partial b_1^{n+1}}{\partial LnK_{1,\alpha}}+b_1^{n+1}\frac{\partial d^{n+1}}{\partial LnK_{1,\alpha}}) \tag{E.63}$$

$$Term6=\frac{\partial\left(\frac{(d^{n+1})^2(\theta^{n+1}-\theta^n)}{\eta\Delta t}\right)}{\partial LnK_{1,\alpha}}=$$

$$\frac{\left(2(\theta^{n+1}-\theta^0)\frac{\partial d^{n+1}}{\partial LnK_{1,\alpha}}+(d^{n+1})^2\frac{\partial\theta}{\partial LnK_{1,\alpha}}\right)\eta\Delta t-(d^{n+1})^2(\theta^{n+1}-\theta^0)\Delta t\frac{\partial\eta}{\partial LnK_{1,\alpha}}}{(\eta\Delta t)^2} \tag{E.64}$$

$$\frac{\partial b_2^{n+1}}{\partial LnK_{1,\alpha}}=\frac{(Term5-\frac{\partial\theta}{\partial LnK_{1,\alpha}}+Term6)(d^{n+1})^2}{2(d^{n+1})^4}$$

$$\frac{-4d^{n+1}\left(2b_1^{n+1}(d^{n+1})-(\theta^{n+1}-\theta^0)+\frac{(d^{n+1})^2(\theta^{n+1}-\theta^n)}{\eta\Delta t}\right)\frac{\partial d^{n+1}}{\partial LnK_{1,\alpha}}}{} \tag{E.65}$$

For T as the primary variable

$$Term5=\frac{\partial\left(2b_1^{n+1}(d^{n+1})\right)}{\partial LnK_{1,\alpha}}=2(d^{n+1}\frac{\partial b_1^{n+1}}{\partial LnK_{1,\alpha}}+b_1^{n+1}\frac{\partial d^{n+1}}{\partial LnK_{1,\alpha}}) \tag{E.66}$$

$$Term6 = \frac{\partial\left(\frac{(d^{n+1})^2(\theta^{n+1}-\theta^n)}{\eta\Delta t}\right)}{\partial LnK_{1,\alpha}} =$$

$$\frac{\left(2(\theta^{n+1}-\theta^0)\frac{\partial d^{n+1}}{\partial LnK_{1,\alpha}}\right)\eta\Delta t-(d^{n+1})^2(\theta^{n+1}-\theta^0)\Delta t\frac{\partial\eta}{\partial LnK_{1,\alpha}}}{(\eta\Delta t)^2} \tag{E.67}$$

$$\frac{\partial b_2^{n+1}}{\partial LnK_{1,\alpha}} = \frac{2(Term5+Term6)(d^{n+1})^2}{4(d^{n+1})^4} -$$

$$\frac{4d^{n+1}\left(2b_1^{n+1}(d^{n+1})-(\theta^{n+1}-\theta^0)+\frac{(d^{n+1})^2(\theta^{n+1}-\theta^n)}{\eta\Delta t}\right)\frac{\partial d^{n+1}}{\partial LnK_{1,\alpha}}}{4(d^{n+1})^4} \tag{E.68}$$

Therefore, the final equation and its derivative are

$$Q_{loss} = \lambda_r A\left[\frac{(\theta^{n+1}-\theta^0)}{d^{n+1}} - b_1^{n+1}\right] \tag{E.69}$$

$$\frac{\partial Q_{loss}}{\partial LnK_{1,\alpha}} = A\left[\frac{(\theta^{n+1}-\theta^0)}{d^{n+1}} - b_1^{n+1}\right]\frac{\partial\lambda_r}{\partial LnK_{1,\alpha}}$$

$$+\lambda_r A\left[\frac{d^{n+1}\frac{\partial\theta}{\partial LnK_{1,\alpha}}-(\theta^{n+1}-\theta^0)\frac{\partial d^{n+1}}{\partial LnK_{1,\alpha}}}{(d^{n+1})^2}-\frac{\partial b_1^{n+1}}{\partial LnK_{1,\alpha}}\right] \tag{E.70}$$

For T as the primary variable, we have

$$\frac{\partial Q_{loss}}{\partial LnK_{1,\alpha}} = A\left[\frac{(\theta^{n+1}-\theta^0)}{d^{n+1}} - b_1^{n+1}\right]\frac{\partial\lambda_r}{\partial LnK_{1,\alpha}}$$

$$+\lambda_r A\left[\frac{-(\theta^{n+1}-\theta^0)\dfrac{\partial d^{n+1}}{\partial LnK_{1,\alpha}}}{(d^{n+1})^2}-\frac{\partial b_1^{n+1}}{\partial LnK_{1,\alpha}}\right] \tag{E.71}$$

E.1.2 Derivatives of Energy Equation for the Off-Diagonal Elements of the Jacobian Matrix

The Jacobian elements for off-diagonal terms (*i* is any arbitrary direction; it can be *j* for the *y* direction, or *k* for *z* direction) related to derivatives with respect to LnK_1 and LnK_2 are

$$\frac{\partial R_E}{\partial LnK_{1,\alpha i\pm 1}}=-\frac{\partial E_{accum}}{\partial LnK_{1,\alpha i\pm 1}}+\frac{\partial E_{conv}}{\partial LnK_{1,\alpha i\pm 1}}+\frac{\partial E_{source}}{\partial LnK_{1,\alpha i\pm 1}}-\frac{\partial E_{loss}}{\partial LnK_{1,\alpha i\pm 1}} \tag{E.72}$$

Derivatives for the Off-Diagonal Elements of *i-1*

The derivatives of each term are described as follows:

Accumulation Term

This term of the equation is zero;

$$\frac{\partial U_f}{\partial LnK_{1,\alpha i-1}}=0 \quad \text{and} \quad \frac{\partial U_f}{\partial LnK_{2,\alpha i-1}}=0$$

Source Term

The source term is not a function of either the left-hand or the right-hand side of the specified gridblock; hence, this term is zero.

$$\frac{\partial q_H}{\partial LnK_{1,\alpha i-1}}=0 \quad \text{and} \quad \frac{\partial q_H}{\partial LnK_{2,\alpha i-1}}=0$$

Convective Term

1. $$\frac{\partial E_{conv}}{\partial LnK_{1,\alpha i-1}} = \frac{\partial(TE_{\beta i}\tilde{K}_i(\Phi_{\beta i}-\Phi_{\beta i+1}) - TE_{\beta i-1}\tilde{K}_i(\Phi_{\beta i-1}-\Phi_{\beta i}))}{\partial LnK_{1,\alpha i-1}}$$
$$= -\tilde{K}_i(\Phi_{\beta i-1}-\Phi_{\beta i})\frac{\partial TE_{\beta i-1}}{\partial LnK_{1,\alpha i-1}} \quad \text{(E.73)}$$

2. $$\frac{\partial E_{conv}}{\partial LnK_{1,\alpha i-1}} = \frac{\partial(-TE_{\beta i+1}\tilde{K}_{i+1}(\Phi_{\beta i+1}-\Phi_{\beta i}) + TE_{\beta i}\tilde{K}_i(\Phi_{\beta i}-\Phi_{\beta i-1}))}{\partial LnK_{1,\alpha i-1}} = 0 \quad \text{(E.74)}$$

3. $$\frac{\partial E_{conv}}{\partial LnK_{1,\alpha i-1}} = \frac{\partial(-TE_{\beta i+1}K_{i+1}(\Phi_{\beta i+1}-\Phi_{\beta i}) - TE_{\beta i-1}K_i(\Phi_{\beta i-1}-\Phi_{\beta i}))}{\partial LnK_{1,\alpha i-1}}$$
$$= -K_i(\Phi_{\beta i-1}-\Phi_{\beta i})\frac{\partial TE_{\beta i-1}}{\partial LnK_{1,\alpha i-1}} \quad \text{(E.75)}$$

4. $$\frac{\partial E_{conv}}{\partial LnK_{1,\alpha i-1}} = \frac{\partial(TE_{\beta i}K_{i+1}(\Phi_{\beta i}-\Phi_{\beta i+1}) + TE_{\beta i}K_i(\Phi_{\beta i}-\Phi_{\beta i-1}))}{\partial LnK_{1,\alpha i-1}} = 0 \quad \text{(E.76)}$$

Conduction Term

The derivatives of the four scenarios, described in Section E.1.1, are as follows (derivatives refer to the cases of H_t and T as primary variables):

1. $$\frac{\partial E_{cond}}{\partial LnK_{1,\alpha i-1}} = \frac{\partial\left(\tilde{\lambda}_{av}\,|_{i\to i+1}\,(T_i - T_{i+1}) - \tilde{\lambda}_{av}\,|_{i-1\to i}\,(T_{i-1}-T_i)\right)}{\partial LnK_{1,\alpha i-1}}$$
$$= -(T_{i-1}-T_i)\frac{\partial \tilde{\lambda}_{av}\,|_{i-1\to i}}{\partial LnK_{1,\alpha i-1}} - \tilde{\lambda}_{av}\,|_{i-1\to i}\,\frac{\partial T_{i-1}}{\partial LnK_{1,\alpha i-1}} \quad \text{(E.77)}$$

For T as the primary variable,

$$\frac{\partial E_{cond}}{\partial LnK_{1,\alpha i-1}} = -(T_{i-1}-T_i)\frac{\partial \tilde{\lambda}_{av}\,|_{i-1\to i}}{\partial LnK_{1,\alpha i-1}} \quad \text{(E.78)}$$

2. $$\frac{\partial E_{cond}}{\partial LnK_{1,\alpha i-1}} = \frac{\partial\left(-\tilde{\lambda}_{av}\,|_{i\to i+1}\,(T_{i+1}-T_i)+\tilde{\lambda}_{av}\,|_{i-1\to i}\,(T_i-T_{i-1})\right)}{\partial LnK_{1,\alpha i-1}}$$

$$= (T_i - T_{i-1})\frac{\partial \tilde{\lambda}_{av}\,|_{i-1\to i}}{\partial LnK_{1,\alpha i-1}} - \tilde{\lambda}_{av}\,|_{i-1\to i}\,\frac{\partial T_{i-1}}{\partial LnK_{1,\alpha i-1}} \tag{E.79}$$

For *T* as the primary variable,

$$\frac{\partial E_{cond}}{\partial LnK_{1,\alpha i-1}} = (T_i - T_{i-1})\frac{\partial \tilde{\lambda}_{av}\,|_{i-1\to i}}{\partial LnK_{1,\alpha i-1}} \tag{E.80}$$

3. $$\frac{\partial E_{cond}}{\partial LnK_{1,\alpha i-1}} = \frac{\partial\left(-\tilde{\lambda}_{av}\,|_{i\to i+1}\,(T_{i+1}-T_i)-\tilde{\lambda}_{av}\,|_{i-1\to i}\,(T_{i-1}-T_i)\right)}{\partial LnK_{1,\alpha i-1}}$$

$$= -(T_{i-1} - T_i)\frac{\partial \tilde{\lambda}_{av}\,|_{i-1\to i}}{\partial LnK_{1,\alpha i-1}} - \tilde{\lambda}_{av}\,|_{i-1\to i}\,\frac{\partial T_{i-1}}{\partial LnK_{1,\alpha i-1}} \tag{E.81}$$

For *T* as the primary variable,

$$\frac{\partial E_{cond}}{\partial LnK_{1,\alpha i-1}} = -(T_{i-1} - T_i)\frac{\partial \tilde{\lambda}_{av}\,|_{i-1\to i}}{\partial LnK_{1,\alpha i-1}} \tag{E.82}$$

4. $$\frac{\partial E_{cond}}{\partial LnK_{1,\alpha i-1}} = \frac{\partial\left(\tilde{\lambda}_{av}\,|_{i\to i+1}\,(T_i-T_{i+1})+\tilde{\lambda}_{av}\,|_{i-1\to i}\,(T_i-T_{i-1})\right)}{\partial LnK_{1,\alpha i-1}}$$

$$= (T_i - T_{i-1})\frac{\partial \tilde{\lambda}_{av}\,|_{i-1\to i}}{\partial LnK_{1,\alpha i-1}} - \tilde{\lambda}_{av}\,|_{i-1\to i}\,\frac{\partial T_{i-1}}{\partial LnK_{1,\alpha i-1}} \tag{E.83}$$

For T as the primary variable,

$$\frac{\partial E_{cond}}{\partial LnK_{1,\alpha i-1}} = (T_i - T_{i-1})\frac{\partial \tilde{\lambda}_{av}\,|_{i-1\to i}}{\partial LnK_{1,\alpha i-1}} \tag{E.84}$$

Heat-Loss Term

The heat-loss derivatives for off-diagonal terms are zero.

$$\frac{\partial Q_{loss}}{\partial LnK_{1,\alpha i-1}} = 0$$

Derivatives for the Off-Diagonal Elements of *i+1*

The derivatives of each term are described as follows:

Accumulation Term

The accumulation term is not a function of neighborhood gridblocks; hence,

$$\frac{\partial U_f}{\partial LnK_{1,\alpha i+1}} = 0 \quad \text{and} \quad \frac{\partial U_f}{\partial LnK_{2,\alpha i+1}} = 0$$

Source Term

The source term is also zero for off-diagonal terms.

$$\frac{\partial q_H}{\partial LnK_{1,\alpha i+1}} = 0 \quad \text{and} \quad \frac{\partial q_H}{\partial LnK_{2,\alpha i+1}} = 0$$

Convective Term

1. $$\frac{\partial E_{conv}}{\partial LnK_{1,\alpha i+1}} = \frac{\partial (TE_{\beta i}\tilde{K}_i(\Phi_{\beta i} - \Phi_{\beta i+1}) - TE_{\beta i-1}\tilde{K}_i(\Phi_{\beta i-1} - \Phi_{\beta i}))}{\partial LnK_{1,\alpha i+1}}$$
$$= 0 \qquad \text{(E.85)}$$

2. $$\frac{\partial E_{conv}}{\partial LnK_{1,\alpha i+1}} = \frac{\partial (-TE_{\beta i+1}\tilde{K}_{i+1}(\Phi_{\beta i+1} - \Phi_{\beta i}) + TE_{\beta i}\tilde{K}_i(\Phi_{\beta i} - \Phi_{\beta i-1}))}{\partial LnK_{1,\alpha i+1}}$$
$$= -\tilde{K}_{i+1}(\Phi_{\beta i+1} - \Phi_{\beta i})\frac{\partial TE_{\beta i+1}}{\partial LnK_{1,\alpha i+1}} \qquad \text{(E.86)}$$

3. $$\frac{\partial E_{conv}}{\partial LnK_{1,\alpha i+1}} = \frac{\partial(-TE_{\beta i+1}K_{i+1}(\Phi_{\beta i+1}-\Phi_{\beta i}) - TE_{\beta i-1}K_i(\Phi_{\beta i-1}-\Phi_{\beta i}))}{\partial LnK_{1,\alpha i+1}}$$
$$= -K_{i+1}(\Phi_{\beta i+1}-\Phi_{\beta i})\frac{\partial TE_{\beta i+1}}{\partial LnK_{1,\alpha i+1}} \quad \text{(E.87)}$$

4. $$\frac{\partial E_{conv}}{\partial LnK_{1,\alpha i+1}} = \frac{\partial(TE_{\beta i}K_{i+1}(\Phi_{\beta i}-\Phi_{\beta i+1}) + TE_{\beta i}K_i(\Phi_{\beta i}-\Phi_{\beta i-1}))}{\partial LnK_{1,\alpha i+1}}$$
$$= 0 \quad \text{(E.88)}$$

Conduction Term

The derivatives in the case of four scenarios, described in Section E.1.1, are as follows (derivatives are with respect to H_t and T):

1. $$\frac{\partial E_{cond}}{\partial LnK_{1,\alpha i+1}} = \frac{\partial\left(\tilde{\lambda}_{av}|_{i\to i+1}(T_i - T_{i+1}) - \tilde{\lambda}_{av}|_{i-1\to i}(T_{i-1}-T_i)\right)}{\partial LnK_{1,\alpha i+1}}$$
$$= (T_i - T_{i+1})\frac{\partial \tilde{\lambda}_{av}|_{i\to i+1}}{\partial LnK_{1,\alpha i+1}} - \tilde{\lambda}_{av}|_{i\to i+1}\frac{\partial T_{i+1}}{\partial LnK_{1,\alpha i+1}} \quad \text{(E.89)}$$

when T is the primary variable,

$$\frac{\partial E_{cond}}{\partial LnK_{1,\alpha i+1}} = (T_i - T_{i+1})\frac{\partial \tilde{\lambda}_{av}|_{i\to i+1}}{\partial LnK_{1,\alpha i+1}} \quad \text{(E.90)}$$

2. $$\frac{\partial E_{cond}}{\partial LnK_{1,\alpha i+1}} = \frac{\partial\left(-\tilde{\lambda}_{av}|_{i\to i+1}(T_{i+1} - T_i) + \tilde{\lambda}_{av}|_{i-1\to i}(T_i - T_{i-1})\right)}{\partial LnK_{1,\alpha i+1}}$$
$$= -\frac{\partial \tilde{\lambda}_{av}|_{i\to i+1}}{\partial LnK_{1,\alpha i+!}}(T_{i+1}-T_i) - \tilde{\lambda}_{av}|_{i\to i+1}\frac{\partial T_{i+1}}{\partial LnK_{1,\alpha i+1}} \quad \text{(E.91)}$$

when T is the primary variable,

$$\frac{\partial E_{cond}}{\partial LnK_{1,\alpha i+1}} = -\frac{\partial \tilde{\lambda}_{av}\,|_{i\to i+1}}{\partial LnK_{1,\alpha i+1}}(T_{i+1}-T_i) \tag{E.92}$$

3. $$\frac{\partial E_{cond}}{\partial LnK_{1,\alpha i+1}} = \frac{\partial\left(-\tilde{\lambda}_{av}\,|_{i\to i+1}\,(T_{i+1}-T_i) - \tilde{\lambda}_{av}\,|_{i-1\to i}\,(T_{i-1}-T_i)\right)}{\partial LnK_{1,\alpha i+1}}$$

$$= -(T_{i+1}-T_i)\frac{\partial \tilde{\lambda}_{av}\,|_{i\to i+1}}{\partial LnK_{1,\alpha i+1}} - \tilde{\lambda}_{av}\,|_{i\to i+1}\,\frac{\partial T_{i+1}}{\partial LnK_{1,\alpha i+1}} \tag{E.93}$$

when T is the primary variable,

$$\frac{\partial E_{cond}}{\partial LnK_{1,\alpha i+1}} = -(T_{i+1}-T_i)\frac{\partial \tilde{\lambda}_{av}\,|_{i\to i+1}}{\partial LnK_{1,\alpha i+1}} \tag{E.94}$$

4. $$\frac{\partial E_{cond}}{\partial LnK_{1,\alpha i+1}} = \frac{\partial\left(\tilde{\lambda}_{av}\,|_{i\to i+1}\,(T_i-T_{i+1}) + \tilde{\lambda}_{av}\,|_{i-1\to i}\,(T_i-T_{i-1})\right)}{\partial LnK_{1,\alpha i+1}}$$

$$= (T_i-T_{i+1})\frac{\partial \tilde{\lambda}_{av}\,|_{i\to i+1}}{\partial LnK_{1,\alpha i+1}} - \tilde{\lambda}_{av}\,|_{i\to i+1}\,\frac{\partial T_{i+1}}{\partial LnK_{1,\alpha i+1}} \tag{E.95}$$

When T is the primary variable,

$$\frac{\partial E_{cond}}{\partial LnK_{1,\alpha i+1}} = (T_i-T_{i+1})\frac{\partial \tilde{\lambda}_{av}\,|_{i\to i+1}}{\partial LnK_{1,\alpha i+1}} \tag{E.96}$$

Heat-Loss Term

The heat-loss term for off-diagonal elements is zero.

$$\frac{\partial Q_{loss}}{\partial LnK_{1,\alpha i+1}} = 0 \tag{E.97}$$

E.2 DERIVATIVES OF THE ENERGY EQUATION WITH RESPECT TO MOLE NUMBER OF COMPONENT

The derivative equations for on-diagonal and off-diagonal elements with respect to *Ni* are the same for LnK_i by replacing of LnK_i by N_i.

E.3 DERIVATIVES OF THE ENERGY EQUATION WITH RESPECT TO PRESSURE

The derivatives of the conservation of the energy equation for the diagonal and off-diagonal terms are described as follows:

E.3.1 Derivatives for the Diagonal Elements of the Jacobian Matrix

The formula of the derivatives of the energy equation with respect to pressure is

$$\frac{\partial R_E}{\partial P_i} = -\frac{\partial E_{accum}}{\partial P_i} + \frac{\partial E_{conv}}{\partial P_i} + \frac{\partial E_{source}}{\partial P_i} - \frac{\partial E_{loss}}{\partial P_i} \tag{E.98}$$

Each term of the equation is presented in a separate section.

Accumulation Term

By taking the derivative of the accumulation term of the energy equation

$$E_{Acc} = \frac{U^{n+1} - U^n}{\Delta t} \tag{E.99}$$

$$U = (1-\phi)\zeta_r U_r + \phi \zeta_f U_f \tag{E.100}$$

$$\frac{\partial E_{Acc}}{\partial P}=\frac{1}{\Delta t}\,\phi\,(U_f\frac{\partial \zeta_f}{\partial P}+\ \zeta_f\frac{\partial U_f}{\partial P}) \tag{E.101}$$

The following is the internal energy of the fluid and rock.

$$U_f=H_f-\frac{P}{\zeta_f} \tag{E.102}$$

$$U_r=\ A_r(T-T_{ini})+0.5B_r\,(T^2-T_{ini}{}^2) \tag{E.103}$$

The first term of the derivative of the energy equation with respect to pressure is

$$\frac{\partial E_{accum}}{\partial P_i}=\frac{\partial H_f}{\partial P_i}+\frac{P}{\zeta_f{}^2}\frac{\partial \zeta_f}{\partial P_i} \tag{E.104}$$

Source Term

The heat rate derivative term with respect to pressure is

$$\frac{\partial q_H}{\partial P_i}=C\frac{(H_t)_{inj}}{(V_t)_{inj}}\frac{\partial\left[\sum_{\beta=1}^{n_p}\lambda_{\beta i}\left(P_{wf}-P_{\beta i}\right)\right]}{\partial P_i} \tag{E.105}$$

$$\frac{\partial q_H}{\partial P_i}=C\frac{(H_t)_{inj}}{(V_t)_{inj}}\sum_{\beta=1}^{n_p}\left[\left(\frac{\mu_{\beta i}\dfrac{\partial k_{r\beta i}}{\partial P_i}-k_{r\beta i}\dfrac{\partial \mu_{\beta i}}{\partial P_i}}{\mu_{\beta i^2}}\right)\left(P_{wf}-P_{\beta i}\right)-\lambda_{\beta i}\right]$$

$$=C_i\frac{(H_t)_{inj}}{(V_t)_{inj}}\sum_{\beta=1}^{n_p}\left[\left(\frac{\mu_{\beta i}\dfrac{\partial k_{r\beta i}}{\partial S_{\beta i}}\dfrac{\partial S_{\beta i}}{\partial P_i}-k_{r\beta i}\dfrac{\partial \mu_{\beta i}}{\partial P_i}}{\mu_{\beta i}{}^2}\right)\left(P_{wf}-P_{\beta i}\right)-\lambda_{\beta i}\right] \tag{E.106}$$

Convective Term

$$E_{conv} = V_b \nabla . \sum_{\beta=o,g,aq} (\zeta_\beta H_\beta \vec{v}_\beta) \tag{E.107}$$

where

$$\bar{v}_\beta = -\vec{\vec{K}} \lambda_{r\beta} (K \nabla P_\beta - \gamma_\beta \nabla D) \tag{E.108}$$

$$TE_{\beta i} = \zeta_{\beta i} \lambda_{\beta i} H_{\beta i} \tag{E.109}$$

$$\frac{\partial TE_{\beta i}}{\partial P_i} = V_b \frac{\partial (\zeta_{\beta i} \lambda_{\beta i} H_{\beta i})}{\partial P_i} =$$

$$V_b (\lambda_{\beta i} H_{\beta i} \frac{\partial \zeta_{\beta i}}{\partial P_i} + \zeta_{\beta i} H_{\beta i} \frac{\partial \lambda_{\beta i}}{\partial P_i} + \zeta_{\beta i} \lambda_{\beta i} \frac{\partial H_{\beta i}}{\partial P_i}) \tag{E.110}$$

1. $$\frac{\partial E_{conv}}{\partial P_i} = \frac{\partial (TE_{\beta i} \tilde{K}_i (\Phi_{\beta i} - \Phi_{\beta i+1}) - TE_{\beta i-1} \tilde{K}_i (\Phi_{\beta i-1} - \Phi_{\beta i}))}{\partial P_i}$$

$$= \tilde{K}_i (\Phi_{wi} - \Phi_{wi+1}) \frac{\partial TE_{\beta i}}{\partial P_i} + TE_{\beta i} \tilde{K}_i + TE_{\beta i-1} \tilde{K}_i \tag{E.111}$$

2. $$\frac{\partial E_{conv}}{\partial P_i} = \frac{\partial (-TE_{\beta i+1} \tilde{K}_{i+1} (\Phi_{\beta i+1} - \Phi_{\beta i}) + TE_{\beta i} \tilde{K}_i (\Phi_{\beta i} - \Phi_{\beta i-1}))}{\partial P_i}$$

$$= TE_{\beta i+1} \tilde{K}_{i+1} + \tilde{K}_i (\Phi_{\beta i} - \Phi_{\beta i+1}) \frac{\partial TE_{\beta i}}{\partial P_i} + TE_{\beta i} \tilde{K}_i \tag{E.112}$$

3. $$\frac{\partial E_{conv}}{\partial P_i} = \frac{\partial (-TE_{\beta i+1} K_{i+1} (\Phi_{\beta i+1} - \Phi_{\beta i}) - TE_{\beta i-1} K_i (\Phi_{\beta i-1} - \Phi_{\beta i}))}{\partial P_i}$$

$$= TE_{\beta i+1} K_{i+1} + TE_{\beta i-1} K_i \tag{E.113}$$

4. $$\frac{\partial E_{conv}}{\partial P_i} = \frac{\partial (TE_{\beta i} K_{i+1} (\Phi_{\beta i} - \Phi_{\beta i+1}) + TE_{\beta i} K_i (\Phi_{\beta i} - \Phi_{\beta i-1}))}{\partial P_i}$$

$$= K_{i+1} (\Phi_{\beta i} - \Phi_{\beta i+1}) \frac{\partial TE_{\beta i}}{\partial P_i} + TE_{\beta i} K_{i+1} +$$

$$K_i (\Phi_{\beta i} - \Phi_{\beta i+1}) \frac{\partial TE_{\beta i}}{\partial P_i} + TE_{\beta i} K_i \tag{E.114}$$

Conduction Term

The conductivity can be a constant or a variable as described in Section E.1.1. The derivative expressions of this term with respect to pressure are the same as LnK_i by replacing of LnK_i by P.

Heat-Loss Term

The derivative expressions of this term with respect to pressure are same as for LnK_i by replacing of LnK_i by P.

E.3.2 Derivatives for the Off-Diagonal Elements of the Jacobian Matrix

The Jacobian matrix elements for the off-diagonal terms (i is arbitrary direction; it can be j for the y direction or k for the z direction) related to derivatives with respect to pressure are given by

$$\frac{\partial R_E}{\partial P_{i\pm1}} = -\frac{\partial E_{accum}}{\partial P_{i\pm1}} + \frac{\partial E_{conv}}{\partial P_{i\pm1}} + \frac{\partial E_{source}}{\partial P_{i\pm1}} - \frac{\partial E_{loss}}{\partial P_{i\pm1}} \tag{E.115}$$

Derivatives for the Off-Diagonal Elements of *i*-1

The derivative of energy equation terms with respect to the left-hand side (for example in x direction) of the gridblock i is as follows:

Accumulation Term

This term of the equation is zero; that is

$$\frac{\partial U_f}{\partial P_{i-1}} = 0 \tag{E.116}$$

Source Term

The source term is not a function of the left-hand side or the right-hand side of the specified gridblock; hence, this term is zero.

$$\frac{\partial q_H}{\partial P_{i-1}} = 0 \tag{E.117}$$

Convective Term

The derivatives for this term are as follows:

1. $$\frac{\partial E_{conv}}{\partial P_{i-1}} = \frac{\partial (TE_{\beta i}\tilde{K}_i(\Phi_{\beta i} - \Phi_{\beta i+1}) - TE_{\beta i-1}\tilde{K}_i(\Phi_{\beta i-1} - \Phi_{\beta i}))}{\partial P_{i-1}}$$
$$= -\tilde{K}_i(\Phi_{\beta i-1} - \Phi_{\beta i})\frac{\partial TE_{\beta i-1}}{\partial P_{i-1}} - TE_{\beta i-1}\tilde{K}_i \tag{E.118}$$

2. $$\frac{\partial E_{conv}}{\partial P_{i-1}} = \frac{\partial (-TE_{\beta i+1}\tilde{K}_{i+1}(\Phi_{\beta i+1} - \Phi_{\beta i}) + TE_{\beta i}\tilde{K}_i(\Phi_{\beta i} - \Phi_{\beta i-1}))}{\partial P_{i-1}}$$
$$= -TE_{\beta i}\tilde{K}_i \tag{E.119}$$

3. $$\frac{\partial E_{conv}}{\partial P_{i-1}} = \frac{\partial (-TE_{\beta i+1}K_{i+1}(\Phi_{\beta i+1} - \Phi_{\beta i}) - TE_{\beta i-1}K_i(\Phi_{\beta i-1} - \Phi_{\beta i}))}{\partial P_{i-1}}$$
$$= -K_i(\Phi_{\beta i-1} - \Phi_{\beta i})\frac{\partial TE_{\beta i-1}}{\partial P_{i-1}} - TE_{\beta i-1}K_i \tag{E.120}$$

4. $$\frac{\partial E_{conv}}{\partial P_{i-1}} = \frac{\partial (TE_{\beta i}K_{i+1}(\Phi_{\beta i} - \Phi_{\beta i+1}) + TE_{\beta i}K_i(\Phi_{\beta i} - \Phi_{\beta i-1}))}{\partial P_{i-1}}$$
$$= -TE_{\beta i}K_i \tag{E.121}$$

Conduction Term

The conductivity can be a constant or a variable as described in Section E.1.1. The derivative expressions of this term with respect to pressure are the same as LnK_i by replacing of LnK_i by P.

Heat-Loss Term;

The heat-loss derivatives for the off-diagonal terms are zero.

$$\frac{\partial Q_{loss}}{\partial P_{i-1}} = 0 \tag{E.122}$$

Derivatives for the Off-Diagonal Elements of *i*+1

The derivative of energy equation terms with respect to the right-hand side of the gridblock i (if we consider the x direction) is as follows:

Accumulation Term

The accumulation term is not a function of neighboring gridblocks; hence

$$\frac{\partial U_f}{\partial P_{i+1}} = 0 \tag{E.123}$$

Source Term

The source term is also zero for the off diagonal terms

$$\frac{\partial q_H}{\partial P_{i+1}} = 0 \tag{E.124}$$

Convective Term

The following are the derivatives during the four cases (Section 4.6), of the convection term.

1. $$\frac{\partial E_{conv}}{\partial P_{i+1}} = \frac{\partial (TE_{\beta i}\tilde{K}_i(\Phi_{\beta i} - \Phi_{\beta i+1}) - TE_{\beta i-1}\tilde{K}_i(\Phi_{\beta i-1} - \Phi_{\beta i}))}{\partial P_{i+1}}$$

$$= -TE_{\beta i}\tilde{K}_i \tag{E.125}$$

2. $$\frac{\partial E_{conv}}{\partial P_{i+1}} = \frac{\partial (-TE_{\beta i+1}\tilde{K}_{i+1}(\Phi_{\beta i+1} - \Phi_{\beta i}) + TE_{\beta i}\tilde{K}_i(\Phi_{\beta i} - \Phi_{\beta i-1}))}{\partial P_{i+1}}$$

$$= -\tilde{K}_{i+1}(\Phi_{\beta i+1} - \Phi_{\beta i})\frac{\partial TE_{\beta i+1}}{\partial P_{i+1}} - TE_{\beta i+1}\tilde{K}_{i+1} \tag{E.126}$$

3. $$\frac{\partial E_{conv}}{\partial P_{i+1}} = \frac{\partial (-TE_{\beta i+1}K_{i+1}(\Phi_{\beta i+1} - \Phi_{\beta i}) - TE_{\beta i-1}K_i(\Phi_{\beta i-1} - \Phi_{\beta i}))}{\partial P_{i+1}}$$

$$= -K_{i+1}(\Phi_{\beta i+1} - \Phi_{\beta i})\frac{\partial TE_{\beta i+1}}{\partial P_{i+1}} - TE_{\beta i+1}K_{i+1} \tag{E.127}$$

4. $$\frac{\partial E_{conv}}{\partial P_{i+1}} = \frac{\partial (TE_{\beta i}K_{i+1}(\Phi_{\beta i} - \Phi_{\beta i+1}) + TE_{\beta i}K_i(\Phi_{\beta i} - \Phi_{\beta i-1}))}{\partial P_{i+1}}$$

$$= -TE_{\beta i}K_{i+1} \tag{E.128}$$

Conduction Term

The derivative expressions of this term with respect to pressure are the same as LnK_i by replacing of LnK_i by P.

Heat Loss Term

The heat-loss term for the off diagonal elements is zero.

$$\frac{\partial Q_{loss}}{\partial P_{i+1}} = 0 \tag{E.129}$$

E.4 DERIVATIVES WITH RESPECT TO TEMPERATURE

The derivatives equations for on-diagonal and off-diagonal elements are presented in this section. In the following derivatives, ∂H_{ti}, H_{ti} can be temperature or enthalpy (it is explained for each of the primary variables).

E.4.1 Derivatives for the On-Diagonal Elements of the Jacobian Matrix

The derivatives of the energy equation with respect to temperature or total enthalpy are

$$\frac{\partial R_E}{\partial H_{ti}} = -\frac{\partial E_{accum}}{\partial H_{ti}} + \frac{\partial E_{conv}}{\partial H_{ti}} + \frac{\partial E_{source}}{\partial H_{tii}} - \frac{\partial E_{loss}}{\partial H_{ti}} \tag{E.130}$$

Accumulation Term

The accumulation term and its derivative with respect to temperature are

Something is missing

The derivative with respect to temperature is

$$\frac{\partial E_{Acc}}{\partial T} = \frac{1}{\Delta t}\,\phi\,(U_f \frac{\partial \zeta_f}{\partial T} + \zeta_f \frac{\partial U_f}{\partial T}) \tag{E.131}$$

The derivative of the accumulation term with respect to total enthalpy can be described as follows:

$$\frac{\partial E_{accum}}{\partial H_{ti}} = \frac{\partial H_f}{\partial H_{ti}} + \frac{P}{\zeta_f{}^2} \frac{\partial \zeta_f}{\partial H_{ti}} \tag{E.132}$$

Source Term:

The total heat injection rate is

$$\frac{\partial q_{Hi}}{\partial T_i} = C \frac{(H_t)_{inj}}{(V_t)_{inj}} \frac{\partial \left[\sum_{\beta=1}^{n_p} \lambda_{\beta i} \left(P_{wf} - P_{\beta i} \right) \right]}{\partial T_i} \tag{E.133}$$

$$\frac{\partial q_{Hi}}{\partial T_i} = C \frac{(H_t)_{inj}}{(V_t)_{inj}} \sum_{\beta=1}^{n_p} \left[\left(\frac{\mu_{\beta i} \frac{\partial k_{r\beta i}}{\partial T_i} - k_{r\beta i} \frac{\partial \mu_{\beta i}}{\partial T_i}}{\mu_{\beta i^2}} \right) \left(P_{wf} - P_{\beta i} \right) \right] \tag{E.134}$$

Convective Term

The convection term of the energy equation is

$$E_{conv} = V_b \nabla . \sum_{\beta=o,g,aq} (\zeta_\beta H_\beta \vec{v}_\beta) \tag{E.135}$$

where

$$\bar{v}_\beta = -\vec{\vec{K}} \cdot \lambda_{r\beta} (\nabla P_\beta - \gamma_\beta \nabla D) \tag{E.136}$$

$$TE_{\beta i} = \zeta_{\beta i} \lambda_{\beta i} H_{\beta i} \tag{E.137}$$

$$\frac{\partial TE_{\beta i}}{\partial H_{ti}} = V_b \frac{\partial (\zeta_{\beta i} \lambda_{\beta i} H_{\beta i})}{\partial H_{ti}} = V_b (\lambda_{\beta i} H_{\beta i} \frac{\partial \zeta_{\beta i}}{\partial H_{ti}} + \zeta_{\beta i} H_{\beta i} \frac{\partial \lambda_{\beta i}}{\partial H_{ti}} + \zeta_{\beta i} \lambda_{\beta i} \frac{\partial H_{\beta i}}{\partial H_{ti}}) \tag{E.138}$$

1. $$\frac{\partial E_{conv}}{\partial H_{ti}} = \frac{\partial (TE_{\beta i}\tilde{K}_i(\Phi_{\beta i} - \Phi_{\beta i+1}) - TE_{\beta i-1}\tilde{K}_i(\Phi_{\beta i-1} - \Phi_{\beta i}))}{\partial H_{ti}}$$
$$= \tilde{K}_i(\Phi_{wi} - \Phi_{wi+1})\frac{\partial TE_{\beta i}}{\partial H_{ti}} \quad \text{(E.139)}$$

2. $$\frac{\partial E_{conv}}{\partial H_{ti}} = \frac{\partial (-TE_{\beta i+1}\tilde{K}_{i+1}(\Phi_{\beta i+1} - \Phi_{\beta i}) + TE_{\beta i}\tilde{K}_i(\Phi_{\beta i} - \Phi_{\beta i-1}))}{\partial H_{ti}}$$
$$= \tilde{K}_i(\Phi_{\beta i} - \Phi_{\beta i+1})\frac{\partial TE_{\beta i}}{\partial H_{ti}} \quad \text{(E.140)}$$

3. $$\frac{\partial E_{conv}}{\partial H_{ti}} = \frac{\partial (-TE_{\beta i+1}K_{i+1}(\Phi_{\beta i+1} - \Phi_{\beta i}) - TE_{\beta i-1}K_i(\Phi_{\beta i-1} - \Phi_{\beta i}))}{\partial H_{ti}}$$
$$= 0 \quad \text{(E.141)}$$

4. $$\frac{\partial E_{conv}}{\partial H_{ti}} = \frac{\partial (TE_{\beta i}K_{i+1}(\Phi_{\beta i} - \Phi_{\beta i+1}) + TE_{\beta i}K_i(\Phi_{\beta i} - \Phi_{\beta i-1}))}{\partial H_{ti}}$$
$$= K_{i+1}(\Phi_{\beta i} - \Phi_{\beta i+1})\frac{\partial TE_{\beta i}}{\partial H_{ti}} + K_i(\Phi_{\beta i} - \Phi_{\beta i+1})\frac{\partial TE_{\beta i}}{\partial H_{ti}} \quad \text{(E.142)}$$

Conduction Term

The conductivity can be a constant or a variable. The following equations have been selected for the *x*-direction as examples (same form for other axes).

There are four scenarios (Section E.1.1) for the conduction term:

1. $T_{i+1} < T_i \quad and \quad T_i < T_{i-1}$
$$E_{cond,i+1/2} - E_{cond,i-1/2} = \tilde{\lambda}_{av}|_{i\to i+1}(T_i - T_{i+1}) - \tilde{\lambda}_{av}|_{i-1\to i}(T_{i-1} - T_i) \quad \text{(E.143)}$$

2. $T_{i+1} > T_i \quad and \quad T_i > T_{i-1}$

$$E_{cond,i+1/2} - E_{cond,i-1/2} = -\tilde{\lambda}_{av}\,|_{i\to i+1}\,(T_{i+1} - T_i) + \tilde{\lambda}_{av}\,|_{i-1\to i}\,(T_i - T_{i-1}) \tag{E.144}$$

3. $T_{i+1} > T_i \quad and \quad T_i < T_{i-1}$

$$E_{cond,i+1/2} - E_{cond,i-1/2} = -\tilde{\lambda}_{av}\,|_{i\to i+1}\,(T_{i+1} - T_i) - \tilde{\lambda}_{av}\,|_{i-1\to i}\,(T_{i-1} - T_i) \tag{E.145}$$

4. $T_{i+1} < T_i \quad and \quad T_i > T_{i-1}$

$$E_{cond,i+1/2} - E_{cond,i-1/2} = \tilde{\lambda}_{av}\,|_{i\to i+1}\,(T_i - T_{i+1}) + \tilde{\lambda}_{av}\,|_{i-1\to i}\,(T_i - T_{i-1}) \tag{E.146}$$

$$\frac{\partial \tilde{\lambda}_{av}\,|_{i\to i+1}}{\partial H_{ti}} = 2\frac{(\tilde{\lambda}_{i+1}\frac{\partial \tilde{\lambda}_i}{\partial H_{ti}}(\,\Delta x_i\,\tilde{\lambda}_i + \Delta x_{i+1}\,\tilde{\lambda}_{i+1}) - \Delta x_i\,\tilde{\lambda}_i\,\tilde{\lambda}_{i+1}\frac{\partial \tilde{\lambda}_i}{\partial H_{ti}})}{(\,\Delta x_i\,\tilde{\lambda}_i + \Delta x_{i+1}\,\tilde{\lambda}_{i+1})^2}$$

$$= 2\,\Delta y_i\,\Delta z_i\frac{(\Delta x_{i+1}\tilde{\lambda}_{i+1}^{\,2}\frac{\partial \tilde{\lambda}_i}{\partial H_{ti}})}{(\,\Delta x_i\,\tilde{\lambda}_i + \Delta x_{i+1}\,\tilde{\lambda}_{i+1})^2} \tag{E.147}$$

$$\frac{\partial \tilde{\lambda}_{av}\,|_{i\to i+1}}{\partial H_{ti}} = 2\,\Delta y_i\,\Delta z_i\frac{(\Delta x_i\tilde{\lambda}_i^{\,2}\frac{\partial \tilde{\lambda}_{i+1}}{\partial H_{ti}})}{(\,\Delta x_i\,\tilde{\lambda}_i + \Delta x_{i+1}\,\tilde{\lambda}_{i+1})^2} \tag{E.148}$$

The derivatives in the case of four scenarios (Section E.1.1) are as follows:

1. $$\frac{\partial E_{cond}}{\partial H_{ti}} = \frac{\partial\left(\tilde{\lambda}_{av}\,|_{i\to i+1}\,(T_i - T_{i+1}) - \tilde{\lambda}_{av}\,|_{i-1\to i}\,(T_{i-1} - T_i)\right)}{\partial H_{ti}}$$

$$\frac{\partial E_{cond}}{\partial H_{ti}} = (T_i - T_{i+1})\frac{\partial \tilde{\lambda}_{av}\,|_{i\to i+1}}{\partial H_{ti}} + \tilde{\lambda}_{av}\,|_{i\to i+1}\frac{\partial T_i}{\partial H_{ti}}$$

$$-(T_{i-1} - T_{i+1})\frac{\partial \tilde{\lambda}_{av}\,|_{i-1\to i}}{\partial H_{ti}} + \tilde{\lambda}_{av}\,|_{i-1\to i}\frac{\partial T_i}{\partial H_{ti}} \tag{E.149}$$

2.
$$\frac{\partial E_{cond}}{\partial H_{ti}} = \frac{\partial\left(-\tilde{\lambda}_{av}\,|_{i\to i+1}\,(T_{i+1}-T_i)+\tilde{\lambda}_{av}\,|_{i-1\to i}\,(T_i-T_{i-1})\right)}{\partial H_{ti}}$$
$$\frac{\partial E_{cond}}{\partial H_{ti}} = -\frac{\partial \tilde{\lambda}_{av}\,|_{i\to i+1}}{\partial H_{ti}}(T_{i+1}-T_i)+\tilde{\lambda}_{av}\,|_{i\to i+1}\,\frac{\partial T_i}{\partial H_{ti}}$$
$$+\frac{\partial \tilde{\lambda}_{av}\,|_{i-1\to i}}{\partial H_{ti}}(T_i-T_{i-1})+\tilde{\lambda}_{av}\,|_{i-1\to i}\,\frac{\partial T_i}{\partial H_{ti}} \qquad \text{(E.150)}$$

3.
$$\frac{\partial E_{cond}}{\partial H_{ti}} = \frac{\partial\left(-\tilde{\lambda}_{av}\,|_{i\to i+1}\,(T_{i+1}-T_i)-\tilde{\lambda}_{av}\,|_{i-1\to i}\,(T_{i-1}-T_i)\right)}{\partial H_{ti}}$$
$$\frac{\partial E_{cond}}{\partial H_{ti}} = -(T_{i+1}-T_i)\frac{\partial \tilde{\lambda}_{av}\,|_{i\to i+1}}{\partial H_{ti}}+\tilde{\lambda}_{av}\,|_{i\to i+1}\,\frac{\partial T_i}{\partial H_{ti}}$$
$$-(T_{i-1}-T_i)\frac{\partial \tilde{\lambda}_{av}\,|_{i-1\to i}}{\partial H_{ti}}+\tilde{\lambda}_{av}\,|_{i-1\to i}\,\frac{\partial T_i}{\partial H_{ti}} \qquad \text{(E.151)}$$

4.
$$\frac{\partial E_{cond}}{\partial H_{ti}} = \frac{\partial\left(\tilde{\lambda}_{av}\,|_{i\to i+1}\,(T_i-T_{i+1})+\tilde{\lambda}_{av}\,|_{i-1\to i}\,(T_i-T_{i-1})\right)}{\partial H_{ti}}$$
$$\frac{\partial E_{cond}}{\partial H_{ti}} = (T_i-T_{i+1})\frac{\partial \tilde{\lambda}_{av}\,|_{i\to i+1}}{\partial H_{ti}}+\tilde{\lambda}_{av}\,|_{i\to i+1}\,\frac{\partial T_i}{\partial H_{ti}}$$
$$+(T_i-T_{i-1})\frac{\partial \tilde{\lambda}_{av}\,|_{i-1\to i}}{\partial H_{ti}}+\tilde{\lambda}_{av}\,|_{i-1\to i}\,\frac{\partial T_i}{\partial H_{ti}} \qquad \text{(E.152)}$$

Heat-Loss Term

The derivative-parameters for the heat-loss term are as follows:

$$\frac{\partial d}{\partial H_t}\Big|_{under\ or\ underburden} = \frac{1}{2}\,t\,(\eta t)^{-\frac{1}{2}}\,\frac{\partial \eta}{\partial H_t} \qquad \text{(E.153)}$$

$$\frac{\partial \eta}{\partial H_t} = \frac{C_r\zeta_r\,\dfrac{\partial \lambda_r}{\partial H_t}-\lambda_r\zeta_r\,\dfrac{\partial C_r}{\partial H_t}}{(C_r\zeta_r)^2} \qquad \text{(E.154)}$$

$$Term1 = \frac{\partial\left(\frac{\eta\Delta t(\theta^{n+1}-\theta^{0})}{d^{n+1}}\right)}{\partial H_t} =$$

$$\frac{\left(\Delta t(\theta^{n+1}-\theta^{0})\frac{\partial\eta}{\partial H_t}+\eta\Delta t\frac{\partial\theta^{n+1}}{\partial H_t}\right)d^{n+1}-\left(\eta\Delta t(\theta^{n+1}-\theta^{0})\frac{\partial d^{n+1}}{\partial H_t}\right)}{(d^{n+1})^2} \tag{E.155}$$

$$Term3 = \frac{\partial\left(\frac{(d^{n+1})^3(\theta^{n+1}-\theta^{n})}{\eta\Delta t}\right)}{\partial H_t} =$$

$$\frac{\left(3(d^{n+1})^2(\theta^{n+1}-\theta^{0})\frac{\partial d^{n+1}}{\partial H_t}+(d^{n+1})^3\frac{\partial\theta^{n+1}}{\partial H_t}\right)\eta\Delta t-\Delta t(d^{n+1})^3(\theta^{n+1}-\theta^{0})\frac{\partial\eta}{\partial H_t}}{(\eta\Delta t)^2} \tag{E.156}$$

$$Term4 = \frac{\partial\left(3(d^{n+1})^2+\eta\Delta t\right)}{\partial H_t} = 6d^{n+1}\frac{\partial d^{n+1}}{\partial H_t}+\Delta t\frac{\partial\eta}{\partial H_t} \tag{E.157}$$

$$\frac{\partial b_1^{n+1}}{\partial H_t} = \frac{(Term1-Term3)(3(d^{n+1})^2+\eta\Delta t)-(\frac{\eta\Delta t(\theta^{n+1}-\theta^{0})}{d^{n+1}}+}{(3(d^{n+1})^2+\eta\Delta t)^2}$$

$$\frac{\tau^{n}-\frac{(d^{n+1})^3(\theta^{n+1}-\theta^{n})}{\eta\Delta t})Term4}{} \tag{E.158}$$

$$b_2^{n+1} = \frac{2b_1^{n+1}(d^{n+1})-(\theta^{n+1}-\theta^{0})+\frac{(d^{n+1})^2(\theta^{n+1}-\theta^{n})}{\eta\Delta t}}{2(d^{n+1})^2} \tag{E.159}$$

$$Term5 = \frac{\partial\left(2b_1^{n+1}(d^{n+1})\right)}{\partial H_t} = 2(d^{n+1}\frac{\partial b_1^{n+1}}{\partial H_t}+b_1^{n+1}\frac{\partial d^{n+1}}{\partial H_t}) \tag{E.160}$$

$$Term6 = \frac{\partial\left(\frac{(d^{n+1})^2(\theta^{n+1}-\theta^n)}{\eta\Delta t}\right)}{\partial H_t} = \frac{\left(2(\theta^{n+1}-\theta^0)\frac{\partial d^{n+1}}{\partial P} + (d^{n+1})^2\frac{\partial\theta}{\partial P}\right)\eta\Delta t - (d^{n+1})^2(\theta^{n+1}-\theta^0)\Delta t\frac{\partial\eta}{\partial P}}{(\eta\Delta t)^2} \quad \text{(E.161)}$$

$$\frac{\partial b_2^{n+1}}{\partial H_t} = \frac{2(Term5 - \frac{\partial\theta}{\partial H_t} + Term6)(d^{n+1})^2}{4(d^{n+1})^4} \frac{-4d^{n+1}\left(2b_1^{n+1}(d^{n+1}) - (\theta^{n+1}-\theta^0) + \frac{(d^{n+1})^2(\theta^{n+1}-\theta^n)}{\eta\Delta t}\right)\frac{\partial d^{n+1}}{\partial H_t}}{4(d^{n+1})^4} \quad \text{(E.162)}$$

The heat-loss derivative term for the case of Ht as the primary variable is as follows:

$$\frac{\partial Q_{loss}}{\partial H_t} = A\left[\frac{(\theta^{n+1}-\theta^0)}{d^{n+1}} - b_1^{n+1}\right]\frac{\partial\lambda_r}{\partial H_t} + \lambda_r A\left[\frac{d^{n+1}\frac{\partial\theta}{\partial H_t} - (\theta^{n+1}-\theta^0)\frac{\partial d^{n+1}}{\partial H_t}}{(d^{n+1})^2} - \frac{\partial b_1^{n+1}}{\partial H_t}\right] \quad \text{(E.163)}$$

For T as the primary variable we have,

$$\frac{\partial Q_{loss}}{\partial H_t} = A\left[\frac{(\theta^{n+1}-\theta^0)}{d^{n+1}} - b_1^{n+1}\right]\frac{\partial\lambda_r}{\partial H_t} + \lambda_r A\left[\frac{-(\theta^{n+1}-\theta^0)\frac{\partial d^{n+1}}{\partial H_t}}{(d^{n+1})^2} - \frac{\partial b_1^{n+1}}{\partial H_t}\right] \quad \text{(E.164)}$$

E.4.2 Derivatives for the Off-Diagonal Elements of the Jacobian Matrix

The Jacobian elements for off-diagonal terms (*i* is any arbitrary direction; it can be *j* for *y*-direction or *k* for *z*-direction) related to derivatives with respect to temperature or total enthalpy are

$$\frac{\partial R_E}{\partial H_{ti\pm1}} = -\frac{\partial E_{accum}}{\partial H_{ti\pm1}} + \frac{\partial E_{conv}}{\partial H_{ti\pm1}} + \frac{\partial E_{cond}}{\partial H_{ti\pm1}} + \frac{\partial E_{source}}{\partial H_{ti\pm1}} - \frac{\partial E_{loss}}{\partial H_{ti\pm1}} \tag{E.165}$$

Derivatives for the Off-Diagonal Elements of *i*-1

The derivative of energy equation terms with respect to the left-hand side of the gridblock *i* are described as follows:

Accumulation Term

The accumulation term derivative of a gridblock with respect to the neighboring gridblock properties is zero; hence:

$$\frac{\partial U_f}{\partial H_{ti-1}} = 0 \tag{E.166}$$

Source Term

The derivative of the source term, same as the accumulation term, is zero.

$$\frac{\partial q_H}{\partial H_{ti-1}} = 0 \tag{E.167}$$

Convective Term

There are four scenarios for the convection term (Section 4.6); hence, the derivatives of them are presented by the following equations.

1. $$\frac{\partial E_{conv}}{\partial H_{ti-1}} = \frac{\partial(TE_{\beta i}\tilde{K}_i(\Phi_{\beta i} - \Phi_{\beta i+1}) - TE_{\beta i-1}\tilde{K}_i(\Phi_{\beta i-1} - \Phi_{\beta i}))}{\partial H_{ti-1}}$$
$$= -\tilde{K}_i(\Phi_{\beta i-1} - \Phi_{\beta i})\frac{\partial TE_{\beta i-1}}{\partial H_{ti-1}} \quad \text{(E.168)}$$

2. $$\frac{\partial E_{conv}}{\partial H_{ti-1}} = \frac{\partial(-TE_{\beta i+1}\tilde{K}_{i+1}(\Phi_{\beta i+1} - \Phi_{\beta i}) + TE_{\beta i}\tilde{K}_i(\Phi_{\beta i} - \Phi_{\beta i-1}))}{\partial H_{ti-1}}$$
$$= 0 \quad \text{(E.169)}$$

3. $$\frac{\partial E_{conv}}{\partial H_{ti-1}} = \frac{\partial(-TE_{\beta i+1}K_{i+1}(\Phi_{\beta i+1} - \Phi_{\beta i}) - TE_{\beta i-1}K_i(\Phi_{\beta i-1} - \Phi_{\beta i}))}{\partial H_{ti-1}}$$
$$= -K_i(\Phi_{\beta i-1} - \Phi_{\beta i})\frac{\partial TE_{\beta i-1}}{\partial H_{ti-1}} \quad \text{(E.170)}$$

4. $$\frac{\partial E_{conv}}{\partial H_{ti-1}} = \frac{\partial(TE_{\beta i}K_{i+1}(\Phi_{\beta i} - \Phi_{\beta i+1}) + TE_{\beta i}K_i(\Phi_{\beta i} - \Phi_{\beta i-1}))}{\partial H_{ti-1}}$$
$$= 0 \quad \text{(E.171)}$$

Conduction Term

The derivatives of the four scenarios (Section E.1.1) are as follows:

1. $$\frac{\partial E_{cond}}{\partial H_{ti-1}} = \frac{\partial\left(\tilde{\lambda}_{av}|_{i\to i+1}(T_i - T_{i+1}) - \tilde{\lambda}_{av}|_{i-1\to i}(T_{i-1} - T_i)\right)}{\partial H_{ti-1}}$$
$$= -(T_{i-1} - T_i)\frac{\partial \tilde{\lambda}_{av}|_{i-1\to i}}{\partial H_{ti-1}} - \tilde{\lambda}_{av}|_{i-1\to i}\frac{\partial T_{i-1}}{\partial H_{ti-1}} \quad \text{(E.172)}$$

2. $$\frac{\partial E_{cond}}{\partial H_{ti-1}} = \frac{\partial\left(-\tilde{\lambda}_{av}\mid_{i\to i+1}(T_{i+1}-T_i)+\tilde{\lambda}_{av}\mid_{i-1\to i}(T_i-T_{i-1})\right)}{\partial H_{ti-1}}$$
$$= (T_i - T_{i-1})\frac{\partial \tilde{\lambda}_{av}\mid_{i-1\to i}}{\partial H_{ti-1}} - \tilde{\lambda}_{av}\mid_{i-1\to i}\frac{\partial T_{i-1}}{\partial H_{ti-1}} \quad \text{(E.173)}$$

3. $$\frac{\partial E_{cond}}{\partial H_{ti-1}} = \frac{\partial\left(-\tilde{\lambda}_{av}\mid_{i\to i+1}(T_{i+1}-T_i)-\tilde{\lambda}_{av}\mid_{i-1\to i}(T_{i-1}-T_i)\right)}{\partial H_{ti-1}}$$
$$= -(T_{i-1} - T_i)\frac{\partial \tilde{\lambda}_{av}\mid_{i-1\to i}}{\partial H_{ti-1}} - \tilde{\lambda}_{av}\mid_{i-1\to i}\frac{\partial T_{i-1}}{\partial H_{ti-1}} \quad \text{(E.174)}$$

4. $$\frac{\partial E_{cond}}{\partial H_{ti-1}} = \frac{\partial\left(\tilde{\lambda}_{av}\mid_{i\to i+1}(T_i-T_{i+1})+\tilde{\lambda}_{av}\mid_{i-1\to i}(T_i-T_{i-1})\right)}{\partial H_{ti-1}}$$
$$= (T_i - T_{i-1})\frac{\partial \tilde{\lambda}_{av}\mid_{i-1\to i}}{\partial H_{ti-1}} - \tilde{\lambda}_{av}\mid_{i-1\to i}\frac{\partial T_{i-1}}{\partial H_{ti-1}} \quad \text{(E.175)}$$

Heat Loss Term

The derivative of the source term, same as the accumulation term, is zero.

$$\frac{\partial Q_{loss}}{\partial H_{ti-1}} = 0 \quad \text{(E.176)}$$

Derivatives for the Off-Diagonal Elements of *i*+1

The derivative of energy equation terms with respect to the right-hand side of the gridblock *i* are as follows:

Accumulation Term

The derivative of the accumulation is zero for this part.

$$\frac{\partial U_f}{\partial H_{ti+1}} = 0 \quad \text{(E.177)}$$

Source Term

The derivative of the injection heat rate is

$$\frac{\partial q_H}{\partial H_{ti+1}} = 0 \tag{E.178}$$

Convective Term

The derivatives of the four different cases (Section 4.6) of the convection terms are as follows:

1.
$$\frac{\partial E_{conv}}{\partial H_{ti+1}} = \frac{\partial (TE_{\beta i}\tilde{K}_i(\Phi_{\beta i} - \Phi_{\beta i+1}) - TE_{\beta i-1}\tilde{K}_i(\Phi_{\beta i-1} - \Phi_{\beta i}))}{\partial H_{ti+1}}$$
$$= 0 \tag{E.179}$$

2.
$$\frac{\partial E_{conv}}{\partial H_{ti+1}} = \frac{\partial (-TE_{\beta i+1}\tilde{K}_{i+1}(\Phi_{\beta i+1} - \Phi_{\beta i}) + TE_{\beta i}\tilde{K}_i(\Phi_{\beta i} - \Phi_{\beta i-1}))}{\partial H_{ti+1}}$$
$$= -\tilde{K}_{i+1}(\Phi_{\beta i+1} - \Phi_{\beta i})\frac{\partial TE_{\beta i+1}}{\partial H_{ti+1}} \tag{E.180}$$

3.
$$\frac{\partial E_{conv}}{\partial H_{ti+1}} = \frac{\partial (-TE_{\beta i+1}K_{i+1}(\Phi_{\beta i+1} - \Phi_{\beta i}) - TE_{\beta i-1}K_i(\Phi_{\beta i-1} - \Phi_{\beta i}))}{\partial H_{ti+1}}$$
$$= -K_{i+1}(\Phi_{\beta i+1} - \Phi_{\beta i})\frac{\partial TE_{\beta i+1}}{\partial H_{ti+1}} \tag{E.181}$$

4.
$$\frac{\partial E_{conv}}{\partial H_{ti+1}} = \frac{\partial (TE_{\beta i}K_{i+1}(\Phi_{\beta i} - \Phi_{\beta i+1}) + TE_{\beta i}K_i(\Phi_{\beta i} - \Phi_{\beta i-1}))}{\partial H_{ti+1}}$$
$$= 0 \tag{E.182}$$

Conduction Term

The derivatives of the four scenarios (Section E.1.1) are as follows:

1. $$\frac{\partial E_{cond}}{\partial H_{ti+1}} = \frac{\partial\left(\tilde{\lambda}_{av}\mid_{i\to i+1}(T_i - T_{i+1}) - \tilde{\lambda}_{av}\mid_{i-1\to i}(T_{i-1} - T_i)\right)}{\partial H_{ti+1}}$$
$$= (T_i - T_{i+1})\frac{\partial \tilde{\lambda}_{av}\mid_{i\to i+1}}{\partial H_{ti+1}} - \tilde{\lambda}_{av}\mid_{i\to i+1}\frac{\partial T_{i+1}}{\partial H_{ti+1}} \quad \text{(E.183)}$$

2. $$\frac{\partial E_{cond}}{\partial H_{ti+1}} = \frac{\partial\left(-\tilde{\lambda}_{av}\mid_{i\to i+1}(T_{i+1} - T_i) + \tilde{\lambda}_{av}\mid_{i-1\to i}(T_i - T_{i-1})\right)}{\partial H_{ti+1}}$$
$$= -\frac{\partial \tilde{\lambda}_{av}\mid_{i\to i+1}}{\partial H_{ti+1}}(T_{i+1} - T_i) - \tilde{\lambda}_{av}\mid_{i\to i+1}\frac{\partial T_{i+1}}{\partial H_{ti+1}} \quad \text{(E.184)}$$

3. $$\frac{\partial E_{cond}}{\partial H_{ti+1}} = \frac{\partial\left(-\tilde{\lambda}_{av}\mid_{i\to i+1}(T_{i+1} - T_i) - \tilde{\lambda}_{av}\mid_{i-1\to i}(T_{i-1} - T_i)\right)}{\partial H_{ti+1}}$$
$$= -(T_{i+1} - T_i)\frac{\partial \tilde{\lambda}_{av}\mid_{i\to i+1}}{\partial H_{ti+1}} - \tilde{\lambda}_{av}\mid_{i\to i+1}\frac{\partial T_{i+1}}{\partial H_{ti+1}} \quad \text{(E.185)}$$

4. $$\frac{\partial E_{cond}}{\partial H_{ti+1}} = \frac{\partial\left(\tilde{\lambda}_{av}\mid_{i\to i+1}(T_i - T_{i+1}) + \tilde{\lambda}_{av}\mid_{i-1\to i}(T_i - T_{i-1})\right)}{\partial H_{ti+1}}$$
$$= (T_i - T_{i+1})\frac{\partial \tilde{\lambda}_{av}\mid_{i\to i+1}}{\partial H_{ti+1}} - \tilde{\lambda}_{av}\mid_{i\to i+1}\frac{\partial T_{i+1}}{\partial H_{ti+1}} \quad \text{(E.186)}$$

Heat-Loss term

This parameter for this case is zero; therefore

$$\frac{\partial Q_{loss}}{\partial H_{ti+1}} = 0 \quad \text{(E.187)}$$

E.5 MULTIPHASE REACTIONS FOR THERMAL RECOVERY

In-situ combustion (ISC) or air injection is the process of injecting oxygen into the oil reservoir for its reaction with the heaviest components of the crude oil and oxidizing it. The process results in enhanced oil recovery by heating the reservoir and increasing the pressure. This chapter concerns the study and modeling of the in-situ combustion process and the implementation of necessary reaction formalism for that purpose.

This method is usually used for reservoirs with very viscous or heavy oil, which is difficult to produce by conventional methods. The mechanism of ISC constitutes burning some of the oil (in-situ oil) in the reservoir to create a combustion zone which moves toward the production well. The steam drive method or the intense gas drive can be used for the recovery of oil. To start the process, sometimes a heater or an igniter is lowered into the injection well and then oxygen is injected into the well. Afterwards, the heater or the igniter is turned on until ignition takes place. The heater is removed after heating up the surrounding rocks, but the air injection is continued to sustain the moving combustion front. Sometimes, water is injected with air simultaneously or alternatively to produce steam for better heat utilization and reduction of injection rate.

In the mechanism of reaction in ISC, the injected or any oxidant gas should pass through the burning region or zone to move the burning front. In the burning zone, four processes can be achieved. First, oxygen diffuses from bulk gas flow to the interface of the fuel and then (the second process) oxygen is absorbed and reacts with fuel. The third part is desorbing the combustion products and finally, the products are transferred to the gas bulk stream. The slowest step is the limiting or the controlling part of the overall rate. In the steady-state condition, the rate of each series should be equal.

E.5.1 Chemical Reaction Model

The general chemical reaction equation and related rate equation are as follows:

$$aA + bB \rightarrow cC + dD \tag{E.188}$$

$$R = K_0 e^{-\frac{E}{RT}} C_A^{n_A} C_B^{n_B} \tag{E.189}$$

K_0 is the reaction rate constant or the Arrhenius constant, E is the activation energy of the reaction and n_A and n_B are order of reaction in the reactant components A and B, respectively. The chemical reaction rate equations have been determined in the laboratory for specific cases, i.e. rock/oil.

The kinetic model which can be considered to have different phases and which addresses reactions possibly happening between different components in the phases can be expressed as follows:

$$R_i = \phi \sum_{\beta=1}^{n_p} S_\beta r_{i\beta} + (1-\phi) r_{is} \tag{E.190}$$

where R_i, $r_{i\beta}$, and r_{is} are the reaction rate of component *i* in total volume, reaction rate of component *i* in phase β, and reaction rate in solid phase, respectively. The reaction rate for each component for each phase in reaction *r* and reaction rate for component *i* in total volume by considering no solid phase in the system can be written as follows:

$$r_{i\beta r} = A_r e^{-\frac{1.8E_r}{RT}} (\zeta_{\beta ir} x_{i,\beta ir})^{n_{i,r}} \tag{E.191}$$

$$R_i = V_b \phi e^{-\frac{1.8E_r}{RT}} \sum_{\beta=1}^{n_p} S_{\beta ir} \prod_{i=1\ldots N_{RC,r}} A_r (\zeta_{\beta ir} x_{i,\beta ir})^{n_{i,r}} \tag{E.192}$$

A_r is the reaction rate constant, E_r is the activation energy of reaction r, $S_{\beta ir}$ and $\zeta_{\beta ir}$ are the saturation and the density of the phase β of the ith reactant in reaction r, and $x_{i,\beta ir}$ is the mole fraction of component i in phase β of the ith reactant in reaction r. $N_{RC,r}$ is the number of reactants in reaction r.

Consider, for example, the oxidation of a heavy oil component. Oil is considered as component 1, oxygen is component 2, and carbon dioxide and water are components 3 and 4, respectively. The reaction equation is

$$s_{1,r} Oil_1 + s_{2,r} O_2 \rightarrow s_{3,r} CO_2 + s_{4,r} H_2O \tag{E.193}$$

In this reaction, reactants oil and oxygen are in phases 2, which are oil phase. By definition, if the stoichiometric coefficient of the first reactant (in above equation, s_{1r}) is considered equal to one, the reaction rate of this equation, considering Eq. (7.3), is as follows:

$$Oil_1 + \frac{s_{2,r}}{s_{1,r}} O_2 \rightarrow \frac{s_{3,r}}{s_{1,r}} CO_2 + \frac{s_{4,r}}{s_{1,r}} H_2O \tag{E.194}$$

$$R_1 = V_b \phi A_r e^{-\frac{1.8E_r}{RT}} S_2 (\zeta_2 x_{1,2})^{n_{1,r}} (\zeta_2 x_{2,2})^{n_{2,r}} \tag{E.195}$$

For the first reactant, its molar and heat rate per day for a gridblock can be written as follows:

$$R_1 = R[\frac{Lbmole\,of\,the\,Oil_1}{Day}] = V_b \phi A_r e^{-\frac{1.8E_r}{RT}} S_2 (\zeta_2 x_{1,2})^{n_{1,r}} (\zeta_2 x_{2,2})^{n_{2,r}} \tag{E.196}$$

$$Hr[\frac{Btu}{Day}] = R_1 \hat{H}_r \tag{E.197}$$

$\hat{H}_r$ is the heat of reaction per Lbmol of the component, i.e. in this example, it is Btu per Lbmole of oil component. For exothermic reactions, this value is negative and for endothermic reactions it is positive.

Let us rewrite the material balance and energy equations from Chapters 3 and 4.

$$V_b \frac{\partial(\phi N_i)}{\partial t} + V_b \nabla \cdot \sum_{j=a,v,o} (x_{ij} . \xi_j . \bar{v}_j) = \dot{q}_i + R_i \qquad i = 1 \ldots n_c + 1 \tag{E.198}$$

$$V_b \frac{\partial U^T}{\partial t} + V_b \nabla \cdot \sum_{j=a,v,o} (\zeta_j h_j \vec{v}) - V_b \nabla . (\lambda_T \nabla T) = -\dot{Q}_L + \dot{q}_H - H_r \tag{E.199}$$

The component molar rates, and also the reaction heat rate in this example, to be used in material balance and energy equations are

$$R_{Oil_1} = -V_b \phi A_r e^{-\frac{1.8E_r}{RT}} S_2 (\zeta_2 x_{1,2})^{n_{1,r}} (\zeta_2 x_{2,2})^{n_{2,r}} = -R_r \tag{E.200}$$

$$R_{O_2} = -\frac{s_{2,r}}{s_{1,r}} R_r \tag{E.201}$$

$$R_{CO_2} = \frac{s_{3,r}}{s_{1,r}} R_r \tag{E.202}$$

$$R_{H_2O} = \frac{s_{4,r}}{s_{1,r}} R_r \tag{E.203}$$

$$H_r = R_r \hat{H}_r \tag{E.204}$$

E.5.2 Implementation of the Reaction Model

To have chemical reaction in each gridblock, component molar rates and reaction heat rate should be added into the material balance and the energy equations. In other words, the derivatives of the reaction-rate-equation should also be added to derivatives of the material balance and energy equations.

Derivatives of the reaction rate equation are expressed as given below:

$$\frac{\partial R_{r,i}}{\partial LnK_{1,\alpha}} = s_{r,i} V_b \phi e^{-\frac{1.8E_r}{RT}} \left[\prod_{i=1\ldots N_{RC,r}} A_r (\zeta_{\beta ir} x_{i,\beta ir})^{n_{i,r}} \sum_{\beta=1}^{n_p} \frac{\partial S_{\beta ir}}{\partial LnK_{1,\alpha}} + \right.$$
$$\left. \sum_{\beta=1}^{n_p} S_{\beta ir} A_r n_{ir} (\zeta_{\gamma ir} x_{i,\gamma ir})^{n_{i,r}-1} \left(\zeta_{\gamma ir} \frac{\partial x_{i,\gamma ir}}{\partial LnK_{1,\alpha}} + x_{i,\gamma ir} \frac{\partial \zeta_{\gamma ir}}{\partial LnK_{1,\alpha}} \right) \right] \tag{E.205}$$

The derivative of the reaction rate with respect to $\partial LnK_{2,\alpha}$ and ∂N_α are the same as for $\partial LnK_{1,\alpha}$, and the derivative with respect to pressure and temperature are as follow:

$$\frac{\partial R_{r,i}}{\partial P} = s_{r,i} V_b e^{-\frac{1.8E_r}{RT}} \left[\frac{\partial \phi}{\partial P} \sum_{\beta=1}^{n_p} S_{\beta ir} \prod_{i=1\ldots N_{RC,r}} A_r (\zeta_{\beta ir} x_{i,\beta ir})^{n_{i,r}} + \right.$$
$$\left. \phi \left(\prod_{i=1\ldots N_{RC,r}} A_r (\zeta_{\beta ir} x_{i,\beta ir})^{n_{i,r}} \sum_{\beta=1}^{n_p} \frac{\partial S_{\beta ir}}{\partial P} + \right. \right.$$

$$\sum_{\beta=1}^{n_p} S_{\beta ir}\, A_r\, n_{ir} (\zeta_{\gamma ir} x_{i,\gamma ir})^{n_{i,r}-1} \left(\zeta_{\gamma ir} \frac{\partial x_{i,\gamma ir}}{\partial P} + x_{i,\gamma ir} \frac{\partial \zeta_{\gamma ir}}{\partial P} \right) \Bigg) \Bigg] \tag{E.206}$$

$$\frac{\partial R_{r,i}}{\partial T} = s_{r,i} V_b \phi e^{-\frac{1.8E_r}{RT}} \Bigg[\prod_{i=1\ldots N_{RC,r}} A_r (\zeta_{\beta ir} x_{i,\beta ir})^{n_{i,r}} \sum_{\beta=1}^{n_p} \frac{\partial S_{\beta ir}}{\partial T} +$$
$$\sum_{\beta=1}^{n_p} S_{\beta ir}\, A_r\, n_{ir} (\zeta_{\gamma ir} x_{i,\gamma ir})^{n_{i,r}-1} \left(\zeta_{\gamma ir} \frac{\partial x_{i,\gamma ir}}{\partial T} + x_{i,\gamma ir} \frac{\partial \zeta_{\gamma ir}}{\partial T} \right) \Bigg]$$
$$-\frac{1.8}{R} \left(\frac{\partial E_r}{\partial T} - \frac{E_r}{T} \right) \tag{E.207}$$

For energy equations, the following expression can be used for the derivatives of the reaction heat-rate.

$$\frac{\partial H_r}{\partial LnK_{1,\alpha}} = \hat{H}_r \frac{\partial R_{r,i}}{\partial LnK_{1,\alpha}} \tag{E.208}$$

The derivative of the reaction heat rate with respect to $\partial LnK_{2,\alpha}$, ∂N_α, ∂P are the same as for $\partial LnK_{1,\alpha}$, and the derivative with respect temperature are as follows:

$$\frac{\partial H_r}{\partial T} = \hat{H}_r \frac{\partial R_{r,i}}{\partial T} + R_{r,i} \frac{\partial \hat{H}_r}{\partial T} \tag{E.209}$$

Appendix F

Evaluation of Jacobian Elements for Electrical Heating Model

F.1 DERIVATIVES FOR ELECTRICAL HEATING MODEL

The derivative of the following equation and the related derivatives for the electrical heating model are described in this section.

$$R_I = \frac{V_{i-1,j,k} - V_{i,j,k}}{R_{i-1,j,k} + R_{i,j,k}} - \frac{V_{i,j,k} - V_{i+1,j,k}}{R_{i,j,k} + R_{i+1,j,k}} + \frac{V_{i,j-1,k} - V_{i,j,k}}{R_{i,j-1,k} + R_{i,j,k}} - \frac{V_{i,j,k} - V_{i,j+1,k}}{R_{i,j,k} + R_{i,j+1,k}}$$

$$+ \frac{V_{i,j,k-1} - V_{i,j,k}}{R_{i,j,k-1} + R_{i,j,k}} - \frac{V_{i,j,k} - V_{i,j,k+1}}{R_{i,j,k} + R_{i,j,k+1}} \qquad \text{(F.1)}$$

The equation has been written for the *x*-direction; similar equations can be written for other directions.

Derivatives of the Electrical Current Equation With Respect to Primary Variables

For each primary variable, the diagonal and the off-diagonal elements are as follows.

The Diagonal Elements of the Jacobian Matrix

The derivatives of the output terms of the gridblock *i*-1 are

$$\left(\frac{\partial R_I}{\partial LnK_{1,\alpha}}\right)_{i-1,j,k} = \frac{\partial\left(\frac{V_{i-1,j,k} - V_{i,j,k}}{R_{i-1,j,k} + R_{i,j,k}}\right)}{\partial(LnK_{1,\alpha})_{i-1,j,k}}$$

$$= (V_{i-1,j,k} - V_{i,j,k}) \frac{-\frac{\partial R_{i-1,j,k}}{\partial (LnK_{1,\alpha})_{i-1,j,k}}}{(R_{i-1,j,k} + R_{i,j,k})^2} \tag{F.2}$$

The derivatives of the input terms of the gridblock *i* are

$$\left(\frac{\partial R_I}{\partial LnK_{1,\alpha}} \right)_{i,j,k} = \frac{\partial \left(\frac{V_{i-1,j,k} - V_{i,j,k}}{R_{i-1,j,k} + R_{i,j,k}} \right)}{\partial (LnK_{1,\alpha})_{i,j,k}}$$

$$= (V_{i-1,j,k} - V_{i,j,k}) \frac{-\frac{\partial R_{i,j,k}}{\partial (LnK_{1,\alpha})_{i,j,k}}}{(R_{i-1,j,k} + R_{i,j,k})^2} \tag{F.3}$$

The derivatives with respect to $LnK_{2\alpha}$, number of mole per pore volume, pressure, and temperature are the same as for $LnK_{1\alpha}$.

Derivatives of the Current Equation with Respect to Voltage

The derivatives of the output terms of the gridblock *i*-1 are

$$\left(\frac{\partial R_I}{\partial V} \right)_{i-1,j,k} = \frac{1}{R_{i-1,j,k} + R_{i,j,k}} \tag{F.4}$$

The derivatives of the input terms of the gridblock *i* are

$$\left(\frac{\partial R_I}{\partial V} \right)_{i,j,k} = \frac{-1}{R_{i-1,j,k} + R_{i,j,k}} \tag{F.5}$$

The Off-Diagonal Elements of the Jacobian Matrix

The following are the derivatives with respect to the left-hand side and the right-hand side of the current equation in the *x* and *y* directions and also the top and bottom in the *z* direction.

The derivatives of the output term of the gridblock *i*-1 with respect to the right-hand side of the grid block *i*-1 are

$$\frac{\partial(R_I)_{i-1,j,k}}{\partial(LnK_{1,\alpha})_{i,j,k}} = \frac{\partial\left(\frac{V_{i-1,j,k}-V_{i,j,k}}{R_{i-1,j,k}+R_{i,j,k}}\right)}{\partial(LnK_{1,\alpha})_{i,j,k}}$$

$$= (V_{i-1,j,k}-V_{i,j,k})\frac{-\frac{\partial R_{i,j,k}}{\partial(LnK_{1,\alpha})_{i,j,k}}}{(R_{i-1,j,k}+R_{i,j,k})^2} \qquad \text{(F.6)}$$

The derivatives of the input term of the gridblock *i* with respect to left-hand side of the gridblock *i* are

$$\frac{\partial(R_I)_{i,j,k}}{\partial(LnK_{1,\alpha})_{i-1,j,k}} = \frac{\partial\left(\frac{V_{i-1,j,k}-V_{i,j,k}}{R_{i-1,j,k}+R_{i,j,k}}\right)}{\partial(LnK_{1,\alpha})_{i-1,j,k}}$$

$$= (V_{i-1,j,k}-V_{i,j,k})\frac{-\frac{\partial R_{i-1,j,k}}{\partial(LnK_{1,\alpha})_{i-1,j,k}}}{(R_{i-1,j,k}+R_{i,j,k})^2} \qquad \text{(F.7)}$$

Derivatives of the Current Equation with Respect to Voltage

The derivatives of the output term of the gridblock *i*-1 with respect to the right-hand side of the gridblock *i*-1 are

$$\frac{\partial (R_I)_{i-1,j,k}}{\partial (V)_{i,j,k}} = \frac{1}{R_{i-1,j,k} + R_{i,j,k}} \tag{F.8}$$

The derivatives of the input term of the gridblock *i* with respect to the left-hand side of the gridblock *i* are

$$\frac{\partial (R_I)_{i,j,k}}{\partial (V)_{i-1,j,k}} = \frac{-1}{R_{i-1,j,k} + R_{i,j,k}} \tag{F.9}$$

F.2 DERIVATIVES OF THE HEAT GENERATION EQUATION RELATED TO ELECTRICAL CURRENT INTO ENERGY EQUATION

The heat generation equation for each gridblock in three dimensions is

$$\begin{aligned} Q_{gen\_i} = {} & (I_{i-1\to i,j,k})^2 R_{i-1/2\to i,j,k} + (I_{i\to i+1,j,k})^2 R_{i\to i+1/2,j,k} \\ & + (I_{i,j-1\to j,k})^2 R_{i,j-1/2\to j,k} + (I_{i,j\to j+1,k})^2 R_{i,j\to j+1/2,k} \\ & + (I_{i,j,k-1\to k})^2 R_{i,j,k-1/2\to k} + (I_{i,j,k\to k+1})^2 R_{i,j,k\to k+1/2} \end{aligned} \tag{F.10}$$

If we consider the equation for the *x* direction,

$$I_{i\to i+1} = \frac{V_i - V_{i+1}}{R_i + R_{i+1}} \tag{F.11}$$

$$Q_{gen,i} = (I_{i\to i+1})^2 R_i = \left(\frac{V_i - V_{i+1}}{R_i + R_{i+1}} \right)^2 R_i \tag{F.12}$$

$$Q_{gen,i+1} = (I_{i\to i+1})^2 R_{i+1} = \left(\frac{V_i - V_{i+1}}{R_i + R_{i+1}} \right)^2 R_{i+1} \tag{F.13}$$

The derivatives of the above equation with respect to primary variables are calculated by the following equations. Later, they are used for heat generation derivative for each gridblock in the Jacobian matrix related to the energy equation. For each current equation of two neighborhood gridblocks, two different equations can be written.

The heat generation term for gridblock *i*-1 related to current equation between *i*-1 and *i* is given by

$$Q_{gen,i-1} = (I_{i-1\to i})^2 R_{i-1} = \left(\frac{V_{i-1} - V_i}{R_{i-1} + R_i} \right)^2 R_{i-1} \tag{F.14}$$

The derivatives of on-diagonal elements for gridblock *i* are

$$\frac{\partial (Q_{gen})_{i-1}}{\partial (LnK_{1,\alpha})_{i-1}} = (V_{i-1} - V_i)^2 \frac{\partial R_{i-1}}{\partial (LnK_{1,\alpha})_{i-1}} \left(\frac{1}{(R_{i-1} + R_i)^2} - \frac{2.R_{i-1}}{(R_{i-1} + R_i)^3} \right) \tag{F.15}$$

The same equation can be written for $LnK_{2\alpha}$., number of mole per pore volume, pressure, and temperature. The equation for voltage is as follows:

$$\frac{\partial (Q_{gen})_{i-1}}{\partial (V)_{i-1}} = 2 \left(\frac{R_{i-1}}{(R_{i-1} + R_i)^2} \right) (V_{i-1} - V_i) \tag{F.16}$$

The derivatives of off-diagonal elements, which are the derivatives of the heat generation for gridblock *i*-1 with respect to primary variables of the right-hand side of gridblock *i*, are given by

$$\frac{\partial (Q_{gen})_{i-1}}{\partial (LnK_{1,\alpha})_i} = (V_{i-1} - V_i)^2 \frac{\partial R_i}{\partial (LnK_{1,\alpha})_i} \frac{-2.R_{i-1}}{(R_{i-1} + R_i)^3} \tag{F.17}$$

The same equation can be used for $LnK_{2\alpha}$ number of moles, pressure, and temperature. The following equation describes the case for voltage

$$\frac{\partial(Q_{gen})_{i-1}}{\partial(V)_i} = -2\left(\frac{R_{i-1}}{(R_{i-1}+R_i)^2}\right)(V_{i-1}-V_i) \tag{F.18}$$

The heat generation term for gridblock *i* related to current equation between *i*-1 and *i* is given by

$$Q_{gen,i} = (I_{i-1\to i})^2 R_i = \left(\frac{V_{i-1}-V_i}{R_{i-1}+R_i}\right)^2 R_i \tag{F.19}$$

The derivatives of on-diagonal elements for gridblock *i* are

$$\frac{\partial(Q_{gen})_i}{\partial(LnK_{1,\alpha})_i} = (V_{i-1}-V_i)^2 \frac{\partial R_i}{\partial(LnK_{1,\alpha})_i}\left(\frac{1}{(R_{i-1}+R_i)^2} - \frac{2.R_i}{(R_{i-1}+R_i)^3}\right)$$

The same equation can be used for $LnK_{2\alpha}$ number of moles, pressure, and temperature. The following equation describes the case for voltage

$$\frac{\partial(Q_{gen})_i}{\partial(V)_i} = -2\left(\frac{R_i}{(R_{i-1}+R_i)^2}\right)(V_{i-1}-V_i) \tag{F.20}$$

The derivatives of off-diagonal elements, which are the derivatives of heat generation for gridblock *i* with respect to the primary variables of the left-hand side gridblock *i*-1, are

$$\frac{\partial (Q_{gen})_i}{\partial (LnK_{1,\alpha})_{i-1}} = \left(V_{i-1} - V_i\right)^2 \frac{\partial R_{i-1}}{\partial (LnK_{1,\alpha})_{i-1}} \frac{-2.R_i}{(R_{i-1} + R_i)^3} \tag{F.21}$$

They are the same equation $LnK_{2\alpha}$., number of mole per pore volume, pressure, and temperature. The following equation describes the case for voltage

$$\frac{\partial (Q_{gen})_i}{\partial (V)_{i-1}} = 2\left(\frac{R_i}{(R_{i-1} + R_i)^2}\right)\left(V_{i-1} - V_i\right) \tag{F.22}$$

F.3 DERIVATIVE OF RESISTIVITY WITH RESPECT TO PRIMARY VARIABLES

The derivatives of the resistance and the conductivity for each gridblock, which are used in the derivative equations, are shown in this section.

$$\sigma_{w,p}(T, \phi_f, S_w) = \sigma_{w,p}(T)\left[\phi_f^{1.7}\, S_w^2 / 0.88\right], \quad p = i, j, k \tag{F.23}$$

$$\sigma_p = \sigma_{w,p}(T, \phi_f, S_w) + \sigma_{r,p}(T)(1 - \phi_v) + \sigma_{s,p}(T)(\phi_v - \phi_f) + \sigma_{o,p}(T).\phi_f.S_o\,, p = i, j, k \tag{F.24}$$

If we consider the equation in the x direction, we have

$$R_i = \frac{\Delta x / 2}{\Delta y\, \Delta z} \frac{1}{\sigma_i} \tag{F.25}$$

$$\frac{\partial R_i}{\partial \mathrm{P}} = \frac{\Delta x / 2}{\Delta y\, \Delta z} \frac{\partial\left(\frac{1}{\sigma_i}\right)}{\partial \mathrm{P}} = \frac{\Delta x / 2}{\Delta y\, \Delta z} \frac{-\partial \sigma_i}{\sigma_i^2} \tag{F.26}$$

where P is the primary variable

$$\frac{\partial \sigma_p}{\partial LnK_{1,jc,p}} = \frac{\partial \sigma_{aq,p}}{\partial S_{aq}} \frac{\partial S_{aq,P}}{\partial LnK_{1,jc,p}} + \sigma_{o,p}(T)\phi_f \frac{\partial S_{o,P}}{\partial LnK_{1,jc,p}} \tag{F.27}$$

The same equation can be used for $LnK_{2\alpha}$ number of moles, pressure, and temperature; thus, we have

$$\frac{\partial \sigma_p}{\partial P_p} = \frac{\partial \sigma_{aq,p}}{\partial S_{aq}} \frac{\partial S_{aq,P}}{\partial P_p} - \sigma_{o,p}(T)\frac{\partial \phi_v}{\partial P_p} + \sigma_{s,p}(T)\frac{\partial \phi_v}{\partial P_p} -$$
$$\sigma_{s,p}(T)\frac{\partial \phi_f}{\partial P_p} + \sigma_{o,p}(T)\phi_f \frac{\partial S_{o,P}}{\partial P_p} + \sigma_{o,p}(T)S_{o,P}\frac{\partial \phi_f}{\partial P_p} \tag{F.28}$$

$$\frac{\partial \sigma_p}{\partial T_p} = \frac{\partial \sigma_{aq,p}}{\partial T_p} + (1-\phi_v)\frac{\partial \sigma_{r,p}(T)}{\partial T_p} + (\phi_v - \phi_f)\frac{\partial \sigma_{s,p}(T)}{\partial T_p}$$
$$+\sigma_{o,p}(T)\phi_f \frac{\partial S_{o,P}}{\partial T_p} + S_{o,P}\phi_f \frac{\partial \sigma_{o,p}(T)}{\partial P_p} \tag{F.29}$$

If there is no solid phase,

$$\sigma_p = \sigma_{aq,p}(T, \phi_f, S_w) + \sigma_{r,p}(T)(1-\phi_v) + \sigma_{o,p}(T)\phi S_o, \quad p = i, j, k \tag{F.30}$$

$$\frac{\partial \sigma_p}{\partial P_p} = \frac{\partial \sigma_{aq,p}}{\partial S_{aq}} \frac{\partial S_{aq,P}}{\partial P_p} - \sigma_{o,p}(T)\frac{\partial \phi_{v,p}}{\partial P_p} + (1-\phi_v)\frac{\partial \sigma_{o,p}(T)}{\partial T_p} +$$
$$\sigma_{o,p}(T)\phi_f \frac{\partial S_{o,P}}{\partial T_p} + +\sigma_{o,p}(T)S_{o,P}\frac{\partial \phi}{\partial P_p} \tag{F.31}$$

$$\frac{\partial \sigma_p}{\partial T_p} = \frac{\partial \sigma_{aq,p}}{\partial T_p} + (1-\phi_v)\frac{\partial \sigma_{r,p}(T)}{\partial T_p}$$
$$+\sigma_{o,p}(T)\phi_f \frac{\partial S_{o,P}}{\partial T_p} + S_{o,P}\phi_f \frac{\partial \sigma_{o,p}(T)}{\partial T_p} \tag{F.32}$$

$$\sigma_{aq,p}(T, \phi_f, S_w) = \sigma_{aq_i,p}(T)\left[\phi_f^{1.7} S_{aq}^2 / 0.88\right], \quad p = i, j, k \tag{F.33}$$

$$\frac{\partial \sigma_{aq,p}}{\partial LnK_{1,jc,p}} = (\sigma_{aq_i,p}(T)/0.88)\left(2S_{aq}\phi_f^{1.7}\frac{\partial S_{aq}}{\partial LnK_{1,jc,p}}\right) \tag{F.34}$$

The same equation can be used for $LnK_{2\alpha}$ number of moles, pressure and temperature; thus, we have

$$\frac{\partial \sigma_{aq,p}}{\partial P_p} = (\sigma_{aq_i,p}(T)/0.88)\left(1.7\phi_{f,p}^{0.7}S_{aq,p}^2\frac{\partial \phi_{f,p}}{\partial P_p} + 2S_{aq}\phi_f^{1.7}\frac{\partial S_{aq,p}}{\partial P_p}\right) \tag{F.35}$$

$$\frac{\partial \sigma_{aq,p}}{\partial T_p} = (\phi_{f,p}^{0.7}/0.88)\left(2S_{aq,p}\sigma_{aq_i,p}(T)\frac{\partial S_{aq,p}}{\partial T_p} + S_{aq,p}^2\frac{\partial \sigma_{aq_i,p}(T)}{\partial T_p}\right) \tag{F.36}$$

Appendix G

Keywords and Input Files

G.1 KEYWORDS

Following are the keywords used in the models.

ENERGY	Thermal model flag
HKCONST	Constant thermal conductivity coefficient flag
HKROCK	Constant value of rock thermal conductivity
HEATLOSS	Heat loss calculation flag
HKCONSTS	Constant surrounding thermal conductivity flag
HKROCKS	Constant value of surrounding thermal conductivity
ACPR1	Rock heat capacity
ACPR1S	Surrounding heat capacity
ACPI	Ideal gas heat capacity coefficients of each component for polynomial equation
TMEINI1	Initial temperature for each gridblock
TEMPERATURE (IW)	Injection temperature for well IW
VISCOCORRW	Andrade correlation flag for water, if this flag is OFF, the Grabowski equation is used
VISCOCORRO	Andrade correlation flag for oil
AVISO	Andrade equation constants for each component
VISCOTABLEW	Viscosity table look-up flag for water

VISCOTABLEO	Viscosity table look-up flag for oil
VISCOTABLEG	Viscosity table look-up flag for gas
N_DATV	Number of data for viscosity
T_DATAV	Temperature corresponding to viscosity data
WVIS	Viscosity of water for each temperature
OVIS	Viscosity of oil for each temperature
GVIS	Viscosity of gas for each temperature
ELECTHEAT	Flag for electrical heating model flag
VOLTGINI1	Initial voltage for each gridblock
VOLTAGE (IW)	Voltage in location IW
COND_CONST	Constant electrical conductivity
N_DATAE	Number of data for electrical conductivity
T_DATAE	Temperature corresponding to electrical conductivity data
CONDW	Electrical conductivity of water for each temperature
CONDO	Electrical conductivity of oil for each temperature
CONDR	Electrical conductivity of rock for each temperature
ISTD	In-situ thermal desorption option flag
QISTD(IW)	Injection heat of ISTD option for well IW
REACTION	Reaction option flag
NREAC	Number of reactions
ICBR(IR)	Based component for stoichiometric reaction calculation in reaction IR
ICIR(IR,JP,IC)	Index for each component (IC) to be exist in each phase (JP) in reaction (IR)

CCIR(IR,IC)	Components stoichimetric coefficient for each reaction
RIN(IR,IC)	Component order for the component IC which exist in reaction IR
EACT(IR)	Activation energy for each reaction
RK0(IR)	Reaction constant for each reaction(IR)
HREAC(IR)	Heat of reaction IR
TREF	Reference temperature for chemical phase behavior calculation
HBNTm	Slope of bimodal curve, m=0,1,2
ACPP()	Heat capacity of the phases for chemical flooding in BTU/(Lbm.F)
NESM	Index for effective salinity formula method, 1 is for CSE=C51/(1+BETAT.(T-Tref) and 2 is for CSE=C51.(1+BETAT.(T-Tref)
OPTS	Flag for calculation of optimum salinity, if ON it is calculated directly if OFF it is calculated using upper and lower values
C51	Coefficient to calculate salinity to calculate directly
C51L	Coefficient to calculate lower salinity value
C51U	Coefficient to calculate upper salinity
BETAT	Coefficient to calculate salinity
SCMC	Slope to calculate critical micelle concentration of surfactant CMC= SCMC(T-Tref) +RCMC
RCMC	Intercept of the critical micelle concentration of surfactant equation

WATERCOMPO	Flag for output of thermal model
WATERCOMPO2	Flag for output of thermal model

G.2 INPUT FILES

The input files for different chapters are as follows:

G.2.1 Input Files for Chapter 3, Four-Phase Model

```
TITLE(2)="3-D 6-COMPONENT GAS INJECTION"
DESCRIPTION()=
"THICKNESS (FT) : 100"
"LENGTH (FT) : 560"
"WIDTH (FT) : 560"
"GRID BLOCKS : 7x7x3"
COMPOSITIONAL_MODEL
$DEBUGS
TIMEEND = 365
$ I/O OPTIONS
OUTLEVEL = 1
PROCOUT
OUTPUT_PRE
OUTPUT_SAT
OUTPUT_OIL
OUTPUT_GAS
OUTPUT_WEL
OUTPUT_HIS
WELLFILE = "6COMP.WEL"
HISDATA_NUM = 2000
OUTPUT_TIME() =  100 1000 2000 3000 3650
$NO_CRASH
$OUTPUT FREQUENCY
ISTEP(,,)=1
JSTEP(,,)=1
KSTEP(,,)=1
$ FAULT BLOCK AND MESH DATA
METHOD = 2
DOWN() = 0 0 1
NX(1) = 7  NY(1) = 7  NZ(1) = 3
MES = "cart"
DX() = 80  DY() = 80  DZ() = 20 30 50
$ COMPOUND NAMES
COMPOUND(1) = "C1"      COMPOUND(2) = "C3"
COMPOUND(3) = "C6"      COMPOUND(4) = "C10"
```

```
COMPOUND(5) = "C15"     COMPOUND(6) = "C20"
$ COMPOUND CRITICAL TEMPERATURES
CRIT()  343.0 665.7 913.4 1111.8 1270.0 1380.0
$ COMPOUND CRITICAL PRESSURES
CRIP()  667.8 616.3 436.9 304.0 200.0 162.0
$ COMPOUND CRITICAL VOLUMES
CRIV()  1.599 3.211 5.923 10.087 16.696 21.484
$ COMPOUND ACEN
ACEN()  0.013 0.152 0.301 0.488 0.650 0.850
$ COMPOUND MOL WEIGHTS
MOLW()  16.0 44.1 86.2 142.3 206.0 282.0
$ COMPOUND PARA
PARA()  71.00 151.0 271.0 431.0 631.0 831.0
$ MAX NUMBER OF PHASES
NPHASE = 4
$ MAXNEWT MAX NUMBER OF NEWTON ITERATION
MAXNEWT = 20
$ Initial rock & water properties
ROCKZ = 0.000001  ROCKP = 1500
H2OZ = 0.000003  H2OP = 14.696  H2OD = 3.468
SURTF = 60.0  SURPS = 14.696
RESTF = 160.0
$ TOLERANCE
CVGOPT = 2
TOL_FLASH = 0.0001
TOL_VOLUME = 0.0001
TOL_MASS = 0.0001
TOL_WATER = 0.0001
$ POROSITY
POROSITY1() = 0.35
$ PERMEABILITIES
XPERM1() = 10
YPERM1() = 10
ZPERM1() = 10
XYPERM1() = 0
XZPERM1() = 0
YZPERM1() = 0
$ INITIAL WATER SATURATION
SWINI1() = 0.17
$ INITIAL WATER CELL PRESSURE
PINI1() = 1400.0
$ INITIAL PHASE VISCOSITIES AT EACH CELL
VIS1() = 1.0
$ INITIAL COMPOSITIONS
ZXY1(,,,1) = .5
ZXY1(,,,2) = .03
ZXY1(,,,3) = .07
ZXY1(,,,4) = .2
ZXY1(,,,5) = .15
ZXY1(,,,6) = .05
$ RELPERM DATA
RELP 2
NRELFUN  1
```

```
ENDPT() = 0.4 0.9 0.9
SR() = 0.3 0.1 0.0
EXPN() = 3.0 2.0 2.0
$ ============== WELL SPECIFICATIONS ==============
NUMWELL = 2
$ --- The first well ---
WELLNAME(1) = "INJECTOR 1"
KINDWELL(1) = 2
WELLTOP(1 TO 3,1,1) = 40 40 0
WELLBOTTOM(1 TO 3,1,1) = 40 40 100
DIAMETER(1,1) = 1.0
PRLIMIT(1) = 14695
WELLPQ(1) Block
  Interpolation Linear
  Extrapolation Constant
$ --- Lb-mole/day
  Data  0.      2634.597
EndBlock
$ --- The 2nd well ---
WELLNAME(2) = "PRODUCER 1"
KINDWELL(2) = 3
WELLTOP(1 TO 3,1,2) = 520 520 0
WELLBOTTOM(1 TO 3,1,2) = 520 520 100
DIAMETER(1,2) = 1.0
WELLPQ(2) Block
  Interpolation Linear
  Extrapolation Constant
  Data  0.   1300.
EndBlock
EndInitial
$ TRANSIENT DATA INPUT BLOCKS
BeginTime  0.0
TIME_CONTROL = 2
DELTIM = 1  DTIMMUL = 1.0  DTIMMAX = 30 DTIMMIN = 0.1
TUNE = 0.5  DCMAX = 0.5  DAQCMAX = 0.5  DPMAX = 0.5  DSMAX = 0.5
WZ() 0.77 0.20 0.01 0.01 0.005 0.005 0.0
EndTime
```

G.2.2 Input Files for Chapter 4, EOS-Thermal Model

```
TITLE(2)="1-D 4-COMPONENT "
DESCRIPTION()=
"THICKNESS (FT) : 20"
"LENGTH (FT) : 250"
"WIDTH (FT) : 50"
"GRID BLOCKS : 50x1x1"
COMPOSITIONAL_MODEL
$DEBUGS
TIMEEND = 600.0
$ I/O OPTIONS
OUTLEVEL = 1
$SPLINEOUT
$GEOMOUT
PROCOUT
OUTPUT_PRE
$OUTPUT_NPH
OUTPUT_SAT
OUTPUT_OIL
OUTPUT_GAS
OUTPUT_DEN
OUTPUT_WEL
OUTPUT_HIS
WELLFILE = "4COMP.WEL"
HISDATA_NUM = 300
OUTPUT_TIME() =  10 20 30 40 50 100 200 300 500 900
$NO_CRASH
$OUTPUT FREQUENCY
ISTEP(,,)=1
JSTEP(,,)=1
KSTEP(,,)=1
$ FAULT BLOCK AND MESH DATA
METHOD = 2
DOWN() = 0 0 1
NX(1) = 50  NY(1) = 1  NZ(1) = 1
MES = "cart"
DX() = 50  DY() = 50  DZ() = 20
$ COMPOUND NAMES
COMPOUND(1) = "C6"
COMPOUND(2) = "C10"
COMPOUND(3) = "C15"
COMPOUND(4) = "H2O"
WATERCOMP
$ COMPOUND CRITICAL TEMPERATURES
CRIT() 913.4 1120.11 1270.0 1165.47
$ COMPOUND CRITICAL PRESSURES
CRIP() 436.9 367.647 200.0 3198.72
$ COMPOUND CRITICAL VOLUMES
```

```
CRIV() 5.923 8.415 16.696 0.91465
$ COMPOUND ACEN
ACEN() 0.301 0.443774 0.650 0.344
$ COMPOUND MOL WEIGHTS
MOLW() 86.2 134.0 206.0 18.015
$ COMPOUND PARA
PARA() 271.0 622.1 631.0 52.0
$ BINARY INTERACTION COEFFICIENS
BINC(,) = 0.0   0.0028 0.01097  0.48
          0.0028   0.0 0.02657  0.48
          0.01097 0.02657  0.0  0.48
          0.48    0.48     0.48 0.0
$ MAX NUMBER OF PHASES
NPHASE = 4
$ MAXNEWT MAX NUMBER OF NEWTON ITERATION
MAXNEWT = 20
$ Initial rock & water properties
ROCKZ = 0.00004  ROCKP = 14.7
H2OZ = 0.000003  H2OP = 14.696  H2OD = 3.468
SURTF = 60.0  SURPS = 14.696
RESTF = 240.0
$ TOLERANCE
CVGOPT = 1
TOL_FLASH = 0.001
TOL_VOLUME = 0.001
TOL_MASS = 0.001
TOL_WATER = 0.001
TOL_ENERGY = 0.001
$ POROSITY
POROSITY1() = 0.3
$ PERMEABILITIES
XPERM1() = 200
YPERM1() = 200
ZPERM1() = 200
XYPERM1() = 0
XZPERM1() = 0
YZPERM1() = 0
$ INITIAL WATER SATURATION
SWINI1() = 0.000000000000017
$ INITIAL WATER CELL PRESSURE
PINI1() = 500.0
$ INITIAL PHASE VISCOSITIES AT EACH CELL
VIS1() = 1.0
$ INITIAL COMPOSITIONS
ZXY1(,,,1) = .05
ZXY1(,,,2) = .15
ZXY1(,,,3) = .3
ZXY1(,,,4) = .5
$RELPERM DATA
RELP 2
$MODREL(1) = 3
NRELFUN  1
ENDPT() = 0.4 0.7 0.5
```

```
SR() = 0.2 0.25 0.06
EXPN() = 2.5 2.0 1.5
ENERGY
ACPR1 = 35.0
HKCONST
HKROCK = 35.0
HEATLOSS
HKCONSTS
HKROCKS = 25.0
ACPI(,)= -4.4082 0.5815 -0.0003116 0.00000006504 0.0
         -0.45171 0.054851 -0.00003 0.00000000646  0.0
         -0.203 0.044 -0.000796 0.0000001722 0.0
          32.24 0.001924 0.00001055 -0.000000003596 0.0
TMEINI1() = 550.0
$END OF ENERGY DATA
$ ============== WELL SPECIFICATIONS ==============
NUMWELL = 2
$ --- The first well ---
WELLNAME(1) = "INJECTOR 1"
KINDWELL(1) = 2
WELLTOP(1 TO 3,1,1) = 25 25 0
WELLBOTTOM(1 TO 3,1,1) = 25 25 20
DIAMETER(1,1) = 1.0
TEMPERATURE(1) = 800.0
PRLIMIT(1) = 14695
WELLPQ(1) Block
  Interpolation Linear
  Extrapolation Constant
     Data  0.    300.0
EndBlock
$ --- The 2nd well ---
WELLNAME(2) = "PRODUCER 1"
KINDWELL(2) = 3
WELLTOP(1 TO 3,1,2) = 2475 25 0
WELLBOTTOM(1 TO 3,1,2) = 2475 25 20
DIAMETER(1,2) = 1.0
WELLPQ(2) Block
  Interpolation Linear
  Extrapolation Constant
  Data  0.   500.
EndBlock
EndInitial
$ TRANSIENT DATA INPUT BLOCKS
BeginTime  0.0
TIME_CONTROL = 2
DELTIM = 0.01  DTIMMUL = 1.0  DTIMMAX = 30 DTIMMIN = 0.00001
TUNE = 0.5  DCMAX = 0.5  DAQCMAX = 0.5  DPMAX = 0.4 DSMAX = 0.4 DTMAX =
0.4
WZ()  0.0001 0.0001 0.0001 0.9997 0
EndTime
```

```
TITLE(2)="2-D 4-COMPONENT "
DESCRIPTION()=
"THICKNESS (FT) : 80"
"LENGTH (FT) : 50"
"WIDTH (FT) : 400"
"GRID BLOCKS : 8x1x8"
COMPOSITIONAL_MODEL
$DEBUGS
TIMEEND = 1700.0
$ I/O OPTIONS
OUTLEVEL = 1
$SPLINEOUT
$GEOMOUT
PROCOUT
OUTPUT_PRE
$OUTPUT_NPH
OUTPUT_SAT
OUTPUT_OIL
OUTPUT_GAS
OUTPUT_DEN
OUTPUT_WEL
OUTPUT_HIS
WELLFILE = "3COMP.WEL"
HISDATA_NUM = 300
OUTPUT_TIME() =  10 20 30 40 50 100 200 300 500 900
$NO_CRASH
$OUTPUT FREQUENCY
ISTEP(,,)=1
JSTEP(,,)=1
KSTEP(,,)=1
$ FAULT BLOCK AND MESH DATA
METHOD = 2
DOWN() = 0 0 1
NX(1) = 8  NY(1) = 1  NZ(1) = 8
MES = "cart"
DX() = 50  DY() = 50  DZ() = 10
$ COMPOUND NAMES
COMPOUND(1) = "C6"
COMPOUND(2) = "C10"
COMPOUND(3) = "C15"
COMPOUND(4) = "H2O"
WATERCOMP
$ COMPOUND CRITICAL TEMPERATURES
CRIT() 913.4 1120.11 1270.0 1165.47
$ COMPOUND CRITICAL PRESSURES
CRIP() 436.9 367.647 200.0 3198.72
$ COMPOUND CRITICAL VOLUMES
CRIV() 5.923 8.415 16.696 0.91465
$ COMPOUND ACEN
ACEN() 0.301 0.443774 0.650 0.344
$ COMPOUND MOL WEIGHTS
MOLW() 86.2 134.0 206.0 18.015
```

```
$ COMPOUND PARA
PARA() 271.0 622.1 631.0 52.0
$ BINARY INTERACTION COEFFICIENS
BINC(,) = 0.0   0.0028 0.01097  0.48
          0.0028   0.0 0.02657  0.48
          0.01097 0.02657  0.0  0.48
          0.48    0.48     0.48 0.0
$ MAX NUMBER OF PHASES
NPHASE = 4
$ MAXNEWT MAX NUMBER OF NEWTON ITERATION
MAXNEWT = 20
$ Initial rock & water properties
ROCKZ = 0.00005  ROCKP = 14.7
H2OZ = 0.000003  H2OP = 14.696  H2OD = 3.468
SURTF = 60.0  SURPS = 14.696
RESTF = 240.0
$ TOLERANCE
CVGOPT = 1
TOL_FLASH = 0.001
TOL_VOLUME = 0.001
TOL_MASS = 0.001
TOL_WATER = 0.001
TOL_ENERGY = 0.001
$ POROSITY
POROSITY1() = 0.2
$ PERMEABILITIES
XPERM1() = 100
YPERM1() = 100
ZPERM1() = 100
XYPERM1() = 0
XZPERM1() = 0
YZPERM1() = 0
$ INITIAL WATER SATURATION
SWINI1() = 0.000000000000017
$ INITIAL WATER CELL PRESSURE
PINI1() = 600.0
$ INITIAL PHASE VISCOSITIES AT EACH CELL
VIS1() = 1.0
$ INITIAL COMPOSITIONS
ZXY1(,,,1) = .2
ZXY1(,,,2) = .2
ZXY1(,,,3) = .3
ZXY1(,,,4) = .3
$RELPERM DATA
RELP 2
$ NRELFUN 1 for corey, more to be added later
NRELFUN  1
$ data for each phase : water, phase 2 and phase 3
ENDPT() = 0.8 0.7 0.
SR() = 0.25 0.15 0.06
EXPN() = 2.5 2.0 1.5
ENERGY
ACPR1 = 35.0
```

```
HKCONST
HKROCK = 35.0
HEATLOSS
HKCONSTS
HKROCKS = 25.0
$VISCOCORRW
VISCOCORRO
AVISO(,) = -4.034 835.35
-4.460 1286.2
-4.648 1654.4
-5.353 1515.7
ACPI(,)= -4.4082 0.5815 -0.0003116 0.00000006504 0.0
         -0.45171 0.054851 -0.00003 0.00000000646  0.0
         -0.203 0.044 -0.000796 0.0000001722 0.0
          32.24 0.001924 0.00001055 -0.000000003596 0.0
TMEINI1() = 550.0
$ ============== WELL SPECIFICATIONS ==============
NUMWELL = 2
$ --- The first well ---
WELLNAME(1) = "INJECTOR 1"
KINDWELL(1) = 2
WELLTOP(1 TO 3,1,1) = 25 25 0
WELLBOTTOM(1 TO 3,1,1) = 25 25 80
DIAMETER(1,1) = 1.0
TEMPERATURE(1) = 800.0
PRLIMIT(1) = 14695
WELLPQ(1) Block
  Interpolation Linear
  Extrapolation Constant
     Data  0.    1000.0
EndBlock
$ --- The 2nd well ---
WELLNAME(2) = "PRODUCER 1"
KINDWELL(2) = 3
WELLTOP(1 TO 3,1,2) = 375 25 0
WELLBOTTOM(1 TO 3,1,2) = 375 25 80
DIAMETER(1,2) = 1.0
WELLPQ(2) Block
  Interpolation Linear
  Extrapolation Constant
  Data  0.   600.
EndBlock
EndInitial
$ TRANSIENT DATA INPUT BLOCKS
BeginTime  0.0
TIME_CONTROL = 2
DELTIM = 0.01  DTIMMUL = 1.0  DTIMMAX = 30 DTIMMIN = 0.00001
TUNE = 0.5  DCMAX = 0.5  DAQCMAX = 0.5  DPMAX = 0.3  DSMAX = 0.5 DTMAX =
0.3
WZ()  0.0001 0.0001 0.0001 0.9997 0
EndTime
```

```
TITLE(2)="3-D 4-COMPONENT "

DESCRIPTION()=
"THICKNESS (FT) : 30"
"LENGTH (FT) : 320"
"WIDTH (FT) : 320"
"GRID BLOCKS : 8x8x3"
COMPOSITIONAL_MODEL
$DEBUGS
TIMEEND = 2000
$ I/O OPTIONS
OUTLEVEL = 1
$SPLINEOUT
$GEOMOUT
PROCOUT
OUTPUT_PRE
$OUTPUT_NPH
OUTPUT_SAT
OUTPUT_OIL
OUTPUT_GAS
OUTPUT_DEN
OUTPUT_WEL
OUTPUT_HIS
WELLFILE = "3COMP.WEL"
HISDATA_NUM = 300
OUTPUT_TIME() =  10 20 30 40 50 100 200 300 500 900
$NO_CRASH
$OUTPUT FREQUENCY
ISTEP(,,)=1
JSTEP(,,)=1
KSTEP(,,)=1
$ FAULT BLOCK AND MESH DATA
METHOD = 2
DOWN() = 0 0 1
NX(1) = 8  NY(1) = 8  NZ(1) = 3
MES = "cart"
DX() = 40  DY() = 40  DZ() = 10
$ COMPOUND NAMES
COMPOUND(1) = "C6"
COMPOUND(2) = "C10"
COMPOUND(3) = "C15"
COMPOUND(4) = "H2O"
WATERCOMP
$ COMPOUND CRITICAL TEMPERATURES
CRIT() 913.4 1120.11 1270.0 1165.47

$ COMPOUND CRITICAL PRESSURES
CRIP() 436.9 367.647 200.0 3198.72

$ COMPOUND CRITICAL VOLUMES
CRIV() 5.923 8.415 16.696 0.91465

$ COMPOUND ACEN
```

```
ACEN() 0.301 0.443774 0.650 0.344

$ COMPOUND MOL WEIGHTS
MOLW() 86.2 134.0 206.0 18.015

$ COMPOUND PARA
PARA() 271.0 622.1 631.0 52.0

$ BINARY INTERACTION COEFFICIENS
BINC(,) = 0.0   0.0028 0.01097  0.48
          0.0028   0.0 0.02657  0.48
          0.01097 0.02657  0.0  0.48
          0.48    0.48     0.48 0.0
$ MAX NUMBER OF PHASES
NPHASE = 4
$ MAXNEWT MAX NUMBER OF NEWTON ITERATION
MAXNEWT = 20
$ Initial rock & water properties
ROCKZ = 0.0001  ROCKP = 14.7
H2OZ = 0.000003  H2OP = 14.696  H2OD = 3.468
SURTF = 60.0  SURPS = 14.696
RESTF = 240.0
$ TOLERANCE
CVGOPT = 1
TOL_FLASH = 0.001
TOL_VOLUME = 0.001
TOL_MASS = 0.001
TOL_WATER = 0.001
TOL_ENERGY = 0.001
$ POROSITY
POROSITY1() = 0.3
$ PERMEABILITIES
XPERM1() = 100
YPERM1() = 100
ZPERM1() = 100
XYPERM1() = 0
XZPERM1() = 0
YZPERM1() = 0
$ INITIAL WATER SATURATION
SWINI1() = 0.000000000000017
$ INITIAL WATER CELL PRESSURE
PINI1() = 600.0
$ INITIAL PHASE VISCOSITIES AT EACH CELL
VIS1() = 1.0
$ INITIAL COMPOSITIONS
ZXY1(,,,1) = .15
ZXY1(,,,2) = .2
ZXY1(,,,3) = .25
ZXY1(,,,4) = .4
$RELPERM DATA
RELP 2
$MODREL(1) = 3
NRELFUN  1
```

```
$ data for each phase : water, phase 2 and phase 3
ENDPT() = 0.8 0.7 0.5
SR() = 0.25 0.15 0.06
EXPN() = 2.5 2.0 1.5
ENERGY
ACPR1 = 35.0
HKCONST
HKROCK = 35.0
HEATLOSS
HKCONSTS
HKROCKS = 35.0
ACPI(,)= -4.4082 0.5815 -0.0003116 0.00000006504 0.0
         -0.45171 0.054851 -0.00003 0.00000000646  0.0
         -0.203 0.044 -0.000796 0.0000001722 0.0
          32.24 0.001924 0.00001055 -0.000000003596 0.0
TMEINI1() = 590.0
$ ============== WELL SPECIFICATIONS ==============
NUMWELL = 2
$ --- The first well ---
WELLNAME(1) = "INJECTOR 1"
KINDWELL(1) = 2
WELLTOP(1 TO 3,1,1) = 20 20 0
WELLBOTTOM(1 TO 3,1,1) = 20 20 60
DIAMETER(1,1) = 1.0
TEMPERATURE(1) = 1000.0
VOLTAGE(1) = -100.0
PRLIMIT(1) = 14695
WELLPQ(1) Block
  Interpolation Linear
  Extrapolation Constant
      Data  0.    1000.0
EndBlock
$ --- The 2nd well ---
WELLNAME(2) = "PRODUCER 1"
KINDWELL(2) = 3
WELLTOP(1 TO 3,1,2) = 300 300 0
WELLBOTTOM(1 TO 3,1,2) = 300 300 60
DIAMETER(1,2) = 1.0
VOLTAGE(2) = 100.0
WELLPQ(2) Block
  Interpolation Linear
  Extrapolation Constant
  Data  0.   600.
EndBlock
EndInitial
$ TRANSIENT DATA INPUT BLOCKS
BeginTime  0.0
TIME_CONTROL = 2
DELTIM = 0.01  DTIMMUL = 1.0  DTIMMAX = 30 DTIMMIN = 0.00001
TUNE = 0.5  DCMAX = 0.5  DAQCMAX = 0.5  DPMAX = 0.5  DSMAX = 0.5 DTMAX =
0.5
WZ()  0.0001 0.0001 0.0001 0.9997 0
EndTime
```

```
TITLE(2)="1-D 6-COMPONENT"
DESCRIPTION()=
"THICKNESS (FT) : 40"
"LENGTH (FT) : 2000"
"WIDTH (FT) : 40"
"GRID BLOCKS : 50x1x1"
COMPOSITIONAL_MODEL
$DEBUGS
TIMEEND = 3650
$ I/O OPTIONS
OUTLEVEL = 1
PROCOUT
OUTPUT_PRE
OUTPUT_SAT
OUTPUT_OIL
OUTPUT_GAS
OUTPUT_DEN
OUTPUT_WEL
OUTPUT_HIS
WELLFILE = "3COMP.WEL"
HISDATA_NUM = 30000
OUTPUT_TIME() =  10 20 30 40 50 100 200 300 500 900
$NO_CRASH
$OUTPUT FREQUENCY
ISTEP(,,)=1
JSTEP(,,)=1
KSTEP(,,)=1
$ FAULT BLOCK AND MESH DATA
METHOD = 2
DOWN() = 0 0 1
NX(1) = 50  NY(1) = 1  NZ(1) = 1
MES = "cart"
DX() = 40  DY() = 40  DZ() = 40
$ COMPOUND NAMES
COMPOUND(1) = "C10"
COMPOUND(2) = "C15"
COMPOUND(3) = "C19"
COMPOUND(4) = "C25"
COMPOUND(5) = "C26+"
COMPOUND(6) = "H2O"
WATERCOMP
$ COMPOUND CRITICAL TEMPERATURES
CRIT() 1120.11 1270.0 1388.13 1499.19 1710.33 1165.47
$ COMPOUND CRITICAL PRESSURES
CRIP() 367.647 200.0 221.38 174.05 140.0 3206.2
$ COMPOUND CRITICAL VOLUMES
CRIV() 8.415 16.696 15.89 19.63 25.95 0.91465
$ COMPOUND ACEN
ACEN() 0.443774 0.650 0.790075 0.965388 3.06 0.344
$ COMPOUND MOL WEIGHTS
MOLW() 134.0 206.0 263.0 337.0 450.0 18.015
$ COMPOUND PARA
```

```
PARA() 622.1 631.0 685.9 827.3 996.6 52.0
$ MAX NUMBER OF PHASES
NPHASE = 4
$ MAXNEWT MAX NUMBER OF NEWTON ITERATION
MAXNEWT = 20
$ Initial rock & water properties
ROCKZ = 0.0001  ROCKP = 14.7
H2OZ = 0.000003  H2OP = 14.696  H2OD = 3.468
SURTF = 60.0  SURPS = 14.696
RESTF = 240.0
$ TOLERANCE
CVGOPT = 1
TOL_FLASH = 0.001
TOL_VOLUME = 0.001
TOL_MASS = 0.001
TOL_WATER = 0.001
TOL_ENERGY = 0.001
$ POROSITY
POROSITY1() = 0.3
$ PERMEABILITIES
XPERM1() = 250
YPERM1() = 100
ZPERM1() = 100
XYPERM1() = 0
XZPERM1() = 0
YZPERM1() = 0
$ INITIAL WATER SATURATION
SWINI1() = 0.000000000000017
$ INITIAL WATER CELL PRESSURE
PINI1() = 650
$ INITIAL PHASE VISCOSITIES AT EACH CELL
VIS1() = 1.0
$ INITIAL COMPOSITIONS
ZXY1(,,,1) = 0.0001
ZXY1(,,,2) = 0.0002
ZXY1(,,,3) = 0.0002
ZXY1(,,,4) = 0.0005
ZXY1(,,,5) = 0.199
ZXY1(,,,6) = 0.8
$RELPERM DATA
RELP 2
NRELFUN  1
ENDPT() = 0.9 0.55 0.6
SR() = 0.12 0.2 0.06
EXPN() = 2.5 2.0 1.5
ENERGY
ACPR1 = 35.0
HKCONST
HKROCK = 35.0
HEATLOSS
HKCONSTS
HKROCKS = 20.0
ACPI(,)= -0.45171 0.054851 -0.00003 0.00000000646  0.0
```

```
          -0.203 0.044 -0.000796 0.0000001722 0.0
          -0.15171 0.00054851 -0.00003 0.00000000646  0.0
          -0.11171 0.00054851 -0.00003 0.00000000646  0.0
           40.833 4.532 -0.00181 0.0 0.0
           32.24 0.001924 0.00001055 -0.000000003596 0.0
TMEINI1() = 560.0
$ ============== WELL SPECIFICATIONS ==============
NUMWELL = 2
$ --- The first well ---
WELLNAME(1) = "INJECTOR 1"
KINDWELL(1) = 1
WELLTOP(1 TO 3,1,1) = 20 20 0
WELLBOTTOM(1 TO 3,1,1) = 20 20 40
DIAMETER(1,1) = 1.0
TEMPERATURE(1) = 1000.0
PRLIMIT(1) = 14695
WELLPQ(1) Block
  Interpolation Linear
  Extrapolation Constant
     Data  0.    700.0
EndBlock
$ --- The 2nd well ---
WELLNAME(2) = "PRODUCER 1"
KINDWELL(2) = 3
WELLTOP(1 TO 3,1,2) = 1980 20 0
WELLBOTTOM(1 TO 3,1,2) = 1980 20 40
DIAMETER(1,2) = 1.0
WELLPQ(2) Block
  Interpolation Linear
  Extrapolation Constant
  Data  0.   630.
EndBlock
EndInitial
$ TRANSIENT DATA INPUT BLOCKS
BeginTime  0.0
TIME_CONTROL = 2
DELTIM = 0.01  DTIMMUL = 1.0  DTIMMAX = 30 DTIMMIN = 0.00001
TUNE = 0.5  DCMAX = 0.5  DAQCMAX = 0.5  DPMAX = 0.5  DSMAX = 0.5 DTMAX =
0.5
WZ()  0.0001 0.0001 0.0001 0.0001 0.0001 0.9995 0
EndTime
```

```
TITLE(2)="2-D 6-COMPONENT"
DESCRIPTION()=
"THICKNESS (FT) : 50"
"LENGTH (FT) : 500"
"WIDTH (FT) : 50"
"GRID BLOCKS : 50x1x5"
COMPOSITIONAL_MODEL
$DEBUGS
TIMEEND = 1300
$ I/O OPTIONS
OUTLEVEL = 1
PROCOUT
OUTPUT_PRE
$OUTPUT_NPH
OUTPUT_SAT
OUTPUT_OIL
OUTPUT_GAS
OUTPUT_DEN
OUTPUT_WEL
OUTPUT_HIS
WELLFILE = "6COMP.WEL"
HISDATA_NUM = 300
OUTPUT_TIME() =  10 20 30 40 50 100 200 300 500 900
$NO_CRASH
$OUTPUT FREQUENCY
ISTEP(,,)=1
JSTEP(,,)=1
KSTEP(,,)=1
$ FAULT BLOCK AND MESH DATA
METHOD = 2
DOWN() = 0 0 1
NX(1) = 10  NY(1) = 1  NZ(1) = 5
MES = "cart"
DX() = 50  DY() = 50  DZ() = 10
$ COMPOUND NAMES
COMPOUND(1) = "C10"
COMPOUND(2) = "C15"
COMPOUND(3) = "C19"
COMPOUND(4) = "C25"
COMPOUND(5) = "C26+"
COMPOUND(6) = "H2O"
WATERCOMP
$ COMPOUND CRITICAL TEMPERATURES
CRIT() 1120.11 1270.0 1388.13 1499.19 1710.33 1165.47
$ COMPOUND CRITICAL PRESSURES
CRIP() 367.647 200.0 221.38 174.05 140.0 3206.2
$ COMPOUND CRITICAL VOLUMES
CRIV() 8.415 16.696 15.89 19.63 25.95 0.91465
$ COMPOUND ACEN
ACEN() 0.443774 0.650 0.790075 0.965388 3.06 0.344
$ COMPOUND MOL WEIGHTS
MOLW() 134.0 206.0 263.0 337.0 450.0 18.015
```

```
$ COMPOUND PARA
PARA() 622.1 631.0 685.9 827.3 996.6 52.0
NPHASE = 4
$ MAXNEWT MAX NUMBER OF NEWTON ITERATION
MAXNEWT = 20
$ Initial rock & water properties
ROCKZ = 0.0001  ROCKP = 14.7
H2OZ = 0.000003  H2OP = 14.696  H2OD = 3.468
SURTF = 60.0  SURPS = 14.696
RESTF = 240.0
$ TOLERANCE
CVGOPT = 1
TOL_FLASH = 0.001
TOL_VOLUME = 0.001
TOL_MASS = 0.001
TOL_WATER = 0.001
TOL_ENERGY = 0.001
$ POROSITY
POROSITY1() = 0.3
$ PERMEABILITIES
XPERM1() = 100
YPERM1() = 100
ZPERM1() = 100
XYPERM1() = 0
XZPERM1() = 0
YZPERM1() = 0
$ INITIAL WATER SATURATION
SWINI1() = 0.000000000000017
$ INITIAL WATER CELL PRESSURE
PINI1() = 650
$ INITIAL PHASE VISCOSITIES AT EACH CELL
VIS1() = 1.0
$ INITIAL COMPOSITIONS
ZXY1(,,,1) = 0.0001
ZXY1(,,,2) = 0.0002
ZXY1(,,,3) = 0.0002
ZXY1(,,,4) = 0.0005
ZXY1(,,,5) = 0.199
ZXY1(,,,6) = 0.8
$RELPERM DATA
RELP 2
NRELFUN  1
ENDPT() = 0.9 0.55 0.6
SR() = 0.15 0.2 0.06
EXPN() = 2.5 2.0 1.5
ENERGY
ACPR1 = 35.0
HKCONST
HKROCK = 35.0
HEATLOSS
HKCONSTS
HKROCKS = 20.0
ACPI(,)= -0.45171 0.054851 -0.00003 0.00000000646  0.0
```

```
          -0.203 0.044 -0.000796 0.0000001722 0.0
          -0.15171 0.00054851 -0.00003 0.00000000646  0.0
          -0.11171 0.00054851 -0.00003 0.00000000646  0.0
           40.833 4.532 -0.00181 0.0 0.0
           32.24 0.001924 0.00001055 -0.000000003596 0.0
TMEINI1() = 560.0
$ ============== WELL SPECIFICATIONS ==============
NUMWELL = 2
$ --- The first well ---
WELLNAME(1) = "INJECTOR 1"
KINDWELL(1) = 2
WELLTOP(1 TO 3,1,1) = 25 25 0
WELLBOTTOM(1 TO 3,1,1) = 25 25 50
DIAMETER(1,1) = 1.0
TEMPERATURE(1) = 800.0
PRLIMIT(1) = 14695
WELLPQ(1) Block
  Interpolation Linear
  Extrapolation Constant
     Data  0.    500.0
EndBlock
$ --- The 2nd well ---
WELLNAME(2) = "PRODUCER 1"
KINDWELL(2) = 3
WELLTOP(1 TO 3,1,2) = 475 25 0
WELLBOTTOM(1 TO 3,1,2) = 475 25 50
DIAMETER(1,2) = 1.0
WELLPQ(2) Block
  Interpolation Linear
  Extrapolation Constant
  Data  0.   650.
EndBlock
EndInitial
$ TRANSIENT DATA INPUT BLOCKS
BeginTime  0.0
TIME_CONTROL = 2
DELTIM = 0.01  DTIMMUL = 1.0  DTIMMAX = 30 DTIMMIN = 0.00001
TUNE = 0.5  DCMAX = 0.5  DAQCMAX = 0.5  DPMAX = 0.5  DSMAX = 0.5 DTMAX =
0.5
WZ()  0.0001 0.0001 0.0001 0.0001 0.0001 0.9995 0
EndTime
```

G.2.3 Input files for Chapter 5, Electrical Heating Model

```
TITLE(2)="1-D 6-COMPONENT "
DESCRIPTION()=
"THICKNESS (FT) : 40"
"LENGTH (FT) : 2000"
"WIDTH (FT) : 40"
"GRID BLOCKS : 50x1x1"
COMPOSITIONAL_MODEL
$DEBUGS
TIMEEND = 3650
$ I/O OPTIONS
OUTLEVEL = 1
PROCOUT
OUTPUT_PRE
OUTPUT_SAT
OUTPUT_OIL
OUTPUT_LIQ_2
OUTPUT_TEMP
OUTPUT_VOLT
OUTPUT_GAS
OUTPUT_DEN
OUTPUT_WEL
OUTPUT_HIS
WELLFILE = "3COMP.WEL"
HISDATA_NUM = 30000
OUTPUT_TIME() =  10 20 30 40 50 100 200 300 500 900
$NO_CRASH
$OUTPUT FREQUENCY
ISTEP(,,)=1
JSTEP(,,)=1
KSTEP(,,)=1
$ FAULT BLOCK AND MESH DATA
METHOD = 2
DOWN() = 0 0 1
NX(1) = 50  NY(1) = 1  NZ(1) = 1
MES = "cart"
DX() = 40  DY() = 40  DZ() = 40
$ COMPOUND NAMES
COMPOUND(1) = "C10"
COMPOUND(2) = "C15"
COMPOUND(3) = "C19"
COMPOUND(4) = "C25"
COMPOUND(5) = "C26+"
COMPOUND(6) = "H2O"
WATERCOMP
$ COMPOUND CRITICAL TEMPERATURES
CRIT() 1120.11 1270.0 1388.13 1499.19 1710.33 1165.47
$ COMPOUND CRITICAL PRESSURES
```

```
CRIP() 367.647 200.0 221.38 174.05 140.0 3206.2
$ COMPOUND CRITICAL VOLUMES
CRIV() 8.415 16.696 15.89 19.63 25.95 0.91465
$ COMPOUND ACEN
ACEN() 0.443774 0.650 0.790075 0.965388 2.06 0.344
$ COMPOUND MOL WEIGHTS
MOLW() 134.0 206.0 263.0 337.0 450.0 18.015
$ COMPOUND PARA
PARA() 622.1 631.0 685.9 827.3 996.6 52.0
$ MAX NUMBER OF PHASES
NPHASE = 4
$ MAXNEWT MAX NUMBER OF NEWTON ITERATION
MAXNEWT = 20
$ Initial rock & water properties
ROCKZ = 0.0001  ROCKP = 14.7
H2OZ = 0.000003  H2OP = 14.696  H2OD = 3.468
SURTF = 60.0  SURPS = 14.696
RESTF = 240.0
$ TOLERANCE
CVGOPT = 1
TOL_FLASH = 0.001
TOL_VOLUME = 0.001
TOL_MASS = 0.001
TOL_WATER = 0.001
TOL_ENERGY = 0.001
$ POROSITY
POROSITY1() = 0.3
$ PERMEABILITIES
XPERM1() = 250
YPERM1() = 100
ZPERM1() = 100
XYPERM1() = 0
XZPERM1() = 0
YZPERM1() = 0
$ INITIAL WATER SATURATION
SWINI1() = 0.000000000000017
$ INITIAL WATER CELL PRESSURE
PINI1() = 650
$ INITIAL PHASE VISCOSITIES AT EACH CELL
VIS1() = 1.0
$ INITIAL COMPOSITIONS
ZXY1(,,,1) = 0.0001
ZXY1(,,,2) = 0.0002
ZXY1(,,,3) = 0.0002
ZXY1(,,,4) = 0.0005
ZXY1(,,,5) = 0.199
ZXY1(,,,6) = 0.8
$RELPERM DATA
RELP 2
$MODREL(1) = 3
NRELFUN  1
ENDPT() = 0.9 0.55 0.6
SR() = 0.12 0.2 0.06
```

```
EXPN() = 2.5 2.0 1.5
ENERGY
ACPR1 = 35.0
HKCONST
HKROCK = 35.0
HEATLOSS
HKCONSTS
HKROCKS = 20.0
ACPI(,)= -0.45171 0.054851 -0.00003 0.00000000646  0.0
         -0.203 0.044 -0.000796 0.0000001722 0.0
         -0.15171 0.00054851 -0.00003 0.00000000646  0.0
         -0.11171 0.00054851 -0.00003 0.00000000646  0.0
          0.9833 4.532 -0.00181 0.0 0.0
          32.24 0.001924 0.00001055 -0.000000003596 0.0
TMEINI1() = 560.0
ELECTHEAT
COND_CONST
N_DATAE 3
T_DATAE()= 582.0 762.0 942.0
CONDW()= 0.8 1.6 2.4
CONDO()= 0.0 0.0 0.0
CONDR()= 0.0 0.0 0.0
VOLTGINI1() = 0.0
$ ============== WELL SPECIFICATIONS ==============
NUMWELL = 2
$ --- The first well ---
WELLNAME(1) = "INJECTOR 1"
KINDWELL(1) = 1
WELLTOP(1 TO 3,1,1) = 20 20 0
WELLBOTTOM(1 TO 3,1,1) = 20 20 40
DIAMETER(1,1) = 1.0
TEMPERATURE(1) = 560.001
VOLTAGE(1) = 200.0
PRLIMIT(1) = 14695
WELLPQ(1) Block
  Interpolation Linear
  Extrapolation Constant
     Data  0.    900.0
EndBlock
$ --- The 2nd well ---
WELLNAME(2) = "PRODUCER 1"
KINDWELL(2) = 3
WELLTOP(1 TO 3,1,2) = 1980 20 0
WELLBOTTOM(1 TO 3,1,2) = 1980 20 40
DIAMETER(1,2) = 1.0
VOLTAGE(2) = 0.0
WELLPQ(2) Block
  Interpolation Linear
  Extrapolation Constant
  Data  0.   650.
EndBlock
EndInitial
$ TRANSIENT DATA INPUT BLOCKS
```

```
BeginTime  0.0
TIME_CONTROL = 2
DELTIM = 0.01  DTIMMUL = 1.0  DTIMMAX = 30 DTIMMIN = 0.00001
TUNE = 0.5  DCMAX = 0.5  DAQCMAX = 0.5  DPMAX = 0.5  DSMAX = 0.5 DTMAX =
0.5
WZ()  0.0001 0.0001 0.0001 0.0001 0.0001 0.9995 0
EndTime



TITLE(2)="2-D 6-OMPONENT "
DESCRIPTION()=
"THICKNESS (FT) : 30"
"LENGTH (FT) : 800"
"WIDTH (FT) : 40"
"GRID BLOCKS : 20x1x3"
COMPOSITIONAL_MODEL
$DEBUGS
TIMEEND = 3650
$ I/O OPTIONS
OUTLEVEL = 1
PROCOUT
OUTPUT_PRE
$OUTPUT_NPH
OUTPUT_SAT
OUTPUT_OIL
OUTPUT_GAS
OUTPUT_DEN
OUTPUT_WEL
OUTPUT_HIS
WELLFILE = "3COMP.WEL"
HISDATA_NUM = 30000
OUTPUT_TIME() =  10 20 30 40 50 100 200 300 500 900
$NO_CRASH
$OUTPUT FREQUENCY
ISTEP(,,)=1
JSTEP(,,)=1
KSTEP(,,)=1
$ FAULT BLOCK AND MESH DATA
METHOD = 2
DOWN() = 0 0 1
NX(1) = 20  NY(1) = 1  NZ(1) = 3
MES = "cart"
DX() = 40  DY() = 40  DZ() = 10
$ COMPOUND NAMES
COMPOUND(1) = "C10"
COMPOUND(2) = "C15"
COMPOUND(3) = "C19"
COMPOUND(4) = "C25"
COMPOUND(5) = "C26+"
COMPOUND(6) = "H2O"
WATERCOMP
```

```
$ COMPOUND CRITICAL TEMPERATURES
CRIT() 1120.11 1270.0 1388.13 1499.19 1710.33 1165.47
$ COMPOUND CRITICAL PRESSURES
CRIP() 367.647 200.0 221.38 174.05 140.0 3206.2
$ COMPOUND CRITICAL VOLUMES
CRIV() 8.415 16.696 15.89 19.63 25.95 0.91465
$ COMPOUND ACEN
ACEN() 0.443774 0.650 0.790075 0.965388 3.06 0.344
$ COMPOUND MOL WEIGHTS
MOLW() 134.0 206.0 263.0 337.0 450.0 18.015
$ COMPOUND PARA
PARA() 622.1 631.0 685.9 827.3 996.6 52.0
NPHASE = 4
$ MAXNEWT MAX NUMBER OF NEWTON ITERATION
MAXNEWT = 20
$ Initial rock & water properties
ROCKZ = 0.0001  ROCKP = 14.7
H2OZ = 0.000003  H2OP = 14.696  H2OD = 3.468
SURTF = 60.0  SURPS = 14.696
RESTF = 240.0
$ TOLERANCE
CVGOPT = 1
TOL_FLASH = 0.001
TOL_VOLUME = 0.001
TOL_MASS = 0.001
TOL_WATER = 0.001
TOL_ENERGY = 0.001
$ POROSITY
POROSITY1() = 0.3
$ PERMEABILITIES
XPERM1() = 200
YPERM1() = 200
ZPERM1() = 100
XYPERM1() = 0
XZPERM1() = 0
YZPERM1() = 0
$ INITIAL WATER SATURATION
SWINI1() = 0.000000000000017
$ INITIAL WATER CELL PRESSURE
PINI1() = 650
$ INITIAL PHASE VISCOSITIES AT EACH CELL
VIS1() = 1.0
$ INITIAL COMPOSITIONS
ZXY1(,,,1) = 0.0001
ZXY1(,,,2) = 0.0002
ZXY1(,,,3) = 0.0002
ZXY1(,,,4) = 0.0005
ZXY1(,,,5) = 0.199
ZXY1(,,,6) = 0.8
$RELPERM DATA
RELP 2
NRELFUN  1
ENDPT() = 0.9 0.55 0.6
```

```
SR() = 0.12 0.2 0.06
EXPN() = 2.5 2.0 1.5
ENERGY
ACPR1 = 35.0
HKCONST
HKROCK = 35.0
HEATLOSS
HKCONSTS
HKROCKS = 20.0
ACPI(,)= -0.45171 0.054851 -0.00003 0.00000000646  0.0
         -0.203 0.044 -0.000796 0.0000001722 0.0
         -0.15171 0.00054851 -0.00003 0.00000000646  0.0
         -0.11171 0.00054851 -0.00003 0.00000000646  0.0
          40.833 4.532 -0.00181 0.0 0.0
          32.24 0.001924 0.00001055 -0.000000003596 0.0
TMEINI1() = 560.0
ELECTHEAT
N_DATAE 3
T_DATAE()= 582.0 762.0 942.0
CONDW()= 0.8 1.6 2.4
CONDO()= 0.00 .00 0.00
CONDR()= 0.00 .00 0.00
VOLTGINI1() = 0.0
$ ============== WELL SPECIFICATIONS ==============
NUMWELL = 2
$ --- The first well ---
WELLNAME(1) = "INJECTOR 1"
KINDWELL(1) = 1
WELLTOP(1 TO 3,1,1) = 20 20 0
WELLBOTTOM(1 TO 3,1,1) = 20 20 30
DIAMETER(1,1) = 1.0
TEMPERATURE(1) = 560.001
VOLTAGE(1) = 0.0
PRLIMIT(1) = 14695
WELLPQ(1) Block
  Interpolation Linear
  Extrapolation Constant
     Data  0.    700.0
EndBlock
$ --- The 2nd well ---
WELLNAME(2) = "PRODUCER 1"
KINDWELL(2) = 3
WELLTOP(1 TO 3,1,2) = 780 20 0
WELLBOTTOM(1 TO 3,1,2) = 780 20 30
DIAMETER(1,2) = 1.0
VOLTAGE(2) = 200.0
WELLPQ(2) Block
  Interpolation Linear
  Extrapolation Constant
  Data  0.   635.
EndBlock
EndInitial
$ TRANSIENT DATA INPUT BLOCKS
```

```
BeginTime  0.0
TIME_CONTROL = 2
DELTIM = 0.01  DTIMMUL = 1.0  DTIMMAX = 30 DTIMMIN = 0.00001
TUNE = 0.5  DCMAX = 0.5  DAQCMAX = 0.5  DPMAX = 0.5  DSMAX = 0.5 DTMAX =
0.5
WZ()  0.0001 0.0001 0.0001 0.0001 0.0001 0.9995 0
EndTime



TITLE(2)="3-D 6-COMPONENT "
DESCRIPTION()=
"THICKNESS (FT) : 50"
"LENGTH (FT) : 500"
"WIDTH (FT) : 500"
"GRID BLOCKS : 20x20x5"
COMPOSITIONAL_MODEL
$DEBUGS
TIMEEND = 3650
$ I/O OPTIONS
OUTLEVEL = 1
PROCOUT
OUTPUT_PRE
OUTPUT_SAT
OUTPUT_OIL
OUTPUT_LIQ_2
OUTPUT_TEMP
OUTPUT_VOLT
OUTPUT_GAS
OUTPUT_DEN
OUTPUT_WEL
OUTPUT_HIS
WELLFILE = "6COMP.WEL"
HISDATA_NUM = 30000
OUTPUT_TIME() =  10 20 30 40 50 100 200 300 500 900
$NO_CRASH
$OUTPUT FREQUENCY
ISTEP(,,)=1
JSTEP(,,)=1
KSTEP(,,)=1
$ FAULT BLOCK AND MESH DATA
METHOD = 2
DOWN() = 0 0 1
NX(1) = 20  NY(1) = 20  NZ(1) = 5
MES = "cart"
DX() = 25  DY() = 25  DZ() = 10
$ COMPOUND NAMES
COMPOUND(1) = "C10"
COMPOUND(2) = "C15"
COMPOUND(3) = "C19"
COMPOUND(4) = "C25"
COMPOUND(5) = "C26+"
```

```
COMPOUND(6) = "H2O"
WATERCOMP
$ COMPOUND CRITICAL TEMPERATURES
CRIT() 1120.11 1270.0 1388.13 1499.19 1710.33 1165.47
$ COMPOUND CRITICAL PRESSURES
CRIP() 367.647 200.0 221.38 174.05 140.0 3206.2
$ COMPOUND CRITICAL VOLUMES
CRIV() 8.415 16.696 15.89 19.63 25.95 0.91465
$ COMPOUND ACEN
ACEN() 0.443774 0.650 0.790075 0.965388 2.06 0.344
$ COMPOUND MOL WEIGHTS
MOLW() 134.0 206.0 263.0 337.0 450.0 18.015
$ COMPOUND PARA
PARA() 622.1 631.0 685.9 827.3 996.6 52.0
$ MAX NUMBER OF PHASES
NPHASE = 4
$ MAXNEWT MAX NUMBER OF NEWTON ITERATION
MAXNEWT = 20
$ Initial rock & water properties
ROCKZ = 0.0001  ROCKP = 14.7
H2OZ = 0.000003  H2OP = 14.696  H2OD = 3.468
SURTF = 60.0  SURPS = 14.696
RESTF = 240.0
$ TOLERANCE
CVGOPT = 1
TOL_FLASH = 0.001
TOL_VOLUME = 0.001
TOL_MASS = 0.001
TOL_WATER = 0.001
TOL_ENERGY = 0.001
$ POROSITY
POROSITY1() = 0.3
$ PERMEABILITIES
XPERM1() = 100
YPERM1() = 100
ZPERM1() = 100
XYPERM1() = 0
XZPERM1() = 0
YZPERM1() = 0
$ INITIAL WATER SATURATION
SWINI1() = 0.000000000000017
$ INITIAL WATER CELL PRESSURE
PINI1() = 650
$ INITIAL PHASE VISCOSITIES AT EACH CELL
VIS1() = 1.0
$ INITIAL COMPOSITIONS
ZXY1(,,,1) = 0.0001
ZXY1(,,,2) = 0.0002
ZXY1(,,,3) = 0.0002
ZXY1(,,,4) = 0.0005
ZXY1(,,,5) = 0.199
ZXY1(,,,6) = 0.8
$RELPERM DATA
```

```
RELP 2
$MODREL(1) = 3
NRELFUN  1
ENDPT() = 0.7 0.55 0.6
SR() = 0.1 0.2 0.06
EXPN() = 2.5 2.0 1.5
ENERGY
ACPR1 = 35.0
HKCONST
HKROCK = 35.0
HEATLOSS
HKCONSTS
HKROCKS = 20.0
ACPI(,)= -0.45171 0.054851 -0.00003 0.00000000646  0.0
         -0.203 0.044 -0.000796 0.0000001722 0.0
         -0.15171 0.00054851 -0.00003 0.00000000646  0.0
         -0.11171 0.00054851 -0.00003 0.00000000646  0.0
          0.98 4.532 -0.00181 0.0 0.0
          32.24 0.001924 0.00001055 -0.000000003596 0.0
TMEINI1() = 560.0
ELECTHEAT
COND_CONST
N_DATAE 3
T_DATAE()= 582.0 762.0 942.0
CONDW()= 0.6 1.6 2.4
CONDO()= 0.00 .00 0.00
CONDR()= 0.15 0.2 0.3
VOLTGINI1() = 0.0
$ ============== WELL SPECIFICATIONS ==============
NUMWELL = 2
$ --- The first well ---
WELLNAME(1) = "INJECTOR 1"
KINDWELL(1) = 1
WELLTOP(1 TO 3,1,1) = 12.5 12.5 0
WELLBOTTOM(1 TO 3,1,1) = 12.5 12.5 50
DIAMETER(1,1) = 1.0
TEMPERATURE(1) = 560.001
VOLTAGE(1) = 0.0
PRLIMIT(1) = 14695
WELLPQ(1) Block
  Interpolation Linear
  Extrapolation Constant
     Data  0.    750.0
EndBlock
$ --- The 2nd well ---
WELLNAME(2) = "PRODUCER 1"
KINDWELL(2) = 3
WELLTOP(1 TO 3,1,2) = 487.5 487.5 0
WELLBOTTOM(1 TO 3,1,2) = 487.5 487.5 50
DIAMETER(1,2) = 1.0
VOLTAGE(2) = 300.0
WELLPQ(2) Block
  Interpolation Linear
```

```
  Extrapolation Constant
  Data  0.   650.
EndBlock
EndInitial
$ TRANSIENT DATA INPUT BLOCKS
BeginTime  0.0
TIME_CONTROL = 2
DELTIM = 0.01  DTIMMUL = 1.0  DTIMMAX = 30 DTIMMIN = 0.00001
TUNE = 0.5  DCMAX = 0.5  DAQCMAX = 0.5  DPMAX = 0.5  DSMAX = 0.5 DTMAX =
0.5
WZ()  0.0001 0.0001 0.0001 0.0001 0.0001 0.9995 0
EndTime
```

G.2.4 Input files for Chapter 6, Hot Chemical Flooding Model

```
TITLE(2) = "1-D HOT-CHEMICAL FLOODING  DATA"
DESCRIPTION()=
"THICKNESS (FT) : 20 "
"LENGTH (FT) : 2000 "
"WIDTH (FT) : 20 "
"GRID BLOCKS : 100X1x1"
COMPOSITIONAL_MODEL
TIMEEND = 365
$ I/O OPTIONS
OUTLEVEL = 1
OUTPUT_PRE
OUTPUT_SAT
OUTPUT_VIS
OUTPUT_HIS
OUTPUT_AQ
OUTPUT_TRAP
OUTPUT_RELP
OUTPUT_IFT
OUTPUT_TEMP
OUTPUT_TIME() = 50 100 150 200 250 300 365
ISTEP(,,) = 1
JSTEP(,,) = 1
KSTEP(,,) = 1
$ FAULT BLOCK AND MESH DATA
METHOD = 2
DOWN() = 0 0 1
MES = "cart"
NX(1) = 100  NY(1) = 1  NZ(1) = 1
DX() = 20  DY() = 20  DZ() = 20
$ COMPOUND NAMES
COMPOUND(1) = "C10"
```

```
$ COMPOUND CRITICAL TEMPERATURES
CRIT() 1111.8
$ COMPOUND CRITICAL PRESSURES
CRIP() 304.0
$ COMPOUND CRITICAL VOLUMES
CRIV() 12.087
$ COMPOUND ACEN
ACEN() 0.488
$ COMPOUND MOL WEIGHTS
MOLW() 142.3
$ COMPOUND PARA
PARA() 431.0
$ MAX NUMBER OF PHASES
NPHASE = 4
$ Initial rock & water properties
ROCKZ = 0.00000  ROCKP = 14.7
H2OZ = 0.000003  H2OP = 14.7  H2OD = 3.467
SURTF = 60.0  SURPS = 14.7
RESTF = 60.0
$ TOLERANCE
CVGOPT = 1
TOL_FLASH = 0.0001
TOL_VOLUME = 0.0001
TOL_MASS = 0.0001
TOL_WATER = 0.0001
TOL_ENERGY = 0.001
MAXNEWT = 100
$ POROSITY
POROSITY1() = 0.2
$ PERMEABILITIES
XPERM1() = 500
YPERM1() = 500
ZPERM1() = 500
$ INITIAL WATER SATURATION
SWINI1() = 0.70
$ INITIAL WATER CELL PRESSURE
PINI1() = 20.0
$ INITIAL PHASE VISCOSITIES AT EACH CELL
VIS1() = 1.00
$ INITIAL COMPOSITIONS
ZXY1(,,,1) = 1.000
$ NUMERICAL METHOD
IMPAQCOMP
NAQCOMP 4
AQCOMPNAM() = "SALT" "SURFACTANT" "TRACER" "POLYMER"
AQCOMPTYPE() = 4 3 1 2
AQCOMPINIT() = 0.17 0.00 0.00 0.00
$ SURFACTANT PARAMETERS
EPSME 0.0001
HBNC70 0.07
HBNC71 0.04
CSEL7 0.177
CSEU7 0.25
```

```
AD31 1.5
AD32 0.5
B3D 1000.
$ IFT PARAMETERS
AHUH 9
CHUH 0.2
XIFTW 1.3
$ POLYMER PARAMETERS
AP1 81
AP2 2700
AP3 2500
SLOPP 0.0
AD41 0.0
AD42 0.0
B4D 100.0
$ RELPERM DATA
RELP 2
NRELFUN 1
ITRAP
ENDPTLOW() = 0.106 0.800 0.000
ENDPTHIGH() = 1.000 1.000 0.000
SRLOW() = 0.140 0.250 0.000
SRHIGH() = 0.000 0.000 0.000
EXPNLOW() = 2.100 1.700 0.000
EXPNHIGH() = 0.480 1.500 0.000
TL() = 364 59074 364
TAUL() = 1 1 1
ENERGY
VISCOCORRO
AVISO(,) = -0.978166136 558.61
VISCOCORRW
AVISW(,) = -4.89 1384.89
ACPR1 = 35.021
HKCONST
HKROCK = 25.0
HEATLOSS
HKCONSTS
HKROCKS = 25.02
TMEINI1()=520.0
ACPI(,)= -4.22 0.306 -0.0001585 0.0000000322 0.0
TREF 520.0
HBNT0 0.00017
HBNT1 0.00017
HBNT2 0.00017
ACPP() 1.0 0.5 1.0
NESM 1
C51L 0.177
BETAL 0.00415
C51U 0.25
BETAU 0.00415
CMCV
SCMC 0.0
RCMC 0.0001
```

```
CSEL7REF 0.177
CSEU7REF 0.25

NUMWELL = 2
WELLNAME(1) = "FIRST WELL"
KINDWELL(1) = 2
WELLTOP(1 TO 3,1,1) = 10 10 0
WELLBOTTOM(1 TO 3,1,1) = 10 10 20
DIAMETER(1,1) = 1.0
TEMPERATURE(1)=650.0
PRLIMIT(1) = 14000
WELLPQ(1) Block
  Interpolation Linear
  Extrapolation Constant
  Data  0.0  100.0
EndBlock
WELLNAME(2) = "SECOND WELL"
KINDWELL(2) = 3
WELLTOP(1 TO 3,1,2) = 1990 10 0
WELLBOTTOM(1 TO 3,1,2) = 1990 10 20
DIAMETER(1,2) = 1.0
WELLPQ(2) Block
  Interpolation Linear
  Extrapolation Constant
  Data  0.0  20.0
EndBlock
EndInitial
$ TRANSIENT DATA INPUT BLOCKS
BeginTime    0.0
TIME_CONTROL = 2
DELTIM = 0.1  DTIMMUL = 1.0  DTIMMAX = .3  DTIMMIN = 0.1
TUNE = 0.1 DPMAX = 0.5 DSMAX = 0.5 DCMAX = 0.5 DAQCMAX = 0.5 DTMAX = 0.5
WZ(,1) = 0 1
AQCOMP_WFINJ(,1) = 0.17 0.01 1.00 0.05
EndTime
BeginTime    64
WZ(,1) = 0 1
AQCOMP_WFINJ(,1) = 0.17 0.00 0.00 0.05
EndTime



TITLE(2) = "2-D HOT-CHEMICAL FLOODING DATA"
DESCRIPTION()=
"THICKNESS (FT) : 20 "
"LENGTH (FT) : 320 "
"WIDTH (FT) : 320 "
"GRID BLOCKS : 8X8x1"
COMPOSITIONAL_MODEL
TIMEEND = 365
$ I/O OPTIONS
OUTLEVEL = 1
OUTPUT_PRE
```

```
OUTPUT_SAT
OUTPUT_VIS
OUTPUT_HIS
OUTPUT_AQ
OUTPUT_TRAP
OUTPUT_RELP
OUTPUT_IFT
OUTPUT_TEMP
OUTPUT_TIME() = 50 100 150 200 250 300 365
ISTEP(,,) = 1
JSTEP(,,) = 1
KSTEP(,,) = 1
$ FAULT BLOCK AND MESH DATA
METHOD = 2
DOWN() = 0 0 1
MES = "cart"
NX(1) = 8  NY(1) = 8  NZ(1) = 1
DX() = 40  DY() = 40  DZ() = 20
$ COMPOUND NAMES
COMPOUND(1) = "C10"
$ COMPOUND CRITICAL TEMPERATURES
CRIT() 1111.8
$ COMPOUND CRITICAL PRESSURES
CRIP() 304.0
$ COMPOUND CRITICAL VOLUMES
CRIV() 12.087
$ COMPOUND ACEN
ACEN() 0.488
$ COMPOUND MOL WEIGHTS
MOLW() 142.3
$ COMPOUND PARA
PARA() 431.0
$ MAX NUMBER OF PHASES
NPHASE = 4
$ Initial rock & water properties
ROCKZ = 0.00000  ROCKP = 14.7
H2OZ = 0.000003  H2OP = 14.7  H2OD = 3.467
SURTF = 60.0  SURPS = 14.7
RESTF = 60.0
$ TOLERANCE
CVGOPT = 1
TOL_FLASH = 0.0001
TOL_VOLUME = 0.0001
TOL_MASS = 0.0001
TOL_WATER = 0.0001
TOL_ENERGY = 0.0001
MAXNEWT = 100
$ POROSITY
POROSITY1() = 0.2
$ PERMEABILITIES
XPERM1() = 500
YPERM1() = 500
ZPERM1() = 500
```

```
$ INITIAL WATER SATURATION
SWINI1() = 0.70
$ INITIAL WATER CELL PRESSURE
PINI1() = 20.0
$ INITIAL PHASE VISCOSITIES AT EACH CELL
VIS1() = 1.00
$ INITIAL COMPOSITIONS
ZXY1(,,,1) = 1.000
$ NUMERICAL METHOD
IMPAQCOMP
NAQCOMP 4
AQCOMPNAM() = "SALT" "SURFACTANT" "TRACER" "POLYMER"
AQCOMPTYPE() = 4 3 1 2
AQCOMPINIT() = 0.17 0.00 0.00 0.00
$ SURFACTANT PARAMETERS
EPSME 0.0001
HBNC70 0.07
HBNC71 0.04
CSEL7 0.177
CSEU7 0.25
AD31 1.5
AD32 0.5
B3D 1000.
$ IFT PARAMETERS
AHUH 9
CHUH 0.2
XIFTW 1.3
$ POLYMER PARAMETERS
AP1 81
AP2 2700
AP3 2500
SLOPP 0.0
AD41 0.0
AD42 0.0
B4D 100.0
$ RELPERM DATA
RELP 2
NRELFUN 1
ITRAP
ENDPTLOW() = 0.106 0.800 0.000
ENDPTHIGH() = 1.000 1.000 0.000
SRLOW() = 0.140 0.250 0.000
SRHIGH() = 0.000 0.000 0.000
EXPNLOW() = 2.100 1.700 0.000
EXPNHIGH() = 0.480 1.500 0.000
TL() = 364 59074 364
TAUL() = 1 1 1
ENERGY
VISCOCORRO
AVISO(,) = -0.978166136 558.61
VISCOCORRW
AVISW(,) = -4.89 1384.89
ACPR1 = 35.021
```

```
HKCONST
HKROCK = 25.0
HEATLOSS
HKCONSTS
HKROCKS = 25.02
TMEINI1()=520.0
ACPI(,)= -4.22 0.306 -0.0001585 0.0000000322 0.0
TREF 520.0
HBNT0 0.00017
HBNT1 0.00017
HBNT2 0.00017
ACPP() 1.0 0.5 1.0
NESM 1
C51L 0.177
BETAL 0.00415
C51U 0.25
BETAU 0.00415
CMCV
SCMC 0.0
RCMC 0.0001
CSEL7REF 0.177
CSEU7REF 0.25

NUMWELL = 2
WELLNAME(1) = "FIRST WELL"
KINDWELL(1) = 2
WELLTOP(1 TO 3,1,1) = 20 20 0
WELLBOTTOM(1 TO 3,1,1) = 20 20 20
DIAMETER(1,1) = 1.0
TEMPERATURE(1)=650.0
PRLIMIT(1) = 14000
WELLPQ(1) Block
  Interpolation Linear
  Extrapolation Constant
  Data  0.0  200.0
EndBlock
WELLNAME(2) = "SECOND WELL"
KINDWELL(2) = 3
WELLTOP(1 TO 3,1,2) = 300 300 0
WELLBOTTOM(1 TO 3,1,2) = 300 300 20
DIAMETER(1,2) = 1.0
WELLPQ(2) Block
  Interpolation Linear
  Extrapolation Constant
  Data  0.0  20.0
EndBlock
EndInitial
$ TRANSIENT DATA INPUT BLOCKS
BeginTime    0.0
TIME_CONTROL = 2
DELTIM = 0.1  DTIMMUL = 1.0  DTIMMAX = 1.0  DTIMMIN = 0.1
TUNE = 0.1 DPMAX = 0.5 DSMAX = 0.5 DCMAX = 0.5 DAQCMAX = 0.5 DTMAX = 0.5
WZ(,1) = 0 1
```

```
AQCOMP_WFINJ(,1) = 0.17 0.01 1.00 0.05
EndTime
BeginTime    64
WZ(,1) = 0 1
AQCOMP_WFINJ(,1) = 0.17 0.00 0.00 0.05
EndTime



TITLE(2) = "3-D HOT-CHEMICAL FLOODING DATA"
DESCRIPTION()=
"THICKNESS (FT) : 20 "
"LENGTH (FT) : 320 "
"WIDTH (FT) : 320 "
"GRID BLOCKS : 8X8x4"
COMPOSITIONAL_MODEL
TIMEEND = 365
$ I/O OPTIONS
OUTLEVEL = 1
OUTPUT_PRE
OUTPUT_SAT
OUTPUT_VIS
OUTPUT_HIS
OUTPUT_AQ
OUTPUT_TRAP
OUTPUT_RELP
OUTPUT_IFT
OUTPUT_TEMP
OUTPUT_TIME() = 50 100 150 200 250 300 365
ISTEP(,,) = 1
JSTEP(,,) = 1
KSTEP(,,) = 1
$ FAULT BLOCK AND MESH DATA
METHOD = 2
DOWN() = 0 0 1
MES = "cart"
NX(1) = 8  NY(1) = 8  NZ(1) = 4
DX() = 40  DY() = 40  DZ() = 5
$ COMPOUND NAMES
COMPOUND(1) = "C10"
$ COMPOUND CRITICAL TEMPERATURES
CRIT() 1111.8
$ COMPOUND CRITICAL PRESSURES
CRIP() 304.0
$ COMPOUND CRITICAL VOLUMES
CRIV() 12.087
$ COMPOUND ACEN
ACEN() 0.488
$ COMPOUND MOL WEIGHTS
MOLW() 142.3
$ COMPOUND PARA
PARA() 431.0
```

```
$ MAX NUMBER OF PHASES
NPHASE = 4
$ Initial rock & water properties
ROCKZ = 0.00000  ROCKP = 14.7
H2OZ = 0.000003  H2OP = 14.7  H2OD = 3.467
SURTF = 60.0  SURPS = 14.7
RESTF = 60.0
$ TOLERANCE
CVGOPT = 1
TOL_FLASH = 0.0001
TOL_VOLUME = 0.0001
TOL_MASS = 0.0001
TOL_WATER = 0.0001
TOL_ENERGY = 0.0001
MAXNEWT = 100
$ POROSITY
POROSITY1() = 0.2
$ PERMEABILITIES
XPERM1() = 500
YPERM1() = 500
ZPERM1() = 500
$ INITIAL WATER SATURATION
SWINI1() = 0.70
$ INITIAL WATER CELL PRESSURE
PINI1() = 20.0
$ INITIAL PHASE VISCOSITIES AT EACH CELL
VIS1() = 1.00
$ INITIAL COMPOSITIONS
ZXY1(,,,1) = 1.000
$ NUMERICAL METHOD
IMPAQCOMP
NAQCOMP 4
AQCOMPNAM() = "SALT" "SURFACTANT" "TRACER" "POLYMER"
AQCOMPTYPE() = 4 3 1 2
AQCOMPINIT() = 0.17 0.00 0.00 0.00
$ SURFACTANT PARAMETERS
EPSME 0.0001
HBNC70 0.07
HBNC71 0.04
CSEL7 0.177
CSEU7 0.25
AD31 1.5
AD32 0.5
B3D 1000.
$ IFT PARAMETERS
AHUH 9
CHUH 0.2
XIFTW 1.3
$ POLYMER PARAMETERS
AP1 81
AP2 2700
AP3 2500
SLOPP 0.0
```

```
AD41 0.0
AD42 0.0
B4D 100.0
$ RELPERM DATA
RELP 2
NRELFUN 1
ITRAP
ENDPTLOW() = 0.106 0.800 0.000
ENDPTHIGH() = 1.000 1.000 0.000
SRLOW() = 0.140 0.250 0.000
SRHIGH() = 0.000 0.000 0.000
EXPNLOW() = 2.100 1.700 0.000
EXPNHIGH() = 0.480 1.500 0.000
TL() = 364 59074 364
TAUL() = 1 1 1
ENERGY
VISCOCORRO
AVISO(,) = -0.978166136 558.61
VISCOCORRW
AVISW(,) = -4.89 1384.89
ACPR1 = 35.021
HKCONST
HKROCK = 25.0
HEATLOSS
HKCONSTS
HKROCKS = 25.02
TMEINI1()=520.0
ACPI(,)= -4.22 0.306 -0.0001585 0.0000000322 0.0
TREF 520.0
HBNT0 0.00017
HBNT1 0.00017
HBNT2 0.00017
ACPP() 1.0 0.5 1.0
NESM 1
C51L 0.177
BETAL 0.00415
C51U 0.25
BETAU 0.00415
CMCV
SCMC 0.0
RCMC 0.0001
CSEL7REF 0.177
CSEU7REF 0.25


NUMWELL = 2
WELLNAME(1) = "FIRST WELL"
KINDWELL(1) = 2
WELLTOP(1 TO 3,1,1) = 20 20 0
WELLBOTTOM(1 TO 3,1,1) = 20 20 20
DIAMETER(1,1) = 1.0
TEMPERATURE(1)=650.0
PRLIMIT(1) = 14000
```

```
WELLPQ(1) Block
  Interpolation Linear
  Extrapolation Constant
  Data  0.0  200.0
EndBlock
WELLNAME(2) = "SECOND WELL"
KINDWELL(2) = 3
WELLTOP(1 TO 3,1,2) = 300 300 0
WELLBOTTOM(1 TO 3,1,2) = 300 300 20
DIAMETER(1,2) = 1.0
WELLPQ(2) Block
  Interpolation Linear
  Extrapolation Constant
  Data  0.0  20.0
EndBlock
EndInitial
$ TRANSIENT DATA INPUT BLOCKS
BeginTime    0.0
TIME_CONTROL = 2
DELTIM = 0.1  DTIMMUL = 1.0  DTIMMAX = 3.0  DTIMMIN = 0.1
TUNE = 0.1 DPMAX = 0.5 DSMAX = 0.5 DCMAX = 0.5 DAQCMAX = 0.5 DTMAX = 0.5
WZ(,1) = 0 1
AQCOMP_WFINJ(,1) = 0.17 0.01 1.00 0.05
EndTime
BeginTime    64
WZ(,1) = 0 1
AQCOMP_WFINJ(,1) = 0.17 0.00 0.00 0.05
EndTime
```

Nomenclature

A_r	Reaction rate constant
C_p	Heat capacity
C_{pw}	Water compressibility
C_r	Rock heat capacity
C_{SEL}	Lower limit effective salinity
C_{SEOP}	Optimum effective salinity
C_{SEU}	Upper limit effective salinity
d	Diffusion length
D	Depth
D_{ij}	Diffusivity coefficient
E	Activation energy
f	Fugacity
F	Flux
g	Gravitational acceleration
G	Gibbs free energy
$\vec{\vec{G}}$	Hessian matrix
h	Molar enthalpy
h_t	Thickness of the reservoir

H_{BNC} Height of binodal curve

$\hat{H}_r$ Heat of reaction

I Coordinate direction

J Coordinate direction

$\vec{\vec{J}}$ Jacobian

k_r Relative permeability

K Equilibrium ratio

K_o Arrhenius constant

$\tilde{K}$ Harmonic mean of permeability on a Cartesian grid

$\vec{\vec{K}}$ Permeability tensor

L Phase molar ratio

m Element of the Hessian matrix

MW Molecular weight

n Element of the Hessian matrix

n_A Number of aqueous components

n_b Number of gridblocks

n_c Number of hydrocarbon components

N Number of component moles

P Pressure

P_C Critical pressure

PI Productivity index

$\dot{q}$ Fluid production/injection rate

$\dot{Q}_L$ Heat- Loss

R Universal gas constant

R_E Residual of energy

R_F Residual of equilibrium

R_M Residual of component mass conservation

R_P Resistance factor

R_r Reaction rate

R_V Residual of volume constraint

S Saturation

t Time

t_D Dimensionless time

t_1 Execution time on single processor

t_n Execution time on N processor

T Temperature

T_C Critical temperature

u Internal energy

$\vec{v}$ Volumetric flux

V Bulk volume

V_P Pore volume

x Mole fraction

x_D Dimensionless length

$\vec{y}$ Trial phase composition

$\vec{z}$ Specific overall composition

Z Compressibility factor

Greek symbols

δ Binary interaction coefficient

Φ Flow potential

ϕ Porosity

φ Fugacity coefficient

γ Specific gravity

η Thermal diffusivity

λ_r Relative mobility

μ Viscosity

μ^* Low pressure viscosity

θ Volumetric heat capacity

ρ Density

σ Diagonal tensor of electrical conductivity

Δ_x Grid size in the x direction

Δ_y Grid size in the y direction

Δ_z Grid size in the z direction

ω Acentric factor

ψ Real scalar electrical potential

ξ Phase molar density

Subscript

a Aqueous

α Component index

b Bulk

β Phase index

f Fluid

g Gas phase

i Component index

j Phase index

m Matrix

o Oleic

oil Oil phase

r Relative

s Surrounding

v Vapor

w Well

Superscript

T	Total
$^\circ$	Reference

Acronyms

ACSS	Accelerated Successive Substitution Method
CMC	Critical Micelle Concentration
GPAS	General Purpose Adaptive Simulator
IMPES	Implicit Pressure-Explicit Saturation
IPARS	Integrated Parallel Accurate Reservoir Simulation
MPI	Message Passing Interface
PETSC	The Portable, Extensible Toolkit for Scientific Computation
VAPEX	Vapor Extraction

Bibliography

Abbas A.A., and Shedid S.A.: "Experimental Investigation of the Feasibility of Steam/Chemical Steam Flooding Processes through Horizontal Wells," Paper SPE 68767 presented at SPE Conference, Jakarta, Indonesia, April 2001.

Abdalla, A., and Coast, K.H.: "A Three-Phase Experimental and Numerical Simulation Study of the Steam Flood Process," Paper SPE 3600 presented at the 46th Annual Fall Meeting of the Society of the Petroleum Engineers of AIME, New Orleans, Louisiana, October 1971.

Abou-Kassem, J.H.: "Practical considerations in developing numerical simulators for thermal recovery," Journal of Petroleum Science and Engineering, 1981, V.15, pp.281-290.

Abu-Khamsin, S.A., Bringham, W.E., and Ramey, H.J.Jr: "Reaction Kinetics of Fuel Formation for In-Situ Combustion," Paper SPE 15736, SPE Reservoir Engineering, V.3 (4), 1988, pp.1308-1316.

Acs, G., Doleschall, S., and Farkas, E.: "General Purpose compositional Model," *SPEJ*, 1985, V.25 (4), pp.543-553.

Akin, S, Castanier, L.M., and Brigham, W.E.: "Effect of Temperature on Heavy Oil/Water Relative Permeabilities," Paper SPE 54120 presented at SPE International Thermal Operations Symposium, Bakersfield, California, March 1999.

Al-hadhrani H. S. and Blunt M. J.: "Thermally Induced Wettability Alteration to Improve Oil Recovery in Fractured Reservoirs," Paper SPE 59289 presented at SPE/DOE Improved Oil Recovery Symposium, Tulsa, Oklahoma, April 2000.

Ali, F.S.M.: "Multiphase, Multidimensional Simulation of In-Situ Combustion," Paper SPE 6896 presented at SPE 52nd Annual Technical Conference and Exhibition, Denver, Colorado, October 1977.

Aoudia, M., and Wade, W. H.: "Optimum microemulsions formulated with propoxylated Guerbet alcohol and propoxylated tridecyl alcohol sodium sulfates," Journal of Dispersion Science and Technology, 1995, V.16 (2), pp. 115-35.

Andrade, E.N., da C, Phi. Mag., 1934, V.7, P.698.

Austad, T. and Skule, S.: "Chemical flooding of oil reservoirs, effects of temperature and pressure on the middle phase solubilization parameters close to optimum flood

conditions," *Colloids and Surfaces*, A: Physicochemical and Engineering Aspects, 1996, V.108(2/3), pp. 243-252.

Ayatollahi, Sh., Lashanizadegan, A., and Kazemi, H.: "Temperature Effects on the Oil Relative Permeability during Tertiary Gas Oil Gravity Drainage (GOGD)," Energy & Fuel J., 2005, V.19, pp. 977-983.

Baker, R.S., and Bierschenk, J.M.: "In-Situ Thermal Destruction makes Stringent Soil and Sediment Cleanup Goals Attainable," Presented in Proceeding of the Forth Tri-Service Environmental Technology Symposium, San Diego, California, June 2001.

Balay, S., Gropp, W., MnInnes, L.C., and Smith, B.: PETSc 2.0 User Manual, Argonne National Laboratory, ANL-95/11-Revision 2.0.22. April 1998.

Bang, Vishal.: "Phase Behavior Study of Hydrocarbon-Water-Alcohol Mixture," MS. Thesis, The University of Texas at Austin, 2005.

Bell, C.W.: "Electrolitically Promoting the Flow of Oil from a Well," U.S. Patent No.2799641, 1957.

Bell, C.W., and Titus, C.H.: "Electro-Thermal Process for Production of Offshore Oil through Onshore Wells," U.S. Patent No.3724543, 1973.

Bell, C.W., and Titus, C.H.: "Electro-Thermal Process for Promoting Oil Recovery," U.S. Patent No.3782465, 1974.

Bell, C.W., and Titus, C.H., and Wittle, J.K.: "In-Situ Method for Yielding a Gas from a Subsurface Formation of Hydrocarbon Material," U.S. Patent No.4473114, 1985.

Bourrel, M., and Schechter, R.S.: *Microemulsions and Related Systems,* Marcle Dekker; New York, 1988, P.483.

Bowen, G., and Crumpton, P.: "A New Formulation for the Implicit Compositional Simulation of Miscible Gas Injection Processes," Paper SPE 79692 presented at SPE Reservoir Simulation Symposium, Houston, Texas, February 2003.

Branco, C.M., and Rodrigues, F.: "A semi-Implicit Formulation for Compositional Reservoir Simulation," Paper SPE 27053 , SPE Advanced Technology Series, 1995, V.4 (1), pp.171-177.

Brantferger, K. M.: "Development of a Thermodynamically Consistent, Fully Implicit, Compositional, Equation-Of-State, Steamflood Simulator," PhD Dissertation, University of Texas at Austin, May 1991.

Briens, F.J.L., Wu, C.H., Gazdag, J., and Wang, L.H.: "Compositional Reservoir Simulation in Parallel Supercomputing Environments," Paper SPE 21214 presented at the 11th

SPE Symposium on Reservoir simulation of the Society of Petroleum Engineers, Anaheim, California, February 1991.

Buchwalter, J.K., and Miller, C.A.: "A New Simplified Compositional Simulator," Paper SPE 25858 presented at SPE Rocky Mountain Regional/Low Permeability Reservoirs Symposium, Denver, Colorado, April 1993.

Cao, H., and Aziz, K.: "Performance of IMPSAT and IMPSAT-AIM Models in Compositional Simulations," ," Paper SPE 77720 presented at the SPE Annual Technical Conference and Exhibition, San Antonio, Texas, October 2002.

Chan, M.Y.S., and Sarioglu, G.: "Numerical Modeling of Cyclically Steamed and Fractured Oil-Sand Reservoirs," Paper SPE 22369 presented at the International Meeting on Petroleum Engineering, Beijing, China, March 1992.

Chang, Y.B.: "Development and Application of an Equation of State Compositional Simulator," Ph.D. Dissertation, The University of Texas at Austin, 1990.

Chein, M.C.H., Lee, S.T., and Chen, W.H.: "A New Fully Implicit Compositional Simulator," SPE 13385, presented at the 8th SPE Symposium on Reservoir simulation of the Society of Petroleum Engineers, Dallas, TX, 1985.

Chein, M.C.H., Yardumain, H.E., Chung, E.Y., and Todd, W.W.: "The Formulation of a Thermal Simulation Model in a Vectorized, General Purpose Reservoir Simulator," Paper SPE 18418 presented at the Tenth SPE Symposium on Reservoir Simulation, Houston, Texas, February 1989.

Chilingar, G.V., Chang, K.S., Davis, J.E., Farhangi, H.J., Adamson, L.G., and Sawabini, S.: "Possible Use of Direct Electrical Current for Augmenting Reservoir Energy during Petroleum Production," The Compass, 1968, V.45 (4), pp.272-285.

Chilingar, G.V., El-Nassir, A., and Stevens, R.G.: "Effect of Electrical Current on Permeability of Sandstone Cores," Journal of Petroleum Technology, 1970, V.22 (7), pp. 830-836.

Chilingar, G.V., Loo, W.W., Khilyux, L.F., and Katz, S.A.: "Electro-bioremediation of Soil Contaminated with Hydrocarbons and Metals," Energy Sources, 1997, V.19, pp. 129-146.

Chute, F.S., and Vermeulen, F.E.: "Present and Potential Application of Electromagnetic Heating in the In-situ Recovery of Oil," OSTARA Journal of Research, 1988, V.4, pp. 19-33.

Cicek, O. and Ertekin, T.: "Development and Testing of a New 3D Field Scale Fully Implicit Multi-Phase Compositional Steam Injection Simulator," Paper SPE 35516 presented at European 3D Reservoir Modeling Conference, Norway, April 1996.

Cicek, O.: "Numerical Simulation of Steam Displacement of Oil in Naturally Fractured Reservoirs Using Fully Implicit Compositional Formulation: A Comparative Analysis of the Effects of Capillary and Gravitational Forces in Matrix/Fracture Exchange Term," Paper SPE 97005 presented at SPE Annual Technical Conference and Exhibition, Dallas, Texas, October 2005.

Cieck, O.: "Modeling and Designing Oil Recovery by Steam Injection in Naturally Fractured Reservoirs," Paper SPE 93574 presented at SPE Western Regional Meeting, Irvine, California, 2005.

Cinar, M., Castainer, L.M., Kovscek, A.R.: " Improved Analysis of the Kinetics of Crude-Oil In-Situ Combustion," Paper SPE 113948 presented at Western Regional and Pacific Section AAPG Joint Meeting, Bakersfield, California, 2008.

Closmann, P.J., Waxman, M.H., and Deeds, C.T.: "Steady-State Tar/Water Relative Permeabilities in Peace River Cores at Elevated Termprature," Paper SPE 14227 presented at SPE 60th Annual Technical Conference and Exhibition, Las Vegas, Nevada, September 1985.

Coats, K.H., George, W.D., Chu, C., and Marcum, B.E.: "Three-Dimensional Simulation of Steam Flooding," Trans., AIME, 1974, V.257, pp. 573-592.

Coats, K.H.: "Simulation of Steam Flooding with Distillation and Solution Gas," *SPEJ,* 1976. V.16 (5), pp. 235-247.

Coats, K.H.: "A Highly Implicit Steam Flood Model," *SPEJ*, 1978, V.18 (5), pp. 369- 383.

Coats, K.H.: "In-Situ Combustion Model," *SPEJ*, 1980, V. 20(6), pp.533 – 554.

Collins, D.A., Nghiem, L.X., and Li, Y.-K.: "An Efficient Approach to Adaptive-Implicit Compositional Simulation with an Equation of State," Paper SPE 15133 presented at the 56th Annual California Regional Meting of the Society of Petroleum Engineers, Oakland, CA, 1986.

Corey, A.T.: "The Interrelation between Gas and Oil Relative Permeabilities," Producers Monthly, November 1954, pp. 38-41.

Crookston, R.B., Culham, W.E., and Chen, W.H.: "A Numerical Simulation Model for Thermal Recovery Processes," *SPEJ*, 1979, V.20 (1), pp. 37-58.

Crowson, F. L., and Gill, W.G.: "Method and Apparatus for Secondary Recovery of Oil," U.S. Patent No. 3605888, 1971.

DeBaun, D., Byer, T., Childs, P., Chen, J., Saaf, F., Wells, M., Liu, J., Cao, H., Pianelo, L., Tialkraj, V., Crumpton, P., Walsh, D., Yardomian, H., Zorzynski, R., Lim, K.T., Schrader, M., Zapata, V., Noleon, J., and Tchelepi, H.: "An Extensible Architecture

for Next Generation Scalable Parallel Reservoir Simulation," Paper SPE 93274 presented at SPE Reservoir Simulation Symposium, Houston, Texas, 2005.

Dwarakanath, V., Pope, G. A.: "Surfactant Phase Behavior with Field Degreasing Solvent," *Environmental Science and Technology*, 2000, V.34 (22), pp. 4842-8.

Dogru, A.H., Sunaidi, H.A., Fung, L.S., Habiballah, W.A., Al-Zamel, N., Li, K.G.: "A parallel Reservoir Simulator for Large-Scale Reservoir Simulation," SPE Reservoir Evaluation and Engineering Journal, 2002, V.7 (1), pp. 11-23.

Douglas, J. Jr., Blair, P.M., and Wagner, R.j.: "Calculation of Linear Waterflood Behavior Including the Effects of Capillary Pressure", Petroleum Transactions, AIME, 1958, V.213, pp. 96-102.

Douglas, J. Jr., Peaceman, D.W., and Rachford, H.H.: "A Method for Calculating Multi-Dimensional Immiscible Displacements," Petroleum Transactions, AIME, 1959, V.216, pp. 297-308.

Edmondson, T.A.: "Effects of Temperature on Water Flooding," J. Can. Pet.Tech., 1965, pp. 263-242.

Elliot, Lucas J., Pope, Gary A., and John, Russell T.: "In-Situ Thermal Remediation of Contaminant below the Water Table," Paper SPE 81204 presented at SPE/EPA /DOE Exploration and Production Environmental Conference in San Antonio, Texas, March 2003.

Fagin, R.G., and Stewart, C.H.: "A New Approach to the Two-Dimensional Multiphase Reservoir Simulator," Paper SPE 1188 presented at SPE Annual Fall Meeting, Denver, Colorado, October 1965.

Fahes, M. and Firoozabadi, A.: "Wettability Alteration to Intermediate Gas-Wetting in Gas/Condensate Reservoir at High Temperatures," Paper SPE 96184 presented at the SPE Annual Technical Conference and Exhibition, Dallas, Texas, October 2005.

Farough Ali, S.M..: "Steam Injection Theories - A Unified Approach," Paper SPE 10746 presented at SPE California Regional Meeting, San Francisco, California, March 1982.

Fassihi, M.R., Brigham, W.E., and Ramey, H.J.Jr.: "Reaction Kinetics of In-Situ Combustion: Part 1- Observations," SPEJ, October 1983, V.4, pp.399-416.

Fathi.N, N.: "Modeling the Effects of IFT and Wettability on Chemical EOR Processes," PhD Dissertation, University of Texas at Austin, in Progress 2009.

Ferrer, J. and Farouq Ali, S.M.: "A Three-Phase, Two- Dimensional Compositional Thermal Simulator for Steam Injection Process," J. Can. Pet.Tech., 1977, pp. 78-90.

Fussell, L.T. and Fussell, D.D.: "An Iterative Technique for Compositional Reservoir Models," *SPEJ*, 1979, V.19 (4), pp.211-220.

Gai, X., Dean, R.H., Wheeler, M.F.: "Coupled Geomechanical and Reservoir Modeling on Parallel Computers," Paper SPE 79700 presented at SPE Reservoir Simulation Symposium, Houston, Texas, February 2003.

Gill, W.G.: "Method and Apparatus for Secondary Recovery of Oil," U.S. Patent No. 3507330, 1970.

Gill, W. G.: "Electrical Method and Apparatus for Recovery of Oil," U.S. Patent No. 3542066, 1972.

Gill, P.E., and Murray, W.: "Newton-Type Methods for Unconstrained and Linearly Constrained Optimization," Mathematical Programming, 1974, V.4, pp.311-350.

Glandt, C.A. and Chapman, W.G.: "Effect of Water Dissolution in Oil Viscosity," SPERE, February 1995, p. 59.

Godderij, R.R., Bruining, J., and Molenaar, J.: "A Fast 3D Interface Simulator for Steamdrives," Paper SPE 59269 SPE Journal, V. 4(4), December 1999.

Goldstein, A.A., and Price, J.F.: "On Descent from Local Minima," *Math. of Comp*. 1971, V.25 (115), pp.569-574.

Grabowski, J.W., Vinsome, P.K., Lin, R.C., Behie, A., and Rubin, B.: "A Fully Implicit General Purpose Finite Difference Thermal Model for In Situ Combustion and Steam," Paper SPE 8396 presented at Annual Meeting of the Society of Petroleum Engineering of AIME, Las Vegas, Nevada, 1979.

Griswold, J. and Kasch, J.E.: "Hydrocarbon-Water Solubilities at Elevated Temperature and Pressure," Ind. Eng. Chem., 1942, V.34 (7), p.804.

Gropp, W., Morgan, T., Smith, B., Arbogast, T., Dawson, C.N., Lake, L.L., McKinney, D.C., Pope, G.A., Sepehrnoori, K., and Wheeler, M.F.: "New Generation Framework for Petroleum reservoir Simulation," First Annual Report , Advanced Technology Initiative, Argonne National Laboratory and The University of Texas at Austin, May 1996.

Habiballah, W.A., Hayder, M.E., Khan, M.S., Issa, K.M., Zahrani, S.H., Shaikh, A.H., Uwaivyedh, A.H, Tyraskis, T.P., Baddourah, M.A.: "Parallel Reservoir Simulation Utilizing PC-Clusters in Massive Reservoir Simulation Models," Paper SPE 84065 presented at SPE Annual Technical Conference and Exhibition, Denver, Colorado, October 2003.

Hamouda, A.A., Karoussi, O., and Chukwudeme, E.A.: "Relative Permeability as a Function of Temperature, Initial Water Saturation and Flooding Fluid Compositions for Modified Oil-Wet Chalk," Journal of Petroleum Science and Engineering, 2008, V.63, pp.61-72.

Han, C., Delshad, M., Sepehrnoori, K., and Pope, G.A.: "A Fully Implicit, Parallel, Compositional Chemical Flooding Simulator," Paper SPE 97217 presented at SPE Annual Technical Conference and Exhibition, Dallas, Texas, October 2005.

Hansen, K.S., Conley, D.M., Vinegar, H.J., Coles, J.M., Menotti, J.L., and Stegemeier, G.L.: "In-Situ Thermal Desorption of Coal Tar," Proceeding of the Institute of Gas Technology/Gas Research Institute International Symposium on Environmental Biotechnologies and Site Remediation Technologies, Orlando, Forida, December 1998.

Healy, R. N., and Reed, R. L.: "Multiphase Microemulsion Systems," *SPEJ*, June 1976, p.174.

Heidman, J.L.: "High-Temperature Mutual Solubilities of Hydrocarbons and Water. Part II: Ethylbenzene, Ethylcyclohexane, and n-Octane," AICHE J., 1985, V. 31, p. 376.

Hilbert, A. D., "Numerical Simulation of the Electrical Pre-heat and Steam Drive Bitumen Recovery Process for the Athabasca Oil Sands," PhD Dissertation, Department of Electrical Engineering, University of Alberta, 1986.

Iben, I.E.T., Edelstein, W.A, Sheldon, R.B., Shapiro, A.P. Uzgiris, E.E., Scatena, C.R., Blaha, S.R., Silverstein, W.B., Brown, G.R., Stegemeier, G.L., and Vinegar, H.J.: "Thermal Blanket for In-Situ Remediation of Surficial Contamination: A Pilot Test," Environmental Science and Technology, 1966, V.30(11), pp. 3144-3154.

Ishimoto, K.: "One – Dimensional Fully Implicit Compositional Model for Steam Flooding," MS Thesis, University of Texas at Austin, Texas, 1985.

Ishimoto, K., Pope, G.A., and Sepehrnoori, K.: "An Equation of State Steam Simulator," *In Situ*, 1987, V.11 (1), pp.1-37.

Kazemi, H., Vestal, C.R., and Shank, G.D.: "An Efficient Multicomponent Simulator," Paper SPE 6890 presented at 52nd SPE Annual Fall Technical Conference and Exhibition, Denver, Colorado, October 1977.

Kell, G.S.: "Density, Thermal Expansivity and Compressibility of liquid water from 0° to 150° Correlations and Tables for atmospheric Pressure and Saturation," J.Therm. Eng. Data, 1975, V.20, pp.97-105.

Killough, J.E., and Kossack, C.A.: "Fifth Comparison Solution Project: Evaluation of Miscible Flood Simulators," Paper SPE 16000 presented at the 9th SPE Symposium on Reservoir Simulation , San Antonio, Texas, February 1987.

Kristensen, M.R., Gerritsen, M.G., and Thomsen, P.G.: "Coupling Chemical Kinetics and Flashes in Reactive, Thermal and Compositional Reservoir Simulation," Presented at SPE Reservoir Simulation Symposium, Houston, Texas, February 2007.

Lauwerier, H.A.: "The Transport of Heat in an Oil Layer by the Injection of Hot Fluid," Applied Scientific Research., Section A, 1955, V.5, pp.145-150.

Li, D.: "Four-Phase Streamline-Based Compositional Simulation of Gas Injections for a Viscous Oil," Paper SPE 88790 presented at 11th International SPE Conference and Exhibition, Abu Dhabi, U.A.E., October 2004.

Lohrenz, J., Bray, B.G., and Clark, C.R.: "Calculation Viscosities of Reservoir Fluids From Their Compositions," Trans.,AIME, 1964,V.142, pp.159-172.

Longumare, P., Mainguy, M., Lemonnier, P., Onaisi, A., Gerard, Ch. and Koutsabeloulis, N.: "Geomechanics in Reservoir Simulation: Overview of Coupling Method and Field Case Study," Oil & Gas Technology–Rev. IFP, 2002, V.57 (5), pp.471-483.

Luo, Sh., and Barrufet, M.A.: "The Effect of Water-in-Oil Solubility on Oil Reservoir in the Steam-Injection Process," Paper SPE 89407 presented at SPE symposium on Improved Oil Recovery, Tulsa, Oklahoma, 2005.

Maini, B.B, and Batycky, J.P.: "Effect of Temperature on Heavy Oil/Water Relative Permeabilities and Vertically Drilled Core Plugs," J. Pet.Tech., 1985, V.37, pp. 1500-1510.

McGee, B. C. W., Vermeulen, F.E., and Yu, L.: "Field Test of Electrical Heating with Horizontal and Vertical Wells," J. of Can. Pet.Tech, 1999, V.38 (3), pp. 46-53.

McKetta, J.L.Jr. and Katz, D.L.: "Methane-n-Butane-Water System in Two-and Three-Phase Regions," Ind. Eng. Chem. 1948, V. 40, p.835.

Mehra, R.K., Heidman, R.A., and Aziz, K.: "An Accelerated Successive Substitution Algorithm," Can.J.Chem.Eng., 1983, V.61, pp.590-596.

Michelsen, M.K.: "The Isothermal Flash Problem: Part I. Stability," Fluid Phase Equilibria, 1982, V.6, pp.1-19.

Michelsen, M.L., and Mollerup, J.M.: "Thermodynamics Models: Fundamental and Computational Aspects," Tie-Line Publications, Denmark, 2004.

Mifflin, R.T., Watts, J.W. and Weiser, A.: "A Fully Coupled, Fully Implicit Reservoir Simulator for Thermal and other Complex Reservoir Processes," Paper SPE 21252 presented at SPE Symposium on Reservoir Simulation, California, February 1991.

Miller, M.A., and Ramey, H.J Jr.: "Effects of Temperature on Oil/Water Relative Permeabilities of Unconsolidated and Consolidated Sands," J. Pet.Tech., 1985, V.37, pp. 945-953.

Nelson, W.L.: "Solubility of Water in Oil," Oil & Gas J., April 1956, p.140.

Nghiem, L.X., Fong, D.K. and Aziz, K.: "Compositional Modeling with an Equation of State," *SPE J.*, 1981, V.21 (6), pp.687-698.

Nghiem, L.X, and Li, Y.-K.: "Computation of Multiphase Equilibrium Phenomena with an Equation of State," Fluid Phase Equilibria, 1984, V.17, pp.77-95.

Nilsson, J., Gerritsen, M. and Younis, R.: "An Adaptive, High-Resolution Simulator for Steam Injection Processes," Paper SPE 93881 presented at SPE Western Regional Meeting, Irvine, California, April 2005.

Noll, L. A.: "The Effect of Temperature, Salinity, and Alcohol on the Critical Micelle Concentration of Surfactants," Paper SPE 21032 presented at the SPE International Symposium on Oil Field Chemistry, Anaheim, California, February 1991.

Novosad, J.: "Surfactant Retention in Berea Sandstone- Effect of Phase Behavior and Temperature," *SPE J.*, December 1982, pp. 962-70.

Orr, F.M., Jr., Yu, A.D., and Lien, C.L.: "Phase Behavior of CO_2 and Crude Oil in Law Temperature Reservoirs," *SPE J.*, 1981, V.21 (4), pp.480-491.

Parashar, M., Wheeler, J.A., Pope, G., Wang, K., and Wang, P.: "A New Generation EOS Compositional Reservoir Simulator: Part II – Framework and Multiprocessing," Paper SPE 37977 presented at the SPE Reservoir Simulation Symposium, Dallas, Texas, June 1997.

Peaceman, D.W.: "Interpretation of Well-Block Pressures in Numerical Reservoir Simulation," *SPEJ*, 1978, V.18 (3), pp.183-194.

Peaceman, D.W.: "Interpretation of Well-Block Pressure in Numerical Reservoir Simulation with Nonsquare Grid Blocks and Anisotropic Permeability," *SPEJ*, 1983, V.23 (3), pp.531-543.

Peng, D.Y., and Robinson, D.B.: "A New Two-Constant Equation of Sate," Ind. Eng. Chem. /Fundam., 1976, V.15, pp.59-64.

Perschke, D. R.: "Equation of State Behavior Modeling for Compositional Simulator," Ph.D. Dissertation, The University of Texas at Austin, 1988.

Perschke, D. R., Chang, Y., Pope, G.A., and Sepehrnoori, K.: "Comparison of Phase Equilibria Algoritms for an Equation-of-State Compositional Simulator," Submitted to SPE, September 1989.

Polikar, M., Ferracuti, F., Decastro, V., Puttagunta, V.R., and Ali, F.S.M.: "Effects of Temperature on Bitumen-Water End Point Relative Permeabilities and Saturations," J. Can. Pet.Tech., 1986, V.25, pp. 44-50.

Poston, S.W., Israel, S., Hossain, A.K.M.S., Montgomery, E.F.III., and Ramey, H.J Jr.: "The Effect of Temperature on Irreducible Water Saturation and Relative Permeability of Unconsolidated Sands," *SPEJ*, 1970, pp. 171-180.

Puetro, M. C. and Reed, R. L.: "A Three-Parameter Representation of Surfactant Oil Brine Interaction," *SPE J*., August 1983, pp.669-682.

Rastegar, R., and Jessen, K.: "A Flow Based Lumping Approach for Compositional Reservoir Simulation," Paper SPE 119160 presented at the SPE Reservoir Simulation Symposium, Woodlands, Texas, February 2009.

Reis, J.C: "Numerical and Experimental Studies of Produced Oil Composition during Light Oil Steam flooding," presented at the Spring Meeting of the AICHE Symposium on Enhanced Oil Recovery, Orlando, Florida, March 1990.

Rubin, B., and Buchanan, W.L.: "A General Purpose Thermal Model," *SPEJ,* 1985, V.15 (2), pp. 202-214.

Sarapuu, E.: "Method of Underground Electro-linking and Electro-carbonization of Mineral Fuels." US Patent No. 2795279, 1957.

Schembre, J.M., Tang, G. Q. and Kovscek, A.R.: "Effect of Temperature on Relative Permeability for Heavy-Oil Diatomite Reservoirs," Paper SPE 93831 presented at SPE Western Regional Meeting, Irvine, California, 2005.

Shedid, S. Ali and El Abbas A. A.: "Experimental Study of surfactant Alkaline Steam Flood through Vertical Wells," Paper SPE 62562 presented at SPE/AAPG Western Regional Meeting, Long Beach, California, June 2000.

Sheldon, J.W., Harris, C.D., and Bavly, D.: "A Method for General Reservoir Behavior Simulation on Digital Computers," Paper SPE 1521-G presented at 35th Annual Fall Meeting of the Society of Petroleum Engineers, Denver, Colorado, October 1960.

Shinta, A.A. and Firoozabadi, A.: "Prediction Phase Behavior of Water/Reservoir Crude Systems with the Association Concept," Paper SPE 27872, SPE Reservoir Engineering, May 1997.

Shutler, N.D.: "Numerical Three-Phase Simulation of the Linear Steam Flood Process," Trans., AIME, 1969, V. 246, pp.232-246.

Shulter, N.D.: "Numerical Three-Phase Model of the Two-Dimensional Steam Flood Process," *SPEJ*, 1970, V. 10(6), pp.405-417.

Somerton, W.H., J.A. Keese, and S.L. Chu.: "Thermal Behavior of Unconsolidated Oil Sands," Paper SPE 4506 presented at 48th Annual Fall Meeting of the Society of Petroleum Engineers, Las Vegas, Nevada, 1974.

Spillette, A.G., Hillestad, J.G., and Stone, H.L.: "A High-Stability Sequential Solution Approach to Reservoir Simulation," Paper SPE 4542, presented at the 48th Annual Fall Meeting of the Society of Petroleum Engineering of AIME, Las Vegas, NV, 1973.

SATRS 2006.10.: "Steam; Thermal and Advanced Processes Reservoir Simulator," By Computer Modelling Group Ltd.

Stegemeier, G.L. and Vinegar, H.J.: "Soil Remediation by Surface Heating and Vacuum Extraction," Paper SPE 29771 presented at the SPE/EPA Exploration and Production Environmental Conference, Houston, Texas, March 1995.

Stegemeier, G.L. and Vinegar, H.J.: "Thermal Conduction Heating for In-Situ Thermal Desorption of Soil," *Hazardous and Radioactive Waste Treatment Technologies Handbook*, CRC Press, Boca Raton, FL., 2001.

Sufi, A.H., Ramey, H.J Jr., and Brigham, W.E.: "Temperature Effects on Relative Permeabilities of Oil-water," Paper SPE 11071 presented at SPE Annual Fall Technical Conference and Exhibition, New Orleans, Louisiana, September 1982.

Tang, G. Q., and Firoozabadi, A.: "Effect of GOR, Temperature, and Initial water Saturation on Solution-Gas Drive in Heavy-Oil Reservoirs," Paper SPE 71499 presented at SPE Annual Technical Conference and Exhibition, New Orleans, Louisiana, 2001.

Tang, G. Q., and Kovscek A. R.: "Wettability Alteration of Diatomite Induced by Hot-Fluid Injection" Paper SPE 77461 presented at SPE Annual Technical Conference and Exhibition, San Antonio, Texas, 2002.

Thele, K.J., Lake, L.W., and Sepehrnoori, K.: "A Comparison of Three Equation-of-State Compositional Simulators," SPE 12245, presented at the 7th SPE Symposium on Reservoir simulation of the Society of Petroleum Engineers, San Francisco, CA, 1983.

Tikhomolova, K. P., "Electro-Osmosis," Ellis Horwood Publication, New York, 1993.

Titus, C.H., Wittle, J.K., and Bell, C.W.: "Apparatus for Passing Electrical Current Through an Underground Formation," US Patent No.4495990, 1985.

Torabzadey, S.J.: "The Effect of Temperature and Interfacial Tension on Water/Oil Relative Permeabilities of Consolidated Sands," Paper SPE 12689 presented at SPE Enhanced Oil Recovery Symposium, Tulsa, Oklahoma, April 1984.

Tortike, W.S., and Farouq Ali, S.M.: "Saturated-Steam-Property Functional Correlation for Fully Implicit Thermal Reservoir Simulation," SPE Reservoir Eng., 1989, V.4 (4), pp. 471-474.

Trangenstein, J.A.: "Minimization of Gibbs Free Energy in Compositional Reservoir Simulation," SPE/DOE Paper 13520 presented at SPE Reservoir Simulation, Dallas, TX, 1985.

Trangenstein, J.A.: "Customized Minimization Techniques for Phase Equilibrium Computation in Reservoir Simulation," Chem. Eng. Sc., 1987, V.42, pp.2847-2863.

Trangenstein, J.A.: "Analysis of a Model and Sequential Numerical Method for Thermal Reservoir Simulation," presented at the European Conference on the Mathematics of Oil Recovery, University of Cambridge, England, July 1989.

Turek, E.A., Metcalfe, R.S., and Fishback, R.E.: "Phase Behavior of Several CO_2-West Texas Reservoir Oil Systems," *SPERE*, 1988, V.3 (2), pp.505-516.

UTCHEM-9.82.: "Three-Dimensional Chemical Flood Simulator," Prepared by Reservoir Engineering Research Program Center for Petroleum and Geosystems Engineering, The University of Texas at Austin.

Varavei, A., and Sepehrnoori, K.: "An EOS-Based Compositional Thermal Reservoir Simulator," Paper SPE 119154, presented at SPE Reservoir Simulation Symposium, Woodland, Texas, February 2009.

Vinegar, H.J., DeRouffignac, E.P., Menotti, J.L., Coles, J.M., Stegemeier, G.L., Sheldon, R.B., and Edelstein, W.A.: "Remediation of Deep Soil Contaminants Using Thermal Vacuum Wells," Paper SPE 39291, Proceedings of the SPE Annual Technical Conference, San Antonio, Texas, October 1997.

Vinegar, H.J., DeRouffignac, E.P., Rosen, R.L., Stegemeier, G.L., Bonn, M.M., Conley, D.M., Phillips, S.H., Hirsch, J.M., Carl, F.G., Steed, J.R., Arrington, D.H., Brunette, P.T., Mueller, W.M., and Siedhof, T.E.: "In-Situ Thermal Desorption (ISTD) of PCBs," Proceeding of the HazWaste/World Superfund XVIII Conference, Washington, DC, December 1997.

Vinegar, H.J., Stegemeier, G.L., Carl, F.G., Stevenson, J.D., and Dudley, R.J.: "In-Situ Thermal Desorption of Soil Impacted with Chlorinated Solvents," Proceeding of the Annual meetings of the Air and Waste Management Association, Paper No.99-450, 1999.

Vinsome, P.K.W.: "A Numerical of Hot-Water and Steam Drive by the Finite-Difference Method," Paper SPE 5248 presented at the Annual Meeting of the Society of Petroleum Eng. of AIME, Houston, Texas, 1974.

Vinsome, P.K.W., and Westerveld, J.: "A Simple Method for Predicting Cap and Base Rock Heat Losses in Thermal Reservoir Simulators," J. Can. Pet. Tech., July 1980, pp. 87-90.

Voskov, D.V., and Tchelepi, H.A.: "Compositional Parameterization for Multi-Phase Flow in Porous Media," Paper SPE 113492 presented at the SPE/DOE Symposium on Improved Oil Recovery, Tulsa, Oklahoma, April 2008.

Walters, D.A., Settari, A. and. Kry, P.R.: "Poroelastic Effects of Cyclic Steam Stimulation in the Cold Lake Reservoir," Paper SPE 62590 presented at SPE/AAPG Western Regional Meeting, Long Beach, California, June 2000.

Wang, Q and Chao, K.C.: "Vapor-Liquid and Liquid-Liquid Equilibria and Critical States of Water + n-Decane Mixtures," Fluid Phase Equilibria, 1990, V.59, p.207.

Wang, P., Yotov, I., Wheeler, M. F., Arebogast, T., Dawson, C., Parashar, M., and Sepehrnoori, K.: "A New Generation EOS Compositional Reservoir Simulator: Part I-Formulation and Descredization," Paper SPE 37979 presented at the SPE Reservoir Simulation Symposium, Dallas, Texas, June 1997.

Wang, P., Balay, S., Sepehrnoori, K., Wheeler, J., Abate, J., Smith, B., and Pope, G.A.: "A Fully Implicit Parallel EOS Compositional Simulator for Large Scale Reservoir Simulation," Paper SPE 51885 presented at the 15th SPE Reservoir Simulation Symposium, Houston, Texas, February 1999.

Watts, J.W.: "A Compositional Formulation of the pressure and Saturation Equations," *SPERE*, May 1986, V.16 (3), pp.243-252.

Weinstein, H.G., Wheeler, J.A., and Woods, E.G.: "Numerical Model for Thermal Processes," *SPEJ*, 1986, V.17 (2), pp.65-78.

West, W.J., Garvin, W.W., and Sheldon, J.W.: "Solution of the Equations of Unsteady State Two-Phase Flow in Oil reservoirs," Trans., AIME, 1954, V. 201, p.217.

Wheeler, M.J., Arbogast, T., Bryant, S., Eaton, J., Lu, Q., Peszynska, M., Yotoy, I.: "A Parallel Multiblock/Multidomain Approach for Reservoir Simulation," Paper SPE

51884 presented at the SPE Reservoir Simulation Symposium, Houston, Texas, February 1999.

Wilson, G.M.: "A Modified Redlich-Kwong Equation of State-Application to General Physical Data Calculations," 65th National AIChE Meeting, Cleveland, OH, May 1969.

Wittle, J.K., and Bell, C.W.: "Electrochemical Process for Effecting Redox-Enhanced Oil Recovery," U.S. Patent No.6877556 B1, 2005.

Wittle, J.K., and Bell, C.W.: "Method for Enhancing Oil Production Using Electricity," U.S. Patent Application No.2005/0199387 A1, 2005.

Wittle, J.K., Hill, D.G., and Chilingar G.V.: "Direct Current Electrical Enhanced Recovery in Heavy-Oil Reservoirs to Improve Recovery, Reduce Water Cut, and Reduce H_2S Production while Increasing API Gravity," Paper SPE 114012 presented at SPE Western Regional and Pacific Section AAPG Joint Meeting in Bakersfield, California, 2008.

Wong, T.W., Firoozabadi, A., Nutakki, R., and Aziz, K.: "A Comparison of Two Approaches to Compositional and Black Oil Simulation," Paper SPE 15999 presented at the 9th SPE Symposium on reservoir Simulation of the Society of Petroleum Engineers, San Antonio, Texas, February 1987.

Workman, P. E.: "Method of Recovering and Increasing the Production of Oil," U.S. Patent No.1784214, 1930.

Yan, W., Michelsen, M.L., Stenby, E.H., Berenblyum, R.A., and Shapiro, A.A.: "Three-phase Compositional Streamline Simulation and Its Application to WAG," Paper SPE 89440 presented at the SPE/DOE 14th Symposium on Improved Oil Recovery, Tulsa, Oklahoma, April 2004.

Yoshiaki, Ito, Settari, A. and Jha, K.N.: "Development and Application of Pseudo - Functions for Reservoir Simulation to Represent Shear Failure during the Cyclic Steam Process," Paper SPE 25800 presented at SPE International Thermal Operations Symposium, Bakersfield, California, February 1993.

Youngren, G.K.: "Development and Application of an In-Situ Combustion Reservoir Simulator," *SPEJ*, February 1980, pp. 39-51.

Young, L.C. and Stephenson, R.E.: "A Generalized Compositional Approach for Reservoir Simulation," *SPEJ*, October 1983, V.13 (6), pp.727-742.

Young, L.C.: "Continues Compositional Volume-Balance Equations," Paper SPE 66346 presented at the SPE Reservoir Simulation Symposium, Houston, Texas, February 2001.

Zhang, K., Wu, Y.S., Ding, C., Pruess, K., and Elmroth, E.: "Parallel Computing Techniques for Large-Scale Reservoir Simulation Multi-Component and Multiphase Fluid Flow," Paper SPE 66343 presented at the SPE Reservoir Simulation Symposium, Houston, Texas, February 2001.

Ziegler, V. M.: "Laboratory Investigation of High Temperature Surfactant Flooding," *SPERE*, May 1988, pp.586-596.

Vita

Abdoljalil Varavei was born in Khormoj, Iran on August 1, 1972, the son of Setareh Teimouri and Gholamhassan Varavei. After completing Motahari High school, Khormoj, Iran, in 1990, he entered the University of Petroleum Engineering, Ahwaz, Iran, in 1990. He received the degree of Bachelor of Science in Chemical Engineering in 1995. He graduated with a Master of Science in Chemical Engineering from The University of Tehran, Iran in 1996. During the following years he joined the University of Boushehr, Iran as an Instructor. On February 2004, he enrolled the Graduate School at the University of Texas at Austin to pursue a PhD in the Department of Petroleum Engineering.

Permanent address: Khormoj, Boushehr.
Iran.

This dissertation was typed by Abdoljalil Varavei.